TESIS DE LA UNIVERSIDAD DE ZARAGOZA
2024
52

Luis Gabriel Guanabara Keler Gesteira

Design and optimization of polygeneration systems for small buildings

Director/es
Uche Marcuello, Francisco Javier

ISSN 2254-7606

Prensas de la Universidad
Universidad Zaragoza

ISSN 2254-7606

Universidad Zaragoza
1542

Tesis Doctoral

DESIGN AND OPTIMIZATION OF POLYGENERATION SYSTEMS FOR SMALL BUILDINGS

Autor

Luis Gabriel Guanabara Keler Gesteira

Director/es

Uche Marcuello, Francisco Javier

UNIVERSIDAD DE ZARAGOZA
Escuela de Doctorado

Programa de Doctorado en Energías Renovables y Eficiencia Energética

2023

Design and Optimization of Polygeneration Systems for Small Buildings

Ph.D. Thesis

Luis Gabriel Guanabara Keler Gesteira

Advisor

Prof. Francisco Javier Uche Marcuello

2023

To my parents

For your unconditional support during my academic journey, but, above all, for your everlasting love.

Acknowledgments

First, I would like to express my gratitude to my advisor, Professor Javier Uche, for believing in me from the very beginning when I was still in Brazil. His unwavering support, availability, and knowledge sharing have been instrumental in my development as a researcher.

I am grateful to the Federal Institute of Bahia and my research group, NRCA, for taking on the workload during my pursuit of a Ph.D. Additionally, I appreciate the mobility program that allowed me to study in Zaragoza.

My sincere thanks go to Campus Iberus and the EU's Erasmus+ program for making my research stay at the University of Naples Federico II possible. I am also grateful to Professor Francesco Calise and his team, particularly Dr. Francesco Cappiello, Dr. Maria Vicidomini, and Luca Cimmino, for their valuable collaboration.

I extend special thanks to Professor Ignacio Zabalza for his guidance and insights on building energy simulation, which has greatly contributed to my thesis.

Finally, I would like to convey my deepest appreciation to Raíza, my family, and my friends for their unwavering love and support throughout this journey. Their encouragement has provided me with the strength to persevere.

Agradecimientos

Primero, me gustaría expresar mi más sincera gratitud a mi director de tesis, el Profesor Javier Uche, por creer en mí desde el principio cuando aún estaba en Brasil. Su constante apoyo, disponibilidad y compartición de conocimientos han sido fundamentales en mi desarrollo como investigador.

Quiero agradecer al Instituto Federal de Bahía y a mi grupo de investigación, NRCA, por asumir la carga de trabajo durante mi búsqueda del doctorado. Y en especial, al programa de movilidad que me permitió estudiar en Zaragoza.

Quede aquí también reconocida las posibilidades que me ha dado el Campus Iberus y el programa Erasmus+ de la UE, por hacer posible mi estancia de investigación en la Universidad de Nápoles Federico II. Quiero dar las gracias desde aquí al Profesor Francesco Calise y a su equipo, especialmente al Dr. Francesco Cappiello, la Dra. Maria Vicidomini y Luca Cimmino, por su valiosa colaboración y acogida en mi estancia.

Durante mi periodo en Zaragoza, quiero destacar la ayuda del profesor Ignacio Zabalza con su orientación y conocimientos sobre la simulación energética de edificios, que ha contribuido en gran medida a mi tesis.

Por último, me gustaría expresar mi más profundo agradecimiento a Raíza, mi familia y mis amigos por su amor y suporte durante toda esta jornada. Sus palabras me han proporcionado la fuerza para perseverar.

Appended publications

This doctoral thesis is a compendium of publications. The collection is composed of research articles featured in journals that are listed in the global index known as Journal Citation Reports (JCR). They are referred to in the text using the assigned Roman numerals:

I. Zabalza, I.; **Gesteira, L.G.**; Uche, J. *The Impact of Building Energy Codes Evolution on the Residential Thermal Demand*. J Braz. Soc. Mech. Sci. Eng. 2022, 44, 588, doi:10.1007/s40430-022-03898-w.

II. **Gesteira, L.G.**; Uche, J.; de Oliveira Rodrigues, L.K. *Residential Sector Energy Demand Estimation for a Single-Family Dwelling: Dynamic Simulation and Energy Analysis*. J. Sustain. Dev. Energy Water Environ. Syst. 2021, 9, 1–18, doi:10.13044/j.sdewes.d8.0358.

III. **Gesteira, L.G.**; Uche, J. *A Novel Polygeneration System Based on a Solar-Assisted Desiccant Cooling System for Residential Buildings: An Energy and Environmental Analysis*. Sustainability 2022, 14, 3449, doi:10.3390/su14063449.

IV. **Gesteira, L.G.**; Uche, J.; Dejo-Oricain, N. *A Polygeneration System Based on Desiccant Air Conditioning Coupled with an Electrical Storage*. Sustainability 2022, 14, 15784, doi:10.3390/su142315784.

V. **Gesteira, L.G.**; Uche, J.; Cappiello, F.L.; Cimmino, L. *Thermoeconomic Optimization of a Polygeneration System Based on a Solar-Assisted Desiccant Cooling*. Sustainability 2023, 15, 1516, doi:10.3390/su15021516.

VI. Uche, J.; Zabalza, I.; **Gesteira, L.G.**; Martínez-Gracia, A.; Usón, S. *A Sustainable Polygeneration System for a Residential Building*. Applied Sciences 2022, 12, 12992, doi:10.3390/app122412992.

Resumen

Esta tesis doctoral se puede dividir en dos partes principales: la estimación de las demandas energéticas y de agua en edificios residenciales y el desarrollo de sistemas innovadores de poligeneración solar para edificios pequeños. La metodología aplicada desarrolla un procedimiento secuencial sistemático para resolver el problema a tratar, que partió del comportamiento energético de un edificio hasta el diseño de una planta de poligeneración y su optimización energética, económica y ambiental adecuado a dicho edificio.

El ámbito de estudio de la tesis partió de un conjunto de edificios representativos que combinaban diferentes tipos de edificios, códigos técnicos y zonas climáticas de España. Se estimó un patrón genérico de electricidad, calefacción, refrigeración, agua caliente sanitaria y agua dulce mediante simulación aplicando herramientas diversas encontradas en la literatura para cada demanda a servir. Como resultado, se presentaron todos los perfiles de demanda con un intervalo de tiempo de 1 hora para un período de 1 año. Además, se realizó un análisis de confort térmico para validar los requisitos térmicos.

Los diseños de los sistemas de poligeneración para viviendas se basan en configuraciones novedosas, al incluir algunos equipos escasamente investigados en la literatura y en cualquier caso no integrados en un esquema de poligeneración, donde el reparto de energía térmica y eléctrica producida debe gestionarse adecuadamente en las 5 demandas a servir, teniendo en cuenta el tamaño de los sistemas de almacenamiento térmico y eléctrico disponibles. En particular, las principales tecnologías utilizadas son colectores fotovoltaicos/térmicos, ósmosis inversa, baterías convencionales de plomo-ácido, generadores termoeléctricos y acondicionadores de aire con rueda desecante. La planta de poligeneración suministra electricidad, calefacción y refrigeración, agua caliente sanitaria y agua dulce para una aplicación residencial. Los colectores fotovoltaicos/térmicos utilizados para la producción de electricidad y calefacción se aplicaron a todos los diseños.

En el primer trabajo, la planta desarrollada se conectó a la red y se utilizó un dispositivo de ósmosis inversa y un aire acondicionado por desecante para satisfacer las demandas de agua dulce y refrigeración, respectivamente. En el segundo estudio, se evaluó el diseño anterior como una instalación independiente mediante el acoplamiento de una batería de plomo-ácido como respaldo de la independencia de la red eléctrica. El tercer sistema investigado fue la planta de poligeneración anterior conectada a la red, añadiendo paneles fotovoltaicos y una caldera de biomasa para proporcionar flexibilidad para optimizar el uso de los colectores fotovoltaicos/térmicos. Finalmente, se incluyeron generadores termoeléctricos en la configuración anterior, así como una bomba de calor y un enfriador de absorción de un solo efecto para proporcionar refrigeración y una destilación multi-efecto para desalinizar el agua:

en este último sistema, el tamaño del esquema de poligeneración aumenta a un edificio multivivienda, y por tanto es necesario explorar otras tecnologías técnicamente disponibles para mayores demandas energéticas (ciclo de absorción y destilación multi-efecto).

Debido al potencial de integración del edificio con diferentes tecnologías para satisfacer las demandas y los servicios energéticos, se ha utilizado como software principal TRaNsient System Simulation (TRNSYS), que permite diseñar y simular dinámicamente los edificios y los sistemas de poligeneración. Además, permite llevar a cabo análisis de sensibilidad para investigar la mejor configuración de los sistemas. Adicionalmente, se realizó una optimización del diseño para proporcionar la rentabilidad energética, ambiental y económica óptima de las disposiciones propuestas.

En definitiva, esta tesis proporciona todos los pasos para el completo diseño de sistemas de poligeneración sostenibles, utilizando en lo posible la electricidad y el calor producido para servir las demandas residenciales, en especial de viviendas con necesidad de suministro de agua independiente de la red.

Abstract

This Ph.D. thesis comprises two main parts: the estimation of energy and water demands for residential buildings and the development of innovative solar-based polygeneration systems for small buildings. A systemic methodology was employed to address this challenge, beginning with an analysis of the building's energy behavior, followed by the design of an appropriate polygeneration facility, and finally, optimizing its energy efficiency, economic feasibility, and environmental impact for the specific building.

The case study consisted of a set of representative buildings, combining different building types, energy codes, and climate zones within Spain. A generic pattern for electricity, heating, cooling, domestic hot water, and freshwater consumption was determined through simulations using multiple tools to generate these demands. Consequently, all demand profiles were displayed with an hourly resolution over a year. Furthermore, thermal comfort analysis was performed to validate thermal requirements.

The design of a residential polygeneration system is based on novel configurations, as it includes several technologies that have been minimally explored in the existing literature and are not typically integrated into polygeneration schemes. These systems manage the production of thermal and electrical energy to satisfy the five demands of a residential building while considering the capacities of thermal and electrical storage. In particular, the leading technologies used in the systems include photovoltaic/thermal collectors, reverse osmosis, lead-acid battery, thermoelectric generators, and desiccant air conditioning. The polygeneration plant supplies electricity, space heating and cooling, domestic hot water, and freshwater for residential applications. Photovoltaic/thermal collectors, used for both electricity and heating production, were incorporated into all system layouts.

In the first work, the developed plant was grid-connected, consisting of a reverse osmosis device and a desiccant air conditioning system to address freshwater and cooling demands, respectively. The second investigation evaluated the prior configuration as an off-grid facility by incorporating lead-acid battery storage for electricity backup. The third system examined the previous on-grid polygeneration plant with added photovoltaic panels and a biomass boiler, offering flexibility for optimizing the usage of photovoltaic/thermal collectors. Lastly, thermoelectric generators were integrated into the previous design, along with a heat pump and a single-effect absorption chiller for space cooling, and a multi-effect distillation unit for water desalination. The first three systems were applied to a single-family townhouse, while the final configuration was implemented in a medium/large apartment block. Consequently, as the polygeneration system size increased, it became necessary to explore new technologies appropriate for higher energy demands, such as single-effect absorption chillers and multi-effect distillation units.

Due to the potential for integrating various technologies to match the building's demands and energy services, the TRaNsient System Simulation (TRNSYS) software was primarily employed for designing and dynamically simulating the building and polygeneration systems. Furthermore, a sensitivity analysis was carried out to investigate the systems' best setup. Additional design optimization was performed to ensure optimal energy efficiency, environmental impact, and economic profitability for the proposed layouts.

Overall, this thesis provided useful insights into the design of sustainable polygeneration systems, using the produced power and heat to match residential users' needs, particularly in regions facing water scarcity.

Contents

Nomenclature

AC	Alternating Current
AH	Air Heater
AS	Annual Saving
BES	Building Energy Simulation
COP	Coefficient of Performance
CO_2	Carbon Dioxide
ΔCO_2	Carbon Dioxide Saving
ΔCO_{2R}	Carbon Dioxide Saving Ratio
CREST	Centre for Renewable Energy Systems Technology
DB-SE	Basic Document on Energy Savings
DAC	Desiccant Air Conditioning
DC	Direct Current
DHW	Domestic Hot Water
EES	Electrical Energy Storage or Engineering Equation Solver
EU	European Union
GPS	Generalized Pattern Search
HP	Heat Pump
HVAC	Heating, Ventilation, and Air Conditioning
IEA	International Energy Agency
IRR	Internal Rate of Return
ISO	International Organization for Standardization
LHV	Low Heating Value
LCA	Life Cycle Assessment
LCO	Levelized Cost
KPI	Key Performance Indicator
MED	Multi-effect Distillation
MD	Membrane Distillation
NPV	Net Present Value
OC	Operating Cost
PE	Primary Energy

PES	Primary Energy Saving
PES_R	Primary Energy Saving Ratio
PS	Proposed System
PMV	Predicted Mean Vote
PPD	Predicted Percentage of Dissatisfied
PV	Photovoltaic
PVT	Photovoltaic/thermal
RES	Renewable Energy Sources
RO	Reverse Osmosis
RS	Reference System
SCF	Solar Collector Fluid
SEC_R	Specific Energy Consumption
SEAC	Single-effect Absorption Chiller
SOC	State of Charge
SPB	Simple Payback
STREAM	Stochastic Residential Water End Use Model
TES	Thermal Energy Storage
TRNSYS	Transient System Simulation
TI	Total Investment
UN	United Nations

List of figures

List of tables

1 Introduction

1.1 Sustainable polygeneration systems

Over the past two decades, climate change has emerged as a significant concern on the global stage [1]. This is primarily due to the consistent rise in average global temperatures and the severe consequences of greenhouse gas (GHG) emissions in the atmosphere [2]. Therefore, the research community and governments were guided to focus on renewable energy sources (RES) as energy consumption in all sectors has increased [3]. In this framework, European Union (EU) countries have been working towards developing new technologies that prevent the depletion of natural resources and reduce greenhouse gas emissions in the energy systems [4].

Polygeneration systems are a possible sustainable energy solution as it integrates multiple fuels for delivering several utilities [5]. It can be defined as the combined production of two or more energy services (e.g. space heating, hot sanitary water, freshwater, etc.), seeking to take advantage of the maximum efficiency of the consumed resources [6,7]. Furthermore, polygeneration systems combined with RES, can replace conventional technologies and supply multiple energy needs while reducing CO_2 emissions and increasing primary energy savings. This is possible because RES are replenished naturally and emit minimally, if any, carbon dioxide [8].

Renewable energy technologies are crucial in transitioning from fossil fuels that have been relied upon for centuries. Therefore, polygeneration systems are a key point in this energy transition as they are designed to harness one or more renewable sources to simultaneously generate electricity, heating, cooling, and fuels [9]. For residential applications, these systems are employed to produce freshwater instead of fuels [10]. Polygeneration systems can be designed in a diverse range of configurations to accommodate various applications [8]. Additionally, decentralized plants in isolated regions help improve energy accessibility for rural populations [5].

Finally, polygeneration systems are gaining recognition for their ability to promote effective resource consumption reduction, lower CO_2 emissions, and economic savings compared to conventional separate production. They also allow the integration of renewable energy technologies with conventional technologies, making a significant contribution to achieving global goals such as those outlined in the Paris agreement of 2015. Furthermore, polygeneration systems can achieve more than 80% of energy savings in the residential sector with appropriate energy integration, particularly in warm areas such as Mediterranean countries [6].

1.2 Polygeneration systems in the building sector

In the past few years, the International Energy Agency (IEA) [11] and the EU [12] have concentrated on energy consumption, specifically concerning buildings. Buildings are responsible for 57% of final energy consumption and 32% of CO_2 emissions in Africa, 26% of energy consumption and 24% of emissions in Southeast Asia, and 24% and 21% of consumption and emissions, respectively, in Central and South America. In Europe and the United States, buildings account for 40% of energy consumption and 36% of CO_2 emissions [13]. Despite regional variations, the building sector's energy consumption is significant across the globe. Furthermore, around 75% of buildings exhibit energy inefficiency and 80% of the untapped energy efficiency potential offers prospects for economic gains, enhanced energy security, and environmental conservation [14].

At the European level, the initial Directive on Energy Performance of Buildings was introduced in 2002 as Directive 2002/91/CE [15]. It was later amended by Directive 2010/31/EU [16] and Directive (EU) 2018/844 [17]. These changes have progressively led to improvements in building enclosures to minimize energy losses and have been incorporated into national regulations across EU countries. In 2016, the European Commission established guidelines for promoting nearly zero-energy buildings (NZEBs) [18]. Consequently, all EU countries enacted regulatory adjustments to achieve NZEBs for new residential, office, and service buildings by 2020. An NZEB is characterized by its exceptional energy performance, with the minimal energy required being primarily supplied by renewable energy sources [19]. However, designing sustainable buildings that meet such high-performance standards is a complex endeavor [20].

In the coming years, we must intensify our efforts to develop and implement new policies to achieve a fully decarbonized building stock (both new and existing) by 2050. Achieving this ambitious objective requires the development of comprehensive roadmaps and the execution of energy transition strategies, which encompass regulatory changes and financial backing for energy efficiency initiatives. This is especially relevant in existing buildings where enhancements can be more easily accomplished, given their relatively elevated energy usage levels.

Within this context, sustainable solutions must be employed to meet building energy demands more effectively. The integration of advanced renewable energy solutions in building design is becoming increasingly popular in academic research [21]. The deployment of polygeneration systems in buildings offers a promising solution for reducing energy consumption and achieving the NZEBs target [8]. The polygeneration structure can vary widely to be suitable for different building types, including hotels [22], hospitals [23], residences [24], districts [25], offices [26], schools [27], and more. These studies evaluate system performance using dynamic simulation tools based on three main indicators, i.e., technical, economic, and environmental [5].

Finally, over 60% of the total energy consumption in the building sector is attributed to residential users [28]. The residential sector contributes to 28% of global CO_2 emissions and 30% of worldwide final energy consumption, which increase to 38% and 35%, respectively, when including the construction industry's impact [29,30]. Therefore, residential buildings serve as a crucial element in the energy transition and significantly contribute to strategies aimed at reducing climate change and its effects. In line with the latest Intergovernmental Panel on Climate Change (IPCC) report, this sector is a primary target in the effort to restrict global temperature rise to 1.5 °C [31].

1.3 Available technologies for buildings

Recent research has offered sustainable solutions for meeting a building's fundamental needs, according to our state-of-the-art review [32–37]. A sustainable approach for the residential sector is a polygeneration system that simultaneously supplies electricity, heating, cooling, freshwater, and DHW from one or multiple primary sources (Figure 1.1).

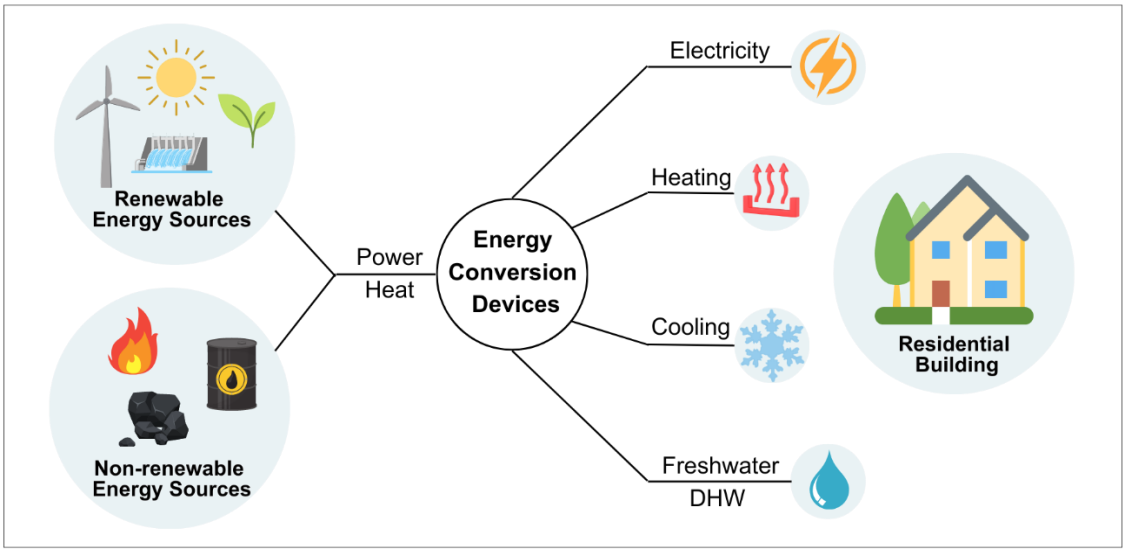

Figure 1.1 Polygeneration system for residential buildings.

A comprehensive evaluation of a polygeneration system based on RES should be examined to identify the most effective integration of technologies for meeting the building's demand. Put simply, various technology combinations can result in distinct designs aimed at achieving the same objective [8]. In each case, simulations are conducted, which include optimizing the design, evaluating energy, environmental, and economic aspects, and assessing the proposed

plant's sensitivity to external factors. Hence, the selection of energy conversion devices relies on factors like input fuels, capacity, cost efficiency, and availability.

Solar energy stands out as the most promising substitute for fossil fuels due to the geographic coincidence of areas with abundant sunlight, significant water scarcity [38], and high demand for cooling. It arrives at Earth's surface via radiation and can be harnessed through two methods: using a solar collector to generate thermal energy or employing a photovoltaic (PV) panel to produce electricity. Furthermore, it can be used for both electricity and heating production through photovoltaic-thermal collectors (PVT). These systems have a combination of solar cells with a solar collector [39–41]. PV and PVT systems are extensively employed as renewable energy solutions in the residential sector. Due to their significance, numerous recent studies have been conducted to enhance their efficiency.

Solar technologies are known to be highly variable due to weather conditions, leading to considerable reliance on the grid when energy production is insufficient or nonexistent, which can negatively impact a plant's profitability [42]. Electricity can be utilized immediately, stored in a suitable energy storage system (EES), or sold back to the grid depending on electricity prices and funding policies. EES transforms electricity into a storable form, which can later be converted back to meet users' needs on-demand, thereby increasing electricity availability [43–45]. EES are grouped into four primary categories: mechanical (e.g., flywheels), electrical (e.g., capacitors), chemical (e.g., electrochemical devices), and fuel cell (e.g., hydrogen storage) [46,47]. They can be employed as standalone energy storage or combined with other energy storage systems for enhanced flexibility and cost reduction [48].

Lead-acid batteries are the most widely used storage technology [49]. Nevertheless, they can result in increased electricity expenses due to the necessity for regular replacement and may release harmful substances during malfunction or disposal. Recent research reveals a rising interest in electrical energy management and usage approaches incorporating EES for building applications [50–54]. Furthermore, EES can operate effectively in a wide range of polygeneration systems, enhancing system stability [56].

In Europe, heating purposes represent about 68% of the residential sector's energy consumption [39]. It is primarily employed for domestic hot water (DHW) production and space heating in buildings. Converting solar radiation into heat is the most simple and direct application of solar energy, with greater potential than other forms of renewable sources [56]. However, due to solar radiation variability, thermal energy storage (TES) is used for mitigating these thermal fluctuations and for covering variable thermal demands while the production system operates continuously at nominal conditions. Consequently, polygeneration systems with TES can yield significant economic, energy, and environmental benefits [6].

Nevertheless, the peak heating demand typically coincides with periods of limited solar radiation in the winter months [57]. Therefore, solar energy can be combined with other RES, such as a biomass boiler (BB) and a thermoelectric generator (TEG), to address the challenges of solar intermittency and ensure continuous and stable operation all year long. Biomass, a solid fuel derived from agricultural waste, has substantial potential as a renewable thermal resource [5]. On the other hand, TEG can increase electricity production from a gradient of temperature through Seebeck's effect [58]. TEG technology is small-sized, lightweight, noiseless, and requires minimal maintenance, making it particularly well-suited for domestic polygeneration schemes [59,60].

The notably greater availability of solar energy during the summer compared to the winter makes it an ideal choice for solar cooling systems [61]. The main advantage of these solutions is the simultaneous occurrence of abundant solar energy and increased space cooling demand in buildings during the summer months. Particularly in hot countries, cooling systems have been the main energy consumer in the residential sector [39].

The concept of solar cooling technologies is based on the operation of thermally-driven devices based on single, double, and multi-effect absorption [62], adsorption [63], or desiccant [64] units with different required temperature levels [65]. Their operation principle consists of using thermal energy, which may be from solar collectors, to activate an ab(d)sorption/desorption process which produces a cooling effect [61]. In absorption cooling systems the most common working fluids are H_2O/LiBr (water is the refrigerant) and NH_3/H_2O (ammonia is the refrigerant). For adsorption cooling systems, the common working pairs are water-zeolite, water-silica gel, and Ammonia-$CaCl_2$. Concerning the desiccant cooling systems (desiccant wheel), silica gel or lithium-chloride solution serve as sorption materials [66].

In general, absorption and adsorption chillers are large and complex, limiting their suitability for medium/large building applications. A more viable thermally-driven cooling technology for small-scale units is a desiccant air conditioning (DAC), offering numerous benefits in terms of operational life, maintenance, and efficiency [67]. Desiccant cooling systems harness the ability of desiccant materials to extract moisture from an airstream through a natural adsorption process. Thus, the latent heat is reduced without cooling the air below its dew point [68]. This allows for the achievement of building thermal comfort by independently controlling sensible and latent loads, resulting in enhanced indoor air quality (IAQ) [69], especially in hot and humid areas such as Mediterranean countries [70].

Today, in many regions across the globe, heat pumps (HP) are widely utilized for cooling purposes. Based on the traditional vapor compression refrigeration cycle, HPs demand a significant amount of electricity to operate [71]. These systems offer high performance, stability, and reliability for cooling. Nevertheless,

despite its high coefficient of performance (COP), HPs may employ harmful refrigerants with global warming and/or ozone depletion potentials, making them an unsustainable option.

Desalination is a way to increase freshwater resources in many parts of the world and it represents a viable and very interesting alternative in the context of water scarcity. Nevertheless, desalination is an intensive energy process, which demands a polygeneration system of power or heat. The thermal technologies include multi-effect distillation (MED) and membrane distillation (MD), while reverse osmosis (RO) is the power-driven membrane-based approach. MED is an interesting technology due to its reduced thermal energy consumption (around 70 °C) and low maintenance requirements [72]. MD is an emerging technology that has the potential to deliver an affordable heat-driven purification method, particularly when combined with waste heat or solar thermal energy [73]. On the other hand, RO stands out as the most efficient seawater desalination method, given its relatively lower energy consumption and high salt rejection [74].

Despite the widespread use of polygeneration systems in various industrial applications, often dependent on non-renewable energy sources [8], there is an untapped potential for innovative building-integrated polygeneration plants, based on RES [75]. Table 1.1 consolidates all the relevant technologies explored in this doctoral thesis that are appropriate for application in residential polygeneration systems.

Table 1.1 Suitable technologies for residential polygeneration systems.

Technology	**Input**	**Output**	**Scale**	**Eff./COP**	**Unit**
PVT collector	Solar	Power Heat	All sizes	0.1-0.18 0.2-0.5	%
PV panel	Solar	Power	All sizes	0.1-0.2	%
Thermoelectric generator	Heat	Power	Small	0.03-0.1	%
Biomass boiler	Biomass	Heat	All sizes	0.7-0.9	%
Desiccant wheel	Heat	Cool	Small	0.5-0.7	-
Absorption chiller	Heat	Cool	Medium/large	0.5-0.7	-
Adsorption chiller	Heat	Cool	Medium/large	0.4-0.6	-
Heat pump	Power	Heat & Cool	All sizes	3.0-6.0	-
Multi-effect distillation	Heat	Freshwater	Medium/large	50-100	kWh_t/m^3
Membrane distillation	Heat	Freshwater	Small	10-250	kWh_t/m^3
Reverse osmosis	Power	Freshwater	All sizes	2.5-4	kWh_e/m^3

1.4 Research gap covered by this Ph.D. thesis

A renewable energy-based polygeneration system enables the integration of different technologies within a single system to address the diverse demands of a user. Scientific literature has predominantly focused on medium and large-scale systems; however, there is an increasing interest in examining small-scale facilities and their potential applications [76]. Developing a decentralized and integrated system that meets both energy and water needs for residential applications is a challenge. The reliable production of multiple energy services for residential buildings is critical for improving sustainability in the 21st century, in line with the new EU Green Deal [77]. Therefore, research in this area is essential given its societal significance and the scarcity of prior knowledge, as evidenced by the current state-of-the-art review.

Although polygeneration facilities demonstrate enhanced overall performance, it is rare to find them meeting all the energy and water demands of a residential building (Table 1.2). Current polygeneration systems face design and optimization issues due to their complex control requirements and their size typically exceeds what is appropriate for residential applications [32]. Consequently, the majority of the related studies are computational-based simulations (not experimental) or industrial applications. Therefore, the expansion of these polygeneration systems depends on a thorough comprehension of their reliability, robustness, self-sufficiency, operational and maintenance needs, and profitability. The latter is influenced by demand fluctuations, external factors such as fuel prices and energy policies, and unit costs of components and installation, which depend on economies of scale, available financing options, and market presence.

This is particularly pertinent in Mediterranean countries like Spain, where the demand for cooling and freshwater is intensified due to the region's hot summers and typical water scarcity. Furthermore, in remote areas, grid connections may not be economically or environmentally feasible because of the higher costs and CO_2 emissions associated with energy and water transportation. In these instances, using local natural resources can provide a more sustainable solution for addressing users' needs [78]. Designing a polygeneration system for self-consumption reduces its dependence on external factors, increasing economic and environmental advantages.

This doctoral thesis introduces a clear and sequential approach to tackling the challenge of integrating technologies typically utilized in large installations. It presents appropriate comprehensive designs for small-scale polygeneration schemes capable of self-sufficiently meeting residential demands. This approach is demonstrated through six previously published works co-authored during the Ph.D. studies [79–84].

Table 1.2 Polygeneration systems state-of-the-art review.

Author	Electricity	Heating	Cooling	DHW	Freshwater
Calise et al. (2019) [85]		✓	✓	✓	✓
El-Emam et al. (2018) [86]	✓		✓	✓	✓
Rashidi et al. (2018) [87]	✓		✓	✓	✓
Calise et al. (2016) [88]	✓	✓	✓		✓
Azhar et al. (2017) [89]	✓	✓	✓		✓
Jana et al. (2015) [90]	✓	✓	✓		✓
Leiva et al. (2017) [91]	✓	✓	✓		✓
Calise et al. (2016) [24]	✓	✓	✓	✓	
Calise et al. (2014) [92]	✓	✓	✓	✓	✓
Calise et al. (2014) [33]	✓	✓	✓	✓	✓
Calise et al. (2015) [93]	✓	✓	✓	✓	✓
Calise et al. (2015) [34]	✓	✓	✓	✓	✓
Calise et al. (2020) [36]	✓	✓	✓	✓	✓
Hogerwaard et al. (2017) [94]	✓	✓	✓	✓	✓
Maraver et al. (2012) [95]	✓	✓	✓	✓	✓
Ahmadi et al. (2014) [96]	✓	✓	✓	✓	✓
Ahmadi et al. (2014) [97]	✓	✓	✓	✓	✓
Figaj et al. (2022) [98]	✓	✓	✓	✓	✓
Luqman et al. (2020) [99]	✓	✓	✓	✓	✓

1.5 Objectives and structure of the thesis

The main objectives of this Ph.D. thesis are: firstly, to explore a comprehensive methodology for accurately estimating energy demands of residential buildings in Spain; and secondly, to model and simulate several solar-based polygeneration systems integrating renewable energy technologies and energy storage, for achieving affordable and sustainable energy solutions for small-scale applications.

This thesis has these main goals:

1. To investigate the impact of building energy codes (BECs) on decreasing thermal demand. In this respect, a set of representative

residential buildings were modeled and simulated to assess heating, cooling, and DHW demands for different climate zones in Spain.

2. To estimate a generic pattern for all main energy demands (electricity, heating, cooling, DHW, and freshwater) required by a single-family townhouse in Spain. All demands were generated for 1 year with a 1-hour time step.
3. To design, model, and optimize an innovative solar-based polygeneration system primarily composed of photovoltaic/thermal collectors, reverse osmosis, and desiccant air conditioning, to meet the demands of a single-family townhouse in Spain. The process began with the development of an on-grid facility, succeeded by an off-grid plant integrated with lead-acid batteries, and concluded with an on-grid plant also incorporating photovoltaic panels and a biomass boiler to serve as a backup for the photovoltaic/thermal collectors and providing optimization flexibility.
4. To extend the previous analysis to a larger scheme, by comparing four configurations of an innovative on-grid solar-based polygeneration system combining photovoltaic/thermal collectors, photovoltaic panels, biomass boiler, thermoelectric generator, heat pump or single-effect absorption chiller, and reverse osmosis or multi-effect distillation for attending the demands of a medium/large apartment block in Spain.

The Ph.D. thesis is organized as follows:

In Chapter 1, a comprehensive literature review of the aspects explored throughout the thesis is provided. This encompasses a summary of the legal framework related to the development of polygeneration systems for residential buildings following global efforts to mitigate climate change. Additionally, the polygeneration systems for residential buildings are presented by examining the integration of technologies and their innovative features. Besides, this chapter outlines the thesis's objective and structure.

In Chapter 2, we introduce the chosen case studies, encompassing all relevant input and design data. This includes climate zones, building types, and energy codes, including building usage and envelope specification (Paper I and II). Additionally, the case study presentation is completed with details on the residential users' demands and the building thermal comfort analysis (Papers I, II, and III).

In Chapter 3, the proposed systems layouts are detailed in specific sections. Several technologies are integrated for achieving sustainable polygeneration systems designed to meet the energy needs of residential buildings. We assess four increasingly complex system arrangements, all of them consisting of a PVT collector’s solar field as the main energy production component (Papers III, IV, V, and VI).

In Chapter 4, the design improvement of the polygeneration systems is discussed. A sensitivity analysis seeks to establish the influence of critical design parameters on the performance of these systems. Additionally, optimization strategies employing energy, environmental, and economic objectives are utilized to find their best configuration (Papers III, IV, V, and VI).

In Chapter 5, the doctoral thesis concludes with a summary of the main findings of the work, the contributions achieved, as well as suggestions for potential future research, encompassing critical aspects associated with the investigated systems.

2 System Definition

The case study encompasses an assortment of representative buildings, based on geometric building typologies, energy regulations, and Spanish climate zones (Paper I). A generic pattern of electricity, heating, cooling, DHW, and freshwater usage was estimated (Paper II). These demand profiles were displayed on an hourly basis for a full year. Additionally, a thermal comfort assessment was conducted to verify the fulfillment of thermal needs (Papers II and III).

2.1 Geographic location and climatic data

Spain is characterized by 15 distinct climate zones, which are categorized based on the severity of winter and summer climates. These classifications are derived from degree-day patterns and solar radiation, as outlined in the Spanish technical building code's energy-saving basic document, DB-HE [100]. The most representative climate zones were chosen based on factors such as the region's size, population, and the inclusion of all winter climate severities, as heating demand surpasses cooling demand in Spain [101]. A detailed description of each climate zone can be found in Table 2.1.

Table 2.1 The main climate conditions of each selected city.

Zone	**Z1**	**Z2**	**Z3**	**Z4**	**Z5**
Location (climate zone)	Almeria	Valencia	Santander	Zaragoza	Burgos
Latitude	36°50′ N	39°28′ N	43°27′ N	41°39′ N	42°21′ N
Altitude above sea level (m)	0	8	1	207	861
Annual average outdoor temperature (ºC)	18.4	17.6	14.6	15.2	12.1
Horizontal global solar radiation (kWh/year)	1829	1615	1279	1656	1549
Average annual wind speed (m/s)	4.1	3.1	5	4.5	4.8
Average annual tap water temperature (ºC)	15.7	14.6	12.8	13.3	10.1

Hourly climate data for energy simulations were obtained from the Meteonorm database, which contains measurements from meteorological stations in the

selected cities. Specifically, Typical Meteorological Year (TMY) data was employed to simulate Spain's climate conditions. Considering the common association among areas with abundant sunlight, significant water scarcity, and high cooling demand, Almería, located on Spain's Mediterranean coast, was chosen as the main case study. The city is known for its high summer climatic severity, which leads to a total annual irradiance of 2,587 kWh/m^2. Figure 2.1 shows the hourly variations in available global solar radiation on a horizontal surface and dry bulb temperature throughout the year at this location. Global solar irradiance includes direct incident beam radiation at the surface, diffuse radiation scattered by atmospheric molecules, and albedo, or the radiation reflected by the surroundings [102].

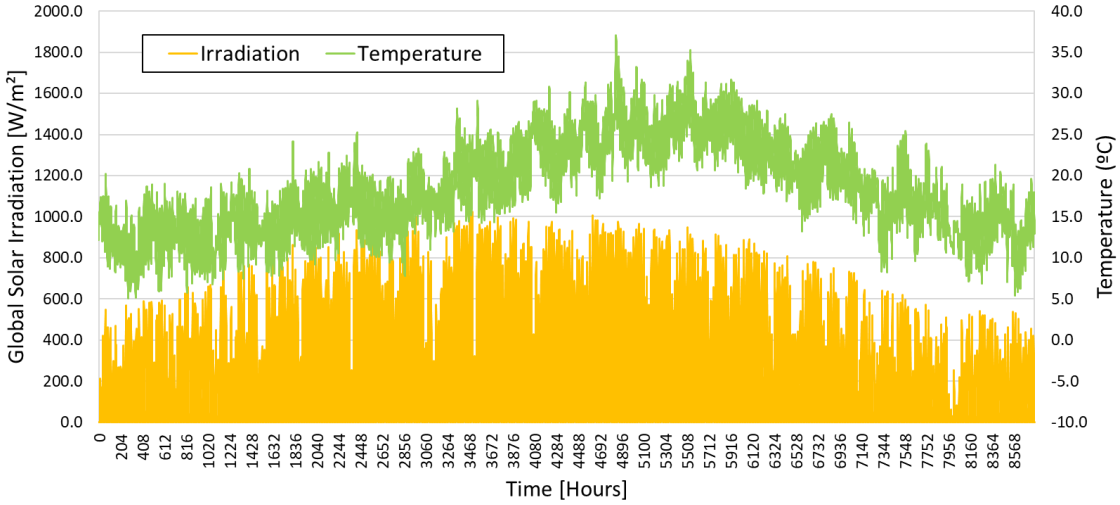

Figure 2.1 Hourly mean solar radiation and ambient temperature, Almería.

2.2 Building types and energy codes

The classification of residential building types was based on data collected from the Spanish Population and Housing Census [103]. Constructive characteristics considered included building-conditioned surfaces, the number of dwellings per building, people per dwelling, floor height, main façade orientation, and the surface area of each thermal envelope element (façades, floors, roofs, and openings). This information enabled the geometric modeling of representative buildings, including a single-family townhouse, a small apartment block, and a medium/large apartment block. Figure 2.2 provides a 3D view of these residential buildings, while Table 2.2 details the main geometric characteristics for each case.

BECs have been instrumental in reducing energy consumption in buildings, but their effectiveness depends on being both mandatory and enforced [104].

Comparative analyses of BECs in neighboring countries with similar climatic conditions support this assertion [105,106]. Over the past 50 years, Spain's national building energy codes have undergone several developments. Five key milestones during this period aimed at enhancing the thermal envelope quality, leading to significant energy demand reductions and improved thermal comfort [107]. The amendments introduced by Directive 2010/31/EU [16] resulted in the 2013 release of the Basic Document of Energy Saving (DB-HE) in the Spanish Technical Building Code [100]. In 2019, this document was updated to incorporate new requirements established in the Directive (EU) 2018/844 [17]. In this study, we employed the latest energy code available during the research period, assuming that the building meets the highest energy efficiency standards.

Table 2.2 Geometric characteristics of the building types.

Building type	**T1**	**T2**	**T3**
Type	Single-family townhouse	Small apartment block	Medium/large apartment block
No. of homes	1	12	80
Total number of people	4	48	240
Useful dwelling surface (m^2)	110	100	70
Total conditioned area (m^2)	110	1200	5600
Total area (m^2)	165	1583	7190
Height per plant (m)	3	3	3
Total volume (m^3)	371.3	4750.2	21568.8
No. of floors above ground	3 (2+attic floor)	7 (6+ground floor)	11 (10+ground floor)
No. of floors below ground	0	0	0
Total building height (m)	7.5	21	33
No. of bedrooms per home	4	4	2
Orientation	North-South	North-South	North-South
Roof type	Pitched roof	Flat roof	Flat roof
Window-to-Wall Ratio, north façade (%)	10	10	10
Window-to-Wall Ratio, south façade (%)	15	15	15
Thermal envelope area (m^2)	178.4	1183.2	6191.2
Compactness[1] (m)	2.08	4.02	3.48
External shades	No	No	No

The DB-ES outlines construction solutions associated with walls, floors, ceiling insulation, windows, and air leakage for each building type and climate zone. It determines the building usage profile under standard operating and

[1] *Compactness* is the ratio between the volume (m^3) enclosed by the thermal envelope of a building and the sum of the thermal exchange surfaces (m^2) of that envelope in contact with the outside air or the ground. It is expressed in m. The compactness of a building is a design variable that affects heat exchange through the thermal envelope, so the greater the compactness, the lower the heat loss through the envelope.

occupancy conditions, which includes working hours, temperature setpoints for heating and cooling, and internal loads related to occupancy, lighting, and other equipment (Table 2.3). Additionally, this document was employed to estimate the daily DHW demand for each building.

Table 2.3 Building usage profile.

Building usage profile			
Setpoint temperature (°C)	Heating season	17	00:00-08:00
		20	08:00-24:00
	Cooling season	27	00:00-08:00
		-	08:00-16:00
		25	16:00-24:00
Occupancy load (W/m^2)	Weekday	3.51	00:00-08:00
		0.88	08:00-16:00
		1.76	16:00-24:00
	Weekend	3.51	00:00-24:00
Lighting load/Equipment load (W/m^2)		1.76	00:00-01:00
		0.44	01:00-08:00
		1.32	08:00-19:00
		2.2	19:00-20:00
		4.4	20:00-24:00
Ventilation rate (1/h)	Heating season	0.4	00:00-24:00
	Cooling season	4	01:00-09:00
		0.4	09:00-01:00
Infiltration rate (1/h)		0.45	00:00-24:00
Daily DHW demand per person (l/day·person)			28

Single-family townhouse

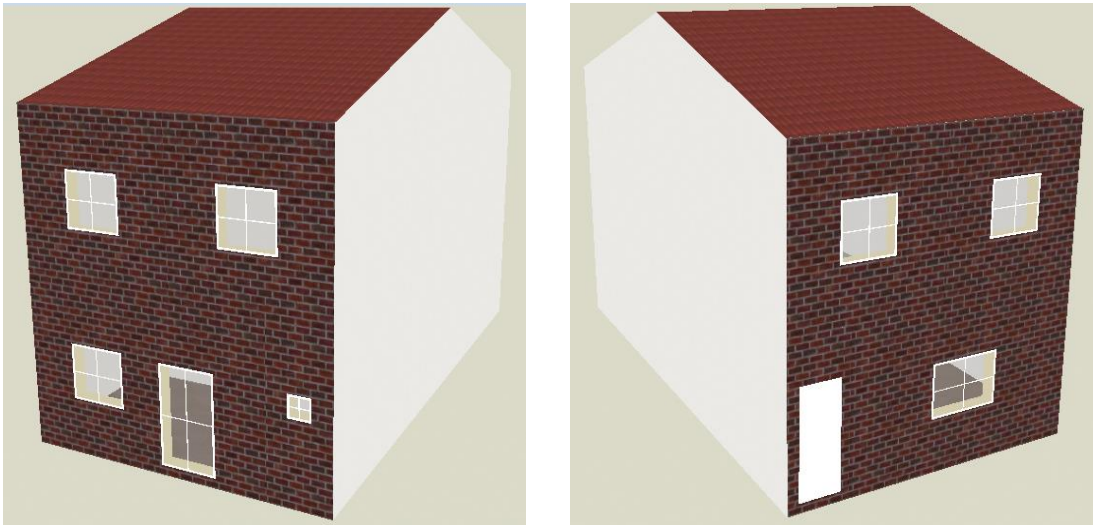

Small apartment block

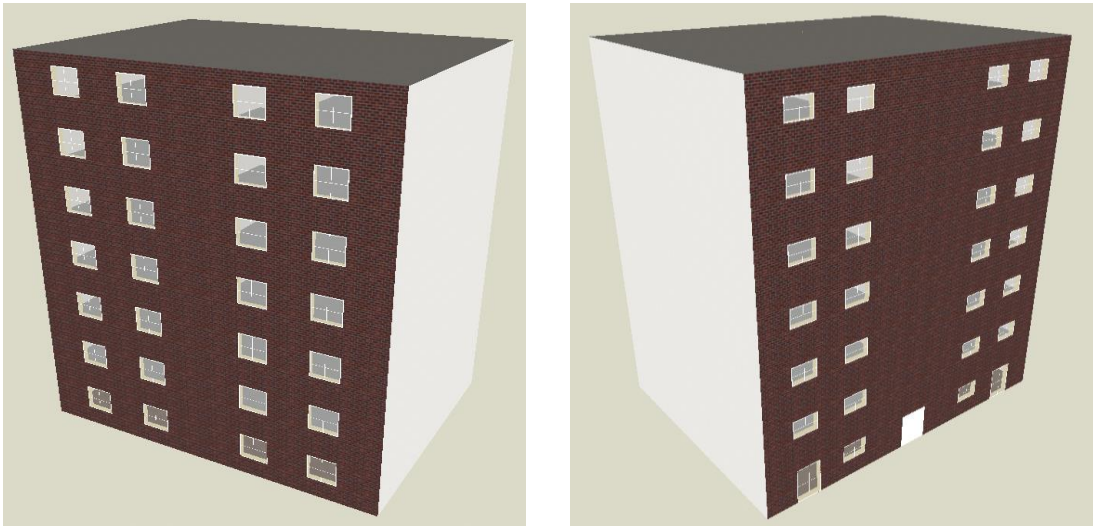

Medium/large apartment block

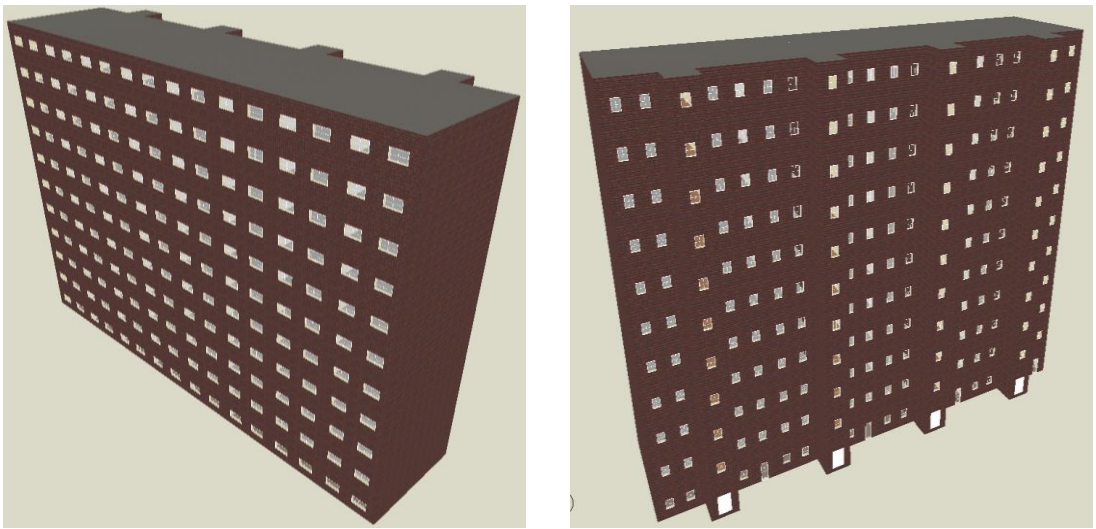

Figure 2.2 3D view of the buildings' south (left) and north façades (right).

2.3 Set of energy demands for residential buildings

To accurately simulate polygeneration systems, it is crucial to estimate detailed demand profiles for the building under study. Energy demand refers to the amount of energy needed to provide energy services for end users. The main residential energy demands include cooling, heating, freshwater, DHW, and electricity. Notably, thermal energy, which encompasses heating, cooling, and DHW, accounts for the largest share of energy consumption, reaching up to 70% in the EU residential sector [79]. This consumption depends on factors such as building thermal characteristics, ventilation, occupancy, and indoor and outdoor climatic conditions [108,109].

Building energy simulation (BES) methods can be employed to estimate energy demand. These models can be categorized as diagnostic or prognostic and based on either laws or data [110]. BES models are mainly prognostic and can be driven by laws or data [111]. Prognostic law-driven models, also known as computational simulations, predict complex systems' behavior based on a set of well-established laws (e.g., energy balance, mass balance, conductivity, heat transfer, etc.). Conversely, prognostic data-driven models use statistical analysis and monitored building data to predict energy demand behavior. A review of the primary research methods, findings, and outcomes concerning total energy use prediction in buildings is available in the literature [112].

In this work, computational simulations (prognostic law-driven models) were used to estimate the thermal demand profiles (heating and cooling). The DesignBuilder simulation tool [113], based on the EnergyPlus engine, was employed to model and simulate the set of buildings. This engine was selected due to its wide international recognition and common use in Spain for issuing energy performance certificates. Although DesignBuilder has proven to be more accurate in estimating building demand by providing a better-detailed building envelope, the tool TRansient SYstem Simulation (TRNSYS) [114] is more suitable for cases requiring energy system simulations, as it integrates the building and energy facility within the same interface. Therefore, we also used the TRNSYS multi-zone building simulation environment, known as TRNBuild, to estimate the heating and cooling demands. The 3D model was developed using the Google SketchUp [115] tool and imported into TRNSYS with the Trnsys3d plug-in [116].

For electricity, DHW, and freshwater demands, prognostic data-driven models were employed to estimate demand profiles. These models detect patterns in the data and accurately predict energy consumption using statistical analysis. A high-resolution stochastic model created by the Centre for Renewable Energy Systems Technology (CREST) was used to produce an electrical demand curve [117]. To estimate the DHW demand, a realistic daily time-dependent simulation

was conducted utilizing the DHWcalc software, designed for the IEA-SHC Task 26, which can create authentic DHW profiles for European countries in various time increments [118]. The STochastic REsidential wAter end-use Model (STREAM), developed and validated by Cominola et al. [119], was used for generating synthetic high-resolution time series of residential freshwater usage at the end-use level.

Energy demand patterns were estimated for an entire year using a 1-hour time step, while the yearly consumption was determined through an integration period of one year (from 0 to 8,760 hours). Specifically, the findings concerning the total amount of each demand for a single-family townhouse in Almería, which served as our base case, can be found summarized in Table 2.4. The electricity, DHW, and freshwater demands are based on the methodologies used to derive them. However, the thermal demands are divided by the software utilized for their estimation.

Table 2.4 Yearly demands for a single-family townhouse, Almería.

Parameter	**Value**	
	DesignBuilder	**TRNSYS**
Freshwater demand [m3/y]	110	
Electricity demand [kWh/y]	3,866	
DHW demand [kWh/y]	2,090	
Cooling demand [kWh/y]	1,526	1,450
Heating demand [kWh/y]	866	941

2.4 Thermal comfort analysis

A thermal comfort analysis can help identify any inefficiencies or poor design in a building's heating, ventilation, and air conditioning (HVAC) system. Understanding the thermal comfort within a building can lead to better decision-making regarding its design and operation, which may include adjustments to insulation, window glazing, or HVAC system sizing and operation. Moreover, BECs have specific requirements that can be assessed using a thermal comfort analysis, helping to ensure compliance and avoid fines or penalties. Achieving a comfortable thermal environment can also improve occupant satisfaction, leading to higher productivity and perceptions of the building. According to ASHRAE 55 [120], thermal comfort is achieved when the occupants' satisfaction level is over 80%.

In this doctoral thesis, a thermal comfort analysis was utilized to validate the thermal requirements of buildings. A built-in subroutine within TRNBuild was used to assess occupants' thermal comfort in a building. This model is developed according to the International Standard Organization (ISO) 7730 standard [121],

described in detail by Fanger [122]. The main calculation procedure establishes two thermal comfort indexes: the Predicted Mean Vote (PMV) and the Predicted Percentage of Dissatisfied (PPD). PMV represents the average thermal sensation experienced by a large group of people exposed to a specific environment, while PPD accounts for the satisfaction level of these occupants.

2.5 Closure

This chapter provided a comprehensive overview of the key input data employed to model the polygeneration systems for residential buildings studied in this Ph.D. thesis. Specifically, the data that were collected and/or obtained include: i) climatic information for each location under consideration, ii) dimensions of the building constructions, iii) details on building envelope and usage, and iv) energy demands for the residences, which encompass electricity, heating, cooling, DHW, and freshwater consumption.

Although five climate zones were analyzed (Paper I), three cities were chosen for the simulation studies. Almería and Valencia were selected due to their specific locations along the Mediterranean coast, characterized by different heating and cooling requirements and water scarcity issues. Zaragoza, on the other hand, was chosen due to its inland position in an arid region, which results in a more severe climate without the issue of freshwater scarcity. It is important to note that Almería was used in all simulations; therefore, this city was explained in detail in this chapter.

In terms of building types (Paper I), an analysis of the Spanish building stock was conducted, and geometric models of representative constructions were developed. Three building types were modeled: a single-family townhouse, a small apartment block, and a medium/large apartment block. The simulations mainly focused on the single-family townhouse, as it represented the smallest application. Nevertheless, to broaden the scope of understanding, the final polygeneration system was designed for a medium/large apartment block.

Building types were modeled following the specifications established in the BEC for each climate zone. Thus, different thermal transmittances were considered for the envelope elements (façades, floors, roofs, and openings) based on the BECs and respective climate zones (Paper I). For this study, we utilized the most recent energy code available during the research period, assuming that the building complies with the highest energy efficiency standards.

Accurate simulation of polygeneration systems requires detailed demand profiles for the building under investigation (Papers I and II). We employed methodologies from the literature based on statistical analysis to estimate electricity, DHW, and freshwater demand profiles. On the other hand, the thermal energy demands (heating and cooling) were calculated using computational

simulations. Two highly regarded software programs were used for estimating building thermal demands.

DesignBuilder software was utilized as it offers greater detail in modeling building envelope elements, such as thermal bridges and fenestrations, leading to more precise estimations of thermal building demands (Paper I). However, as the goal of this study was to simulate polygeneration systems for residential buildings, DesignBuilder was later replaced with TRNSYS simulation studio. TRNSYS is better suited for coupling an integrated energy system to a building, as it simulates both within a single interface. This approach enables real-time interaction between the structure and the system, generating more accurate results (Paper II).

Additionally, a thermal comfort analysis was conducted on the building (Papers II and III). Such an analysis can help identify inefficiencies or inadequate design, as well as determine the size and operational control of the building's HVAC system. Providing a comfortable thermal environment can also improve occupant satisfaction, increase productivity, and ensure compliance with BECs. Thermal comfort was assessed for both the initial building condition without a system installed (Paper II) and following the installation of the polygeneration unit (Paper III).

3 Polygeneration Systems

In this chapter, we present the layout, operation, and control strategy of each polygeneration system developed (Papers III, IV, V, and VI). The initial three system designs were applied to a single-family townhouse, while the fourth was designed for a medium/large apartment block. All polygeneration systems used climate data from cities in Spain and were intended to fulfill residential needs for electricity, heating, cooling, DHW, and freshwater. These systems were broken down into several interconnected subsystems, such as solar loops and power circuits, to ensure the proper functioning of the entire system. The control strategy aimed to maximize the use of thermal and electrical energy produced while minimizing energy losses.

In this Ph.D. thesis, four increasingly complex system layouts were designed and simulated. The first layout (Paper III) features a grid-connected plant with PVT collectors, a reverse osmosis device, and a desiccant air conditioning. The second layout (Paper IV) builds upon the first by disconnecting from the grid and integrating a lead-acid battery and regulator unit to manage the electrical energy produced by the PVT field. The third system (Paper V) extends the first layout by adding PV panels and a biomass boiler for operational flexibility and optimizing PVT collectors' usage. Finally, the fourth layout (Paper VI) evaluates additional technologies, such as thermoelectric generators, heat pumps, single-effect absorption chillers, and multi-effect distillation, as the building size increased. It is important to note that PVT collectors were used for power and heat production in all proposed layouts.

Due to its user-friendly graphical interface, exceptional flexibility, and ability to conduct detailed analyses, the TRaNsient System Simulation (TRNSYS, version 18) software was employed for designing and simulating the dynamic interactions between buildings and polygeneration plants. TRNSYS can process hourly climate data, ensuring a high degree of accuracy in comparison to real-world data. It calculates temperatures, mass flow rates, and thermal and electrical power profiles for all system components based on the inputs. Thus, the operation and control strategy of the system can be optimized by analyzing instantaneous or aggregated data over any selected period, such as hours, days, weeks, months, or years.

The software features a modular structure, allowing each system component to be modeled using subroutines, or types, found in its libraries. Types can be categorized as either built-in components (including collectors, boilers, tanks, pumps, valves, etc.) or user-defined components (such as schedulers, controllers, calculators, etc.). Built-in components have been validated against experimental and/or manufacturer performance data, ensuring highly reliable simulations. Additionally, some components like heat pumps and absorption chillers adopt a data lookup method based on manufacturer data, inherently

validating the model. The mathematical model for the built-in library components can be found in the TRNSYS component mathematical reference.

3.1 System layout with PVT, RO, and DAC

The first system features a grid-connected facility with PVT collectors, a RO unit, and a DAC, to cover all demands of a single-family townhouse located in Almería and Valencia. Electricity generated can either be used on-site or supplied to the grid. On the other hand, to address fluctuations caused by solar radiation intermittence, heat is stored in a TES and employed for space heating and DHW requirements. PVT collectors were selected due to their capacity to simultaneously produce both power and heat. A highly efficient power-driven RO desalting technology was chosen for this system. A RO device, while meeting the building's freshwater needs, also supplies water to the TES for DHW provision. On the other hand, a thermally-driven DAC, ideal for small-scale applications, serves as a space cooling system. Additional elements, such as pumps, pipes, and heat sinks, are also incorporated into the system. Figure 3.1 displays the layout of the first developed polygeneration system.

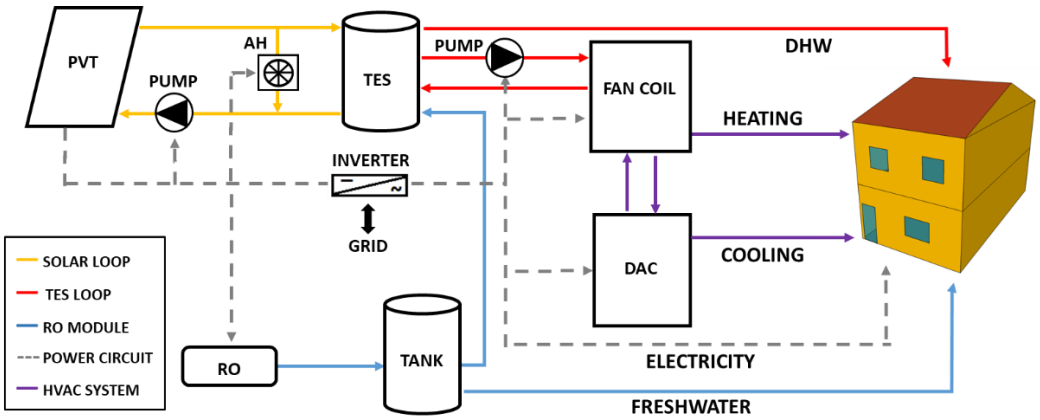

Figure 3.1 First polygeneration system layout.

The solar thermal energy produced heats the solar collector fluid (SCF) as it circulates through the PVT collectors. An air heater (AH) cools the SCF down to avoid damage from overheating when there is low thermal demand from users and high solar energy availability. The TES consists of a hot storage tank with a heat exchanger; it supplies both the HVAC system and the DHW simultaneously. The hot water from the TES is sent to the heating coil or DAC regenerator, depending on whether the user needs heating during winter or cooling during summer, respectively. For DHW, a tempering valve blends hot water from the TES with freshwater from the desalinated water tank.

The electricity demand encompasses both the building's power consumption and the system's power load. The PVT collector's power can be self-consumed, purchased, and sold back to the utility. The grid works as a backup due to the intermittent nature of the solar collectors and the non-simultaneity between production and consumption [75]. A net metering billing arrangement was considered. Under this policy, credits for the excess electricity generated and feed back into the grid can be used within the next 12 months, resulting in an annual near-zero energy balance for the electricity demand. A RO module was simulated as a forcing function of power load and freshwater flow instead of creating a new model type. The desalinated water is sent to a storage tank to meet freshwater needs.

3.2 System layout with PVT, RO, DAC, and EES

The second layout is based on the previous one by disconnecting from the grid and incorporating a lead-acid battery and regulator unit to manage the electrical energy produced by the PVT field. This layout was proposed to address a gap in the literature concerning the analysis of off-grid polygeneration plants with battery storage for residential buildings. A polygeneration unit to cover all demands of a single-family townhouse located in Almería was developed. Figure 3.2 presents the components, loops, and control strategy for the second polygeneration system. Similar to the first layout, the heat produced by the PVT collectors are used for space heating and cooling during winter and summer, respectively, and DHW throughout the year. Conversely, the electrical energy produced is exclusively self-consumed or storage by the single-family townhouse, as this system is not connected to the grid. The selection for electricity storage was lead-acid batteries, which are the most commonly used type.

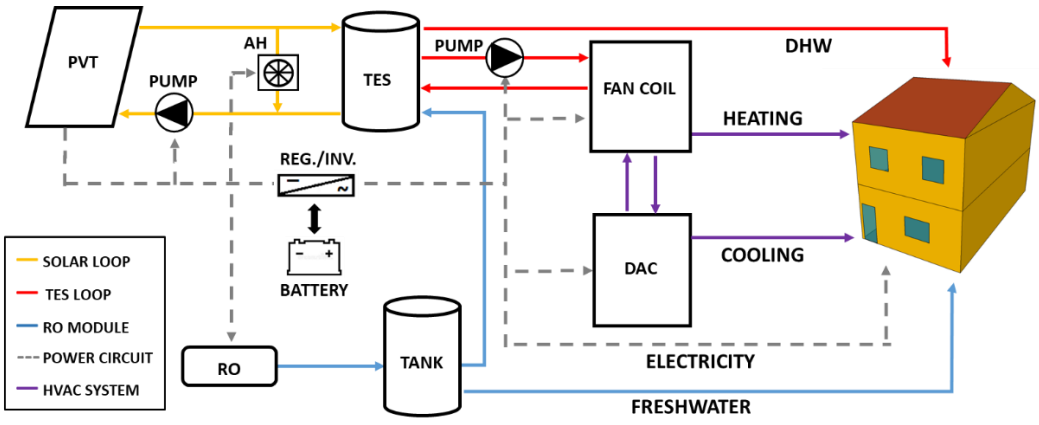

Figure 3.2 Second polygeneration system layout.

The PVT collector's power is sent to a new regulator/inverter for monitoring the battery state of charge (SOC). The inverter converts DC power to an AC output signal waveform [123] and delivers it to the load. The regulator distributes DC power between the solar array and the battery. If the battery is fully charged, surplus energy is dumped. Additionally, the regulator monitors the SOC of a lead-acid storage battery to prevent overcharging or deep discharging. Although batteries for such facilities are often costly and require considerable maintenance [124], they can be economically competitive for remote dwellings due to the higher expenses and distribution losses associated with grid connections [125,126].

3.3 System layout with PVT, PV, BB, RO, and DAC

The third system (Figure 3.3) enhances the first layout by offering greater operational flexibility and more stable demand provision. A polygeneration plant to cover all demands of a single-family townhouse located in Almería was simulated. In this configuration, PVT collectors' usage is optimized with the addition of PV panels for power generation and a biomass boiler (BB) for heat production. When the PVT collectors cannot meet the building's power and heat needs, the PV panels and the BB activate to provide the necessary support. Furthermore, a primary TES is used to mitigate the intermittence of solar radiation, working as a preheater for the BB. The BB supplies the HVAC system and a secondary TES, which ensures the on-demand provision of DHW.

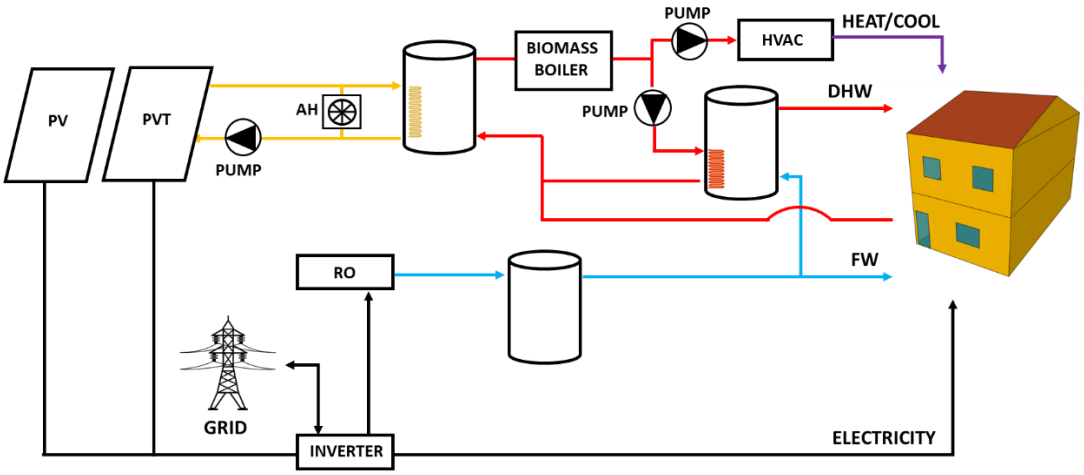

Figure 3.3 Third polygeneration system layout.

In this system, power can be self-consumed, purchased, or sold back to the grid. The grid behaves as a backup due to the non-simultaneity between generation and demand [75]. A net billing policy is implemented, wherein the electricity fed into the grid is valued at a different rate than the electricity withdrawn from the grid. The exported electricity receives payment at a predetermined rate, which is 80% of the purchase price.

3.4 System layout with PVT, PV, BB, TEG, RO/MED, and HP/SEAC

In the fourth layout, the main novelty is the analysis of four different structures of a polygeneration scheme to cover all demands of a medium/large apartment block (80 dwellings) located in Almería, Valencia, and Zaragoza, as seen in Figure 3.4. Different options to produce cooling and desalinated water were checked to find their best integration (whose flows are marked as dashed lines). These technologies were introduced here due to the increase in the building's size. Every combination differs in using a single-effect absorption chiller (SEAC) or a heat pump (HP) for cooling and a membrane technique (RO) or distillation (MED) for water desalination.

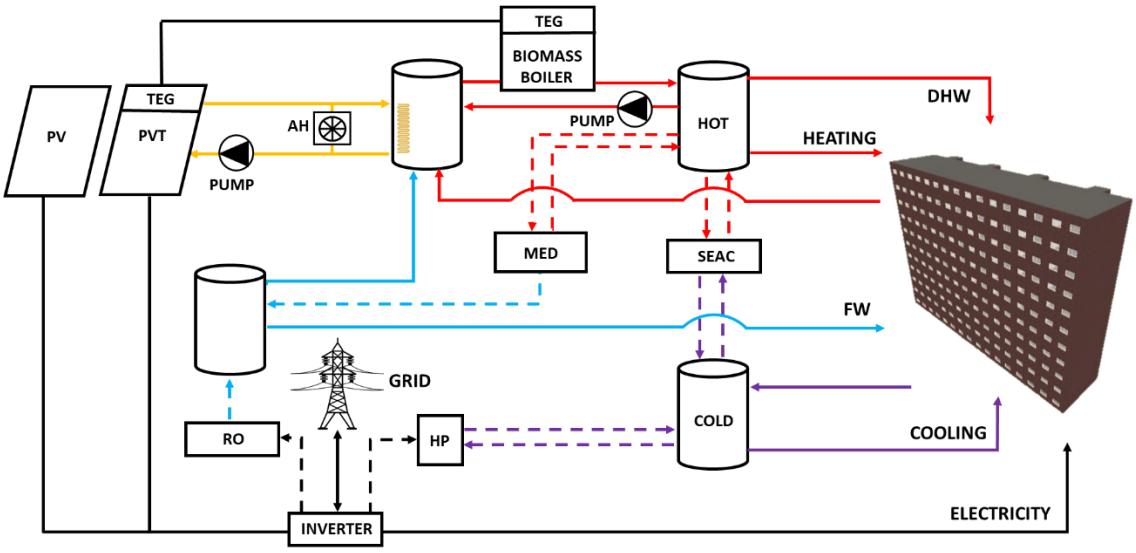

Figure 3.4 Fourth polygeneration system layout.

The solar loop consists of PVT collectors, a solar TES (1), and a heat sink to avoid overheating. PVT collectors, PV panels, and TEGs, installed on the PVT field and the BB, produce electricity. TEG is a small-sized technology suitable for building applications; however, the impact of the electricity supplied by them was

nearly negligible. This on-grid system is based on a yearly net electricity balance. Moreover, it presumes a net billing policy, taking into account different rates for purchasing electricity from, or selling it back to, the grid. The selling back electricity corresponds to 40% of the purchasing price. The solar TES (1) preheats the water fed to the BB. The BB keeps the temperature of the hot water TES (2) stable for activating the cooling or desalinated technologies. The hot water TES (2) supplies DHW, which is covered by a mixture of freshwater, and space heating for the building.

The main difference between the configurations analyzed is the production of cooling and desalinated water. Table 3.1 shows the four combinations analyzed for the polygeneration system depending on the chosen technology. They may require either heat, which will come from the hot water TES (2), or electricity. For cooling, a SEAC or an HP was tested. A cold water TES (3) was used to avoid system start-ups and shutdowns while meeting the space cooling demand. A RO or MED was proposed for seawater desalination.

Table 3.1 Configurations analyzed in the polygeneration scheme.

Service	**A**	**B**	**C**	**D**
Electricity	PVT + PV + TEG			
Heating & DHW	PVT + BB			
Cooling	HP	HP	SEAC	SEAC
Freshwater	MED	RO	RO	MED

In any case, the final design of each option is different in terms of the number of PV panels and PVT collectors, BB power, HP/SEAC capacity, and the size of the hot and cold water TES. Moreover, the BB setpoint and the start-up of the thermally activated technologies (MED, SEAC) may differ slightly depending on the overall integration scheme.

3.5 Closure

In this section, we outlined the design, functioning, and control approach for four increasingly sophisticated polygeneration systems (Papers III, IV, V, and VI). To ensure the optimal performance of a polygeneration facility, it is essential to synchronize all supply and demand aspects. In particular, when dealing with renewable-based polygeneration systems, they must accommodate fluctuating seasonal loads while managing intermittent RES.

The first layout (Paper III) features an innovative, grid-connected solar-driven polygeneration system, primarily composed of PVT collectors, RO, and DAC.

This system was designed to fulfill the requirements of a single-family townhouse in Almería and Valencia. The proposed unit demonstrated its potential for replication in other cities and introduced the small-scale desiccant cooling technology into residential sector polygeneration systems.

The second layout (Paper IV) builds upon the first by disconnecting from the grid and integrating a lead-acid battery and regulator unit to manage the electrical energy produced by the PVT field. The developed system was specifically designed for Almería and used to meet the demands of a single-family townhouse. This system extends the application of the first design to isolated areas as it is disconnected from the grid.

The third system (Paper V) incorporates into the first design PV panels and a biomass boiler to enhance operational flexibility and optimize the use of PVT collectors. The facility meets the demands of a single-family townhouse, which is also situated in Almería. The outcome of this configuration is the size selection of PV panels and PVT collectors in the solar field to satisfy the building's demand, with additional support provided by the BB. Although PVT collectors present higher overall performance than PV panels, as they simultaneously generate power and heat, they may not always be the optimal solution. Hence, by introducing PV panels and a BB to support power and heat production, more efficient use of the PVT collector is achieved.

The fourth layout (Paper VI) evaluates additional technologies, such as TEG, HP, SEAC, and MED by comparing four designs of an on-grid solar-based polygeneration system for meeting the demands of a medium/large apartment block in three different locations in Spain. This facility was applied in two similar sites on the Mediterranean coast (Almería and Valencia) and a more continental climate (Zaragoza). It is essential to highlight that the main consequence of these configurations is the proper selection of desalination and cooling technologies, driven by either power or heat, for larger building applications. For instance, if heat is used to fulfill a demand that can be satisfied by an electrical device with lower specific energy consumption and reduced investment costs, then thermal integration might not be justified.

All systems were designed and simulated using TRNSYS, a modular software that enables each system to be modeled with built-in or custom components (types). Built-in components rely on manufacturer technical data or information from commercially available equipment. Conversely, custom components are programmed to ensure proper system functioning and perform the majority of the analysis. These types might not be available in the TRNSYS built-in library or may execute a specific routine. The Engineering Equation Solver (EES) [127] software was employed to model new types, such as for RO, MED, and TEG. However, due to the slow calculation speed observed when integrating EES and TRNSYS, a simplified version of the RO and MED technologies was integrated into the TRNSYS studio, based on their steady-state condition with fixed

performance parameters. For TEG, a basic model developed in the EES software was implemented in the PVT collectors and the BB types to estimate power generation.

Finally, TRNSYS can process hourly climate data and allow the integration of the building type with all other system components, resulting in highly accurate simulations compared to real-world data. The simulation includes numerous additional components essential for processing the results, such as calculators, integrators, and plotters. As a result, the system's operation and control strategy can be optimized by analyzing instantaneous or aggregated data over any selected period, such as hours, days, weeks, months, or years.

Although TRNSYS offers several advantages, it also has a few disadvantages to consider. The software is complex and requires a significant amount of time and effort to become proficient in its usage. Users need to have a good understanding of system modeling and simulation techniques to effectively utilize the software. Another drawback of TRNSYS is its limited availability of pre-built components. It may not have specific components required for unique or specialized simulations. In such cases, users may need to develop custom components, which can be time-consuming and technically challenging. Lastly, since it is a specialized tool, users might encounter challenges in finding comprehensive documentation or assistance in troubleshooting issues they may encounter while working with the software.

4 Design Improvement

Polygeneration systems are seen as an interesting option to decrease greenhouse gas emissions and economic costs. To create more efficient, sustainable, and cost-effective energy systems, design improvement practices must be used. Systematic design approaches can help achieve these benefits by giving to designers tools to identify suitable technologies for an energy system that meets efficiency, sustainability, and economic goals [128]. These methods offer guidance in assessing the feasibility of several technologies based on design decisions and constraints before the energy system is built. Finally, by evaluating performance criteria, the most advantageous alternatives can be refined and optimized.

Designing polygeneration systems for residential buildings is challenging due to the wide variety of technology options and significant daily and yearly fluctuations in energy demand and prices [129]. Additional factors that add complexity include: i) the intermittency of RES, ii) the non-simultaneous nature of production and consumption, and iii) the incorporation of energy storage, either electrical and/or thermal, which allows for decoupling production from consumption. Design techniques employed in polygeneration systems for residential buildings effectively address these complex energy systems systematically to achieve optimal results under specific conditions [32].

In this chapter, design improvement techniques will be discussed. It is important to note that if modeling is not accurate, simulation and design improvement outcomes will be unrealistic and unhelpful. Furthermore, when designing polygeneration systems, two critical aspects must be addressed: the facility's synthesis (which includes the integrated technologies and their respective capacities) and the operational strategy (such as energy flow rates, electricity trade, etc.) [130]. Therefore, in this work, we carefully modeled the previously developed energy systems and focused on maximizing the design by improving one or more key performance indicators (KPI) associated with energy, environmental, and economic factors.

4.1 Energy model

Energy analysis is based on primary energy saving (PES). PES refers to the reduction in the amount of primary energy sources that need to be used, typically as a result of improved energy efficiency or the use of RES. Primary energy sources include fossil fuels like coal, natural gas, and oil, as well as renewable sources such as solar, wind, and hydropower. These are used to generate secondary energy sources such as electricity and fuels. So, in essence, primary energy saving is about reducing the total amount of primary energy sources

needed to meet our energy demands, which in turn can help to reduce greenhouse gas emissions, save money, and conserve natural resources.

In this work, the energy performance of the proposed system (PS) was compared with a suitable reference system (RS). The PS considers the demand unattended to by RES and the RS supposes all demands produced by conventional technologies based on fossil fuels. The RS consists of a combination of commonly used technologies, such as an electric cooling system (ECS) with a coefficient of performance (COP) of 2.6 and a natural gas boiler (GB) with a thermal efficiency of 0.92 [100]. Additionally, the Spanish electric grid efficiency of 0.42 was taken from the Spanish resolution published by the Institute for Energy Diversification and Saving (IDAE) [131]. The PES and its ratio (PES_R) are calculated as shown in Equations (1) and (2):

$$PES = PE_{RS} - PE_{PS} \quad (1)$$

$$PES_R = \frac{PES}{PE_{RS}} \quad (2)$$

where PE_{RS} and PE_{PS} are, respectively, the energy consumption in the reference and proposed systems.

4.2 Environmental model

Environmental benefits were estimated by the carbon dioxide saving (ΔCO_2). It refers to the reduction in the amount of CO_2 emissions being released into the atmosphere. This reduction can be achieved through various means, such as implementing energy efficiency measures, transitioning to RES, using cleaner fuels, improving waste management techniques, and implementing carbon capture and storage technologies, among others. The concept is crucial in the context of climate change, as carbon dioxide is one of the main greenhouse gases contributing to global warming. By reducing CO_2 emissions, we can help to mitigate the impacts of climate change.

To perform the environmental analysis, the assumptions were a Spanish emission factor for natural gas of 0.25 $kgCO_2/kWh$ [131] and, according to the Spanish Electricity Network (REE), an emission factor associated with electricity generation of 0.19 $kgCO_2/kWh$ [132]. The ΔCO_2 and its ratio (ΔCO_{2R}) are displayed in Equations (3) and (4):

$$\Delta CO_2 = CO_{2,RS} - CO_{2,PS} \quad (3)$$

$$\Delta CO_{2R} = \frac{CO_2}{CO_{2,RS}} \quad (4)$$

where $CO_{2,RS}$ and $CO_{2,PS}$ are, respectively, the carbon dioxide produced by the reference and proposed systems.

4.3 Economic model

In this section, a detailed economic analysis is presented to assess the economic feasibility of the polygeneration plants. Simple payback (SPB) was selected as its key performance indicator. SPB, also known as the payback period, is a basic investment technique used to determine the amount of time it will take to recoup the cost of an investment. It is calculated by dividing the initial investment cost by the annual net cash inflows generated by the project.

In this study, the SPB was obtained as the ratio of the PS total investment (TI) and the annual saving (AS) based on the economic profits of the PS concerning the RS, as shown in Equations (5) and (6):

$$SPB = \frac{TI_{PS}}{AS_{PS}} \quad (5)$$

$$AS_{PS} = OC_{RS} - OC_{PS} \quad (6)$$

where OC_{RS} and OC_{PS} are the operating cost in the reference and proposed systems, respectively.

The operating cost of all components was estimated. In the RS, the utility provides electricity, natural gas, and tap water [133,134]. On the other hand, in the PS, a net billing policy was applied as it allows energy consumers who generate their own electricity from RES to feed the excess energy they produce back into the grid. The electricity exchanged with the grid in the developed on-grid polygeneration systems was valued at different rates to evaluate different scenarios. For the biomass boiler operation, pellets with a fixed lower heating value (LHV) set to 5.2 kWh/kg and a combustion efficiency of 0.85 was considered [37]. Additionally, freshwater can be powered-driven by the national grid, thus electricity consumption aggregates its demand, or thermally-driven, in that case, a desalting system specific energy consumption (SEC_R) of 4 kWh/m^3 was assumed [134]. The yearly operating costs also include a percentage of the investment required for each central technology as a maintenance cost.

Cost functions were introduced to calculate the capital costs of the PS. A percentage of the capital cost can be assumed for the cost of all other components required in the system (pipes, valves, controllers, etc.). A lifetime of a minimum of 20 years for the entire system was assumed, except for the inverter and the RO unit, for which 10 years was considered [135,136]. These investment and installation costs for each technology were taken from the literature and are compiled in Table 4.1.

Table 4.1 Main economic parameters.

Item	Parameter	Value	Unit(s)	Ref.
PV	Inv. & OM	1000, 1	€/kW_p, %/y	[137]
PVT	Inv. & OM	200, 2	€/m^2, %/y	[138]
TES	Investment	495+808·V(m^3)	€	[24]
Inverter	Investment	180	€/kW	[139]
Pumps	Inv. & OM	419+0.03*Q-2.16·10^{-8}·Q^2, 0.5	€, %/y	[140]
BB	Inv. & OM	282, 1	€/kW_{th},%/y	[37,141]
HP	Inv. & OM	350, 0.5	€/kW_{cl}, %/y	[137,142]
SEAC	Inv. & OM	600, 0.2	€/kW_{cl}, %/y	[138,142]
MED	Inv. & OM	1500, 0.5	€/(m^3/d), %/y	[72]
RO	Inv. & OM	800, 1.5	€/(m^3/d), %/y	[143]
DAC	Investment	1090	€/kW_{th}	[144,145]
Electricity (buy)	Price	Variable	€/kWh	[133]
Electricity (sell)	Price	Variable	€/kWh	[133]
Natural gas	Price	0.07	€/kWh	[133]
Biomass pellets	Price	0.052	€/kWh	[146]
Tap water	Price	2.0	€/m^3	[134]

4.4 Sensitivity analysis

Sensitivity analysis is a beneficial tool for exploring how systems react to distinct inputs and scenarios. It is a detailed analysis where the system's parameters are varied to determine the effects of that variation on the system's outcome. Observing how the system's behavior changes in response to parameter variations can offer valuable insights that assist in decision-making, improving performance, or understanding potential risks. In the context of polygeneration systems, sensitivity analysis is used to determine their

performance as a function of the main design variables and/or boundary conditions, while all other parameters are kept fixed.

This doctoral thesis conducted a parametric study to investigate the systems' best setup. The main criteria for achieving a satisfactory system configuration involve ensuring the proper system operation and maximizing performance parameters. The chosen key performance indicators were demand coverage, PES, CO_2 saving, and SPB. Therefore, an iterative method was implemented, focusing on the variation of specific system design parameters or externalities (the price of utilities) to investigate the response of the KPIs.

One of the primary design parameters of a solar-based polygeneration system is the solar field area, which affects energy production. The area of PVT collectors significantly influences the output of thermal and electrical energy, so this factor was used to assess the performance of the polygeneration plants. A similar approach was used with other relevant parameters to determine setpoint temperatures and/or capacities for some components, with an emphasis on selecting the lowest feasible temperature and power levels to minimize energy losses and/or initial investment costs. Additionally, the effect of external factors, including buying and/or selling prices of electricity, natural gas, and biomass, were assessed to comprehend the economic performance trends under several energy cost scenarios.

4.5 System Optimization

Many designers rely on previously described parametric studies to enhance the performance of polygeneration systems. However, these studies usually yield only partial improvement and require substantial labor hours. In a parametric study, all variables except one are held constant, and an attempt is made to optimize the objective function concerning this non-fixed variable. This process is iteratively repeated by modifying other variables. Nonetheless, each time a variable is changed, all other variables usually become sub-optimal and thus require readjustment. This manual method is highly time-intensive and often infeasible for more than two or three independent variables. Therefore, in designing complex systems, which involve many independent variables, numerical optimization is the only practical method for achieving optimization.

Optimization is a powerful instrument in engineering used to identify the optimal value of a system's parameter. It is employed to search for solutions that satisfy an objective function (such as total cost, environmental impact, or thermodynamic efficiency), which can be either minimized or maximized [6]. These numerical methods use iterative computational algorithms to progressively refine the solution until an optimal outcome is achieved. In the context of building and energy system design, numerical optimization techniques are primarily applied to properly size the components and improve resource utilization, to

maximize energy, environmental, or economic benefits. In particular, by using optimization, energy savings between 7% and 32% can be achieved depending on the building location [147].

In this work, we utilized the GenOPT package [148] for the optimization process. GenOpt, a generic optimization program, has been developed to efficiently identify independent variables that improve the performance of energy systems. It is designed for optimization problems where the objective function is computed through a simulation program, specifically for the optimization of building energy consumption or operational costs. Therefore, it is a powerful tool for solving real-world challenges. GenOpt performs optimization of a user-supplied objective function, using a user-selected algorithm. Every optimization algorithm comes with its unique strengths and weaknesses, and the choice of an algorithm often relies on the specific context of the problem, including the nature of the objective function, constraints, and the scale of the problem. As a user of optimization, it is important to have an understanding of these approaches to accurately select and apply the most suitable approach for the problem at hand.

GenOpt incorporates algorithms based on the Generalized Pattern Search (GPS) method [147], which is particularly useful when dealing with complex, nonlinear, or non-differentiable optimization problems where traditional methods may not apply. The Hooke-Jeeves [149] algorithm, which is an example of the GPS method, was applied to address the optimization of the polygeneration systems developed in the previous chapter. It creates a series of iterates, or points within the search space, and at each iterate, a set of directions (the pattern) is searched for improvement. The pattern is designed to ensure a certain degree of progress toward the optimal solution in each iteration, considering the algorithm parameters are set accurately. Following each search, the algorithm adjusts the pattern based on the results and continues the search. This cycle continues until a termination criterion is met, such as a maximum number of iterations or a target accuracy level.

The structure of this algorithm avoids the achievement of local minimum points and uses a dynamic simulation for approximating the objective function. Thus, the TRNOPT type, available in TRNSYS's built-in library, was employed to integrate the optimization algorithm with the dynamic simulation model. This optimization method provides the optimum value in a relatively low number of iterations. The optimization of the polygeneration systems was performed to identify the optimal design parameters that enhance the energy, environmental, and economic efficiency of the systems. Thus, the optimization process embraced PES, ΔCO_2, and SBP as objective functions. Conversely, the solar field (characterized by PVT and PV areas) and thermal and electric storage (represented by thermal tank and battery capacities) were identified as the variables to be optimized.

4.6 Closure

In this chapter, we explored the key performance indicators and the design improvement techniques applied to polygeneration systems. They are used to determine the technologies, component capacities, and operational approaches for energy systems simulated under different conditions. In this study, the findings highlight the advantages of this procedure by presenting the optimal setups achieved for each previously established residential polygeneration system (Table 4.2). Considering the challenge of meeting five demands at 100% for a specific residential building, the optimal configuration for each location, based on the mix of chosen technologies, leads to a unique final design characterized by specific KPIs.

Sensitivity analysis was employed to identify the optimal system configuration by investigating the impact of critical design parameters on the KPIs. It. Specifically, the best configuration is achieved when the KPIs reach their maximum. Paper III presented an ideal system configuration for Almería comprising a 27.2 m^2 PVT field and a TES setpoint of 55 °C, while for Valencia, it included a 32 m^2 PVT field and a TES setpoint of 57 °C. Although both cities are located along the Spanish Mediterranean coast, the variation in results is explained by their differing climatic conditions. Valencia, for instance, has less annual horizontal global solar radiation and a higher thermal demand for heating (1,828 kWh/yr) and cooling (1,567 kWh/yr) compared to Almería.

In Paper V, a sensitivity analysis was carried out to define the optimal design parameters for the PS. The results revealed that the optimal setup was a TES setpoint of 49 °C and a BB setpoint and capacity of 51 °C and 12 kW, respectively. The KPI used in this analysis was the demand coverage, intending to satisfy 100% of all residential needs. Additionally, the same study included a sensitivity analysis to investigate the effects of electricity purchasing and selling prices, as well as natural gas prices, on the economic performance of this system. Higher electricity costs, both for buying and selling, proved to be financially beneficial. It increases both the RS operational cost and the PS economic savings, as it enhances the revenue from sold-back electricity. Conversely, the cost of natural gas was not significantly influential on the system's profitability since its use is limited to the RS for heating and DHW demands.

In Paper VI, the impact of external factors on the polygeneration plant was also investigated. A sensitivity analysis was conducted on the system configurations for each location, varying the biomass and electricity purchase prices. An increase in the cost of biomass decreases the economic feasibility of the systems, as they incorporate a BB, the only technology influenced by this resource. Conversely, an increase in electricity price enhances the systems' economic benefits, as they are capable of producing their own electricity and selling excess power back to the utility. Therefore, the financial results are

strongly dependent on the current prices of electricity and fuels, with future trends likely to enhance the economic KPI of these schemes.

An optimization model was developed to optimize the design of residential energy systems. We used the GenOpt optimization program to iteratively call upon TRNSYS and assess the specified objective function, subject to various technical and physical constraints. The GPS optimization method, performed by GenOPT, is ideal for problems where the objective function is either costly or challenging to evaluate, or where its derivatives are either unavailable or unreliable. However, similar to all optimization techniques, it does not guarantee the identification of the global optimum, especially in problems with several local optima. Therefore, the effectiveness and success of the optimization are significantly influenced by the formulation of the objective function.

In Paper IV, we conducted a comprehensive optimization, taking into account both the PES and ΔCO_2 as objective functions. In terms of design parameters, the number of PVT collectors and batteries was optimized with the main goal of achieving a self-sufficient, off-grid system setup. The optimal number of PVT collectors was established as 30, limited by the size of the building roof. Regarding the lead-acid battery, the optimal value was determined to be 22 batteries, as electricity trading with the grid was not permitted.

In Paper V, the optimization process considered primary design variables like PVT collectors, PV panels, and both types of TES (solar and hot water loops). The SPB economic index was used as the objective function. The optimal SPB of 20.68 years was achieved with the following configuration: 9 PVT collectors, 25 PV panels, and a primary and secondary TES volume of 1.35 m^3 and 0.25 m^3, respectively. However, due to the economy of scale criterion, this configuration is not economically viable unless a capital investment subsidy is added into the equation and the SPB value is significantly reduced.

It is important to note that although the SPB period is easy to calculate and understand, it has certain limitations. It fails to consider factors such as the time value of money, the risk associated with future cash flows, and any benefits that occur beyond the payback period. Consequently, it is common to use additional financial measures like net present value (NPV) or internal rate of return (IRR) in conjunction with the SPB period to obtain a more comprehensive assessment of an investment's profitability. Moreover, it is possible to estimate the levelized cost (LCO) of each demand to evaluate their feasibility in comparison to the utility.

Concerning CO_2 saving, it overlooks emissions generated during the entire lifespan of the proposed installations. To address this limitation, a life cycle assessment (LCA) can be employed as an alternative index to investigate the environmental impact associated with the construction and transportation of materials used in each technology, including the dismantling phase after installation. These metrics, which are discussed in Paper VI to enhance the

environmental and economic analysis, were calculated by another coauthor and are not further explored in this thesis.

Table 4.2 Residential polygeneration systems results.

Layout	Location	Design Variable									Demand Coverage					KPI		
		PVT (m^2)	PV (m^2)	BB (kW)	TEG (kW)	TES1 (m^3)	TES2 (m^3)	TES3 (m^3)	HP/SEAC (kW)	Battery (kWh)	Power (%)	Heat (%)	Cool (%)	DHW (%)	Water (%)	PES_R (%)	$\Delta CO_{2,R}$ (%)	SPB (yr)
1.1	Almería	27.2				2.72					104.1	87.01	97.98	96.05	100	98.62	97.17	
1.2	Valencia	32				3.2					105.7	87.31	97.9	90.15	100	97.57	95.04	
2	Almería	48				4.8				48.4	100	102	105.1	99.83	100	99.88	99.88	
3	Almería	14.4	48.25	12		1.35	0.25				347.2	108	111.3	99.95	100	100	100	20.68
4.A.1	Almería	288	405.3	300	1.20	10	10	5	120		99.7	100	101.9	100	100	64	72	16.06
4.A.2	Valencia	304	405.3	300	1.23	10	10	5	80		100.3	100	103.1	100	100	64.8	74.6	39.84
4.A.3	Zaragoza	480	579	500	2.00	15	12	5	80		100.7	100	101.7	100	100	68.3	77.8	13.72
4.B.1	Almería	96	617.6	100	0.40	7	5	7	100		102.3	100	99.7	100	100	64.6	72.6	6.09
4.B.2	Valencia	112	617.6	100	0.44	7	5	7	70		102.1	100	99.9	100	100	65.4	75	6.14
4.B.3	Zaragoza	144	829.9	300	0.92	10	8	5	70		100.2	100	101.2	100	100	68.3	77.8	6.39
4.C.1	Almería	224	521.1	300	1.06	10	10	7	150		102.2	100	98.9	100	100	65.1	73.3	10.74
4.C.2	Valencia	224	521.1	300	1.07	10	10	7	105		101.5	100	100.7	100	100	65.8	75.5	9.82
4.C.3	Zaragoza	320	714.1	500	1.67	15	15	7	100		100.5	100	99.8	100	100	68.5	78.1	9.39
4.D.1	Almería	256	405.3	300	1.13	12	12	10	170		101.5	100	99.5	100	100	64.5	72.8	43.38
4.D.2	Valencia	256	405.3	300	1.13	12	12	10	140		101.1	100	102	100	100	65.2	75.1	37.56
4.D.3	Zaragoza	320	627.3	500	1.67	18	18	10	140		101.1	100	101.9	100	100	68.2	77.9	21.01

5 Conclusion

In this chapter, this doctoral thesis is concluded by presenting a summary of the main findings of the work, the contributions achieved, as well as suggestions for potential future research, encompassing critical aspects associated with the investigated systems.

5.1 Synthesis

This thesis addresses the complex challenge of designing and optimizing small-scale polygeneration systems for residential buildings, incorporating renewable energy technologies alongside thermal and electric energy storage. Energy, environmental, and economic aspects are the leading objectives, considering the significant limitations set by physical factors and legal regulations. More specifically, in this research work five has addressed five critical topics, which are:

1. The suitable way to estimate a generic pattern for all main energy demands (electricity, heating, cooling, DHW, and freshwater) required by a residential building in Spain (Chapter 2).
2. The introduction of a grid-connected solar-based polygeneration system primarily composed of PVT collectors, RO, and an innovative small-scale desiccant cooling technology to meet the demands of a single-family townhouse in Spain (Chapters 3 and 4).
3. The analysis of the integration of thermal and electric components, especially thermal energy storage and batteries in a polygeneration system suitable for isolated residential buildings (Chapters 3 and 4).
4. The investigation of the optimal design and economic feasibility of a small-scale residential energy system integrating PVT collectors, PV panels, and a biomass boiler. Although PVT collectors can produce simultaneously power and heat, they may not always be the optimal solution (Chapters 3 and 4).
5. The evaluation of additional technologies, such as TEG, HP, SEAC, and MED integrated into an on-grid solar-based polygeneration system for meeting the demands of a medium/large apartment block in three different locations in Spain (Chapters 3 and 4).

Additionally, the comprehensive research scope included: i) a state-of-the-art investigation of the various themes encompassed within this study (Chapter 1); ii) an in-depth comprehension of the representative buildings, energy regulations, and climate zones specific to Spain (Chapter 2); iii) a detailed review of technical, economic, and environmental data related to the technologies and energy resources considered throughout the thesis (Chapter 1); and iv) a custom optimization model designed for enhancing small-scale polygeneration systems

for residential buildings (Chapter 4). A more exhaustive explanation of the topics covered throughout the thesis is presented below.

Chapter 1 showed the state-of-the-art review of various elements explored in this doctoral thesis. It presented an overview of the use of polygeneration systems for residential buildings as an appropriate solution to enhance energy efficiency, while also reducing economic expenses and environmental damage in the residential sector. Additionally, the research gap addressed by this study was outlined, emphasizing its significance in the design of polygeneration systems as a tool to mitigate climate change. The chapter ends by defining the objectives and structure of the thesis.

Chapter 2 introduced a detailed approach for calculating the energy demands of residential buildings. The hourly time series derived from this method were utilized as input data for the simulation and optimization of polygeneration systems. An extensive analysis, based on building types, energy codes, and climate zones, was conducted to generate energy demand profiles for residential buildings. Besides, it highlighted the importance of selecting the suitable method to calculate each hourly energy demand, which includes electricity, heating, cooling, DHW, and freshwater.

Chapter 3 focused on the simulation of grid-connected and standalone polygeneration systems for residential buildings, presenting an increasing level of complexity concerning the integration of different technologies. A detailed overview of the layouts, considering all the technologies studied in the thesis, was presented. It demonstrated the benefits of polygeneration systems, highlighting the feasibility of integrating innovative and consolidated RES-based technologies to enhance energy efficiency and diminish environmental burden. Besides, Moreover, it analyzed the cost-effectiveness of energy supply systems for residential buildings connected to the electric grid. Throughout this study, interesting insights regarding thermal and electric integration were found, especially for cooling and desalting technologies.

Chapter 4 presented the techniques employed to address the design improvement of these energy systems. Optimization was performed to achieve the most effective layout for residential polygeneration systems through the integration of various technologies. An extensive explanation of the technical, environmental, and economic parameters of the energy supply technologies for residential buildings was provided. The optimization model was performed including energy, environmental, and economic objective functions, subject to a range of technical and physical constraints like energy balance, equipment efficiency, and installed capacities, among others. Additionally, the impact of external variables was explored through the utility costs.

5.2 Discussions

Concerning energy demands, higher efforts on new policies will be necessary in the coming years to achieve a completely decarbonized building stock (both new and existing) by 2050. To reach this target, the reduction of thermal demand plays a key role, which can be achieved by enhancing the thermal envelope standards set in the building energy codes. As a result, new patterns of energy demand will be needed in the near future to reflect these regulatory enhancements. In this work, the thermal demands were computed using two software tools: DesignBuilder and TRNSYS. The discrepancy between their outputs was relatively minor, with about a 5% difference for cooling and an 8% difference for heating. This assures the reliability of the obtained results. However, for evaluating energy systems integrated into buildings, TRNSYS presents a better choice as it combines both building and system within the same simulation model, ensuring more reliable outcomes.

A polygeneration system seeks the optimal energy integration solution, which can be achieved either through powered or thermally driven technologies. If heat can serve a demand that could be met with an electrical technology that requires lower equivalent consumption and lower investment cost, thermal integration in a polygeneration scheme might not be justified, as power integration becomes more appealing. In this work, suitable RES-based technologies for small-scale applications were selected. The polygeneration systems were implemented in regions with moderate relative humidity and ambient temperature, appropriated for the operation of the desiccant air conditioning. Regions with water scarcity and isolation were also considered as desalination technologies were incorporated into the systems. Note that wind energy was not very abundant in the selected case studies near the coast, therefore micro-wind turbines were not introduced in the RES mix to supply the primary energy to the proposed schemes.

The polygeneration system developed in this study proved to be adaptable for other cities and introduced a solar-assisted desiccant cooling technology for the residential sector. The DAC system showed a satisfactory performance compared to other thermally-driven cooling technologies. TEG devices, integrated with the PVTs and the BB for additional electricity generation, were also tested. However, their contribution was minimal, providing only 1.5% of the generation achieved with the PVs and PVTs, making them a non-essential option in the proposed configurations. Concerning desalting technologies, RO proved to be the best choice due to its higher efficiency, as the thermally-driven devices excessively increased the required solar field compared to the RO alternative.

In this study, it is assumed that the annual savings remain consistent throughout the system's lifespan. In other words, it is assumed that utility costs remain unchanged. The energy tariff could fluctuate year to year due to factors like inflation or periods of energy scarcity. Nevertheless, it is impractical to predict the trends of climate conditions and future prices over such an extended period.

Hence, the cash flow in this study is calculated considering a constant annual cost-saving over the lifespan of the system. Moreover, policies may promote the adoption of integrated systems based on RES and efficient energy management, especially if a subsidy for capital investment is available. Furthermore, the barrier of the economy of scale might be surpassed with the progression of the small-scale market and technologies.

Regarding the reliability of the polygeneration system results, a meaningful comparison with other references is unfortunately unfeasible, given that the configurations analyzed are not equal to other proposals in the field. Despite this constraint, considering the complexity of the simulations conducted, the detailed energy demands, the reduced simulation time step, and the analysis of the internal temperature and power profiles of the schemes, and the obtained KPIs, we believe that the results obtained have substantial reliability.

5.3 Contributions

This thesis gathered significant data concerning residential buildings and small-scale polygeneration systems. This includes i) information about the building types, energy codes, and climate zones of Spain, ii) technical, economic, and environmental data of different energy supply technologies for small-scale applications, and iii) economic aspects associated with different fuels and the electric grid.

An extensive approach was undertaken to assess all requirements of residential buildings, including electricity, heating, cooling, DHW, and freshwater. This highlighted the importance of selecting the right estimation method for each demand to obtain reliable and suitable results for the simulation and optimization of polygeneration systems.

A state-of-the-art technology for small-scale cooling production, known as desiccant cooling, was presented. Consequently, this thesis assessed the application of this technology in residential buildings from energy, environmental, and economic perspectives, finding it feasible, but less profitable, compared to the existing conventional cooling systems.

An in-depth study was conducted on the thermal and electrical integration involved in the design and optimization of polygeneration systems for residential buildings. In particular, electric energy storage is a key technology for providing electrical integration and for achieving higher shares of renewable energy. However, it was demonstrated that although batteries are considered a key technology for standalone systems, the high capacity required may not be profitable for residential applications.

A methodology was followed to optimize the design of polygeneration systems for residential buildings, whether they are connected to the grid or stand-alone. The optimization model incorporated objective functions related to energy, environment, and economics, while considering various physical and technical constraints like energy balance, equipment efficiency, and capacities. The results clearly illustrated that the design process of energy systems can yield more economical and sustainable solutions.

An assessment was conducted to determine the energy cost implications in future scenarios. The findings revealed that inadequate energy pricing could deviate from the intended goals of encouraging decentralized energy generation and reducing CO_2 emissions. The results obtained herein could help policymakers to take suitable decisions aligned to international policies. Accordingly, regulations that promote energy efficiency and greenhouse gas reduction should facilitate the integration of renewable energy technologies. This implies that renewable energy production can be economically competitive, even without subsidies.

5.4 Future perspectives

Along with the development of this doctoral thesis, many future perspectives have emerged. Some of them are detailed below:

- In the pathway to achieve 100% renewable energy systems, it is crucial to incorporate new technologies and energy resources into the design of polygeneration systems, such as fuel cells, hydrogen, synthetic fuels, and others.
- Innovative TRNSYS types are an interesting topic to be included in the polygeneration models. These new types can help incorporate RES-based emerging technologies not yet available in TRNSYS built-in library, aiming to create more sustainable systems.
- Concerning the simulation models, other software like EES, Matlab, and Fluent could be integrated with TRNSYS for a more comprehensive study.
- Experimental research could be carried out to examine the operation and feasibility of these integrated approaches when applied to complex residential buildings.
- A thorough study of future energy regulations and costs' impact on the economic performance of polygeneration systems would be beneficial, as well as an exploration of the availability of public funding.
- A more in-depth economic analysis of electric energy storage in the design of energy systems coupled with medium/large buildings is recommended.

5 Conclusión

En este capítulo, se concluye esta tesis doctoral presentando un resumen de los principales hallazgos del trabajo, las contribuciones logradas, así como sugerencias para posibles investigaciones futuras, abarcando aspectos críticos asociados con los sistemas investigados.

5.1 Síntesis

Esta tesis aborda el desafío complejo de diseñar y optimizar sistemas de poligeneración a pequeña escala para edificios residenciales, incorporando tecnologías de energía renovable junto con almacenamiento de energía térmica y eléctrica. Los aspectos energéticos, ambientales y económicos son los objetivos principales, considerando las importantes limitaciones impuestas por factores físicos y regulaciones legales. Más específicamente, en este trabajo de investigación se han abordado cinco temas críticos, que son:

1. La forma adecuada de estimar un patrón genérico para todas las demandas energéticas principales (electricidad, calefacción, refrigeración, ACS y agua fresca) requeridas por un edificio residencial en España (Capítulo 2).
2. La introducción de un sistema de poligeneración basado en energía solar conectado a la red, compuesto principalmente por colectores PVT, RO y una innovadora tecnología de refrigeración por desecantes a pequeña escala para satisfacer las demandas de una casa unifamiliar en España (Capítulos 3 y 4).
3. El análisis de la integración de componentes térmicos y eléctricos, especialmente almacenamiento de energía térmica y baterías en un sistema de poligeneración adecuado para edificios residenciales aislados (Capítulos 3 y 4).
4. La investigación del diseño óptimo y la viabilidad económica de un sistema de energía residencial a pequeña escala que integra colectores PVT, paneles PV y una caldera de biomasa. Aunque los colectores PVT pueden producir simultáneamente energía y calor, pueden no ser siempre la solución óptima (Capítulos 3 y 4).
5. La evaluación de tecnologías adicionales, como TEG, HP, SEAC y MED integradas en un sistema de poligeneración basado en energía solar conectado a la red para satisfacer las demandas de un bloque de apartamentos de tamaño medio/grande en tres ubicaciones diferentes en España (Capítulos 3 y 4).

Además, el alcance de la investigación integral incluyó: i) una investigación del estado de la técnica de los diversos temas abordados en este estudio (Capítulo 1); ii) una comprensión profunda de los edificios representativos, las

regulaciones energéticas y las zonas climáticas específicas de España (Capítulo 2); iii) una revisión detallada de los datos técnicos, económicos y ambientales relacionados con las tecnologías y los recursos energéticos considerados a lo largo de la tesis (Capítulo 1); y iv) un modelo de optimización personalizado diseñado para mejorar los sistemas de poligeneración a pequeña escala para edificios residenciales (Capítulo 4). A continuación, se presenta una explicación más exhaustiva de los temas tratados a lo largo de la tesis.

El Capítulo 1 mostró una revisión del estado de la técnica de varios elementos explorados en esta tesis doctoral. Presentó una visión general del uso de los sistemas de poligeneración para edificios residenciales como una solución adecuada para mejorar la eficiencia energética, al mismo tiempo que reduce los gastos económicos y el daño ambiental en el sector residencial. Además, se esbozó la brecha de investigación abordada por este estudio, enfatizando su importancia en el diseño de sistemas de poligeneración como herramienta para mitigar el cambio climático. El capítulo termina definiendo los objetivos y la estructura de la tesis.

El Capítulo 2 introdujo un enfoque detallado para calcular las demandas de energía de los edificios residenciales. Las series de tiempo horarias derivadas de este método se utilizaron como datos de entrada para la simulación y optimización de los sistemas de poligeneración. Se realizó un análisis extenso, basado en tipos de edificios, códigos de energía y zonas climáticas, para generar perfiles de demanda de energía para edificios residenciales. Además, destacó la importancia de seleccionar el método adecuado para calcular cada demanda energética horaria, que incluye electricidad, calefacción, refrigeración, ACS y agua fresca.

El Capítulo 3 se centró en la simulación de sistemas de poligeneración conectados a la red y autónomos para edificios residenciales, presentando un nivel creciente de complejidad en relación con la integración de diferentes tecnologías. Se presentó una visión detallada de las disposiciones, teniendo en cuenta todas las tecnologías estudiadas en la tesis. Demostró los beneficios de los sistemas de poligeneración, destacando la viabilidad de integrar tecnologías basadas en RES innovadoras y consolidadas para mejorar la eficiencia energética y disminuir la carga ambiental. Además, analizó la rentabilidad de los sistemas de suministro de energía para edificios residenciales conectados a la red eléctrica. A lo largo de este estudio, se encontraron percepciones interesantes con respecto a la integración térmica y eléctrica, especialmente para tecnologías de enfriamiento y desalinización.

El Capítulo 4 presentó las técnicas empleadas para abordar la mejora del diseño de estos sistemas energéticos. Se realizó una optimización para lograr la disposición más efectiva para los sistemas de poligeneración residenciales a través de la integración de varias tecnologías. Se proporcionó una explicación extensa de los parámetros técnicos, ambientales y económicos de las

tecnologías de suministro de energía para edificios residenciales. El modelo de optimización se realizó incluyendo funciones objetivo energéticas, ambientales y económicas, sujetas a una serie de restricciones técnicas y físicas como el balance energético, la eficiencia del equipo y las capacidades instaladas, entre otros. Además, se exploró el impacto de las variables externas a través de los costos de los servicios públicos.

5.2 Discusiones

En cuanto a las demandas energéticas, se necesitarán mayores esfuerzos en nuevas políticas en los próximos años para lograr un parque de edificios (tanto nuevos como existentes) completamente descarbonizado para 2050. Para alcanzar este objetivo, la reducción de la demanda térmica juega un papel clave, que se puede lograr mejorando los estándares de la envolvente térmica establecidos en los códigos de energía de los edificios. Como resultado, se necesitarán nuevos patrones de demanda de energía en un futuro cercano para reflejar estas mejoras regulatorias. En este trabajo, las demandas térmicas se calcularon utilizando dos programas de software: DesignBuilder y TRNSYS. La discrepancia entre sus resultados fue relativamente pequeña, con una diferencia de alrededor del 5% para la refrigeración y un 8% para la calefacción. Esto garantiza la fiabilidad de los resultados obtenidos. Sin embargo, para evaluar sistemas energéticos integrados en edificios, TRNSYS es una opción superior ya que combina tanto el edificio como el sistema dentro del mismo modelo de simulación, asegurando resultados más fiables.

Un sistema de poligeneración busca la solución óptima de integración energética, que se puede lograr a través de tecnologías impulsadas por energía eléctrica o térmica. Si el calor puede satisfacer una demanda que podría ser cubierta con una tecnología eléctrica que requiere un consumo equivalente menor y un costo de inversión más bajo, la integración térmica en un esquema de poligeneración puede no estar justificada, ya que la integración de energía se vuelve más atractiva. En este trabajo, se seleccionaron tecnologías basadas en RES adecuadas para aplicaciones a pequeña escala. Los sistemas de poligeneración se implementaron en regiones con humedad relativa y temperatura ambiente moderadas, apropiadas para el funcionamiento del aire acondicionado con rueda desecante. También se consideraron regiones con escasez de agua y aisladas de las redes, ya que se incorporaron tecnologías de desalinización en los sistemas. La minieólica no se ha introducido, por lo general dado que en los emplazamientos analizados su recurso era escaso.

El sistema de poligeneración desarrollado en este estudio demostró ser adaptable para otras ciudades e introdujo una tecnología de refrigeración desecante asistida por energía solar para el sector residencial. El sistema DAC mostró un rendimiento satisfactorio en comparación con otras tecnologías de

refrigeración impulsadas térmicamente. También se probaron dispositivos TEG, integrados con los PVT y la BB para generar electricidad adicional. Sin embargo, su contribución fue mínima, proporcionando solo el 1,5% de la generación lograda con los PV y PVT, lo que los hace una opción prescindible en las configuraciones propuestas. En cuanto a las tecnologías de desalinización, la RO demostró ser la mejor opción debido a su mayor eficiencia, ya que los dispositivos impulsados térmicamente aumentaron excesivamente el campo solar requerido en comparación con la alternativa RO, dados sus elevados costes energéticos específicos (térmicos).

En este estudio, se ha supuesto que los ahorros anuales permanecen constantes durante la vida útil del sistema. En otras palabras, se supone que los costes de los servicios públicos permanecen sin cambios. La tarifa energética podría fluctuar de año en año debido a factores como la inflación o períodos de escasez de energía. Sin embargo, es poco práctico predecir las tendencias de las condiciones climáticas y los precios futuros durante un período tan prolongado y tan imprevisible. Por lo tanto, el flujo de efectivo en este estudio se calcula considerando un ahorro de costes anual constante durante la vida útil del sistema. Además, las políticas pueden promover la adopción de sistemas integrados basados en RES y una gestión energética eficiente, especialmente si está disponible una subvención para la inversión de capital. Además, la barrera de la economía de escala podría superarse con el progreso del mercado y la producción masiva de las tecnologías a pequeña escala.

En cuanto a la fiabilidad de los resultados del sistema de poligeneración, lamentablemente no es factible una comparación significativa con otras referencias de la literatura, dado que las configuraciones analizadas no son exactamente idénticas a las propuestas en otros estudios. A pesar de esta limitación, considerando la complejidad de las simulaciones realizadas, las detalladas demandas energéticas, el paso de tiempo de simulación reducido y el análisis de los perfiles de temperatura y potencia internos de los esquemas, así como de los KPI obtenidos, creemos que los resultados obtenidos tienen una fiabilidad muy alta.

5.3 Contribuciones

Esta tesis recopiló datos significativos sobre edificios residenciales y sistemas de poligeneración a pequeña escala. Esto incluye i) información sobre los tipos de edificios, códigos energéticos y zonas climáticas de España, ii) datos técnicos, económicos y ambientales de diferentes tecnologías de suministro de energía para aplicaciones a pequeña escala, y iii) aspectos económicos asociados con diferentes combustibles y la red eléctrica.

Se utilizó un método detallado para evaluar todos los requisitos de los edificios residenciales, incluyendo electricidad, calefacción, refrigeración, agua

caliente sanitaria y agua dulce. Esto resaltó la importancia de seleccionar el método de estimación adecuado para cada demanda con el fin de obtener resultados confiables y adecuados para la simulación y optimización de los sistemas de poligeneración.

Se presentó una tecnología de vanguardia para la producción de refrigeración a pequeña escala, conocida como refrigeración desecante. En consecuencia, esta tesis evaluó la aplicación de esta tecnología en edificios residenciales desde perspectivas energéticas, ambientales y económicas, encontrando que es factible pero menos rentable en comparación con los sistemas convencionales de refrigeración existentes.

Se llevó a cabo un estudio profundo sobre la integración térmica y eléctrica involucrada en el diseño y optimización de los sistemas de poligeneración para edificios residenciales. En particular, el almacenamiento de energía eléctrica es una tecnología clave para proporcionar integración eléctrica y lograr mayores porcentajes de energía renovable. Sin embargo, se demostró que aunque las baterías se consideran una tecnología clave para sistemas autónomos, la alta capacidad requerida puede no ser rentable para aplicaciones residenciales.

Se siguió una metodología para optimizar el diseño de sistemas de poligeneración para edificios residenciales, ya sea que estén conectados a la red o sean independientes. El modelo de optimización incorporó funciones objetivo relacionadas con la energía, el medio ambiente y la economía, considerando diversas restricciones físicas y técnicas como el balance de energía, la eficiencia de los equipos y sus capacidades. Los resultados ilustraron claramente que el proceso de diseño de los sistemas de energía puede generar soluciones más económicas y sostenibles.

Se realizó una evaluación para determinar las implicaciones de los costos energéticos en escenarios futuros. Los hallazgos revelaron que una tarificación energética inadecuada podría desviarse de los objetivos previstos de fomentar la generación descentralizada de energía y reducir las emisiones de CO_2. En este sentido, las regulaciones que fomenten la eficiencia energética y la reducción de gases de efecto invernadero deberían facilitar la integración de tecnologías de energía renovable. Esto implica que la producción de energía renovable puede ser económicamente competitiva, incluso sin subsidios.

5.4 Perspectivas futuras

Durante el desarrollo de esta tesis doctoral, han surgido muchas perspectivas futuras. Algunas de ellas se detallan a continuación:

- En el camino hacia la consecución de sistemas energéticos 100% renovables, es crucial incorporar nuevas tecnologías y recursos

energéticos en el diseño de sistemas de poligeneración, como las pilas de combustible, el hidrógeno, los combustibles sintéticos, entre otros.

- Los ‘types’ innovadores de TRNSYS son un tema interesante para ser incluido en los modelos de poligeneración. Estos nuevos ‘types’ pueden ayudar a incorporar tecnologías emergentes basadas en fuentes renovables aún no disponibles en la biblioteca de TRNSYS, con el objetivo de crear sistemas más sostenibles.
- Respecto a los modelos de simulación, otros programas como EES, Matlab y Fluent podrían integrarse con TRNSYS para un estudio más completo.
- Se podría llevar a cabo una investigación experimental para examinar la operación y factibilidad de estos enfoques integrados cuando se aplican a edificios residenciales complejos.
- Sería beneficioso un estudio minucioso del impacto de las futuras regulaciones y costos de energía en el rendimiento económico de los sistemas de poligeneración, así como una exploración de la disponibilidad de financiamiento público.
- Se recomienda un análisis económico más profundo del almacenamiento de energía eléctrica en el diseño de sistemas energéticos asociados con edificios medianos/grandes.

References

All the references included in this Ph.D. thesis serve as supporting the research conducted. While certain references were specifically gathered for this work, others have been previously cited in the published papers. This combination of newly collected references and previously utilized sources ensures a solid basis for the thesis.

1. Perkins-Kirkpatrick, S.; Green, D. Chapter 2 - Extreme Heat and Climate Change. In *Heat Exposure and Human Health in the Context of Climate Change*; Elsevier, 2023; pp. 5–36 ISBN 978-0-12-819080-7.
2. Borie, M.; Mahony, M.; Obermeister, N.; Hulme, M. Knowing like a Global Expert Organization: Comparative Insights from the IPCC and IPBES. *Global Environmental Change* **2021**, *68*, 102261, doi:10.1016/j.gloenvcha.2021.102261.
3. Saint Akadiri, S.; Alola, A.A.; Akadiri, A.C.; Alola, U.V. Renewable Energy Consumption in EU-28 Countries: Policy toward Pollution Mitigation and Economic Sustainability. *Energy Policy* **2019**, *132*, 803–810, doi:10.1016/j.enpol.2019.06.040.
4. Köhl, M.; Linser, S.; Prins, K.; Talarczyk, A. The EU Climate Package “Fit for 55” - a Double-Edged Sword for Europeans and Their Forests and Timber Industry. *Forest Policy and Economics* **2021**, *132*, 102596, doi:10.1016/j.forpol.2021.102596.
5. Jana, K.; Ray, A.; Majoumerd, M.M.; Assadi, M.; De, S. Polygeneration as a Future Sustainable Energy Solution – A Comprehensive Review. *Applied Energy* **2017**, *202*, 88–111, doi:10.1016/j.apenergy.2017.05.129.
6. Serra, L.M.; Lozano, M.-A.; Ramos, J.; Ensinas, A.V.; Nebra, S.A. Polygeneration and Efficient Use of Natural Resources. *Energy* **2009**, *34*, 575–586, doi:10.1016/j.energy.2008.08.013.
7. Fell, M.J. Energy Services: A Conceptual Review. *Energy Research & Social Science* **2017**, *27*, 129–140, doi:10.1016/j.erss.2017.02.010.
8. Calise, F.; de Notaristefani di Vastogirardi, G.; Dentice d’Accadia, M.; Vicidomini, M. Simulation of Polygeneration Systems. *Energy* **2018**, *163*, 290–337, doi:10.1016/j.energy.2018.08.052.
9. Gimelli, A.; Muccillo, M. Development of a 1 KW Micro-Polygeneration System Fueled by Natural Gas for Single-Family Users. *Energies* **2021**, *14*, 8372, doi:10.3390/en14248372.
10. Khoshgoftar Manesh, M.H.; Mousavi Rabeti, S.A.; Nourpour, M.; Said, Z. Energy, Exergy, Exergoeconomic, and Exergoenvironmental Analysis of an Innovative Solar-Geothermal-Gas Driven Polygeneration System for Combined Power, Hydrogen, Hot Water, and Freshwater Production. *Sustainable Energy Technologies and Assessments* **2022**, *51*, 101861, doi:10.1016/j.seta.2021.101861.
11. International Energy Agency *Energy and Climate Change: World Energy Outlook Special Report*; Paris, 2015;

12. European Commission *Communication from the Commission to the European Parliament, the Council, the European Economic and Social Committee and the Committee of the Regions: An EU Strategy on Heating and Cooling*; Brussels, 2016;
13. United Nations Environment Programme *Global Status Report for Buildings and Construction: Towards a Zero-Emission, Efficient and Resilient Buildings and Construction Sector*; Nairobi, 2020;
14. EUROPEAN COMMISSION *SET-Plan ACTION N°5 - ISSUES PAPER - Develop New Materials and Technologies for Energy Efficiency Solutions for Buildings*; SET Plan Secretariat: Brussels, 2016;
15. European Union *Directive 2002/91/EC of the European Parliament and of the Council of 16 December 2002 on the Energy Performance of Buildings*; 2003; Vol. 001, pp. 65–71.
16. European Union *Directive 2010/31/EU of the European Parliament and of the Council of 19 May 2010 on the Energy Performance of Buildings*; 2010; Vol. 153, pp. 13–35.
17. European Union *Directive 2018/844 of the European Parliament and the Council of 30 May 2018 Amending Directive 2010/31/EU on the Energy Performance of Buildings and Directive 2012/27/EU on Energy Efficiency*; 2018; Vol. 156, pp. 75–91.
18. European Commission *Commission Recommendation (EU) 2016/1318: On Guidelines for the Promotion of Nearly Zero-Energy Buildings and Best Practices to Ensure That, by 2020, All New Buildings Are Nearly Zero-Energy Buildings*; Official Journal of the European Union: Brussels, 2016; p. 12.
19. D'Agostino, D.; Tzeiranaki, S.T.; Zangheri, P.; Bertoldi, P. Assessing Nearly Zero Energy Buildings (NZEBs) Development in Europe. *Energy Strategy Reviews* **2021**, *36*, 100680, doi:10.1016/j.esr.2021.100680.
20. Mazuroski, W.; Berger, J.; Delinchant, B.; Wurtz, F.; Mendes, N. A Technique to Improve the Design of Near-Zero Energy Buildings. *J Braz. Soc. Mech. Sci. Eng.* **2022**, *44*, 228, doi:10.1007/s40430-022-03416-y.
21. Calise, F.; Cappiello, F.L.; Cimmino, L.; Dentice d'Accadia, M.; Vicidomini, M. Dynamic Simulation and Thermoeconomic Analysis of a Hybrid Renewable System Based on PV and Fuel Cell Coupled with Hydrogen Storage. *Energies* **2021**, *14*, 7657, doi:10.3390/en14227657.
22. Buonomano, A.; Calise, F.; Palombo, A.; Vicidomini, M. Energy and Economic Analysis of Geothermal–Solar Trigeneration Systems: A Case Study for a Hotel Building in Ischia. *Applied Energy* **2015**, *138*, 224–241, doi:10.1016/j.apenergy.2014.10.076.
23. Calise, F.; Dentice d'Accadia, M.; Libertini, L.; Quiriti, E.; Vicidomini, M. A Novel Tool for Thermoeconomic Analysis and Optimization of Trigeneration Systems: A Case Study for a Hospital Building in Italy. *Energy* **2017**, *126*, 64–87, doi:10.1016/j.energy.2017.03.010.
24. Calise, F.; Dentice d'Accadia, M.; Figaj, R.D.; Vanoli, L. A Novel Solar-Assisted Heat Pump Driven by Photovoltaic/Thermal Collectors: Dynamic Simulation and Thermoeconomic Optimization. *Energy* **2016**, *95*, 346–366, doi:10.1016/j.energy.2015.11.071.

25. Carotenuto, A.; Figaj, R.D.; Vanoli, L. A Novel Solar-Geothermal District Heating, Cooling and Domestic Hot Water System: Dynamic Simulation and Energy-Economic Analysis. *Energy* **2017**, *141*, 2652–2669, doi:10.1016/j.energy.2017.08.084.
26. Angrisani, G.; Entchev, E.; Roselli, C.; Sasso, M.; Tariello, F.; Yaïci, W. Dynamic Simulation of a Solar Heating and Cooling System for an Office Building Located in Southern Italy. *Applied Thermal Engineering* **2016**, *103*, 377–390, doi:10.1016/j.applthermaleng.2016.04.094.
27. Calise, F. Thermoeconomic Analysis and Optimization of High Efficiency Solar Heating and Cooling Systems for Different Italian School Buildings and Climates. *Energy and Buildings* **2010**, *42*, 992–1003, doi:10.1016/j.enbuild.2010.01.011.
28. Poel, B.; van Cruchten, G.; Balaras, C.A. Energy Performance Assessment of Existing Dwellings. *Energy and Buildings* **2007**, *39*, 393–403, doi:10.1016/j.enbuild.2006.08.008.
29. International Energy Agency *Energy Technology Perspectives 2020*; Paris, 2020;
30. International Energy Agency *World Energy Balances 2020*; Paris, 2020;
31. Masson-Delmotte, V.; Pörtner, H.-O.; Skea, J.; Zhai, P.; Roberts, D.; Shukla, P.R.; Pirani, A.; Pidcock, R.; Chen, Y.; Lonnoy, E.; et al. An IPCC Special Report on the Impacts of Global Warming of 1.5°C above Pre-Industrial Levels and Related Global Greenhouse Gas Emission Pathways, in the Context of Strengthening the Global Response to the Threat of Climate Change, Sustainable Development, and Efforts to Eradicate Poverty.
32. Rong, A.; Su, Y. Polygeneration Systems in Buildings: A Survey on Optimization Approaches. *Energy and Buildings* **2017**, *151*, 439–454, doi:10.1016/j.enbuild.2017.06.077.
33. Calise, F.; Cipollina, A.; Dentice d'Accadia, M.; Piacentino, A. A Novel Renewable Polygeneration System for a Small Mediterranean Volcanic Island for the Combined Production of Energy and Water: Dynamic Simulation and Economic Assessment. *Applied Energy* **2014**, *135*, 675–693, doi:10.1016/j.apenergy.2014.03.064.
34. Calise, F.; Dentice d'Accadia, M.; Piacentino, A. Exergetic and Exergoeconomic Analysis of a Renewable Polygeneration System and Viability Study for Small Isolated Communities. *Energy* **2015**, *92*, 290–307, doi:10.1016/j.energy.2015.03.056.
35. Calise, F.; Macaluso, A.; Piacentino, A.; Vanoli, L. A Novel Hybrid Polygeneration System Supplying Energy and Desalinated Water by Renewable Sources in Pantelleria Island. *Energy* **2017**, *137*, 1086–1106, doi:10.1016/j.energy.2017.03.165.
36. Calise, F.; Cappiello, F.L.; Vicidomini, M.; Petrakopoulou-Robinson, F. Water-Energy Nexus: A Thermoeconomic Analysis of Polygeneration Systems for Small Mediterranean Islands. *Energy Conversion and Management* **2020**, *220*, 113043, doi:10.1016/j.enconman.2020.113043.
37. Mouaky, A.; Rachek, A. Thermodynamic and Thermo-Economic Assessment of a Hybrid Solar/Biomass Polygeneration System under the

Semi-Arid Climate Conditions. *Renewable Energy* **2020**, *156*, 14–30, doi:10.1016/j.renene.2020.04.019.
38. Chen, Q.; Alrowais, R.; Burhan, M.; Ybyraiymkul, D.; Shahzad, M.W.; Li, Y.; Ng, K.C. A Self-Sustainable Solar Desalination System Using Direct Spray Technology. *Energy* **2020**, *205*, 118037, doi:10.1016/j.energy.2020.118037.
39. Alobaid, M.; Hughes, B.; Calautit, J.K.; O'Connor, D.; Heyes, A. A Review of Solar Driven Absorption Cooling with Photovoltaic Thermal Systems. *Renewable and Sustainable Energy Reviews* **2017**, *76*, 728–742, doi:10.1016/j.rser.2017.03.081.
40. Chow, T.T. A Review on Photovoltaic/Thermal Hybrid Solar Technology. *Applied Energy* **2010**, *87*, 365–379, doi:10.1016/j.apenergy.2009.06.037.
41. Zondag, H. Flat-Plate PV-Thermal Collectors and Systems: A Review. *Renewable and Sustainable Energy Reviews* **2008**, *12*, 891–959, doi:10.1016/j.rser.2005.12.012.
42. Calise, F.; Cappiello, F.L.; Dentice d'Accadia, M.; Vicidomini, M. Thermo-Economic Analysis of Hybrid Solar-Geothermal Polygeneration Plants in Different Configurations. *Energies* **2020**, *13*, 2391, doi:10.3390/en13092391.
43. Aneke, M.; Wang, M. Energy Storage Technologies and Real Life Applications – A State of the Art Review. *Applied Energy* **2016**, *179*, 350–377, doi:10.1016/j.apenergy.2016.06.097.
44. Olabi, A.G. Renewable Energy and Energy Storage Systems. *Energy* **2017**, *136*, 1–6, doi:10.1016/j.energy.2017.07.054.
45. Chen, Y.; Liu, Y.; Wang, Y.; Wang, D.; Dong, Y. The Research on Solar Photovoltaic Direct-Driven Air Conditioning System in Hot-Humid Regions. *Procedia Engineering* **2017**, *205*, 1523–1528, doi:10.1016/j.proeng.2017.10.427.
46. Yekini Suberu, M.; Wazir Mustafa, M.; Bashir, N. Energy Storage Systems for Renewable Energy Power Sector Integration and Mitigation of Intermittency. *Renewable and Sustainable Energy Reviews* **2014**, *35*, 499–514, doi:10.1016/j.rser.2014.04.009.
47. Liu, T.; Yang, Z.; Duan, Y.; Hu, S. Techno-Economic Assessment of Hydrogen Integrated into Electrical/Thermal Energy Storage in PV+ Wind System Devoting to High Reliability. *Energy Conversion and Management* **2022**, *268*, 116067, doi:10.1016/j.enconman.2022.116067.
48. Fan, M.; Lu, S. Benefit Analysis and Preliminary Decision-Making of Electrical and Thermal Energy Storage in the Regional Integrated Energy System. *Journal of Energy Storage* **2022**, *55*, 105816, doi:10.1016/j.est.2022.105816.
49. Chen, H.; Cong, T.N.; Yang, W.; Tan, C.; Li, Y.; Ding, Y. Progress in Electrical Energy Storage System: A Critical Review. *Progress in Natural Science* **2009**, *19*, 291–312, doi:10.1016/j.pnsc.2008.07.014.
50. Hazelton, J.; Bruce, A.; MacGill, I. A Review of the Potential Benefits and Risks of Photovoltaic Hybrid Mini-Grid Systems. *Renewable Energy* **2014**, *67*, 222–229, doi:10.1016/j.renene.2013.11.026.
51. Wollny, M.; Tapanlis, S. Hybrid Backup Power Solutions for Unstable Grids. In: 4th European Conference on PV-Hybrids and Mini-Grids.

52. Dekker, J.; Nthontho, M.; Chowdhury, S. Economic Analysis of PV/ Diesel Hybrid Power Systems in Different Climatic Zones of South Africa. *Int J Electr Power Energy Syst* **2012**, *40*, 104–112.
53. Schroeter, A.; Martin, S. Profitable and Affordable Energy Services for Remote Areas in Lao PDR: Private-Public Partnership as Mutual Leverage for Hybrid Village Grids in Areas of the National Grid.; Athens.
54. Wiser, R.; Millstein, D.; Mai, T.; Macknick, J.; Carpenter, A.; Cohen, S.; Cole, W.; Frew, B.; Heath, G. The Environmental and Public Health Benefits of Achieving High Penetrations of Solar Energy in the United States. *Energy* **2016**, *113*, 472–486, doi:10.1016/j.energy.2016.07.068.
55. Zhang, C.; Wei, Y.-L.; Cao, P.-F.; Lin, M.-C. Energy Storage System: Current Studies on Batteries and Power Condition System. *Renewable and Sustainable Energy Reviews* **2018**, *82*, 3091–3106, doi:10.1016/j.rser.2017.10.030.
56. Ge, T.S.; Wang, R.Z.; Xu, Z.Y.; Pan, Q.W.; Du, S.; Chen, X.M.; Ma, T.; Wu, X.N.; Sun, X.L.; Chen, J.F. Solar Heating and Cooling: Present and Future Development. *Renewable Energy* **2018**, *126*, 1126–1140, doi:10.1016/j.renene.2017.06.081.
57. Calise, F. High Temperature Solar Heating and Cooling Systems for Different Mediterranean Climates: Dynamic Simulation and Economic Assessment. *Applied Thermal Engineering* **2012**, *32*, 108–124, doi:10.1016/j.applthermaleng.2011.08.037.
58. Pintanel, M.T.; Martínez-Gracia, A.; Galindo, M.P.; Bayod-Rújula, Á.A.; Uche, J.; Tejero, J.A.; del Amo, A. Analysis of the Experimental Integration of Thermoelectric Generators in Photovoltaic–Thermal Hybrid Panels. *Applied Sciences* **2021**, *11*, 2915, doi:10.3390/app11072915.
59. Børset, M.T.; Wilhelmsen, Ø.; Kjelstrup, S.; Burheim, O.S. Exploring the Potential for Waste Heat Recovery during Metal Casting with Thermoelectric Generators: On-Site Experiments and Mathematical Modeling. *Energy* **2017**, *118*, 865–875, doi:10.1016/j.energy.2016.10.109.
60. Jouhara, H.; Żabnieńska-Góra, A.; Khordehgah, N.; Doraghi, Q.; Ahmad, L.; Norman, L.; Axcell, B.; Wrobel, L.; Dai, S. Thermoelectric Generator (TEG) Technologies and Applications. *International Journal of Thermofluids* **2021**, *9*, 100063, doi:10.1016/j.ijft.2021.100063.
61. Al-Alili, A.; Hwang, Y.; Radermacher, R. Review of Solar Thermal Air Conditioning Technologies. *International Journal of Refrigeration* **2014**, *39*, 4–22, doi:10.1016/j.ijrefrig.2013.11.028.
62. Calise, F.; Palombo, A.; Vanoli, L. Maximization of Primary Energy Savings of Solar Heating and Cooling Systems by Transient Simulations and Computer Design of Experiments. *Applied Energy* **2010**, *87*, 524–540, doi:10.1016/j.apenergy.2009.08.033.
63. Alam, K.C.A.; Saha, B.B.; Akisawa, A. Adsorption Cooling Driven by Solar Collector: A Case Study for Tokyo Solar Data. *Applied Thermal Engineering* **2013**, *50*, 1603–1609, doi:10.1016/j.applthermaleng.2011.09.028.
64. Calise, F.; Dentice d'Accadia, M.; Roselli, C.; Sasso, M.; Tariello, F. Desiccant-Based AHU Interacting with a CPVT Collector: Simulation of

Energy and Environmental Performance. *Solar Energy* **2014**, *103*, 574–594, doi:10.1016/j.solener.2013.11.001.
65. Srikhirin, P.; Aphornratana, S.; Chungpaibulpatana, S. A Review of Absorption Refrigeration Technologies. *Renewable and Sustainable Energy Reviews* **2001**, *5*, 343–372, doi:10.1016/S1364-0321(01)00003-X.
66. Riaz, F.; Qyyum, M.A.; Bokhari, A.; Klemeš, J.J.; Usman, M.; Asim, M.; Awan, M.R.; Imran, M.; Lee, M. Design and Energy Analysis of a Solar Desiccant Evaporative Cooling System with Built-In Daily Energy Storage. *Energies* **2021**, *14*, 2429, doi:10.3390/en14092429.
67. Elmer, T.; Worall, M.; Wu, S.; Riffat, S. An Experimental Study of a Novel Integrated Desiccant Air Conditioning System for Building Applications. *Energy and Buildings* **2016**, *111*, 434–445, doi:10.1016/j.enbuild.2015.11.065.
68. Heidari, A.; Roshandel, R.; Vakiloroaya, V. An Innovative Solar Assisted Desiccant-Based Evaporative Cooling System for Co-Production of Water and Cooling in Hot and Humid Climates. *Energy Conversion and Management* **2019**, *185*, 396–409, doi:10.1016/j.enconman.2019.02.015.
69. Angrisani, G.; Minichiello, F.; Roselli, C.; Sasso, M. Desiccant HVAC System Driven by a Micro-CHP: Experimental Analysis. *Energy and Buildings* **2010**, *42*, 2028–2035, doi:10.1016/j.enbuild.2010.06.011.
70. Lafuenti, I.; Colangelo, G.; Milanese, M.; De Risi, A. New Solutions for the Use of Solar Cooling in Hot and Humid Weather Conditions. *REPQJ* **2012**, 424–430, doi:10.24084/repqj10.334.
71. Jani, D.B.; Mishra, M.; Sahoo, P.K. Solid Desiccant Air Conditioning – A State of the Art Review. *Renewable and Sustainable Energy Reviews* **2016**, *60*, 1451–1469, doi:10.1016/j.rser.2016.03.031.
72. Mata-Torres, C.; Escobar, R.A.; Cardemil, J.M.; Simsek, Y.; Matute, J.A. Solar Polygeneration for Electricity Production and Desalination: Case Studies in Venezuela and Northern Chile. *Renewable Energy* **2017**, *101*, 387–398, doi:10.1016/j.renene.2016.08.068.
73. Ibrar, I.; Yadav, S.; Naji, O.; Alanezi, A.A.; Ghaffour, N.; Déon, S.; Subbiah, S.; Altaee, A. Development in Forward Osmosis-Membrane Distillation Hybrid System for Wastewater Treatment. *Separation and Purification Technology* **2022**, *286*, 120498, doi:10.1016/j.seppur.2022.120498.
74. Ghalavand, Y.; Hatamipour, M.S.; Rahimi, A. A Review on Energy Consumption of Desalination Processes. *Desalination and Water Treatment* **2014**, 1–16, doi:10.1080/19443994.2014.892837.
75. Pina, E.A.; Lozano, M.A.; Serra, L.M. A Multiperiod Multiobjective Framework for the Synthesis of Trigeneration Systems in Tertiary Sector Buildings. *Int J Energy Res* **2019**, er.5006, doi:10.1002/er.5006.
76. Homa, M.; Pałac, A.; Żołądek, M.; Figaj, R. Small-Scale Hybrid and Polygeneration Renewable Energy Systems: Energy Generation and Storage Technologies, Applications, and Analysis Methodology. *Energies* **2022**, *15*, 9152, doi:10.3390/en15239152.
77. European Commission *Communication from the Commission to the European Parliament, the Council, the European Economic and Social*

Committee and the Committee of the Regions: The European Green Deal; Brussels, 2019;
78. Chu, W.; Calise, F.; Duić, N.; Østergaard, P.A.; Vicidomini, M.; Wang, Q. Recent Advances in Technology, Strategy and Application of Sustainable Energy Systems. *Energies* **2020**, *13*, 5229, doi:10.3390/en13195229.
79. Zabalza, I.; Gesteira, L.G.; Uche, J. The Impact of Building Energy Codes Evolution on the Residential Thermal Demand. *J Braz. Soc. Mech. Sci. Eng.* **2022**, *44*, 588, doi:10.1007/s40430-022-03898-w.
80. Gesteira, L.G.; Uche, J.; de Oliveira Rodrigues, L.K. Residential Sector Energy Demand Estimation for a Single-Family Dwelling: Dynamic Simulation and Energy Analysis. *J. Sustain. Dev. Energy Water Environ. Syst.* **2021**, *9*, 1–18, doi:10.13044/j.sdewes.d8.0358.
81. Gesteira, L.; Uche, J. A Novel Polygeneration System Based on a Solar-Assisted Desiccant Cooling System for Residential Buildings: An Energy and Environmental Analysis. *Sustainability* **2022**, *14*, 3449, doi:10.3390/su14063449.
82. Gesteira, L.G.; Uche, J.; Dejo-Oricain, N. A Polygeneration System Based on Desiccant Air Conditioning Coupled with an Electrical Storage. *Sustainability* **2022**, *14*, 15784, doi:10.3390/su142315784.
83. Gesteira, L.G.; Uche, J.; Cappiello, F.L.; Cimmino, L. Thermoeconomic Optimization of a Polygeneration System Based on a Solar-Assisted Desiccant Cooling. *Sustainability* **2023**, *15*, 1516, doi:10.3390/su15021516.
84. Uche, J.; Zabalza, I.; Gesteira, L.G.; Martínez-Gracia, A.; Usón, S. A Sustainable Polygeneration System for a Residential Building. *Applied Sciences* **2022**, *12*, 12992, doi:10.3390/app122412992.
85. Calise, F.; d'Accadia, M.D.; Vicidomini, M. Optimization and Dynamic Analysis of a Novel Polygeneration System Producing Heat, Cool and Fresh Water. *Renewable Energy* **2019**, *143*, 1331–1347, doi:10.1016/j.renene.2019.05.051.
86. El-Emam, R.S.; Dincer, I. Development and Assessment of a Novel Solar Heliostat-Based Multigeneration System. *International Journal of Hydrogen Energy* **2018**, *43*, 2610–2620, doi:10.1016/j.ijhydene.2017.12.026.
87. Rashidi, H.; Khorshidi, J. Exergoeconomic Analysis and Optimization of a Solar Based Multigeneration System Using Multiobjective Differential Evolution Algorithm. *Journal of Cleaner Production* **2018**, *170*, 978–990, doi:10.1016/j.jclepro.2017.09.201.
88. Calise, F.; d'Accadia, M.D.; Macaluso, A.; Piacentino, A.; Vanoli, L. Exergetic and Exergoeconomic Analysis of a Novel Hybrid Solar–Geothermal Polygeneration System Producing Energy and Water. *Energy Conversion and Management* **2016**, *115*, 200–220, doi:10.1016/j.enconman.2016.02.029.
89. Azhar, M.S.; Rizvi, G.; Dincer, I. Integration of Renewable Energy Based Multigeneration System with Desalination. *Desalination* **2017**, *404*, 72–78, doi:10.1016/j.desal.2016.09.034.
90. Jana, K.; De, S. Sustainable Polygeneration Design and Assessment through Combined Thermodynamic, Economic and Environmental Analysis. *Energy* **2015**, *91*, 540–555, doi:10.1016/j.energy.2015.08.062.

91. Leiva-Illanes, R.; Escobar, R.; Cardemil, J.M.; Alarcón-Padilla, D.-C. Thermoeconomic Assessment of a Solar Polygeneration Plant for Electricity, Water, Cooling and Heating in High Direct Normal Irradiation Conditions. *Energy Conversion and Management* **2017**, *151*, 538–552, doi:10.1016/j.enconman.2017.09.002.
92. Calise, F.; Dentice d'Accadia, M.; Piacentino, A. A Novel Solar Trigeneration System Integrating PVT (Photovoltaic/Thermal Collectors) and SW (Seawater) Desalination: Dynamic Simulation and Economic Assessment. *Energy* **2014**, *67*, 129–148, doi:10.1016/j.energy.2013.12.060.
93. Calise, F.; d'Accadia, M.; Piacentino, A.; Vicidomini, M. Thermoeconomic Optimization of a Renewable Polygeneration System Serving a Small Isolated Community. *Energies* **2015**, *8*, 995–1024, doi:10.3390/en8020995.
94. Hogerwaard, J.; Dincer, I.; Naterer, G.F. Solar Energy Based Integrated System for Power Generation, Refrigeration and Desalination. *Applied Thermal Engineering* **2017**, *121*, 1059–1069, doi:10.1016/j.applthermaleng.2017.03.116.
95. Maraver, D.; Uche, J.; Royo, J. Assessment of High Temperature Organic Rankine Cycle Engine for Polygeneration with MED Desalination: A Preliminary Approach. *Energy Conversion and Management* **2012**, *53*, 108–117, doi:10.1016/j.enconman.2011.08.013.
96. Ahmadi, P.; Dincer, I.; Rosen, M.A. Thermoeconomic Multi-Objective Optimization of a Novel Biomass-Based Integrated Energy System. *Energy* **2014**, *68*, 958–970, doi:10.1016/j.energy.2014.01.085.
97. Ahmadi, P.; Dincer, I.; Rosen, M.A. Multi-Objective Optimization of a Novel Solar-Based Multigeneration Energy System. *Solar Energy* **2014**, *108*, 576–591, doi:10.1016/j.solener.2014.07.022.
98. Figaj, R.; Żołądek, M.; Homa, M.; Pałac, A. A Novel Hybrid Polygeneration System Based on Biomass, Wind and Solar Energy for Micro-Scale Isolated Communities. *Energies* **2022**, *15*, 6331, doi:10.3390/en15176331.
99. Luqman, M.; Al-Ansari, T. Thermodynamic Analysis of an Energy-Water-Food (Ewf) Nexus Driven Polygeneration System Applied to Coastal Communities. *Energy Conversion and Management* **2020**, *205*, 112432, doi:10.1016/j.enconman.2019.112432.
100. Spanish Ministry of Development Updating of the Energy Saving Document DB-HE of the Technical Building Code 2019.
101. Aranda-Usón, A.; Ferreira, G.; López-Sabirón, A.M.; Mainar-Toledo, M.D.; Zabalza Bribián, I. Phase Change Material Applications in Buildings: An Environmental Assessment for Some Spanish Climate Severities. *Science of The Total Environment* **2013**, *444*, 16–25, doi:10.1016/j.scitotenv.2012.11.012.
102. Lemos, L.F.L.; Starke, A.R.; Boland, J.; Cardemil, J.M.; Machado, R.D.; Colle, S. Assessment of Solar Radiation Components in Brazil Using the BRL Model. *Renewable Energy* **2017**, *108*, 569–580, doi:10.1016/j.renene.2017.02.077.
103. Spanish National Institute of Statistics *Population and Housing Census*; 2011;

104. Nejat, P.; Jomehzadeh, F.; Taheri, M.M.; Gohari, M.; Abd. Majid, M.Z. A Global Review of Energy Consumption, CO 2 Emissions and Policy in the Residential Sector (with an Overview of the Top Ten CO 2 Emitting Countries). *Renewable and Sustainable Energy Reviews* **2015**, *43*, 843–862, doi:10.1016/j.rser.2014.11.066.
105. Allard, I.; Nair, G.; Olofsson, T. Energy Performance Criteria for Residential Buildings: A Comparison of Finnish, Norwegian, Swedish, and Russian Building Codes. *Energy and Buildings* **2021**, *250*, 111276, doi:10.1016/j.enbuild.2021.111276.
106. Bienvenido-Huertas, D.; Oliveira, M.; Rubio-Bellido, C.; Marín, D. A Comparative Analysis of the International Regulation of Thermal Properties in Building Envelope. *Sustainability* **2019**, *11*, 5574, doi:10.3390/su11205574.
107. Reis, I.F.G.; Figueiredo, A.; Samagaio, A. Modeling the Evolution of Construction Solutions in Residential Buildings' Thermal Comfort. *Applied Sciences* **2021**, *11*, 2427, doi:10.3390/app11052427.
108. Foucquier, A.; Robert, S.; Suard, F.; Stéphan, L.; Jay, A. State of the Art in Building Modelling and Energy Performances Prediction: A Review. *Renewable and Sustainable Energy Reviews* **2013**, *23*, 272–288, doi:10.1016/j.rser.2013.03.004.
109. Murugan, S.; Horák, B. A Review of Micro Combined Heat and Power Systems for Residential Applications. *Renewable and Sustainable Energy Reviews* **2016**, *64*, 144–162, doi:10.1016/j.rser.2016.04.064.
110. *Global Sensitivity Analysis: The Primer*; Saltelli, A., Ed.; John Wiley: Chichester, England ; Hoboken, NJ, 2008; ISBN 978-0-470-05997-5.
111. Coakley, D.; Raftery, P.; Keane, M. A Review of Methods to Match Building Energy Simulation Models to Measured Data. *Renewable and Sustainable Energy Reviews* **2014**, *37*, 123–141, doi:10.1016/j.rser.2014.05.007.
112. Yoshino, H.; Hong, T.; Nord, N. IEA EBC Annex 53: Total Energy Use in Buildings—Analysis and Evaluation Methods. *Energy and Buildings* **2017**, *152*, 124–136, doi:10.1016/j.enbuild.2017.07.038.
113. DesignBuilder Software Ltd DesignBuilder.
114. TRNSYS: A Transient System Simulation Program. Solar Energy Laboratory, University of Wisconsin, Madison, USA, 2006.
115. Google SketchUp Is a Registered Trademark 2009.
116. OpenStudio Plugin for Google SketchUp3D 2009.
117. Richardson, I.; Thomson, M.; Infield, D.; Clifford, C. Domestic Electricity Use: A High-Resolution Energy Demand Model. *Energy and Buildings* **2010**, *42*, 1878–1887, doi:10.1016/j.enbuild.2010.05.023.
118. Jordan, U.; Vajen, K. Tool for the Generation of Domestic Hot Water (DHW) Profiles on a Statistical Basis Version 2.02b (March 2017). 22.
119. Cominola, A.; Giuliani, M.; Castelletti, A.; Rosenberg, D.E.; Abdallah, A.M. Implications of Data Sampling Resolution on Water Use Simulation, End-Use Disaggregation, and Demand Management. *Environmental Modelling & Software* **2018**, *102*, 199–212, doi:10.1016/j.envsoft.2017.11.022.

120. ANSI/ASHRAE Standard 55 *Thermal Environmental Conditions for Human Occupancy*; The Society: New York, 2013;
121. International Organization for Standardization (ISO) ISO 7730:1994, Moderate Thermal Environments – Determination of the PMV and PPD Indices and Specification of the Conditions for Thermal Comfort, ISO Standard, p 26, Geneva, Switzerland 1994.
122. Fanger, P.O. *Thermal Comfort. Analysis and Applications in Environmental Engineering*; Danish Technical Press: Copenhagen, 1970;
123. Havrlík, M.; Libra, M.; Poulek, V.; Kouřím, P. Analysis of Output Signal Distortion of Galvanic Isolation Circuits for Monitoring the Mains Voltage Waveform. *Sensors* **2022**, *22*, 7769, doi:10.3390/s22207769.
124. Gómez Melgar, S.; Sánchez Cordero, A.; Videras Rodríguez, M.; Andújar Márquez, J.M. Matching Energy Consumption and Photovoltaic Production in a Retrofitted Dwelling in Subtropical Climate without a Backup System. *Energies* **2020**, *13*, 6026, doi:10.3390/en13226026.
125. Lubello, P.; Pasqui, M.; Mati, A.; Carcasci, C. Assessment of Hydrogen-Based Long Term Electrical Energy Storage in Residential Energy Systems. *Smart Energy* **2022**, *8*, 100088, doi:10.1016/j.segy.2022.100088.
126. MendezQuezada, V.H.; RivierAbbad, J.; GomezSanRoman, T. Assessment of Energy Distribution Losses for Increasing Penetration of Distributed Generation. *IEEE Trans. Power Syst.* **2006**, *21*, 533–540, doi:10.1109/TPWRS.2006.873115.
127. Klein, S.A.; Alvarado, F.L. Engineering Equation Solver (EES) 2014.
128. Andiappan, V. State-Of-The-Art Review of Mathematical Optimisation Approaches for Synthesis of Energy Systems. *Process Integr Optim Sustain* **2017**, *1*, 165–188, doi:10.1007/s41660-017-0013-2.
129. Tapia-Ahumada, K.; Pérez-Arriaga, I.J.; Moniz, E.J. A Methodology for Understanding the Impacts of Large-Scale Penetration of Micro-Combined Heat and Power. *Energy Policy* **2013**, *61*, 496–512, doi:10.1016/j.enpol.2013.06.010.
130. Wakui, T.; Kawayoshi, H.; Yokoyama, R. Optimal Structural Design of Residential Power and Heat Supply Devices in Consideration of Operational and Capital Recovery Constraints. *Applied Energy* **2016**, *163*, 118–133, doi:10.1016/j.apenergy.2015.10.154.
131. Instituto para la Diversificación y Ahorro de la Energia (IDAE) *CO2 Emission Factors and Primary Energy Coefficients for Different Final Energy Sources Consumed in the Building Sector in Spain*; 2014;
132. Red Eléctrica Española (REE) *CO2 Emissions of Electricity Generation in Spain*; Madrid, Spain, 2021;
133. Pinto, E.S.; Serra, L.M.; Lázaro, A. Optimization of the Design of Polygeneration Systems for the Residential Sector under Different Self-consumption Regulations. *Int J Energy Res* **2020**, *44*, 11248–11273, doi:10.1002/er.5738.
134. Uche, J.; Acevedo, L.; Círez, F.; Usón, S.; Martínez-Gracia, A.; Bayod-Rújula, Á.A. Analysis of a Domestic Trigeneration Scheme with Hybrid Renewable Energy Sources and Desalting Techniques. *Journal of Cleaner Production* **2019**, *212*, 1409–1422, doi:10.1016/j.jclepro.2018.12.006.

135. Calise, F.; Figaj, R.D.; Vanoli, L. A Novel Polygeneration System Integrating Photovoltaic/Thermal Collectors, Solar Assisted Heat Pump, Adsorption Chiller and Electrical Energy Storage: Dynamic and Energy-Economic Analysis. *Energy Conversion and Management* **2017**, *149*, 798–814, doi:10.1016/j.enconman.2017.03.027.
136. Calise, F.; Cappiello, F.L.; Vanoli, R.; Vicidomini, M. Economic Assessment of Renewable Energy Systems Integrating Photovoltaic Panels, Seawater Desalination and Water Storage. *Applied Energy* **2019**, *253*, 113575, doi:10.1016/j.apenergy.2019.113575.
137. Calise, F.; Cappiello, F.L.; Dentice d'Accadia, M.; Petrakopoulou, F.; Vicidomini, M. A Solar-Driven 5th Generation District Heating and Cooling Network with Ground-Source Heat Pumps: A Thermo-Economic Analysis. *Sustainable Cities and Society* **2022**, *76*, 103438, doi:10.1016/j.scs.2021.103438.
138. Calise, F.; Cappiello, F.L.; Dentice d'Accadia, M.; Vicidomini, M. Dynamic Simulation, Energy and Economic Comparison between BIPV and BIPVT Collectors Coupled with Micro-Wind Turbines. *Energy* **2020**, *191*, 116439, doi:10.1016/j.energy.2019.116439.
139. Buonomano, A.; Calise, F.; Dentice d'Accadia; Vicidomini, M. A Hybrid Renewable System Based on Wind and Solar Energy Coupled with an Electrical Storage: Dynamic Simulation and Economic Assessment. **2018**, *155*, 174–189.
140. Buonomano, A.; Calise, F.; Ferruzzi, G.; Vanoli, L. A Novel Renewable Polygeneration System for Hospital Buildings: Design, Simulation and Thermo-Economic Optimization. *Applied Thermal Engineering* **2014**, *67*, 43–60, doi:10.1016/j.applthermaleng.2014.03.008.
141. Instituto para la Diversificación y Ahorro de la Energía (IDAE) *Renewable Energy Plan in Spain 2005-2010*; 2005;
142. Pina, E.A.; Lozano, M.A.; Serra, L.M. Allocation of Economic Costs in Trigeneration Systems at Variable Load Conditions Including Renewable Energy Sources and Thermal Energy Storage. *Energy* **2018**, *151*, 633–646, doi:10.1016/j.energy.2018.03.083.
143. Esrafilian, M.; Ahmadi, R. Energy, Environmental and Economic Assessment of a Polygeneration System of Local Desalination and CCHP. *Desalination* **2019**, *454*, 20–37, doi:10.1016/j.desal.2018.12.004.
144. Angrisani, G.; Roselli, C.; Sasso, M.; Tariello, F. Dynamic Performance Assessment of a Micro-Trigeneration System with a Desiccant-Based Air Handling Unit in Southern Italy Climatic Conditions. *Energy Conversion and Management* **2014**, *80*, 188–201, doi:10.1016/j.enconman.2014.01.028.
145. Angrisani, G.; Roselli, C.; Sasso, M. Experimental Assessment of the Energy Performance of a Hybrid Desiccant Cooling System and Comparison with Other Air-Conditioning Technologies. *Applied Energy* **2015**, *138*, 533–545.
146. Instituto para la Diversificación y Ahorro de la Energía (IDAE) *Biomass Price Report for Thermal Uses*; Madrid, Spain, 2020;
147. Wetter, M.; Wright, J. COMPARISON OF A GENERALIZED PATTERN SEARCH AND A GENETIC ALGORITHM OPTIMIZATION METHOD.

148. Wetter, M. GenOpt - A Generic Optimization Program.; Rio de Janeiro, Brazil, 2001; pp. 601–608.
149. Hooke, R.; Jeeves, T.A. "Direct Search'' Solution of Numerical and Statistical Problems. *J. ACM* **1961**, *8*, 212–229, doi:10.1145/321062.321069.

A. Appendix

The thesis is based on a compilation of manuscripts published in international journals. The impact factors and scope of the corresponding journals are listed below.

I. Journal of the Brazilian Society of Mechanical Sciences and Engineering (ISSN: 1806-3691): Impact Factor: 2.361. JCR category rank: Q3 (Mechanical Engineering).

II. Journal of Sustainable Development of Energy, Water, and Environment Systems (ISSN: 1848-9257): JCI category rank: Q3 (Environmental Sciences).

III. Sustainability (ISSN: 2071-1050): Impact Factor: 3.889. JCR category rank: Q2 (Environmental Sciences).

IV. Sustainability (ISSN: 2071-1050): Impact Factor: 3.889. JCR category rank: Q2 (Environmental Sciences).

V. Sustainability (ISSN: 2071-1050): Impact Factor: 3.889. JCR category rank: Q2 (Environmental Sciences).

VI. Applied Sciences (ISSN: 2076-3417): Impact Factor: 2.838. JCR category rank: Q2: Engineering, Multidisciplinary.

A.1 Paper I

Journal of the Brazilian Society of Mechanical Sciences and Engineering (2022) 44:588
https://doi.org/10.1007/s40430-022-03898-w

TECHNICAL PAPER

The impact of building energy codes evolution on the residential thermal demand

Ignacio Zabalza[1] · Luis Gabriel Gesteira[1] · Javier Uche[1]

Received: 30 June 2022 / Accepted: 31 October 2022

Abstract
The building stock decarbonization by 2050 requires the implementation of an energy transition strategy. Building energy codes must be considered to minimize the energy consumption of the residential sector. This paper aims to evaluate the evolution of the building energy codes of Spain based on energy simulation. A quantitative assessment of the residential thermal demand according to the new energy efficiency requirements introduced in national regulations over the years was performed. Heating, cooling, and domestic hot water demands were assessed for 60 cases modeled in DesignBuilder, combining different building geometric typologies, energy codes, and climate zones. Heating presented the largest contribution to the total energy demand reaching up to 75%. The codes' evolution led to a significant reduction in heating and a slighter decrease in cooling. The results showed an average energy demand improvement of 50% from the first regulatory release to the latest one.

Keywords Energy simulation · Energy efficiency · Building energy codes · Thermal demand · Residential sector

1 Introduction

The residential sector accounts for 28% of global carbon dioxide emissions and 30% of global final energy consumption, figures that rise to 38% and 35%, respectively, if the contribution of the construction industry is also accounted for. In 2019, these percentages presented an energy consumption of 151 EJ and an emission of 10 $GtCO_2$ due to buildings' direct and indirect impact [1, 2]. Moreover, buildings accounted for 57% of final energy consumption and 32% of CO_2 emissions in Africa, 26% of final energy consumption and 24% of CO_2 emissions in Southeast Asia, and 24% and 21% of energy consumption and emissions, respectively, in Central and South America. In Europe, buildings were responsible for 40% of energy consumption and 36% of CO_2 emissions, with similar figures in the USA [3]. Although the building impact varies according to the geographical region considered, its contribution is relevant worldwide.

The decarbonization of the building stock by 2050 requires the development of roadmaps and the implementation of energy transition strategies that include regulatory changes and support for investments in energy efficiency for existing buildings. Therefore, building energy codes (BECs) come out as an essential instrument to reduce building energy consumption, especially if they are mandatory and enforced by the local government [4]. Energy codes use energy standards as the technical basis for specifying how buildings must be constructed or performed in order to save energy effectively, with some variations according to the regional climate [5]. Furthermore, using renewable energy sources, such as solar energy [6] and biomass [7], is another way to move forward decarbonization since they are replenished by nature and emit little to no greenhouse gases.

Focusing on the European level, in 2002, the first Directive on Energy Performance of Buildings was enacted — Directive 2002/91/CE— [8], later modified first by Directive 2010/31/EU [9] and then by Directive (EU) 2018/844 [10]. This Directive led to a progressive tightening of regulations regarding the thermal envelope of buildings in the EU countries. Therefore, all EU countries approved regulatory changes to achieve nearly zero energy buildings (NZEBs) for all-new residential, office, and service buildings by 2020. NZEB is defined as a building with a very high-energy

Technical Editor: Ahmad Arabkoohsar.

✉ Ignacio Zabalza
izabal@unizar.es

[1] CIRCE Research Institute, University of Zaragoza, Calle María de Luna, 5, 50018 Zaragoza, Spain

Published online: 17 November 2022

performance, where a very low-amount of energy required should be covered as much as possible by renewable energy sources [11]. Nevertheless, the design of sustainable buildings is not a simple task, as it must achieve such high levels of performance [12]. Thus, higher efforts on new policies must be made over the next years to reach a building stock (new and existing) decarbonized by 2050. To achieve this goal, thermal demand reduction is a key point, which can be achieved by improving the thermal envelope established on the BECs [13].

Previous studies have analyzed the effect of new BECs on building energy efficiency in different countries, such as India [14], several states of the USA [15], and other comparative studies in neighboring countries with similar climate conditions [16, 17]. In particular, Bianco and Marmori [18] presented a novel bottom-up model, based on the definition of building archetypes to estimate energy consumption evolution in the Italian residential sector according to four different energy efficiency scenarios. Merini et al. (2020) [19] examined the thermal demands in a single reference building by comparing the current regulations of Morocco and Spain in a single climate zone (similar in both countries) using DesignBuilder as a simulation tool. Monzón-Chavarrías et al. [20] used the official national tools to quantify the reduction obtained in demand, energy consumption, and CO_2 emissions by implementing different refurbishment solutions in an old housing block to comply with current Spanish and Portuguese regulations, considering two different climate zones in each country. Gangolells et al. [21] made an energy mapping of the Spanish building stock, analyzing nearly 130,000 energy performance certificates collected from a specific Spanish Region (Catalonia). Additionally, Cerezo-Narváez et al. [22] used the TRNSYS simulation tool to quantify energy savings achieved by upgrading an old single-family house in Andalusia (south of Spain) to the latest national building energy code. Likewise, Gesteira et al. [23] performed a simulation in TRNSYS to estimate the demand of a single-family townhouse located in Almeria, on the Mediterranean coast of Spain, meeting the national BEC requirements.

Other studies have investigated innovative solutions for promoting building energy savings. In this framework, Ebrahimi-Moghadam et al. [24] proposed five types of light shelves as a passive-enhancement method for building energy saving. The results revealed that the light shelves caused an annual average improvement of 18%, 11%, and 7% in the building demand for heating, cooling, and electricity, respectively. Gasparin et al. [25] developed an innovative non-uniform adaptive method to determine the optimal insulation thickness of external walls as thermal insulation can reduce energy consumption associated with heating or cooling in buildings. The method improved in 25% the building's thermal efficiency. Sadripour et al. [26] used a ceiling fan with a central heating system during the winter to save energy inside a building. The effective room temperature increased by 0.35 °C, which could be used to reduce the radiators' temperature, thereby reducing 37% of energy consumption. Vaishnani et al. [27] computationally modeled a cross-ventilation system with asymmetric openings positions to examine the effects of natural ventilation in a wind-driven system. The provision of natural ventilation in buildings is associated with reductions in energy consumption with HVAC systems by the circulation of air within the building, without the help of any mechanical systems.

Over the past years, new BECs have been launched worldwide. They establish minimum energy-efficient design and construction requirements and outline uniform requirements for new buildings as well as additions and renovations. Furthermore, the BECs drive the innovation of new energy-efficient solutions forward. In this work, a significant number of building types, climate zones, and BECs from the last 50 years in Spain were computationally simulated. Despite their importance, to date, previous studies have not assessed the evolution of BECs applied to residential buildings over such a long period. In fact, they considered only regulatory changes in recent years.

This paper aims to propose a procedure based on an energy simulation tool (DesignBuilder) to assess heating, cooling, and domestic hot water thermal demand of residential buildings according to the evolution of the national building energy code requirements. To this end, the following specific objectives are proposed:

- Propose a procedure that can be easily replicated in any country.
- Apply the proposed procedure to a case study (Spain), selecting a comprehensive set of building types and climate zones.
- Model a set of representative buildings using an energy simulation tool commonly used in the architecture field to estimate the demands.
- Analyze the building thermal demands for heating, cooling, and domestic hot water (DHW) broken down by building type, climate zone, and BECs in the last 50 years.
- Assess whether the BECs contribute to achieving thermal demand reduction.

2 Materials and methods

This section describes the procedure proposed to assess the residential thermal demand according to the national BEC evolution. The procedure can be summarized in the following steps:

1. Selecting representative climate zones and climate data.
2. Setting the period to be analyzed and the corresponding BECs.
3. Defining the building clusters.
4. Assigning constructive solutions.
5. Defining the usage profile.
6. Estimating the air renewal rate.
7. Modeling, simulating and analyzing the results.

First, it is necessary to identify the most representative climate zones of the country. The zone selection can be based on criteria such as the area covered or the local population. In case of official climate zoning lack, the Köppen–Geiger [28] climate classification can be used as a reference. This classification sets five climate types subdivided into thirty types depending on outside temperatures, rainfall, and local vegetation. The climate data are based on the synthesis of weather data collected over long periods (usually between 10 and 30 years). The main climate variables of a typical year for each zone can be obtained by a variety of free or paid databases, such as EnergyPlus weather data [29], NOAA's National Centers for Environmental Information (NCEI) climate data [30], and Meteonorm [31]. In general, the energy simulation tools require input temperature, humidity, solar radiation, and wind parameters on an hourly basis for an entire year.

The next step is defining the period to be analyzed and the BECs under effect during this time. It must consider the regulatory updates that directly or indirectly affect the building energy efficiency. BECs cover the building itself, for instance, the walls, floors, ceiling insulation, windows, and air leakage. However, some regulatory changes regarding accessibility, building structure, fire safety, etc., can be ignored during this analysis.

The definition of the representative building stock can be done through the population and home census. Besides, it is possible to find international data hubs, including information about thermal quality, size, age, and type of buildings from different countries [32], such as the ENTRANZE [33] and ODYSSEE [34] databases. The building stock is divided into different typological clusters considering each constructive characteristic: building conditioned surfaces, number of dwellings per building, number of people per dwelling, number of floors, the height of each floor, the orientation of the main façade, the surface area of each element of the thermal envelope (façades, floors, roofs, and openings), etc. It allows the geometric modeling of the representative building of each cluster.

Based on the BECs already selected and the building typology considered, constructive solutions can be assigned to each building. In particular, the main constructive solutions are: materials (layer by layer), thermal transmittance value (U-value) for each element of the building's thermal envelope, window transmittance to solar energy, commonly known as a solar factor (g-value), as well as the window-to-wall ratio on each façade. All these data determine the building's one-dimensional thermal losses. Additionally, to calculate two- or three-dimensional losses, it is necessary to set the linear thermal transmittance value (ψ) of the thermal bridges for each BEC and building type.

The next step is defining the usage profile. It is based on ordinary operating and occupancy conditions. At this point, it is necessary to set the working hours and temperature setpoints for heating and cooling, as well as the internal loads (W/m^2) related to occupancy, lighting, and other equipment. In addition, a daily reference demand (l/day) and an hourly profile for the domestic hot water service must be established. All these data related to the user profile can be obtained from the literature or national standards and regulations.

Another relevant input data for the building energy modeling are the air renewal rate due to ventilation and infiltration. Ventilation is the controlled air renewal to ensure indoor air quality, while infiltration is the uncontrolled air renewal depending on the thermal and pressure gradient between the inside and outside of the building and the air permeability of the opening elements (windows and doors) of the thermal envelope. The air renewal data can be obtained from the literature or national regulations. It is presented as the number of air changes per hour (ach) or airflow (m^3/h or $m^3/h{\cdot}m^2$).

Finally, the total number of simulations can be obtained through the number of building types, BECs, and climate zones. In order to organize the simulation process and the result´s analysis, it is convenient to establish a unique code for each simulation case using a set of alphanumeric characters. Several simulation tools can be chosen to estimate the building thermal demand. Most simulation tools calculate the heating and cooling demands through a heat balance considering:

- Thermal losses or gains through the walls, glazing, roof, floor, and thermal bridges.
- Thermal losses or gains associated with ventilation and infiltration.
- Solar gains through glazing and internal gains due to lighting, equipment, and occupancy.

Different calculation methods [35, 36] and modeling and simulation tools [37–39] have been developed and adopted for building energy modeling (BEM). Although they differ in their engine (data modeling, algorithms, hypothesis, etc.), their results are consistent and reliable even if they present some variations among them. Some authors have widely explained these issues [40–46]. Table 1 presents the main features of the most commonly used energy simulation tools

Table 1 List of energy simulation tools for buildings worldwide

Software	Developer	Country	Overview	Type	Engine	References
EnergyPlus	NREL, various DOE national laboratories, academic institutions, and private firms	US	Modeling energy consumption, lighting, plug and process loads, and water use in buildings, including plant integration with heat balance-based zone simulation, multizone air flow, thermal comfort, and photovoltaic systems	Free	DOE-2 and BLAST	[47, 48]
eQUEST	DOE	US	Detailed comparative analysis of building designs and technologies, including energy cost estimating, daylighting and lighting system control, and automatic implementation of energy efficiency measures	Free	DOE-2	[49, 50]
ECOTECT	Autodesk	US	Visual architectural design and analysis tool covering thermal, energy, lighting, shading, acoustics, and cost aspects	Paid discontinued	Self	[51, 52]
TRNSYS/ TRNBuild	University of Wisconsin	US	Detailed multi-zone building model and components for HVAC systems and renewable energy systems. Building input data entered through a dedicated visual interface (TRNBuild)	Paid	Self	[53, 54]
HEED	University of California	US	Easy to use tool that quickly compares multiple design alternatives with few input data, displaying a wide array of graphic outputs	Free	Self	[55]
SUNREL	NREL	US	Hourly building energy simulation program that aids in designing small energy-efficient buildings	Free discontinued	Self	[56]
HAP	Carrier	US	Designing systems and sizing system components as well as modeling annual energy performance and energy costs	Paid	Self	[57]
ESP-r	University of Strathclyde	Scotland	Modeling heat, air, moisture light, and electrical power flow at user-specified spatial and temporal resolution	Free	Self	[58, 59]
BSIM	University of Aalborg	Denmark	Simulating and calculating thermal indoor climate, energy consumption, daylight conditions, synchronous simulation of moisture and energy transport in constructions and spaces. Calculation of natural ventilation and electrical yield from building integrated photovoltaic systems	Paid	Self	[60, 61]
IDA-ICE	EQUA Simulation AB	Sweden	Detailed and dynamic multi-zone simulation application for the study of indoor thermal climate as well as the energy consumption of the entire building	Paid	Modelica based	[62, 63]
IES-VE	IES	Scotland	Analysis tools for the design and retrofit of buildings. It provides building and system designs, allowing them to be optimized concerning comfort criteria and energy use	Paid	Self	[64, 65]

for buildings worldwide. It also includes references to some studies where these tools have been used.

The thermal demand results obtained for each typology, BEC, and climate zone are analyzed and compared. Considering the size difference among the buildings analyzed, the ratio between the thermal demand and the building area can be used to levelize the results. The breakdown of the thermal balance can also be studied to identify possible improvements for the future.

3 Case study

In this section, the proposed procedure is applied to the case study of Spain, which was selected due to its variety of climate zones and relevant regulatory updates in the past 50 years.

3.1 Climate zones and data

The climate zones were selected from the basic document of energy saving of the Spanish technical building code: DB-HE [66]. In Spain, there are 15 climate zones classified according to winter and summer climate severities, calculated based on degree-day patterns and solar radiation. Winter climate severity is divided into five ranges coded from A to E, being A the lowest and E the highest severity. In comparison, summer climate severity is divided into four ranges, from 1 to 4, the first is the lowest and the fourth is the highest severity [67, 68]. In this work, five cities located in five different climate zones were selected following the criteria of area and population. Additionally, all winter climate severities were included as heating demand is much higher than cooling in the Spanish residential buildings [69].

Therefore, the climate zones selected were Z1 (Almeria—A4), Z2 (Valencia—B3), Z3 (Santander—C1), Z4 (Zaragoza—D3), and Z5 (Burgos—E1). Table 2 shows a description of each climate zone. The hourly climate data were taken from the Meteonorm database for the energy simulation. These data are measured from meteorological stations in each selected city [31]. Furthermore, the average monthly temperature of the tap water for each city was also taken from the Spanish regulation [70] to calculate the domestic hot water demand.

3.2 Time period and BECs

In Spain, the national building energy codes have evolved in the past 50 years. During this period, five new milestones were launched proposing the improvement of the thermal envelope quality. In 1979, the first building standard was approved, reported on the NBE-CT-79 [71], which for the first time limited the heat losses through the building thermal envelope depending on the location. This regulation forced the introduction of minimum thermal insulation in new building envelopes. Twenty-seven years later, the previous building standard was replaced by the Spanish Technical Building Code [72] to comply with the first Directive on Building Energy Performance (Directive 2002/91/CE [8]). The amendments introduced by the Directive 2010/31/EU [9] led to the release of the Basic Document of Energy Saving of the Spanish Technical Building Code in 2013 [73]. In 2019, this document was updated [66], including the new requirements established in the Directive (EU) 2018/844 [10].

This paper considered four of five milestones, neglecting the last update as the BECs chosen were enough to analyze its evolution. Therefore, as shown in Table 3, the BECs were classified as S1 (before 1979), S2 (from 1979 to 2006), S3 (from 2007 to 2013), and S4 (from 2014 to 2019).

3.3 Building clusters and constructive solutions

The typological clusters definition regarding the residential building stock in Spain was based on the data collected from the Population and Housing Census [74]. Three building types were considered, T1 for a single-family semi-detached house, T2 for a small block of flats between party walls, and T3 for a medium/large block of flats. The main geometric characteristics for each case are detailed in Table 4.

The following figures present a 3D view (Fig. 1) and the floor plans (Fig. 2) of the building types considered.

Table 2 Description of the main climate conditions of the selected cities. *Source*: [31, 66, 70]

Zone	Z1	Z2	Z3	Z4	Z5
Location (climate zone)	Almeria (A4)	Valencia (B3)	Santander (C1)	Zaragoza (D3)	Burgos (E1)
Latitude	36°50′ N	39°28′ N	43°27′ N	41°39′ N	42°21′ N
Altitude above sea level (m)	0	8	1	207	861
Annual average outdoor temperature (ºC)	18.4	17.6	14.6	15.2	12.1
Horizontal global solar radiation (kWh/year)	1829	1615	1279	1656	1549
Average annual wind speed (m/s)	4.1	3.1	5	4.5	4.8
Average annual temperature of tap water (ºC)	15.7	14.6	12.8	13.3	10.1

Table 3 Period and national building energy code considered

BEC	S1	S2	S3	S4
Period	Before 1979	1979—2006	2007—2013	2014—2019
Regulation	No energy efficiency requirements	Basic Building Norm: NBE-CT 79 [71]	Technical Building Code: CTE-DB-HE 2006 [72]	Technical Building Code: CTE-DB-HE 2013 [73]

Table 4 Geometric characteristics of the three building types considered

Building type	T1	T2	T3
Type	Single-family semi-detached house	Small block of flats between party walls	Medium/large block of flats
No. of homes	1	12	80
Total number of people	4	48	240
Useful surface per dwelling (m^2)	110	100	70
Total conditioned area (m^2)	110	1200	5600
Total area (m^2)	165	1583	7190
Height per plant (m)	3	3	3
Total volume (m^3)	371.3	4750.2	21,568.8
No. of floors above ground	3 (2 + attic floor)	7 (6 + ground floor)	11 (10 + ground floor)
No. of floors below ground	0	0	0
Total building height (m)	7.5	21	33
No. of bedrooms per home	4	4	2
Orientation	North–South	North–South	North–South
Roof type	Pitched roof	Flat roof	Flat roof
Window-to-wall ratio, north façade (%)	10	10	10
Window-to-wall ratio, south façade (%)	15	15	15
Thermal envelope area (m^2)	178.4	1183.2	6191.2
Compactness[a] (m)	2.08	4.02	3.48
External shades	No	No	No

[a] *Compactness* is the ratio between the volume (m^3) enclosed by the thermal envelope of a building and the sum of the thermal exchange surfaces (m^2) of that envelope in contact with the outside air or the ground. It is expressed in m. The compactness of a building is a design variable that affects heat exchange through the thermal envelope, so the greater the compactness, the lower the heat loss through the envelope

The building types were modeled according to the requirements established in each BEC for each climate zone. As shown in Table 5, different U-values were considered for the thermal envelope elements based on the BECs and climate zones.

Additionally, the thickness of the thermal insulation and the window type for each climate zone was defined depending on the building age. Regarding the doors, only the outside doors were modeled, so for the internal doors, the same composition of the internal partitions was assumed. It is worth noting that the convective coefficients of inside and outside surfaces for each enclosure were calculated through the simulation tool algorithm.

Thermal bridges were also estimated through the linear thermal transmittance (ψi) based on the internal dimensions of the building types. The values of ψ_i were taken from the atlas of thermal bridges of the Spanish Technical Building Code [75] and the user manual of the energy certification software for existing buildings CE3x [76]. Table 6 shows the thermal bridge values according to the BECs.

In this study, the thermal demand of a set of 60 buildings was assessed due to the combination of three building types, four BECs, and five climate zones. Each case was coded using six characters: *TiSjZk*; being *i*, *j*, and *k* numerical values (1, 2, 3, etc.). *T*, *S*, and *Z* correspond to the building types, standards, and climate zones, respectively.

3.4 Usage profile

The usage profile considered is included in the Spanish regulation [66] and consists of the following aspects:

- Heating is available from January to May and from October to December, with a setpoint of 20 °C from 8:00 a.m. to 11:59 p.m., and 17 °C from 0:00 a.m. to 7:59 a.m.

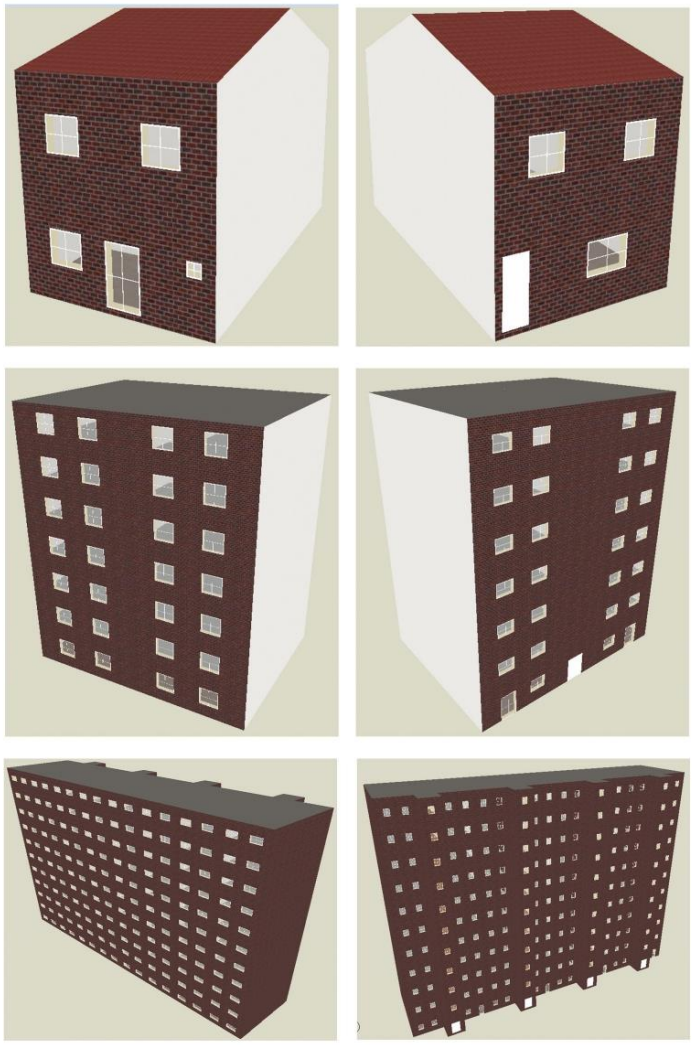

Fig. 1 3D view of the South façade (left) and the North façade (right) of the building types T1 (top), T2 (center), and T3 (bottom)

- Cooling is available from June to September, with a set-point of 25 °C from 4:00 p.m. to 11:59 p.m. and 27 °C from 0:00 a.m. to 7:59 a.m. From 8:00 a.m. to 3:59 p.m., cooling is not available.
- A metabolic rate of 117.21 W/person and an occupancy density of 0.03 people/m^2 resulted in a thermal load per person of 3.51 W/m^2. The hourly distribution on working days is 100% from 0:00 a.m. to 7:59 a.m., 25% from 8:00 a.m. to 3:59 p.m. and 50% from 4:00 p.m. to 11:59 p.m. A 100% occupancy is considered 24 h a day on Saturdays and holidays. 61% of the occupancy load is sensitive, while 39% corresponds to latent load.
- Internal heat gains from equipment and lighting of 4.40 W/m^2 in both cases, according to the following

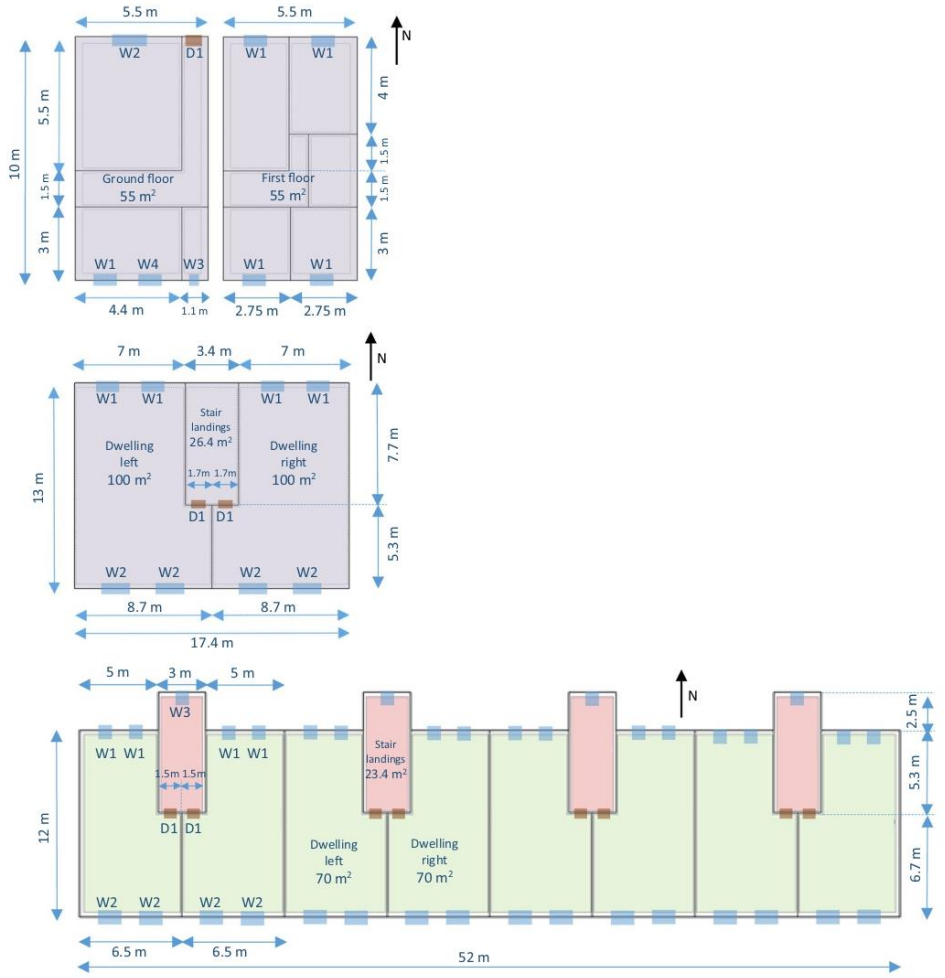

Fig. 2 Ground floor plan (left) and first-floor plan (right) of the building type T1[a] (above) and typical floor plan of the building types T2[b] (center) and T3.[c] (below). [a]Height from the floor of the plant (z) and windows dimensions (width × height) in T1: W1: z = 1 m, 1 m × 1 m; W2: z = 1 m, 1.3 m × 1 m; W3: z = 1.5 m, 0.4 m × 0.4 m; W4: z = 0 m, 1 m × 1.8 m. Doors dimensions (width × height) in T1: D1: 0.8 m × 2 m. [b]Height from the floor of the plant (z) and windows dimensions (width × height) in T2: W1: z = 1 m, 1.3 m × 1 m; W2: z = 1 m, 1.4 m × 1.4 m. Doors dimensions (width × height) in T2: D1: 0.8 m × 2 m. The ground floor in T2 consists of two premises instead of two dwellings, in addition to an entrance door (1.5 m × 2 m) to the portal-stairs and two doors (1.3 m × 2 m) for the entrance to the two premises. [c]Height from the floor of the plant (z) and windows dimensions (width × height) in T3: W1: z = 1 m, 0.8 m × 1 m; W2: z = 1 m, 1.46 m × 1 m; W3: z = 1 m, 0.7 m × 1 m. Doors dimensions (width × height) in T3: D1: 0.8 m × 2 m. The ground floor in T3 consists of four premises instead of eight dwellings, in addition to four entrance doors (1.4 m × 2 m) to the four portals-stairs and four doors (0.8 m × 2 m) for the entrance to the four premises

Table 5 Characteristic U-values (W/m^{2}K) of the thermal envelope of buildings depending on the climate zone and the BEC. *Source*: Author elaboration based on [71–73]

Element	S1	S2	S3	S4
External wall	Z1-Z5: 2.5	Z1: 1.8 Z2: 1.8 Z3: 1.6 Z4: 1.4 Z5: 1.4	Z1: 0.94 Z2: 0.82 Z3: 0.73 Z4: 0.66 Z5: 0.57	Z1: 0.50 Z2: 0.38 Z3: 0.29 Z4: 0.27 Z5: 0.25
Roof	Z1-Z5: 2.5	Z1: 1.4 Z2: 1.4 Z3: 1.2 Z4: 0.9 Z5: 0.7	Z1: 0.50 Z2: 0.45 Z3: 0.41 Z4: 0.38 Z5: 0.35	Z1: 0.47 Z2: 0.33 Z3: 0.23 Z4: 0.22 Z5: 0.19
Party walls and horizontal/vertical internal partitions between zones with different uses	Z1-Z5: 2.5	Z1-Z5: 1.94	Z1: 1.22 Z2: 1.07 Z3: 0.95 Z4: 0.86 Z5: 0.74	Z1: 1.25 Z2: 1.10 Z3: 0.95 Z4: 0.85 Z5: 0.70
Horizontal internal partitions between zones with the same use	Z1-Z5: 2.5	Z1-Z5: 1.6	Z1-Z5: 1.2	Z1: 1.80 Z2: 1.55 Z3: 1.35 Z4: 1.20 Z5: 1.00
Vertical internal partitions between zones with the same use	Z1-Z5: 2.5	Z1-Z5: 1.94	Z1-Z5: 1.2	Z1: 1.4 Z2: 1.2 Z3: 1.2 Z4: 1.2 Z5: 1.0
Ground floor	Z1-Z5: 2.35	Z1: 1.4 Z2: 1.4 Z3: 1.2 Z4: 0.9 Z5: 0.7	Z1: 0.94 Z2: 0.82 Z3: 0.73 Z4: 0.66 Z5: 0.57	Z1: 0.50 Z2: 0.38 Z3: 0.29 Z4: 0.27 Z5: 0.25
South-facing windows without obstacles (high solar gain) considering the window-to-wall ratio of 15%	Z1-Z5: 5.7	Z1-Z5: 5.7	Z1: 5.7 Z2: 5.7 Z3: 4.4 Z4: 3.5 Z5: 3.1	Z1: 2.6 Z2: 2.1 Z3: 1.9 Z4: 1.8 Z5: 1.9
North-facing windows without obstacles (low solar gain) considering the window-to-wall ratio of 10%	Z1-Z5: 5.7	Z1-Z5: 5.7	Z1: 5.7 Z2: 5.4 Z3: 4.4 Z4: 3.5 Z5: 3.1	Z1: 2.6 Z2: 2.0 Z3: 1.6 Z4: 1.4 Z5: 1.3

Table 6 Characteristic values of the linear thermal transmittance ψ_i (W/mK) of thermal bridges for the buildings according to the BECs. *Source*: Author elaboration based on [75, 76]

Thermal bridge	S1 & S2	S3 & S4
Junction Roof-Wall	0.44	0.25
Junction Wall-Ground floor	0.20	0.20
Junction Wall-Internal floor	0.60	0.20
The lintel above the window or door	0.80	0.1
Sill below window	0.50	0.1
Jamb at window or door	0.50	0.05

schedule: 10% from 1:00 a.m. to 7:59 a.m., 30% from 8:00 a.m. to 6:59 p.m., 50% from 7:00 p.m. to 7:59 p.m., 100% from 8:00 p.m. to 11:59 p.m. and 50% from 0:00 a.m. to 0:59 a.m. 90% of equipment load is sensitive, while 10% is latent. Regarding the sensitive part, 70% is transmitted by convection and 30% by radiation. On the other hand, lighting load is 50% transmitted by convection, 30% by long-wave radiation (thermal), and 20% by short-wave radiation (visible).

- A specific domestic hot water (DHW) demand of 28 l/person·day with a setpoint temperature of 60 °C.
- Same hourly profile of the DHW demand per day (see Fig. 3).

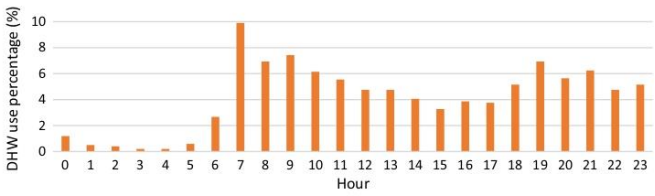

Fig. 3 Hourly profile of the daily DHW demand. *Source*: Author elaboration based on [76]

Table 7 Building ventilation rate (ach) considered based on the period and the building construction age. *Source*: Author elaboration based on [77–79]

Building type	S1	S2	S3	S4
June to September, 01:00 a.m.—08:59 a.m				
T1, T2 and T3	4	4	4	4
June to September, 09:00 a.m.—00:59 a.m. and October to May, 00:00 a.m.—23:59 p.m				
T1	0.63	0.63	0.69	0.40
T2	0.63	0.63	0.73	0.44
T3	0.63	0.63	0.67	0.46

The method reported in the Spanish regulation [66] was used to estimate the daily DHW demand for each building. It consists of multiplying the specific DHW demand by the number of people in each dwelling. In the case of housing blocks, this result can be corrected by a factor based on the number of houses in the block. Thus, for the T1 building, the daily DHW demand was 140 l/day = 28 l/person·day · 5 people (4 bedrooms). For the T2 case, the demand was 1,512 l/day = 28 l/person·day · 5 people/dwelling · 12 dwellings · 0.9 (simultaneity factor). For T3, the demand was 5,040 l/day = 28 l/person·day · 3 people/dwelling (2 bedrooms) · 80 dwellings · 0.75 (simultaneity factor).

3.5 Air renewal (ventilation and infiltration)

As shown in Table 7, the ventilation rate considered for all cases during the summer nights (from June to September) is 4 ach, which is associated with windows opening [77]. During all other seasons, the ventilation rate varies depending on the building's age and type. The ventilation rate for the S4 was based on the last update of the Basic Document on Salubrity of the Spanish Technical Building Code [78]. Regarding the S3, the first version of the Basic Document on Salubrity of the Spanish Technical Building Code [79] was considered. For the S1 and S2, a default value of 0.63 ach [77] was assumed for all building types, as there was no specific regulation regarding air renewal in these BECs' periods.

Regarding uncontrolled ventilation, known as infiltration, Table 8 shows the air permeability through the windows and doors reported by the BECs for each period considered. Infiltration depends on the thermal and pressure gradient, the wind, and the air permeability of all thermal envelope elements. For the sake of simplicity, an annual mean infiltration rate was considered as a function of the air permeability of the windows. Thus, as shown in Table 9, three possible constant infiltration rates were established based on the results reported by Rodríguez Trejo [80]. Infiltration rate of 0.3 ach for enclosures with very high airtightness (27 m^3/hm^2), 0.45 ach for enclosures with medium airtightness (50

Table 9 Infiltration rates (ach) considered based on the climate zone and the building construction age. *Source*: Author elaboration based on [80]

	S1	S2	S3	S4
Infiltration rate (ach)	0.60	Z1: 0.45 Z2: 0.45 Z3: 0.30 Z4: 0.30 Z5: 0.30	Z1: 0.45 Z2: 0.45 Z3: 0.30 Z4: 0.30 Z5: 0.30	Z1: 0.45 Z2: 0.45 Z3: 0.30 Z4: 0.30 Z5: 0.30

Table 8 Air permeability of windows and doors (m^3/hm^2) in residential buildings depending on the climate zone and the building construction age. *Source*: Author elaboration based on [71–73]

	S1	S2	S3	S4
Air permeability of windows and doors ($m^3/h{\cdot}m^2$)	100	Z1: 50 Z2: 50 Z3: 27 Z4: 27 Z5: 27	Z1: 50 Z2: 50 Z3: 27 Z4: 27 Z5: 27	Z1: 50 Z2: 50 Z3: 27 Z4: 27 Z5: 27

m^3/hm^2), and 0.6 ach for enclosures with low airtightness (100 m^3/hm^2).

3.6 Energy model and simulation

The DesignBuilder simulation tool, based on the EnergyPlus engine, was used to model and simulate the set of 60 buildings. This engine was selected due to its wide international recognition and also because it is one of the calculation engines commonly used in Spain for issuing energy performance certificates. The buildings were modeled, and the thermal demands of heating, cooling, and DHW were estimated. All data were generated on an hourly basis.

4 Results and discussion

The thermal demand results of the 60 building cases performed by DesignBuilder are presented and analyzed in this section. Considering the size difference among the building types, the comparison was based on the ratio between the thermal demand and the building area to levelize the results.

Figure 4 shows the energy demand results broken down into heating, cooling, domestic hot water, and electricity (lighting and equipment). The average energy demand of the 60 building cases was 106.2 kWh/m^2year. Focusing on the BECs, the average energy demand per standard ranged from 144.4 kWh/m^2year for S1 to 73.4 kWh/m^2year for S4. Thus, the improvement achieved by the release of each regulatory update was around 17%, and the total improvement reached up to 50% for the whole time considered. The higher energy demands were found for the TiS1Z5 cases, due to the worse constructive solutions among the standards and the greater heating demand in Burgos. On the contrary, lower energy demands were found for the TiS4Z3 cases, in accordance with the better constructive solutions established in S4 and the lower cooling demand of Santander. It is important to note that DHW demand decreases from T1 to T3 due to the simultaneity factor. Electricity demand, obtained from the internal loads, presents the same value in terms of kWh/m^2year for all cases.

Considering the average energy demand for all building cases, as shown in Fig. 5, heating presented the largest contribution (41%), followed by electricity demand (30%). DHW and cooling accounted for 17% and 12%, respectively. The heating contribution to the total energy demand can significantly vary from 6% (T2S4Z1) to 75% (T3S1Z5) due to the winter climate severity and the thermal envelope quality. On the other hand, the cooling contribution can be negligible in some cases (0.6–3% for TiSjZ3) or reach up to 24% (TiSjZ1) in other cases due to the summer severity of the climate zones. Regarding the DHW and electricity demands, their contribution to the energy demand depends on the other demands. Therefore, lower percentages were found for higher heating and cooling demands (10% and 15% for TiS1Z5, respectively) and higher percentages for lower heating and cooling demands (30% and 45% for TiS4Z3).

Focusing on the heating demand (Table 10), a substantial decrease (50%) is observed between S3 and S4, and notable reductions, although somewhat lower, between S2 and S3 (40%) and the S1 and S2 (30%). These improvements are mostly associated with the better U-values of the thermal envelope and the ventilation rate reduction defined by each BEC. If the analysis is performed with the climate zones, a clear correlation is observed for all buildings and BECs; the higher winter climate severity, the higher the heating demand. On the other hand, comparing the building types, the heating demand is lower for the blocks of flats (T2 and T3) than for the single-family house (T1) because of T1's lower compactness. In addition, the heating demand of T2 is lower than T3 because T2 is between party walls.

Regarding the cooling demand, as shown in Table 11, the higher demands are found in zones with higher summer climate severity (Z1, Z2, and Z4). Conversely, much lower or even negligible values are achieved in zones with lower summer severity (Z5 and Z3). The highest cooling demand does not occur in the highest summer severity zone (Z1). It happens because the climate zones are defined by the Spanish Weather for Energy Calculations [29] for an area instead of a city. Nevertheless, real measured climate data from Meteonorm [31] for each city were considered in the simulation. Thus, Valencia presents the highest cooling demand instead of Almeria.

The cooling results showed a decrease of 11% between S1 and S2, 4% from S2 to S3, and also 4% between S3 and S4. This slight decrease is due to the lack of solar control elements (awnings, shutters, blinds, etc.) for the windows in the BECs requirements. The solar control elements are considered essential to reduce the cooling demand. In fact, this update came up only in the new regulation launched in 2019 [66], which was not considered in this study. The minor differences in the cooling demand between the building types can be explained by their compactness. The building blocks present higher compactness, thus, lower heat losses compared with the single-family house. Therefore, T3 presents the highest cooling demand, followed by T2 and T1, respectively.

Analyzing the heating and cooling thermal balance, it was observed that the heat loss through the thermal envelope and by the air renewal (ventilation and infiltrations) comprised 50% of the total annual thermal loss. However, the relevance of each term in the thermal balance depends on the BEC. Thus, in S1, the thermal envelope was more relevant due to the higher U-values found, while in S4, the air renewal rate had a higher contribution.

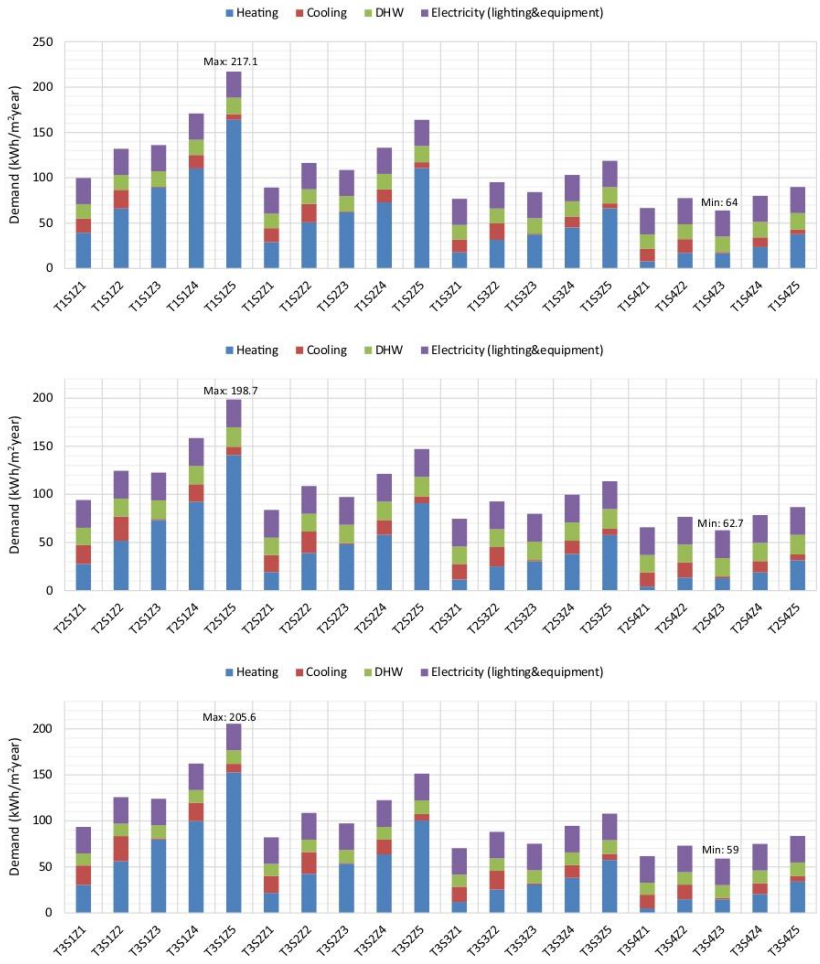

Fig. 4 Energy demand (kWh/m^{2}year) depending on building type, BEC, and climate zone

Regarding the thermal envelope loss breakdown, the walls (including the corresponding thermal bridges) were the most relevant, accounting for 39% of the total annual thermal loss, while glazing accounted for 26%. It is worth noting that the heat losses through the ground were more significant for T1, since T2 and T3 have an unconditioned ground floor behaving as a thermal insulating space. Moreover, focusing on the air renewal losses, ventilation accounted for 64%, and 36% corresponded to infiltration. Concerning the heat gains, the internal gains (occupancy, lighting, and equipment) accounted for 54% of the total annual thermal gain, while solar gain accounted for 46%. A higher solar contribution was found for climate zones with higher solar radiation (Z1 and Z2) and higher g-value of the windows (S1, S2, and S3).

The DHW demand, as shown in Table 12, is not dependent on the BEC. It is affected solely by the building type and climate zone. The DHW demand is higher in zones with a

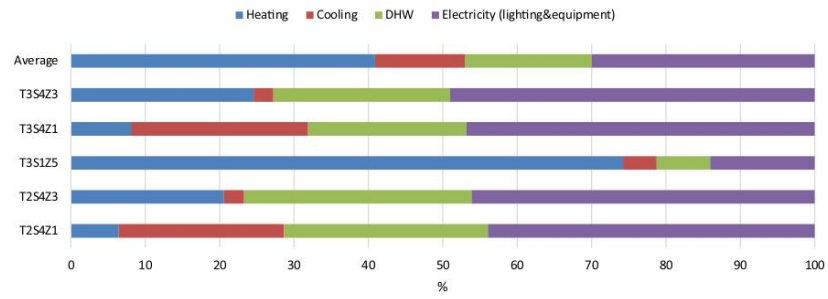

Fig. 5 Breakdown of energy demand (%) in some representative cases

Table 10 Heating demand (kWh/m^{2}year) depending on building type, BEC, and climate zone

Building type	S1	S2	S3	S4
T1	Z1: 39.44	Z1: 29.01	Z1: 17.83	Z1: 7.88
	Z2: 66.03	Z2: 50.94	Z2: 31.65	Z2: 17.30
	Z3: 89.36	Z3: 62.04	Z3: 37.47	Z3: 16.89
	Z4: 110.39	Z4: 73.02	Z4: 45.24	Z4: 23.55
	Z5: 163.88	Z5: 110.78	Z5: 66.26	Z5: 37.88
T2	Z1: 27.62	Z1: 19.31	Z1: 11.52	Z1: 4.22
	Z2: 51.80	Z2: 38.92	Z2: 25.17	Z2: 13.47
	Z3: 73.39	Z3: 48.11	Z3: 30.45	Z3: 12.89
	Z4: 92.26	Z4: 58.01	Z4: 38.10	Z4: 18.84
	Z5: 140.95	Z5: 90.86	Z5: 57.53	Z5: 31.59
T3	Z1: 30.33	Z1: 21.60	Z1: 11.87	Z1: 5.00
	Z2: 56.08	Z2: 42.51	Z2: 25.39	Z2: 14.70
	Z3: 79.83	Z3: 53.32	Z3: 30.99	Z3: 14.49
	Z4: 99.69	Z4: 63.67	Z4: 38.10	Z4: 20.45
	Z5: 152.60	Z5: 100.29	Z5: 57.72	Z5: 33.95

Table 11 Cooling demand (kWh/m^{2}year) depends on the building type, BEC, and the climate zone

Building type	S1	S2	S3	S4
T1	Z1: 15.55	Z1: 15.43	Z1: 14.16	Z1: 13.87
	Z2: 20.78	Z2: 20.16	Z2: 18.18	Z2: 15.09
	Z3: 0.80	Z3: 0.69	Z3: 0.92	Z3: 1.23
	Z4: 14.76	Z4: 14.43	Z4: 12.11	Z4: 10.83
	Z5: 6.34	Z5: 6.35	Z5: 5.53	Z5: 5.15
T2	Z1: 19.59	Z1: 17.57	Z1: 16.15	Z1: 14.64
	Z2: 25.31	Z2: 22.41	Z2: 20.05	Z2: 15.81
	Z3: 1.12	Z3: 1.07	Z3: 1.23	Z3: 1.69
	Z4: 18.28	Z4: 15.37	Z4: 13.67	Z4: 11.79
	Z5: 8.52	Z5: 7.09	Z5: 6.69	Z5: 6.06
T3	Z1: 21.06	Z1: 18.50	Z1: 16.48	Z1: 14.69
	Z2: 27.24	Z2: 23.65	Z2: 20.33	Z2: 15.94
	Z3: 1.27	Z3: 1.07	Z3: 1.25	Z3: 1.56
	Z4: 19.85	Z4: 15.96	Z4: 13.72	Z4: 11.71
	Z5: 9.28	Z5: 7.23	Z5: 6.62	Z5: 5.93

Table 12 DHW demand (kWh/m^{2}year) depending on building type and climate zone

BEC	T1	T2	T3
S1-S4	Z1: 15.96	Z1: 18.03	Z1: 13.15
	Z2: 16.35	Z2: 18.47	Z2: 13.48
	Z3: 16.99	Z3: 19.19	Z3: 14.00
	Z4: 16.83	Z4: 19.01	Z4: 13.87
	Z5: 17.97	Z5: 20.30	Z5: 14.81

lower mains water temperature. The differences among the building types are due to the simultaneity factor (1, 0.9, and 0.75 for T1, T2, and T3, respectively) and the occupancy (five people per dwelling in T1 and T2 and three people per dwelling in T3). Thus, the higher demand is found in T2 and the lower in T3.

5 Conclusions

A procedure based on energy simulation was proposed to evaluate the improvement in energy efficiency achieved by the changes introduced in the building energy codes. The procedure was applied to the Spanish residential sector, focusing on heating, cooling, and DHW demands. DesignBuilder simulation tool was used to model and simulate 60 different cases, combining three representative building types, four national building energy codes, and five selected climate zones.

The analysis of the thermal demands showed a remarkable decrease in heating, particularly, between S3 and S4 standards. The reduction was mostly impacted by the U-values, and ventilation and infiltration rates required by each BEC. The decrease achieved in cooling was substantial, but

it was much lower than in heating. Further improvements regarding the thermal energy demands should consider higher building compactness, better construction solutions, lower infiltration rate, and new ventilation systems (e.g., with energy recovery).

The DHW demand is not dependent on the BEC. However, it is important to mention that the S3 standard introduced the obligation to cover 30–50% of the DHW demand using renewable or residual energy sources or combined heat and power systems.

Acknowledgments This contribution has been developed from the results obtained in the framework of the project TEGBIOSOL (Ref. number: RTI2018-09886-A-100) "Integration of thermoelectric generators (TEG) in solar PVT collectors and biomass boilers: testing and optimization in polygeneration schemes" funded by Spanish Ministry of Science, Innovation and Universities (MCIU), Spanish State Research Agency (AEI) and European Regional Development Funds (FEDER).

Author contributions All authors contributed to the study conception and design. Material preparation, data collection and analysis were performed by Ignacio Zabalza and Luis Gabriel Gesteira. The first draft of the manuscript was written by Ignacio Zabalza, and all authors commented on previous versions of the manuscript. All authors read and approved the final manuscript.

Funding Open Access funding provided thanks to the CRUE-CSIC agreement with Springer Nature. The authors have no relevant financial or non-financial interests to disclose.

Declarations

Conflict of interest The authors have no competing interests to declare that are relevant to the content of this article.

References

1. International Energy Agency (2020) Energy Technology Perspectives 2020, Paris. https://www.iea.org/reports/energy-technology-perspectives-2020. Accessed 11 Nov 2021.
2. International Energy Agency (2020) World Energy Balances 2020, Paris. https://www.iea.org/data-and-statistics/data-product/world-energy-balances. Accessed 11 Nov 2021.
3. United Nations Environment Programme (2020) Global status report for buildings and construction: towards a zero-emission, efficient and resilient buildings and construction sector. Report, Nairobi
4. Nejat P, Jomehzadeh F, Taheri MM, Gohari M, Abd. Majid MZ (2015) A global review of energy consumption, CO_2 emissions and policy in the residential sector (with an overview of the top ten CO_2 emitting countries). Renew Sustain Energy Rev 43:843–862
5. Bartlett R, Halverson MA, Shankle DL (2003). Understanding building energy codes and standards. https://doi.org/10.2172/900221
6. Sadi M, Arabkoohsar A (2020) Techno-economic analysis of off-grid solar-driven cold storage systems for preventing the waste of agricultural products in hot and humid climates. J Clean Prod 275
7. Sadi M, Chakravarty KH, Behzadi A, Arabkoohsar A (2021) Techno-economic-environmental investigation of various biomass types and innovative biomass-firing technologies for cost-effective cooling in India. Energy 219
8. European Union. Directive 2002/91/EC of the European Parliament and of the Council of 16 December 2002 on the energy performance of buildings. Official J L 001, 04/01/2003, pp 65–71
9. European Union. Directive 2010/31/EU of the European Parliament and of the Council of 19 May 2010 on the energy performance of buildings. Official Journal L 153, 18/06/2010, pp 13–35
10. European Union. Directive (EU) 2018/844 of the European Parliament and the Council of 30 May 2018 amending Directive 2010/31/EU on the energy performance of buildings and Directive 2012/27/EU on energy efficiency. Official J L 156, 19/06/2018, pp 75–91
11. D'Agostino D, Tzeiranaki ST, Zangheri P, Bertoldi P (2021) Assessing nearly zero energy buildings (NZEBs) development in Europe. Energy Strategy Rev 36
12. Mazuroski W, Berger J, Delinchant B, Wurtz F, Mendes N (2022) A technique to improve the design of near-zero energy buildings. J Braz Soc Mech Sci Eng 44(6)
13. Reis IFG, Figueiredo A, Samagaio A (2021) Modeling the evolution of construction solutions in residential buildings' thermal comfort. Appl Sci 11(5):2427. https://doi.org/10.3390/app11052427
14. Kumar G, Thakur B, De S (2021) Energy performance of typical large residential apartments in Kolkata: implementing new energy conservation building codes of India. Clean Technol Environ Policy 23(4):1251–1271
15. Xie Y, Halverson M, Bartlett R, Chen Y, Rosenberg M, Taylor T, et al (2020) Evaluating building energy code compliance and savings potential through large-scale simulation with models inferred by field data. Energies 13(9):2321. https://doi.org/10.3390/en13092321
16. Allard I, Nair G, Olofsson T (2021) Energy performance criteria for residential buildings: a comparison of Finnish, Norwegian, Swedish, and Russian building codes. Energy Build 250:111276. https://doi.org/10.1016/j.enbuild.2021.111276
17. Bienvenido-Huertas D, Oliveira M, Rubio-Bellido C and Marín D (2019) A comparative analysis of the international regulation of thermal properties in building envelope. Sustainability 11(20):5574. https://doi.org/10.3390/su11205574
18. Bianco V, Marmori C (2022) Modelling the deployment of energy efficiency measures for the residential sector. The case of Italy. Sustain Energy Technol Assess 49:101777. https://doi.org/10.1016/j.seta.2021.101777
19. Merini I, Molina-García A, Socorro García-Cascales M, Mahdaoui M, Ahachad M (2020) Analysis and comparison of energy efficiency code requirements for buildings: a Morocco-Spain case study. Energies 13(22):5979. https://doi.org/10.3390/en13225979
20. Monzón-Chavarrías M, López-Mesa B, Resende J, Corvacho H (1961) The nZEB concept and its requirements for residential buildings renovation in Southern Europe: the case of multi-family

buildings from, to 1980 in Portugal and Spain. J Build Eng 2021:34
21. Gangolells M, Casals M, Forcada N, MacArulla M, Cuerva E (2016) Energy mapping of the existing building stock in Spain. J Clean Prod 112:3895–3904
22. Cerezo-Narváez A, Piñero-Vilela J-, Rodríguez-Jara E-, Otero-Mateo M, Pastor-Fernández A and Ballesteros-Pérez P (2021) Energy, emissions and economic impact of the new nZEB regulatory framework on residential buildings renovation: Case study in southern Spain. J Build Eng 42:103054. https://doi.org/10.1016/j.jobe.2021.103054
23. Gesteira LG, Uche J, De Oliveira Rodrigues LK (2021) Residential sector energy demand estimation for a single-family dwelling: dynamic simulation and energy analysis. J Sustain Dev Energy Water Environ Syst 9(2):1080358. https://doi.org/10.13044/j.sdewes.d8.0358
24. Ebrahimi-Moghadam A, Ildarabadi P, Aliakbari K, Arabkoohsar A, Fadaee F (2020) Performance analysis of light shelves in providing visual and thermal comfort and energy savings in residential buildings. J Braz Soc Mech Sci Eng 42:484. https://doi.org/10.1007/s40430-020-02565-2
25. Gasparin S, Berger J, Dutykh D, Mendes N (2019) An innovative method to determine optimum insulation thickness based on non-uniform adaptive moving grid. J Braz Soc Mech Sci Eng 41:173. https://doi.org/10.1007/s40430-019-1670-6
26. Sadripour S, Mollamahdi M, Sheikhzadeh GA, Adibi M (2017) Providing thermal comfort and saving energy inside the buildings using a ceiling fan in heating systems. J Braz Soc Mech Sci Eng 39(10):4219–4230
27. Vaishnani Y, Ali SF, Joshi A, Rakshit D, Wang F (2020) Thermal performance analysis of a naturally ventilated system using PMV models for different roof inclinations in composite climatic conditions. J Braz Soc Mech Sci Eng 42:124. https://doi.org/10.1007/s40430-020-2219-4
28. Peel MC, Finlayson BL, McMahon TA (2007) Updated world map of the Köppen-Geiger climate classification. Hydrol Earth Syst Sci 11(5):1633–1644
29. US Department of Energy (2021) EnergyPlus weather data. https://energyplus.net/weather. Accessed 11 Nov 2021.
30. NOAA's National Centers for Environmental Information. Climate data online. https://www.ncdc.noaa.gov/cdo-web/datasets. Accessed 11 Nov 2021.
31. Meteotest AG. Meteonorm 8. Handbook part I: Software. https://meteonorm.com/assets/downloads/mn81_software.pdf. Accessed 11 Nov 2021.
32. Gulotta TM, Cellura M, Guarino F, Longo S (2021) A bottom-up harmonized energy-environmental models for Europe (BOHEEME): a case study on the thermal insulation of the EU-28 building stock. Energy Build 231:110584. https://doi.org/10.1016/j.enbuild.2020.110584
33. ENTRANZE project. Entranze data tool. https://entranze.enerdata.net. Accessed 11 Nov 2021.
34. ODYSSEE-MURE project. Country profiles. http://www.odyssee-mure.eu. Accessed 11 Nov 2021.
35. Tuominen P, Holopainen R, Eskola L, Jokisalo J, Airaksinen M (2014) Calculation method and tool for assessing energy consumption in the building stock. Build Environ 75:153–160
36. Kalogeras G, Rastegarpour S, Koulamas C, Kalogeras AP, Casillas J, Ferrarini L (2020) Predictive capability testing and sensitivity analysis of a model for building energy efficiency. Build Simul 13(1):33–50
37. Campana JP, Morini GL (2019) BESTEST and en ISO 52016 benchmarking of ALMABuild, a new open-source simulink tool for dynamic energy modeling of buildings. Energies 12(15):2938. https://doi.org/10.3390/en12152938
38. Kamel E, Memari AM (2018) Automated building energy modeling and assessment tool (ABEMAT). Energy 147:15–24
39. Ascione F, Bianco N, Iovane T, Mastellone M, Mauro GM (2021) Conceptualization, development and validation of EMAR: A user-friendly tool for accurate energy simulations of residential buildings via few numerical inputs. J Build Eng 44:102647. https://doi.org/10.1016/j.jobe.2021.102647
40. Sousa J (2012) Energy simulation software for buildings: Review and comparison. In: Carreira P, Amaral V (eds) Proceedings of the first international workshop on information technology for energy applications, Lisbon, Portugal, 6–7 September 2012. CEUR, Lisbon, pp 57–68
41. Choi C, Kim K, Park C, Kim Y (2019) Performance comparison of energy simulation tools according to analysis methods: Focused on existing buildings. Asia Life Sci 3:1365–1377
42. Magni M, Ochs F, de Vries S, Maccarini A, Sigg F (2021) Hourly simulation results of building energy simulation tools using a reference office building as a case study. Data Brief 38:107370. https://doi.org/10.1016/j.dib.2021.107370
43. Magni M, Ochs F, de Vries S, Maccarini A, Sigg F (2021) Detailed cross comparison of building energy simulation tools results using a reference office building as a case study. Energy Build 250:111260. https://doi.org/10.1016/j.enbuild.2021.111260
44. Pernigotto G, Gasparella A (2013) Extensive comparative analysis of building energy simulation codes: Heating and cooling energy needs and peak loads calculation in TRNSYS and EnergyPlus for southern Europe climates. HVAC R Res 19(5):481–492
45. Harish VSKV, Kumar A (2016) A review on modeling and simulation of building energy systems. Renew Sustain Energy Rev 56:1272–1292
46. Crawley DB, Hand JW, Kummert M, Griffith BT (2008) Contrasting the capabilities of building energy performance simulation programs. Build Environ 43(4):661–673
47. Tabadkani A, Tsangrassoulis A, Roetzel A, Li HX (2020) Innovative control approaches to assess energy implications of adaptive facades based on simulation using EnergyPlus. Sol Energy 206:256–268
48. Queiroz N, Westphal FS, Ruttkay Pereira FO (2020) A performance-based design validation study on EnergyPlus for daylighting analysis. Build Environ 183:107088. https://doi.org/10.1016/j.buildenv.2020.107088
49. Xing J, Ren P, Ling J (2015) Analysis of energy efficiency retrofit scheme for hotel buildings using eQuest software: a case study from Tianjin, China. Energy Build 87:14–24
50. Song J, Zhang X, Meng X (2015) Simulation and analysis of a university library energy consumption based on EQUEST. Proc Eng 121:1382–1388. https://doi.org/10.1016/j.proeng.2015.09.028
51. Yang L, He B, Ye M (2014) Application research of ECOTECT in residential estate planning. Energy Build 72:195–202
52. Peng C (2016) Calculation of a building's life cycle carbon emissions based on Ecotect and building information modeling. J Clean Prod 112:453–465
53. Kenai M-, Libessart L, Lassue S, Defer D (2021) Impact of green walls occultation on energy balance: development of a TRNSYS model on a brick masonry house. J Build Eng 44:102634. https://doi.org/10.1016/j.jobe.2021.102634
54. M'Saouri El Bat A, Romani Z, Bozonnet E, Draoui A (2021) Thermal impact of street canyon microclimate on building energy needs using TRNSYS: a case study of the city of Tangier in Morocco. Case Stud Therm Eng 24:100834. https://doi.org/10.1016/j.csite.2020.100834
55. Sabunas A, Kanapickas A (2017) Estimation of climate change impact on energy consumption in a residential building in Kaunas, Lithuania, using HEED software. Energy Procedia 128:92–99. https://doi.org/10.1016/j.egypro.2017.09.020

56. Shaari S, Bowman N (1998) Photovoltaics in buildings: a case study for rural England and Malaysia. Renew Energy 15(1–4):558–561
57. MacGregor WA, Hamdullahpur F, Ugursal VI (1993) Space heating using small-scale fluidized beds: a techno-economic evaluation. Int J Energy Res 17(6):445–466
58. Strachan PA, Kokogiannakis G, Macdonald IA (2008) History and development of validation with the ESP-r simulation program. Build Environ 43(4):601–609
59. Tavares PF, Gaspar AR, Martins AG, Frontini F (2014) Evaluation of electrochromic windows impact in the energy performance of buildings in Mediterranean climates. Energy Policy 67:68–81
60. Liu M, Wittchen KB, Heiselberg PK (2015) Control strategies for intelligent glazed façade and their influence on energy and comfort performance of office buildings in Denmark. Appl Energy 145:43–51
61. Sørensen MJ, Myhre SH, Hansen KK, Silkjær MH, Marszal-Pomianowska AJ, Liu L (2017) Integrated building energy design of a Danish office building based on Monte Carlo simulation method. Energy Procedia 132:93–98. https://doi.org/10.1016/j.egypro.2017.09.646
62. Johari F, Munkhammar J, Shadram F, Widén J (2022) Evaluation of simplified building energy models for urban-scale energy analysis of buildings. Build Environ 211:108684. https://doi.org/10.1016/j.buildenv.2021.108684
63. Hilliaho K, Lahdensivu J, Vinha J (2015) Glazed space thermal simulation with IDA-ICE 4.61 software - Suitability analysis with a case study. Energy Build 89:132–141
64. Al-janabi A, Kavgic M, Mohammadzadeh A, Azzouz A (2019) Comparison of EnergyPlus and IES to model a complex university building using three scenarios: free-floating, ideal air load system, and detailed. J Build Eng 22:262–280
65. Shareef S (2021) The impact of urban morphology and building's height diversity on energy consumption at urban scale. The case study of Dubai. Build Environ 194
66. Spanish Ministry of Development. Royal Decree 732/2019, of December 20th, which modifies the Technical Building Code, approved by Royal Decree 314/2006, of March 17th. BOE no. 311, 27/12/2019.
67. Spanish Ministry of Development. Descriptive document on reference climates – Support document to the Basic Document DB-HE of Energy Saving of the Technical Building Code, 2017.
68. de la Flor FJS, Domínguez SA, Félix JLM, Falcón RG (2008) Climatic zoning and its application to Spanish building energy performance regulations. Energy Build 40(10):1984–1990
69. Aranda-Usón A, Ferreira G, López-Sabirón AM, Mainar-Toledo MD, Zabalza BI (2013) Phase change material applications in buildings: an environmental assessment for some Spanish climate severities. Sci Total Environ 444:16–25
70. State Meteorological Agency of Spain. Municipal climate data. www.aemet.es. Accessed 11 Nov 2021.
71. Presidency of the Spanish Government. Royal Decree 2429/1979, of July 8th, which approves the Basic Building Standard NBE-CT-79 on thermal conditions in buildings. BOE no. 253, 22/10/1979.
72. Spanish Ministry of Housing. Royal Decree 314/2006, of March 17th, approving the Technical Building Code. BOE no. 74, 28/03/2006.
73. Spanish Ministry of Development. Order FOM/1635/2013, of September 10th, which updates the Basic Document DB-HE of Energy Saving of the Technical Building Code, approved by Royal Decree 314/2006, of March 17th. BOE no. 219, 12/09/2013.
74. Spanish National Institute of Statistics (2011) Population and Housing Census. www.ine.es/censos2011_datos/cen11_datos_inicio.htm Accessed 11 Nov 2021.
75. Spanish Ministry of Development (2014) Thermal bridges DA DB-HE/3—support document to the Basic Document DB-HE of Energy Saving of the Technical Building Code
76. Spanish Institute for Energy Diversification and Savings (2015) Manual of technical basics of energy qualification of existing buildings CE3x
77. Spanish Ministry for the Ecological Transition and the Demographic Challenge and Spanish Ministry of Transport, Mobility and Urban Agenda. Technical conditions of the procedures for assessing the energy efficiency of buildings, 2020.
78. Spanish Ministry of Development (2019) Updating of the basic health document DB-HS of the technical building code. https://www.codigotecnico.org/pdf/Documentos/HS/DBHS.pdf. Accessed 11 Nov 2021.
79. Spanish Ministry of Development (2006) Basic Health Document DB-HS of the Technical Building Code. https://www.codigotecnico.org/pdf/Documentos/HS/DBAnteriores/DBHS_200603.pdf. Accessed 11 Nov 2021.
80. Rodríguez Trejo S (2016) Characterization of ventilation in the existing residential buildings. Conciliation between indoor air quality and efficiency in energy renovation. Ph.D. Thesis, Polytechnic University of Madrid, Spain

A.1 Paper II

Journal of Sustainable Development of Energy, Water and Environment Systems

http://www.sdewes.org/jsdewes

Year 2021, Volume 9, Issue 2, 1080358

Residential Sector Energy Demand Estimation for a Single-family Dwelling: Dynamic Simulation and Energy Analysis

***Luis G. Gesteira*[*1], *Javier Uche*[2], *Luanda K. de Oliveira Rodrigues*[3]**

[1]Department of Mechanical Engineering, University of Zaragoza, Calle de Pedro Cerbuna, 12, Zaragoza, Spain
e-mail: 773948@unizar.es

[2]Department of Mechanical Engineering, University of Zaragoza, Calle de Pedro Cerbuna, 12, Zaragoza, Spain
e-mail: javiuche@unizar.es

[3]Department of Mechanical Engineering, Federal Institute of Bahia, R. Emídio dos Santos, s/n – Barbalho, Salvador, Brazil
e-mail: luandakivia@ifba.edu.br

Cite as: Gesteira, L. G., Uche, J., de Oliveira Rodrigues, L. K., Residential Sector Energy Demand Estimation for a Single-family Dwelling: Dynamic Simulation and Energy Analysis, J. sustain. dev. energy water environ. syst., 9(2), 1080358, 2021, DOI: https://doi.org/10.13044/j.sdewes.d8.0358

ABSTRACT

Detailed demand profiles for the residential sector are an important prerequisite for the improvement of building energy efficiency and the development of polygeneration systems. Therefore, the aim of this paper is to provide a generic pattern for each energy demand required for a single-family dwelling. The data of electricity, domestic hot water and freshwater were obtained through literature reported methods of demand profile estimation, whereas heating and cooling have been estimated by TRNSYS software simulation. All methods provide energy consumption profiles with 1-hour time step along 1-year period. Daily, weekly and yearly results are presented. The total dwelling consumption amounts to 3,866 kWh/y of electricity, 941 kWh/y of heating, 1,450 kWh/y of cooling, 41 m^3/y or 2,090 kWh/y of domestic hot water and 110 m^3/y of freshwater. Primary energy saving can achieve up to 13,917 kWh/y in case of renewable energy use and a higher comfort level is felt by the users during summer.

KEYWORDS

Residential sector, Energy demand, Transient System Simulation, Primary energy saving, Thermal comfort, Polygeneration.

INTRODUCTION

Building sector consumption encompasses 40% of global primary energy and contribute to in excess of 30% of carbon dioxide (CO_2) emissions [1]. In particular, the residential users comprehend more than 60% of the total energy consumption of the building sector [2]. Thereby, the research community and governments are paying more attention to energy efficiency and renewable energy technologies application in the residential sector in order to cope with its increasing energy demand.

* Corresponding author

In this framework, the residential sector stands out as one of the most significant energy consumers and highly affected by the actual directives. The energy and environmental policies coincide in highlighting the role of energy efficiency and climate change estimating, in the horizon of 2020, a reduction of its overall emissions to at least 20% below 1990 levels as well as an increase in renewables energy use to 20% [3].

Buildings perform most efficiently if all systems are controlled and integrated. Without upgrading existing appliances, the building efficiency can increase up to 30%, with an appropriate energy integration [4]. Furthermore, energy savings increase with the level of integration and can achieve more than 80% when the system design is optimized [5]. Thus, polygeneration systems pop up as a large potential once it promotes the energy integration required to achieve building energy efficiency and environmental targets.

Polygeneration applied to buildings has been broadly studied in the literature. For instance, Calise *et al.* [6] compared the polygeneration system applied to an office and a gym in different configurations. The proposed system was more profitable in the application with higher hot water demand, in this particular case, the gym. Roseli *et al.* [7] evaluated the integration of an electric heat pump driven by a photovoltaic field in two different configurations. In the first case, the system was connected to the grid. In second configuration, the system was also connected to grid but a battery bank was added as well. In both configurations, the system was applied to a small office and a reduction in primary energy consumption was verified. Acevedo *et al.* [8], designed a system combining Photovoltaic/Thermal (PVT) collectors, an evacuated tube collector and a wind turbine to produce electricity, sanitary hot water and desalted fresh water for a single-family house. Ghaem Sigarchian *et al.* [9] evaluated the effect of the operational modes on the performance of a polygeneration system in a residential building complex in northern Italy.

Uche *et al.* [10] showed experimental tests of a polygeneration pilot plant, for power, freshwater and Domestic Hot Water (DHW) production, designed for a typical family home (four residents) isolated from the power and water networks. Buonomano *et al.* [11] simulated a small trigeneration plant supplied by geothermal and solar energies for a hotel in Ischia, in South Italy. Results showed that the system performance is more dependent on the availability of the geothermal energy than the solar one. Considering a small residential building, Calise *et al.* [12] designed and simulated a system combining solar cooling, solar-assisted heat pump and PVT collector technologies. System performance presented to be highly sensitive to the PVT field area. Angrisani *et al.* [13] studied different solar panel technologies, tilt angles and collecting areas in a simulation of a solar heating and cooling system in an office building located in Southern Italy. The results showed a Primary Energy Saving (PES) and equivalent dioxide carbon emission reduction while compared with conventional system. Calise [14] evaluated energy and economic feasibility of a solar-assisted heating and cooling system for different types of school buildings and Italian climates. Despite the potential of energy saving, the author concluded that the economic profitability can be achieved only in case of public funding policies.

However, in order to promote reliable polygeneration systems simulations, detailed demand profiles of the analyzed building are required. Energy demand can be defined as the energy required by a system to provide energy services to the final users. The main residential demands can be divided into cooling, heating, DHW and electricity (lighting and appliances). It is important to note that the thermal energy (heating and cooling) is the highest consumer and represents 45% of the energy consumption in the EU residential sector [15] and depends on the thermal characteristics of the building, ventilation, indoor and outdoor climatic conditions and energy end-uses [16].

Thus, different methods of Building Energy Simulation (BES) for energy demand estimation can be defined. The models can be classified as diagnoses or prognosis and law or data [17]. Coakley *et al.* [18] describe that models applied to BES are, basically,

prognostics. Although, they can be driven by both law or data. The prognostic law-driven model (computational simulation) is used to predict the behavior of a complex system given a set of well-defined laws (e.g., energy balance, mass balance, conductivity, heat transfer, etc.). Whereas, the prognostic data-driven approach (statistical analysis) uses monitored data from the building to predict accurately the energy demand behavior. The study conducted by Yoshino *et al.* [19] highlighted the main research methods, findings and outcomes regarding the robust prediction of total energy use in buildings.

A few examples of detailed BES for energy demand estimation can be found in the literature. In particular, a study performed by Karlsson *et al.* [20] used three different tools to simulate a low energy terraced house in the south of Sweden. The measured values for total electricity demand ranged from about 6,000 kWh to over 12,000 kWh. Richardson *et al.* [21] presented a high-resolution model to estimate the demand for electricity in a dwelling. This model was validated through samples of 22 houses located in East Midlands, United Kingdom. The model can be modified according to specific requirements and be incorporated into other models. Carvalho [22] carried out a study along a period of 1-year to evaluate the demand for a medium-sized hospital located in the city of Zaragoza in Spain. The demand outcomes showed a maximum heating demand of 50,007.0 kWh/day in January and a maximum cooling demand of 20,170.0 kWh/day in July. Electricity demand achieved a maximum and minimum demand of 9,411.0 kWh/day and 7,802.0 kWh/day, respectively.

Thus, there is a lack of energy demand information regarding the residential sector. This data is indispensable for the simulation of reliable polygeneration systems. For that reason, the aim of this paper is to estimate an hourly generic pattern for all main energy demand required by the residential sector. As a reference case, a single-family dwelling located at the Mediterranean European side is considered. The results can be useful for improving the knowledge about energy demand estimation and providing basis for polygeneration systems simulations applied to the residential sector.

METHOD

The reference case is a single-family townhouse located in the Mediterranean European side. The energy demand patterns estimated are electricity, heating, cooling, DHW and freshwater along 1-year simulation with 1-hour time step.

The reliable tool TRansient SYstem Simulation (TRNSYS) [23] was used to estimate the heating and cooling demands by a detailed energy performance evaluation of the residential building. TRNSYS simulation software evaluates the energy required to maintain a specified building condition (e.g., temperature and humidity). It performs a detailed heat-balance calculation under the influence of external and internal inputs (weather, infiltration, occupancy, lighting, equipment loads, etc.).

On the other hand, electricity, DHW and freshwater demands were obtained by statistical analysis reported at the literature based on studies previously validated. The reference dwelling parameters were used as input for all approaches. Furthermore, a thermal comfort study and PES analysis were performed to validate the assumptions and highlight the importance of the residential sector.

The city of Almería, in the Mediterranean European side of Spain, was selected due to its high summer climatic severity and, therefore, the high total annual irradiance, which accounts to 2,587 kWh/m². Meteonorm weather data of Almería (36° 50' 1" N, 2° 27' 35" W) was used for climatic simulation purpose. Figure 1 shows the hourly variation of available global solar radiation on the horizontal surface and the dry bulb temperature for the whole year in this location. The global solar irradiance encompasses the direct incident beam radiation at the surface, the diffuse radiation that has been scattered through the molecules of the atmosphere and the albedo, radiation reflected by the surroundings [24].

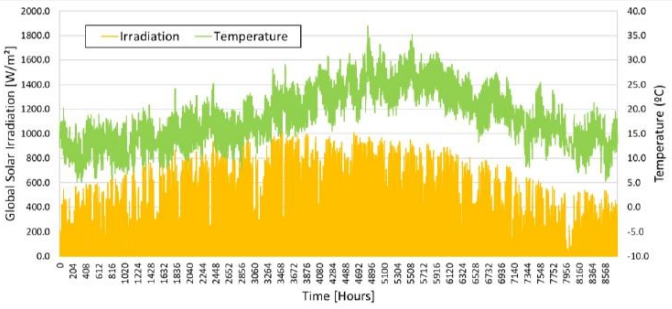

Figure 1. Hourly mean solar radiation and ambient temperature (Almería, Spain)

Heating and cooling demands

The space heating and cooling demand was dynamically simulated with TRNSYS in order to obtain the building thermal behavior. The model utilizes several components from the build-in component library considering both physical components (building, ground temperature, etc.) and controlling devices (schedules, calculators, unit converters, etc.). Moreover, the simulation tool also includes a number of additional components required to run the simulations and to process the results, such as weather data readers, integrators and plotters. All main types used in the proposed system model are listed in Table 1 and showed at Figure 2.

It is important to note that, the software built-in components are validated against experimental and/or performance manufacturers' data. Thus, the results of the simulation of the proposed system are highly reliable. Furthermore, the model under investigation can be analyzed by means of instantaneous or integrated data on whatever time period (hours, days, weeks, months or years). A detailed description of all component models used in the simulation are omitted, however, it is available in the TRNSYS component mathematical reference [23].

Table 1. TRNSYS main types used in the model

Component	Type	Component	Type
Weather data reader	15	Ground temperature	77
Building	56	Schedulers	14
Unit converter	57	Printer/plotter	65

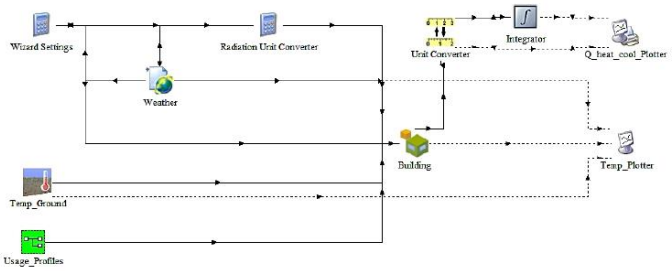

Figure 2. Pictorial view of the BES model in TRNSYS studio

Regarding the main components, the TRNBuild (Type 56) is the building input description tool of TRNSYS studio and simulates the multi-zone building thermal

behavior. TRNBuild is an interface for creating and editing all of the non-geometry information required by the TRNSYS BES model. It allows the user extensive flexibility in editing wall and layer material properties, creating ventilation and infiltration profiles, adding gains, defining radiant ceilings and floors, and positioning occupants for comfort calculations. Furthermore, Meteonorm weather data of Almería, Spain is given by Type 15 and Type 77 calculates the ground-coupled heat transfer according to the IEA Task 34/43 [25].

The usage profile encompasses in a macro all user defined information in order to simplify the TRNSYS main scheme. Figure 3 presents the usage profile macro breakdown. It presents all the inputs required by Type 56 to perform the BES model. In particular, the space heating and cooling thermostat setpoint control, the ventilation and infiltration airflow profiles and the lighting, equipment load and occupancy gains.

Figure 3. Pictorial view of the usage profile macro

The thermal energy demand of a residential building is a function of the building type, size, materials used for construction, occupancy and location [26]. In particular, a typical single-family townhouse of 110 m^2 with four occupants, as shown in Figure 4, was designed. It consists of two floors and an attic with a total height of 7.5 m. The side walls are adiabatic. Fenestration comprehends 10% and 15% of the north and south façade area, respectively. Trnsys3d plugin [27] for Google SketchUP [28] was used to build the 3D dwelling geometry divided in thermal zones for the proper building thermal evaluation. Furthermore, it provides a direct link between SketchUp and TRNBuild for BES.

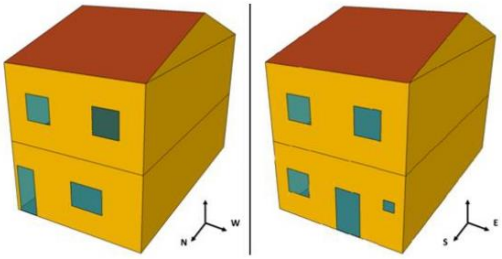

Figure 4. 3D of the reference dwelling

The house envelope comprehends the external walls and roof, the floor and the external doors and windows. The dwelling meets the transmittance thresholds defined by the basic document of energy saving of the Spanish technical building code: BD-ES [29], summarized in Table 2. However, no envelope components layers (material, thickness, density, etc.) were specified. The convective coefficients of the interior and exterior surfaces of each envelop component are calculated using a specific dynamic algorithm

defined in TRNSYS engine. It is worthy to note that no thermal bridges were considered in this study, nor internal walls and doors.

Table 2. Transmittances of building envelope components

Element	Value [W/m^{2}K]
External wall	0.50
External roof	0.47
Floor	0.50
Door	2.20
Window	2.60

Regarding the building usage profile, Table 3 presents the space heating and cooling setpoint temperature operation, the occupancy, lighting and equipment load profiles and the ventilation and infiltration air rate. Ventilation is the controlled air change of the building interior air to ensure its quality, whereas infiltration consists of an uncontrolled air renovation through various elements of the building envelope.

As shown in Table 3, an addition of four air changes per hour in ventilation airflow rate is considered during the cooling season, which represents the opening of windows proposed by [29]. During the whole year, a constant ventilation rate is defined according to the procedure described in the basic document of hygiene, salubrity and environmental protection of the Spanish technical building code: BD-HS [30].

An annual mean infiltration rate was defined according to the fenestration permeability. It is important to note that infiltration depends on the thermal and pressure gradient between the building interior and exterior, the wind and the air permeability of the building envelope. However, for reason of brevity, a constant infiltration rate along the year was defined based on the results of Rodríguez Trejo [31] for an average fenestration tightness.

Table 3. Building usage profile

Setpoint temperature		Heating season	17 °C	00:00-08:00
			20 °C	08:00-24:00
		Cooling season	27 °C	00:00-08:00
			-	08:00-16:00
			25 °C	16:00-24:00
Occupancy load	3.51 W/m²	Weekday	100%	00:00-08:00
			25%	08:00-16:00
			50%	16:00-24:00
		Weekend	100%	00:00-24:00
Lighting load/ Equipment load	4.40 W/m²		50%	00:00-01:00
			10%	01:00-08:00
			30%	08:00-19:00
			50%	19:00-20:00
			100%	20:00-24:00
Ventilation rate		Heating season	0.4 1/h	00:00-24:00
		Cooling season	4 1/h	01:00-09:00
			0.4 1/h	09:00-01:00
Infiltration rate			0.45 1/h	00:00-24:00

Electricity demand

An electrical demand curve was generated using a high-resolution stochastic model of domestic electricity demand developed by the Centre for Renewable Energy Systems Technology (CREST). The model produces 1-hour resolution demand data, disaggregated by end-use, using a bottom-up modelling approach based on patterns of active occupancy and daily activity profiles derived from time-use survey data. This model was validated through samples of 22 houses located in East Midlands, United

Kingdom. The user may configure the month of the year, the total number of residents and whether a weekday or a weekend day simulation is required [21]. The model was adapted to the reference case through the replacement of the climatic data, the appliances selection according to local characteristics and the lighting control calibration.

Domestic Hot Water demand

In order to estimate the DHW demand, a realistic daily time dependent simulation was performed using the DHWcalc software [32] developed for the IEA-SHC Task 26, which can generate realistic DHW profiles for European countries in several time steps. This software has been successfully used and validated in previous literature [33].

For a single-family house, the software considers flow rate distributions for small (washing hands) and medium (dishwasher) draw offs, shower and bath. A pre-defined probability distribution based on Gaussian and step functions assumes a constant probability for draw-offs for small and medium draw offs during daytime and nighttime, respectively. For shower and bath, Gaussian distributions with peaks in the morning and evening, respectively, are defined to describe the probabilities during the day. Each category-profile is generated separately and superposed afterwards [34].

In the particular case, the total mean daily water volume, duration and time step were set based on [29]. The daily water volume was assumed to be 112.0 L/d considering an average consumption per person of 28.0 L/d and four people occupancy. Finally, the software distributes all draw offs throughout the year according to its probability function.

Furthermore, to estimate the DHW thermal demand, a typical outlet temperature of 60 °C was chosen in order to meet the legionella requirement [30] and an annual mean inlet temperature of 16 °C was calculated according to the monthly aqueduct water temperature from Almería reported at [29] and presented at Figure 5.

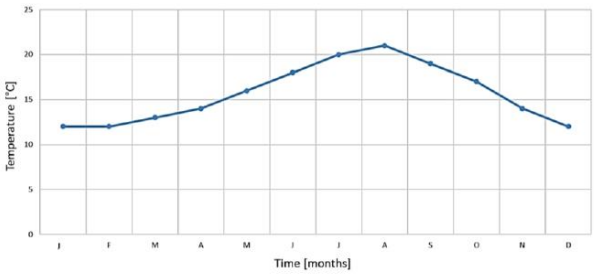

Figure 5. Monthly mean aqueduct water temperature of Almería

Freshwater demand

STochastic REsidential wAter end use Model (STREAM) is a stochastic simulation model for synthetically generating high resolution time series of residential water use at the end-use level developed and validated by Cominola *et al.* [35]. Each water end-use fixture simulated is characterized by its typical consumption pattern, as well as its probability distributions of number of uses per day, single use durations, water demand contribution and time of use during the day. Therefore, the generated profiles represent the heterogeneity of the different fixtures' signatures, with the toilet and the faucet characterized by an almost instantaneous pulse equally distributed during the day, while shower and clothes washers correspond to longer consumption events. The hourly distribution of the shower and the dishwasher consumption contributes to the morning and evening peak, respectively. Whereas the clothes washer is simulated overnight as this use occurs during off-peak times [36].

In this framework, the freshwater consumption of a single-family dwelling with four residents was simulated. The set of fixtures chosen consisted of toilet, faucet, clothes washer and dishwasher. No shower was selected here in order to avoid redundancy once it was considered in the DHW study.

Thermal comfort

The thermal comfort of building users is performed by a built-in subroutine included in TRNSYS to validate the assumptions taken from [29] and [30]. This model is developed according to the International Standard Organization (ISO) 7730 standard [37], described in details by Fanger [38]. The main calculation procedure, reported by Fanger, establishes a statistical correlation between the Predicted Mean Vote (PMV) thermal comfort index and the thermal load acting on the human body:

$$\mathrm{PMV} = L\,(0.0303\mathrm{e}^{-0.036\,\mathrm{M}} + 0.028) \tag{1}$$

The PMV index is calculated according to the energy loss to the environment (L) and the metabolic rate (M) of the users. The PMV is an index that aims to predict the mean value of votes of a group of occupants on the ambient thermal comfort sensation. The index is translated as +3 for a too hot sensation, while −3 as too cold ambient. The 0 value represents a neutral comfort condition. To consider the satisfaction level of the occupants in an ambient, Fanger developed another equation to relate the PMV to the Predicted Percentage of Dissatisfied (PPD), defined as follows:

$$\mathrm{PPD} = 100 - 95e^{-(0.03353\ \mathrm{PMV}^4 + 0.2179\ \mathrm{PMV}^2)} \tag{2}$$

The TRNBULD comfort subroutine includes the procedure to calculate both PMV and PPD as a function of the ambient climatic condition and the person-specific parameters. Regarding the person-specific parameters, a metabolism rate, clothing insulation and air velocity were taken from ASHRAE Standard 55 [39] as it can be seen in Table 4.

Table 4. Thermal comfort parameters

Parameter	Description	Factor
Clothing factor [clo]	Light summer clothing	0.5
Metabolic rate [met]	Seated, light work	1.2
Air velocity [m/s]	Still air	0.2

Energy model

PES analysis was carried out to investigate the building efficiency potential regarding a suitable Reference Case (RS) considering the electricity, DHW, heating, cooling and freshwater production through conventional technologies. The RS consists of an electric vapor compression Air-Conditioning (AC) for space cooling characterized by an average Coefficient of Performance of $\mathrm{COP}_{\mathrm{Cool,RS}} = 2.5$ [40] and a natural Gas Boiler (GB) for DHW and space heating production with an average conversion thermal efficiency $\eta_{\mathrm{th,RS}} = 0.92$ [29]. The national grid for electric demand features an electrical efficiency $\eta_{\mathrm{el,RS}} = 0.46$ [41]. The freshwater demand ($\dot{m}_{\mathrm{FW,dem}}$) is assumed to be provided by a reverse osmosis desalination plant with a specific consumption of $\epsilon_{\mathrm{RS}} = 4$ kWh/m³ [42]. The PES achieved by the RS is calculated as showed in eq. (3):

$$\mathrm{PES} = \left(\frac{P_{\mathrm{El,dem}}}{\eta_{\mathrm{el,RS}}} + \frac{Q_{\mathrm{DHW,dem}} + Q_{\mathrm{Heat,dem}}}{\eta_{\mathrm{th,RS}}} + \frac{P_{\mathrm{Cool,dem}}}{\mathrm{COP}_{\mathrm{Cool,RS}}\,\eta_{\mathrm{el,RS}}} + \frac{\dot{m}_{\mathrm{FW,dem}}\,\epsilon_{\mathrm{RS}}}{\eta_{\mathrm{el,RS}}}\right)_{\mathrm{RS}} \tag{3}$$

where $P_{El,dem}$ is the building electrical demand which is considered to be withdrawn from the national grid. $Q_{DHW,dem}$, $Q_{Heat,dem}$ and $Q_{Cool,dem}$ are the thermal energy demand required to be supplied by a GB for DHW and space heating and by an AC for space cooling, respectively. Whereas, $\dot{m}_{FW,dem}$ is the total freshwater demand provided by a conventional desalination system.

RESULTS AND DISCUSSION

The outcomes of this work is mostly based on generic power and flow rate profiles for a single-family dwelling for each energy demand. Daily, weekly and yearly time bases were used for instantaneous and integrated results of electricity, heating, cooling, DHW and freshwater demands. All simulations were performed based on a 1-year time period (from 0 h to 8,760 h) with 1-hour time step in order to decrease the simulation running time. Nevertheless, all data reported here can be generated in lower time step or mathematically interpolated. The building thermal comfort was analyzed for two scenarios: without an indoor temperature control and controlled by the setpoint temperature established by the BD-ES. Finally, a PES analysis was carried out in order to present the building efficiency potential and verify its BD-ES compliance.

Daily results

In this section, the daily demand behavior for each demand are discussed. Figure 6 shows the heating and cooling demands. It is important to note that heating demand refers to a day in the winter season (February 1st) whereas the cooling daily demand was taken from the summer (August 1st). During the winter, heating is required in the mornings from 08:00 to 13:00. Users' daily routine (work, school, etc.) and the ambient temperature decrease during the night are responsible for this demand. Conversely, during the summer, the cooling demand is required between 16:00 and 24:00. It also coincides with the users' daily routine (after occupation) and a higher ambient temperature due to longer daylight during this season.

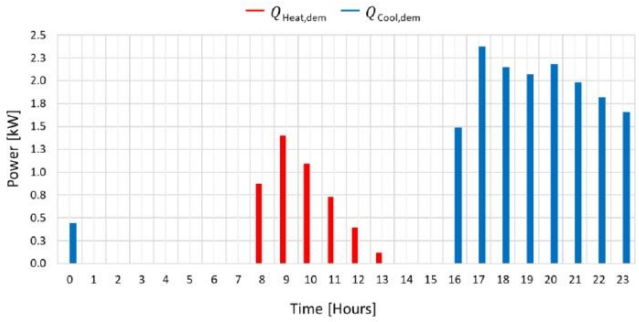

Figure 6. Daily heating and cooling demand

Figure 7 displays the electricity demand profile for January 1st during 24-hours long with 1-hour time step. The greater consumption is shown between 19:00 and 22:00 due to higher occupancy and lighting and appliance use. This period of time represents the daily electric power peak demand.

DHW and freshwater demand profiles were aggregated in Figure 8 based on the data estimated for January 1st. It is worth noting that, DHW has a very characteristic peak at 20:00 due to showering. On the other hand, freshwater is more scattered along the day with a peak at midday (from 11:00 to 12:00) caused mostly by cooking and laundry time.

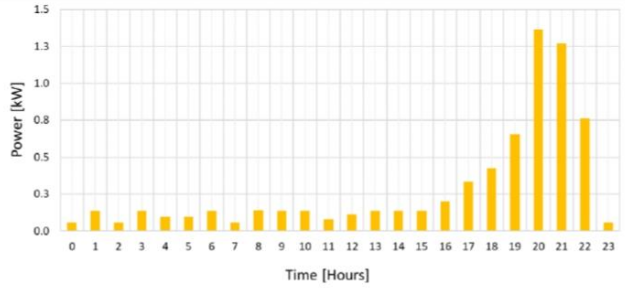

Figure 7. Daily electrical power demand

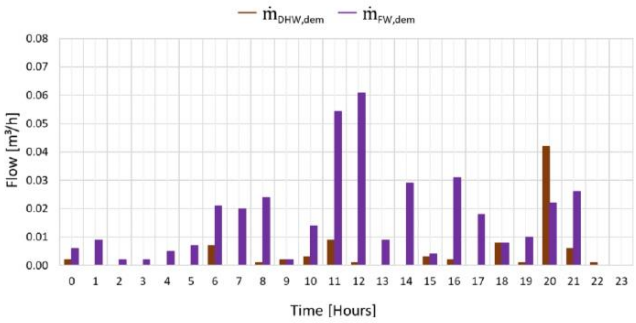

Figure 8. Daily DHW and freshwater flow rate demand

Weekly results

Regarding the weekly demand profile, Figure 9 shows the electrical power consumption for the first week of January. The electricity is the only demand highlighted in this section due to its dissimilar behavior between weekday and weekend. The week ranges from 0 h to 120 h and displays five similar demand patterns, one for each day of the week, as discussed in the previous section. Conversely, the weekend (121 h to 168 h) presents a very different consumption profile. The electricity is used more scattered during the day due to a higher dwelling occupancy and a greater peak is observed between 12:00 and 13:00 (cooking time).

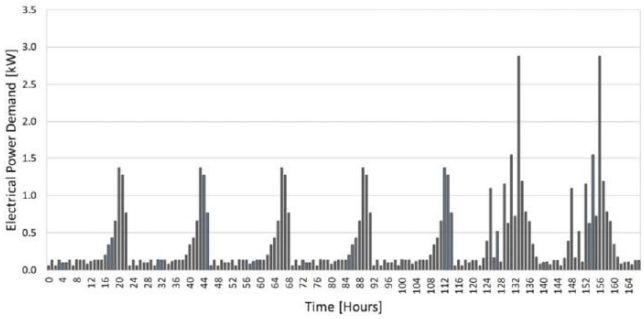

Figure 9. Weekly electrical power demand

Yearly results

In this section, the yearly demand pattern of heating and cooling (Figure 10), electricity (Figure 11), DHW (Figure 12) and freshwater (Figure 13) are displayed with 1-hour time step. In addition, the annual consumption is calculated through a 1-year integration period (form 0 h to 8,760 h). The results of the overall amount of each demand are summarized in Table 5. All yearly demands have been previously validated based on the approach used to generate them.

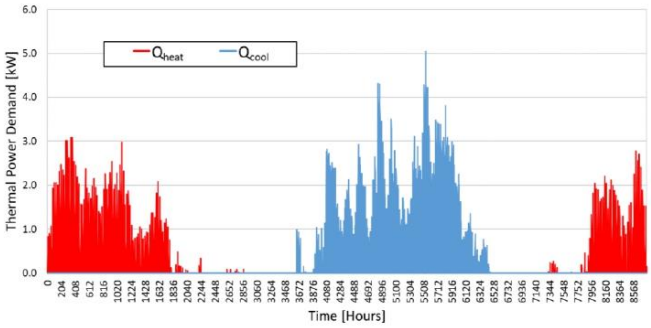

Figure 10. Yearly heating and cooling demand

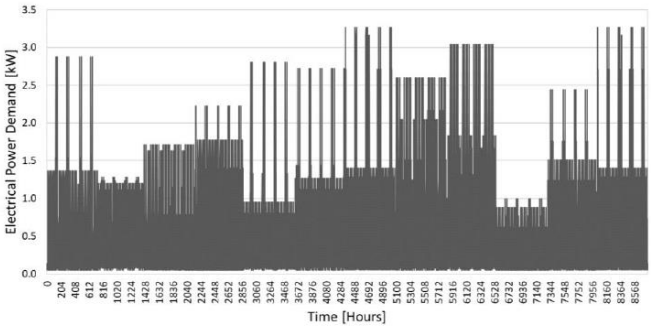

Figure 11. Yearly electricity demand

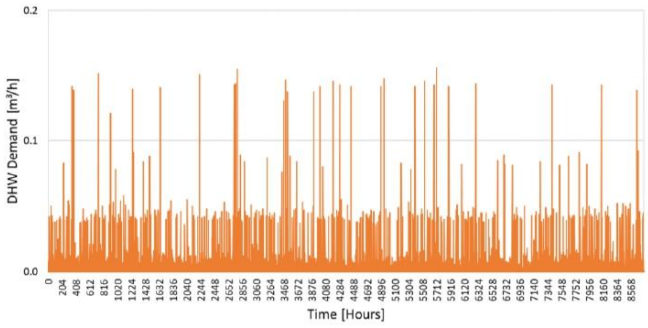

Figure 12. Yearly DHW demand

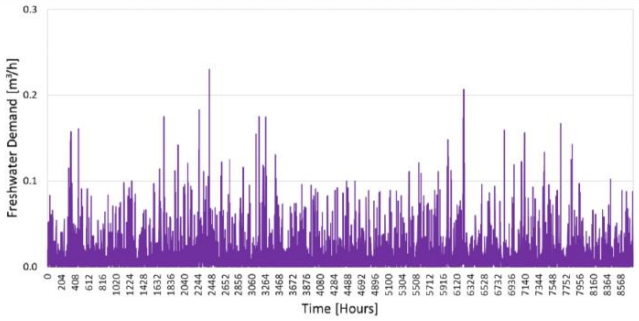

Figure 13. Yearly freshwater demand

Table 5. Yearly results

Parameter	Symbol	Value
Electricity building demand [kWh/y]	$P_{El,dem}$	3,866
DHW building flow demand [m³/y]	$\dot{m}_{DHW,dem}$	41
DHW building thermal demand [kWh/y]	$Q_{DHW,dem}$	2,090
Freshwater building demand [m³/y]	$\dot{m}_{FW,dem}$	110
Cooling building demand [kWh/y]	$Q_{Cool,dem}$	1,450
Heating building demand [kWh/y]	$Q_{Heat,dem}$	941

Figure 10 shows the yearly profile of heating and cooling demand. In particular, the cooling season ranges from June to September and the heating season from October to May. The annual cooling peak (5.05 kW) happens at 18:00 on August 19th, whereas the annual heating peak (3.09 kW) occur at 09:00 on January 8th. The building energy demand of space cooling, $Q_{Cool,dem}$, is 1,450 kWh/y which is higher than the space heating demand $Q_{Heat,dem}$, (941 kWh/y) due to the local weather condition and the setpoint temperature defined by the BD-ES. Nevertheless, the building heating and cooling demands satisfy the BD-ES threshold of 1,650 kWh/y and 2,200 kWh/y for heating and cooling demands, respectively.

Yearly electrical power consumption can be seen at Figure 11. It is important to note that weekly patterns remain constant into a specific month of the year. Spring and autumn seasons present lower difference between weekday and weekend profiles due to the mild temperature of the seasons and more outdoor activities. Summer and winter show higher consumption during the weekend due to higher occupancy and more appliances use. The greater power demands were registered in July and December and an electrical power peak of 3.16 kW was found. In this simulation, October showed the least power consumption along the year. The building electrical power load is due to appliances and lighting use exclusively.

Figure 12 and Figure 13 display the water consumption profile regarding DHW and freshwater, respectively. Both figures show a pattern with lesser season influence all year long because of the constant user need. DHW demand presents a peak of 0.16 m³/h once it considers only a shower. On the other hand, the freshwater consumption can achieve a peak of 0.23 m³/h due to all other building fixtures usage at the same time. Furthermore, the scattered nature of the figures coincide with the distribution of draw offs according to its probability function, duration and time step along the year.

Thermal comfort

First, the building thermal comfort was analyzed without an indoor temperature control, as it can be seen at Figure 14. In this particular case, PMV index ranges from −2

to −3 in the winter season, which is associated to a too cold sensation. In contrast, during the summer, the same index varies up to +2, corresponding to a hot sensation. The PMV is directly related to the PPD index, which establishes the level of building users dissatisfaction. Thus, during the winter 100% of the users are dissatisfied in some occasions, whereas in the summer this dissatisfied percentage varies from 10% to 80%.

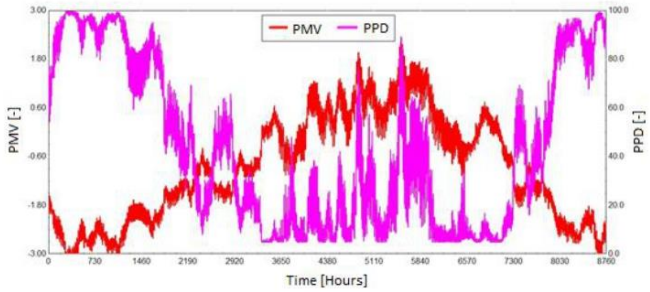

Figure 14. Thermal comfort analysis without temperature control

In order to validate the thermal comfort achieved by the setpoint temperature defined in the BD-ES, another analysis was performed. Figure 15 shows the PMV and PPD indexes. In particular, PMV was considerably improved during summer season, achieving a neutral sensation most of the time and, consequently, reaching up to 90% occupant satisfaction rate. Nevertheless, in the winter, a slightly improvement can be noticed, therefore a cold sensation remains and the level of dissatisfaction is around 80% of the building occupants. According to ASHRAE 55 [39], thermal comfort can be achieved based on 80% occupant satisfaction rate or more. Therefore, applying the BD-ES to the reference case presented in this work, the thermal comfort can only be achieved during the summer season.

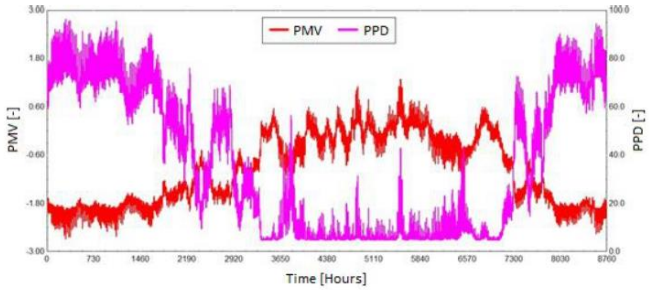

Figure 15. Thermal comfort analysis with temperature control

Primary Energy Saving

The PES applied to the RS was calculated according to eq. (3). Table 6 shows the PES_{RS} breakdown according to the thermal, electrical and freshwater primary energy consumption, as well as the total PES_{RS}.

PES_{RS} achieves up to 13,917 kWh/y for the reference case. It represents a high potential for polygeneration systems application and renewable energy sources usage in the residential sector. Furthermore, the reference case was evaluated according to the maximum non-renewable Primary Energy Consumption ($PEC_{th,max}$) defined by the

BD-ES. For that reason, a thermal Primary Energy Consumption (PEC_{th}) was calculated aggregating all thermal demands (heating, cooling and DHW). In particular, PEC_{th} amounts to 4,556 kWh/y and meets the threshold of 5,400 kWh/y established by the BD-ES.

Table 6. PES breakdown

Demand	Value [kWh/y]
PEC_{th}	4,556
PEC_{el}	8,404
PEC_{FW}	956
PES_{RS}	13,917

CONCLUSIONS

Generic patterns for all energy demands required by the residential sector, in particular a single-family townhouse located at the Mediterranean European side, are presented. Electricity, DHW and fresh water demands were estimated according to parametric algorithms reported in the literature. Whereas, heating and cooling profiles were obtained through a TRNSYS building simulation. All approaches have been previously validated based on statistical and/or experimental data.

Simulations provided reliable data with satisfactory resolution time step along 1-year period. The results were presented in terms of daily, weekly and yearly profiles. Moreover, an annual integration was adopted for all energy demands. The outcomes of the developed study fill a lack of information about residential sector demands found in the literature.

In addition, thermal comfort and PES analysis were performed to validate the reference case against the Spanish normative. The thermal comfort can only be achieved during the summer season. A high percentage of user dissatisfaction was found in the winter. It can be concluded that the BD-ES setpoint temperature assumed for the winter is inadequate to provide thermal comfort satisfaction. PES confirmed the high potential of the residential sector as one of the most significant energy consumers. Furthermore, the maximum non-renewable primary energy consumption defined by the BD-ES was accomplished.

This study can be useful for technicians and policy makers dealing with demand side management as well as polygeneration systems design. The generic energy demand profiles are fully reliable and suitable for realistic simulations in order to integrate and exploit the use of different polygeneration configurations applied to the residential sector. Furthermore, future developments of this work will include a comprehensive analysis of a polygeneration system to supply the reference case demands.

NOMENCLATURE

L	energy loss to the environment	[W/m²]
M	metabolic rate	[W/m²]
$\dot{m}$	mass flow rate	[kg/s]
Q	heat	[kWh]

Greek letters

ϵ	specific consumption	[kWh/m³]
η	efficiency	[-]

Subscripts and superscripts

Cool	cooling
Dem	demand

El	electrical
FW	freshwater
Heat	heating
Max	maximum
Th	thermal

Abbreviations

AC	Air-Conditioning
BES	Building Energy Simulation
CFD	Computational Fluid Dynamics
COP	Coefficient of Performance
CREST	Centre for Renewable Energy Systems Technology
CTE	Technical Construction Code
DB-SE	Basic Document on Energy Savings
DHW	Domestic Hot Water
EU	European Union
GB	Gas Boiler
IEA-SHC	International Energy Agency – Solar Heating and Cooling
ISO	International Organization for Standardization
PEC	Primary Energy Consumption
PES	Primary Energy Saving
PMV	Predicted Mean Vote
PPD	Predicted Percentage of Dissatisfied
RS	Reference System
STREAM	Stochastic Residential Water end use Model
TRNSYS	Transient Systems Simulation

REFERENCES

1. Costa, A., Keane, M. M., Torrens, J. I. and Corry, E., Building Operation and Energy Performance: Monitoring, Analysis and Optimisation Toolkit, *Appl. Energy*, Vol. 101, pp 310-316, 2013, https://doi.org/10.1016/j.apenergy.2011.10.037
2. Poel, B., van Cruchten, G. and Balaras, C. A., Energy Performance Assessment of Existing Dwellings, *Energy Build.*, Vol. 39, No. 4, pp 393-403, 2007, https://doi.org/10.1016/j.enbuild.2006.08.008
3. Europen Commission (EC), EUROPE 2020, A Strategy for Smart, Sustainable and Inclusive Growth, Brussels, Belgium, 2010, https://eur-lex.europa.eu/legal-content/EN/TXT/PDF/?uri=CELEX:52010DC2020&from=en, [Accessed: 07-September-2020]
4. US Department of Energy, Chapter 5: Increasing Efficiency of Building Systems and Technologies, Washington, D. C., USA, 2015, https://www.energy.gov/sites/prod/files/2017/03/f34/qtr-2015-chapter5.pdf, [Accessed: 07-September-2020]
5. Serra, L. M., Lozano, M.-A., Ramos, J., Ensinas, A. V. and Nebra, S. A., Polygeneration and Efficient Use of Natural Resources, *Energy*, Vol. 34, No. 5, pp 575-586, 2009, https://doi.org/10.1016/j.energy.2008.08.013
6. Calise, F., de Notaristefani di Vastogirardi, G., Dentice d'Accadia, M. and Vicidomini, M., Simulation of Polygeneration Systems, *Energy*, Vol. 163, pp 290-337, 2018, https://doi.org/10.1016/j.energy.2018.08.052
7. Roselli, C., Tariello, F. and Sasso, M., Integration of a Photovoltaic System with an Electric Heat Pump and Electrical Energy Storage Serving an Office Building, *J. Sustain. Dev. Energy Water Environ. Syst*, Vol. 7, No. 2, pp 213-228, 2019, https://doi.org/10.13044/j.sdewes.d6.0248

8. Acevedo, L., Uche, J., Del Almo, A., Círez, F., Usón, S., Martínez, A. and Guedea, I., Dynamic Simulation of a Trigeneration Scheme for Domestic Purposes Based on Hybrid Techniques, *Energies*, Vol. 9, No. 12, 1013, 2016, https://doi.org/10.3390/en9121013
9. Ghaem Sigarchian, S., Malmquist, A. and Martin, V., The Choice of Operating Strategy for a Complex Polygeneration System: A Case Study for a Residential Building in Italy, *Energy Convers. Manag.*, Vol. 163, pp 278-291, 2018, https://doi.org/10.1016/j.enconman.2018.02.066
10. Uche, J., Acevedo, L., Círez, F., Usón, S., Martínez-Gracia, A. and Bayod-Rújula, Á. A., Analysis of a Domestic Trigeneration Scheme with Hybrid Renewable Energy Sources and Desalting Techniques, *J. Clean. Prod.*, Vol. 212, pp 1409-1422, 2019, https://doi.org/10.1016/j.jclepro.2018.12.006
11. Buonomano, A., Calise, F., Palombo, A. and Vicidomini, M., Energy and Economic Analysis of Geothermal-Solar Trigeneration Systems: A Case Study for a Hotel Building in Ischia, *Appl. Energy*, Vol. 138, pp 224-241, 2015, https://doi.org/10.1016/j.apenergy.2014.10.076
12. Calise, F., Dentice d'Accadia, M., Figaj, R. D. and Vanoli, L., A Novel Solar-Assisted Heat Pump Driven by Photovoltaic/Thermal Collectors: Dynamic Simulation and Thermoeconomic Optimization, *Energy*, Vol. 95, pp 346-366, 2016, https://doi.org/10.1016/j.energy.2015.11.071
13. Angrisani, G., Entchev, E., Roselli, C., Sasso, M., Tariello, F. and Yaïci, W., Dynamic Simulation of a Solar Heating and Cooling System for an Office Building Located in Southern Italy, *Appl. Therm. Eng.*, Vol. 103, pp 377-390, 2016, https://doi.org/10.1016/j.applthermaleng.2016.04.094
14. Calise, F., Thermoeconomic Analysis and Optimization of High Efficiency Solar Heating and Cooling Systems for Different Italian School Buildings and Climates, *Energy Build.*, Vol. 42, No. 7, pp 992-1003, 2010, https://doi.org/10.1016/j.enbuild.2010.01.011
15. Gierek, A., EU Report About the Strategy for Heating and Cooling (in Portuguese), European Parliament, Industry, Research and Energy Commission, Strasbourg, France, 2016, https://www.europarl.europa.eu/doceo/document/A-8-2016-0232_PT.html, [Accessed: 07-September-2020]
16. Foucquier, A., Robert, S., Suard, F., Stéphan, L. and Jay, A., State of the Art in Building Modelling and Energy Performances Prediction: A Review, *Renew. Sustain. Energy Rev.*, Vol. 23, pp 272-288, 2013, https://doi.org/10.1016/j.rser.2013.03.004
17. Saltelli, A., Ratto, M., Andres, T., Campolongo, F., Cariboni, J., Gatelli, D., Saisana, M. and Tarantola, S., *Global Sensitivity Analysis: The Primer*, John Wiley & Sons, Hoboken, New Jersey, USA, 2008.
18. Coakley, D., Raftery, P. and Keane, M., A Review of Methods to Match Building Energy Simulation Models to Measured Data, *Renew. Sustain. Energy Rev.*, Vol. 37, pp 123-141, 2014, https://doi.org/10.1016/j.rser.2014.05.007
19. Yoshino, H., Hong, T. and Nord, N., IEA EBC Annex 53: Total Energy Use in Buildings—Analysis and Evaluation Methods, *Energy Build.*, Vol. 152, pp 124-136, 2017, https://doi.org/10.1016/j.enbuild.2017.07.038
20. Karlsson, F., Rohdin, P. and Persson, M.-L., Measured and Predicted Energy Demand of a Low Energy Building: Important Aspects when Using Building Energy Simulation, *Build. Serv. Eng. Res. Technol.*, Vol. 28, No. 3, pp 223-235, 2007, https://doi.org/10.1177/0143624407077393
21. Richardson, I., Thomson, M., Infield, D. and Clifford, C., Domestic Electricity Use: A High-Resolution Energy Demand Model, *Energy Build.*, Vol. 42, No. 10, pp 1878-1887, 2010, https://doi.org/10.1016/j.enbuild.2010.05.023

22. Carvalho, M., Thermoeconomic and Environmental Analyses for the Synthesis of Polygeneration Systems in the Residential-Commercial Sector, *Ph.D. Thesis*, Universidad de Zaragoza, Zaragoza, Spain, 2011.
23. TRNSYS: A Transient System Simulation Program, Solar Energy Laboratory, University of Wisconsin, Madison, Wisconsin, USA, 2006.
24. Lemos, L. F. L., Starke, A. R., Boland, J., Cardemil, J. M., Machado, R. D. and Colle, S., Assessment of Solar Radiation Components in Brazil Using the BRL Model, *Renew. Energy*, Vol. 108, pp 569-580, 2017, https://doi.org/10.1016/j.renene.2017.02.077
25. Duffy, M. J., Hiller, M., Bradley, D. E., Keilholz, W. and Thornton, J. W., TRNSYS – Features and Functionalitity for Building Simulation, *Proceedings of the 11th International IBPSA Conference*, p 5, Glasgow, Scotland, July 27-30, 2009.
26. Murugan, S. and Horák, B., A Review of Micro Combined Heat and Power Systems for Residential Applications, *Renew. Sustain. Energy Rev.*, Vol. 64, pp 144-162, 2016, https://doi.org/10.1016/j.rser.2016.04.064
27. OpenStudio Plugin for Google SketchUp3D, 2009, https://www.openstudio.net, [Accessed: 07-September-2020]
28. Google SketchUp is a Registered Trademark, 2009, https://www.sketchup.com/, [Accessed: 07-September-2020]
29. Technical Building Code (CTE), Basic Document Energy Saving (in Spanish), 2017, https://www.codigotecnico.org/pdf/Documentos/HE/DBHE.pdf, [Accessed: 07-September-2020]
30. Technical Building Code (CTE), Basic Document of Health' (in Spanish), 2019, https://www.codigotecnico.org/pdf/Documentos/HS/DBHS.pdf, [Accessed: 07-September-2020]
31. Rodríguez Trejo, S., Building Ventilation Characterization. Trade-Off Between Indoor Air Quality and Energy Rehabilitation Efficiency' (in Spanish), *Ph.D. Thesis*, University of Madrid, Madrid, Spain, 2016.
32. Jordan, U. and Vajen, K., Tool for the Generation of Domestic Hot Water (DHW) Profiles on a Statistical Basis Version 2.02b, Manual, p 22, 2017.
33. Barbu, M., Darie, G. and Siroux, M., Analysis of a Residential Photovoltaic-Thermal (PVT) System in Two Similar Climate Conditions, *Energies*, Vol. 12, No. 19, 3595, 2019, https://doi.org/10.3390/en12193595
34. Influence of the DHW Load Profile on the Fractional Energy Savings: A Case Study of a Solar Combi-System with TRNSYS Simulations, *Fuel Energy Abstr.*, Vol. 43, No. 3, p 200, 2002, https://doi.org/10.1016/S0140-6701(02)85844-1
35. Cominola, A., Giuliani, M., Castelletti, A., Rosenberg, D. E. and Abdallah, A. M., Implications of Data Sampling Resolution on Water Use Simulation, End-Use Disaggregation, and Demand Management, *Environ. Model. Soft.*, Vol. 102, pp 199-212, 2018, https://doi.org/10.1016/j.envsoft.2017.11.022
36. Cominola, A., Giuliani, M., Castelletti, A., Abdallah, A. M. and Rosenberg, D. E., Developing a Stochastic Simulation Model for the Generation of Residential Water End-Use Demand Time Series, *Proceedings of the 8th International Congress on Environmental Modelling and Software (iEMSs 2016)*, p 9, Toulouse, France, 2016.
37. International Organization for Standardization (ISO), ISO 7730:1994, Moderate Thermal Environments – Determination of the PMV and PPD Indices and Specification of the Conditions for Thermal Comfort, ISO Standard, p 26, Geneva, Switzerland, 1994.
38. Fanger, P., *Thermal Comfort: Analysis and Applications in Environmental Engineering*, Danish Technical Press, Copenhagen, Denmark, 1970.

39. American Society of Heating, Refrigerating and Air-Conditioning Engineers (ASHRAE), Standard 55 – Thermal Environmental Conditions for Human Occupancy, Peachtree Corners, Georgia, USA, 2013.
40. Calise, F., Dentice d'Accadia, M., Libertini, L., Quiriti, E. and Vicidomini, M., A Novel Tool for Thermoeconomic Analysis and Optimization of Trigeneration Systems: A Case Study for a Hospital Building in Italy, *Energy*, Vol. 126, pp 64-87, 2017, https://doi.org/10.1016/j.energy.2017.03.010
41. Carotenuto, A., Figaj, R. D. and Vanoli, L., A Novel Solar-Geothermal District Heating, Cooling and Domestic Hot Water System: Dynamic Simulation and Energy-Economic Analysis, *Energy*, Vol. 141, pp 2652-2669, 2017, https://doi.org/10.1016/j.energy.2017.08.084
42. Jia, X., Klemeš, J., J., Varbanov, P. S. and Wan Alwi, S. R., Analyzing the Energy Consumption, GHG Emission, and Cost of Seawater Desalination in China, *Energies*, Vol. 12, No. 3, 463, 2019, https://doi.org/10.3390/en12030463

Paper submitted: 03.06.2020
Paper revised: 07.09.2020
Paper accepted: 08.09.2020

A.1 Paper III

sustainability

MDPI

Article

A Novel Polygeneration System Based on a Solar-Assisted Desiccant Cooling System for Residential Buildings: An Energy and Environmental Analysis

Luis Gabriel Gesteira * and Javier Uche

CIRCE Research Institute, University of Zaragoza, 50018 Zaragoza, Spain; javiuche@unizar.es
* Correspondence: 773948@unizar.es

Abstract: This work aims to design and dynamically simulate a polygeneration system that integrates a solar-assisted desiccant cooling system for residential applications as an alternative to vapor compression systems. The overall plant layout supplies electricity, space heating and cooling, domestic hot water, and freshwater for a single-family townhouse located in the city of Almería in Spain. The leading technologies used in the system are photovoltaic/thermal collectors, reverse osmosis, and desiccant air conditioning. The system model was developed and accurately simulated in the TRNSYS environment for a 1-year simulation with a 5-min time step. Design optimization was carried out to investigate the system's best configuration. The optimal structure showed a satisfactory total annual energy efficiency in solar collectors of about 0.35 and about 0.47 for desiccant air conditioning. Coverage of electricity, space heating and cooling, domestic hot water, and freshwater was 104.1%, 87.01%, 97.98%, 96.05 %, and 100 %, respectively. Furthermore, significant ratios for primary energy saving, 98.62%, and CO_2 saving, 97.17%, were achieved. The users' thermal comfort level was satisfactory over the entire year. Finally, a comparison with an alternative coastal site was performed to extend the polygeneration system's applicability.

Keywords: residential sector; renewable energy; polygeneration system; desiccant air conditioning; TRNSYS; sustainability

Citation: Gesteira, L.G.; Uche, J. A Novel Polygeneration System Based on a Solar-Assisted Desiccant Cooling System for Residential Buildings: An Energy and Environmental Analysis. *Sustainability* **2022**, *14*, 3449. https://doi.org/10.3390/su14063449

Academic Editors: Francesco Liberato Cappiello, Francesco Calise and Maria Vicidomini

Received: 22 February 2022
Accepted: 14 March 2022
Published: 15 March 2022

1. Introduction

In the past half century, population growth and economic development improved awareness about the environmental burdens of conventional energy systems. It directed the research community and governments' attention to alternative energy sources to cope with the increasing energy demand, global climate change, and high levels of greenhouse gas emissions. In recent years, the International Energy Agency (IEA) [1] and the European Union (EU) [2] focused on energy consumption, particularly related to buildings. In 2016, the European Commission developed guidelines for promoting nearly zero-energy buildings (NZEBs) [3], as the building sector is responsible for about 40% of global energy consumption and more than 30% of greenhouse gas emissions [4]. Furthermore, around 75% of buildings are energy inefficient, and 80% of their energy efficiency potential remains an opportunity to explore economic gains, energy security improvements, and environmental protection [5].

In this framework, the application of polygeneration systems within buildings presents an exciting alternative for energy consumption reduction and, consequently, the accomplishment of the NZEBs target [6]. Several research works are available in the literature studying polygeneration systems integrated into diverse building types such as hotels [7], hospitals [8], residences [9], districts [10], offices [11], schools [12], etc., and evaluating the systems' performance with dynamic simulation tools that take into account the buildings' main demands.

Polygeneration systems can achieve more than 80% of energy savings with an appropriate level of energy integration, especially in warm areas such as the European Mediterranean countries [13]. It can replace conventional technologies based on fossil fuels and simultaneously produce several energy services by significantly reducing primary energy consumption and CO_2 emissions. The configuration of polygeneration systems can also vary widely to be suitable for different applications. Input energy may be renewable or non-renewable, while outputs are mainly electricity, heating, cooling, chemicals, liquid or gaseous fuels, and potable water. According to its performance goals, assessments are based on three indicators, i.e., technical, economic, and environmental [14].

Many researchers have evaluated such polygeneration systems using a broad assortment of superstructures and assessment procedures. A polygeneration scheme providing power, heat, and water for a single dwelling was studied in-depth by the authors some years ago. Acevedo et al. [15] designed a system combining photovoltaic/thermal collectors, an evacuated tube collector, and a wind turbine. The system also included two desalination technologies and two types of energy storage devices. Coverage of hot water, freshwater, and power was 99.3%, 100%, and 70%, respectively. Uche et al. [16] reported an experimental study of the same polygeneration system. Those tests showed that daytime assessments of power, freshwater, and sanitary hot water allowed for excellent coverage of scheduled energy and water demands. Flexible operation due to the combined production of power and heat was also observed. An environmental assessment of the pilot unit and its life cycle showed low impacts concerning the conventional supply of energy and water. Finally, Usón et al. [17] investigated the exergy and exergy cost of the previous polygeneration system. The system showed an exergy efficiency of 7.76% in the base case.

Currently, the most deployed cooling technologies in polygeneration systems are vapor compression (VC) systems and absorption (AB) and adsorption (AD) chillers. Besides its high COP, VC systems use harmful refrigerants with global warming and/or ozone depletion potential. Thus, it is not a sustainable option. AB and AD chillers are large and complex, constraining their use in domestic building applications [18]. An alternative cooling technology for small-scale units is desiccant air conditioning (DAC), demonstrating several advantages in operation life, maintenance, and efficiency [18]. A desiccant cooling system uses the capability of desiccant materials to remove moisture from an air stream by a natural adsorption process. Thus, it can achieve thermal comfort for buildings since it can control the sensible and latent loads separately and, consequently, improve the Indoor Air Quality (IAQ) [19].

The recent literature shows a significant research effort regarding various desiccant cooling system configurations. Jani et al. [20] simulated a system with a hybrid desiccant wheel using different configurations for hot and humid climatic conditions. Experimental measurements also observed the influence of operating parameters on system performance. Simulated results were validated as being a good match with the experimentally measured data. Elgendy et al. [21] performed a simulation study on desiccant air conditioning with direct and indirect evaporative coolers using TRNSYS [22]. The study found that desiccant cooling systems with an indirect evaporative cooler have a higher COP. Angrisani et al. [23] examined the desiccant cooling system with three different configurations for the climatic conditions of Italy and compared the performance with the conventional air conditioning system. It was found that 20–25% of primary energy savings can be achieved while CO_2 emissions can also be reduced up to 35–40%. Sopian et al. [24] investigated the desiccant cooling system with one and two stages and in ventilation and recirculation configurations, performed in the TRNSYS [22] simulation studio for Malaysia's hot and humid weather conditions. The two-stage ventilation mode was the best among the other arrangements, presenting a COP of up to 1.06.

Thermal energy sources at low and medium temperatures, typically within 50–80 °C, and obtainable by solar collectors are often used as inputs in DAC applications [25]. Thus, a solar-assisted desiccant cooling system can promote environmental pollution reduction and energy consumption savings. Furthermore, it can also significantly contribute to

the implementation of NZEBs [26]. In particular, Farooq et al. [27] studied dynamic simulation and performance parameters for three ventilation schemes of a DAC based on a photovoltaic-thermal solar collector for the weather of Lahore in Pakistan. The primary energy savings, solar fraction, and thermal efficiency of the solar collector were used to compare its performances. A dynamic analysis of a solar desiccant cooling system was performed by Heidari et al. [28] to produce the cooling effect and freshwater for domestic use. The simulation results showed that the proposed system could provide a comfortable temperature in a hot and humid climate. The system led to an 18.7% saving of CO_2 emissions over a month and economic feasibility, with a payback period of 3 years.

Finally, industrial applications have studied the leading solar cooling technologies integrated into polygeneration schemes for cooling, heating, electricity, and desalinated water production [29]. Thus, it calls for an improvement of existing optimization approaches that considers the synthesis of polygeneration systems supported by renewable energy sources for building applications [30]. Therefore, this study analyses an installation's energy and environmental feasibility in supplying the five demands of a dwelling, as well as its design optimization.

2. Materials and Methods

2.1. System Layout

A simplified layout of the system under investigation in this paper is shown in Figure 1. The proposed system serves a residential building. The technologies included in the system are a photovoltaic/thermal (PVT) collector for electricity and heating, thermal energy storage (TES), reverse osmosis (RO) for freshwater and hot sanitary water demands, and desiccant air conditioning (DAC) for cooling. Additional components were implemented in the system, such as pumps, pipes, heat sinks, etc. The design parameters for all system components were accurately selected to allow the system to operate correctly. In particular, set-point temperatures and dead temperature bands for the components were chosen to minimize the number of on–off events. Pipes simulate the ductwork.

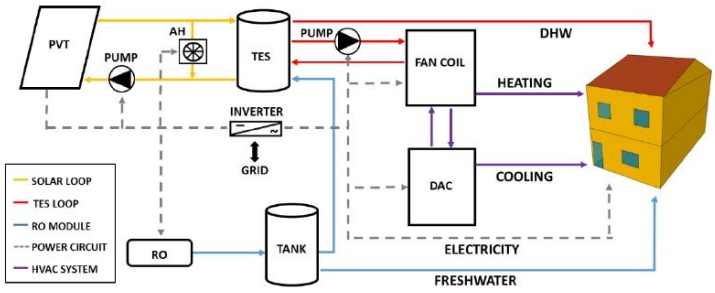

Figure 1. Polygeneration system layout.

The main subsystems included in the system are detailed as follows:

2.1.1. Solar Loop

Solar irradiation is converted into electrical and thermal energy through the PVT collectors. A fixed slope of 35° (no tracking) provides the best irradiation yield for the location of Almería in Spain, according to the Meteonorm weather data simulation. The solar thermal energy produced heats up the solar collector fluid (SCF) circulating through the PVTs. The SCF used in the system is a mixture of water/glycol (60/40). The SCF flow rate of the fixed speed pump is regulated by a controller activated when the PVTs outlet temperature, $T_{out,PVT}$, is 7 °C higher than the temperature at the bottom of the thermal energy storage (TES), $T_{bottom,TES}$, and deactivated when this temperature difference

reaches 2 °C. Thus, the controller stops the pump, preventing the dissipation of the tank's thermal energy.

2.1.2. TES Loop

The thermal energy storage mitigates the fluctuations due to solar radiation variability. It consists of a fluid-filled sensible vertically stratified (4 nodes) energy storage tank with a heat exchanger inside. To avoid the SCF overheating and the PVT electrical efficiency decreasing, a thermostat controls the TES's top temperature with a fixed set point, i.e., $T_{top,TES}$. An air heater (AH) cools the SCF down whenever the PVT's outlet temperature increases the $T_{top,TES}$ over the set point. The heating dissipation capacity of the AH is 20 kW. The TES outputs feed the HVAC system and the DHW simultaneously.

Regarding the DHW, a tempering valve mixes the hot water from the TES with the freshwater from the desalinated water tank. It regulates the outlet temperature for the DHW, $T_{out,DHW}$, equal to 45 °C. The HVAC system provides heating during winter and cooling during summer.

2.1.3. Power Circuit

The electricity system consumption is mostly comprised of the building's electric demand and includes the power loads of pumps, fans, some DAC components, and the RO device. The PVT collector's power is connected to an inverter with peak-power tracking. The inverter converts the DC power from generation to AC and sends it to electric devices. It allows for the purchase and sale of the power back to the utility. When the power produced is higher than the power demand, the surplus power is delivered to the national electric grid. When the energy produced is insufficient to match the power demand, the power is withdrawn from the grid. The grid works as a backup due to the solar collector's intermittent behavior and the non-simultaneity between production and consumption [30].

Furthermore, batteries for these facilities are expensive and require significant maintenance [31]. For simplicity, we assumed an annual near-zero energy balance for the electricity demand. However, as an economic analysis of this study was not performed, a deep discussion on pricing policies was neglected. Detailed analysis on residential sector regulation in Spain is reported by Pinto et al. [32].

2.1.4. RO Module

Membrane-based technology is the most efficient seawater desalination technology due to its comparatively low energy consumption and high salt rejection [33]. Thus, RO seawater desalination was selected to integrate the polygeneration system to provide freshwater. The RO module requires DC power consumption of 110 W, and produces 35 kg/h of freshwater; thus, it presents 3.14 kWh/m^3 of specific consumption [16]. According to its steady performance, the RO module is simulated as a forcing function of power load and freshwater flow instead of a new model type. Thus, it exclusively depends on the electricity, which the grid can attend to, as previously explained. The desalinated water is sent to a tank of 1.0 m^3, and a simple controller prevents overfilling and allows a minimum water capacity of 0.1 m^3.

2.1.5. HVAC System

The TES supplies thermal energy whenever the user requires heating or cooling throughout the year to meet the building HVAC demand. A thermostat inside the thermal building zone controls the setpoint for heating, $T_{set,heat}$, and cooling, $T_{set,cool}$, with a dead band of 2 °C. The seasons of the year activate a single-speed pump to supply hot water for the heating coil or regenerator. In the winter period (from 1 October to 31 May), the thermal energy produced by the PVTs is directly exploited for building space heating through the heating coil. On the other hand, during summer (from 1 June to 30 September), the regenerator uses the PVT's heat energy to drive a DAC system and provide building-space cooling. In addition, the fan airflow calculation is based on the ASHRAE recommendations,

as explained in Ref. [22]. The equation considers the peaks of the heating and cooling demands to calculate the airflow.

2.2. System Model

The proposed system is developed and dynamically simulated in the TRNSYS environment (version 18). It includes several subsystems listed in the previous section. The subsystems are linked to each other to perform the overall system simulation. Some component models are taken from the build-in library of types (e.g., pumps, valves, mixers, diverters, tanks, etc.). Others are user-defined, such as schedulers, controllers, and input data readers. Moreover, the simulation also includes many additional components required to run the simulations and process the results, such as calculators, weather data readers, integrators, and plotters. All main types used in the proposed system model are listed in Table 1.

Table 1. TRNSYS main types used in the proposed system model.

Type	Number	Type	Number
Weather data reader	15	Building	56
Photovoltaic/thermal collector	50	Single-speed fan	146
Inverter	48	Desiccant wheel	716
Fixed flow pump	114	Evaporative coolers	506
Diverter	11	Heat recovery wheel	760
Mixer	11	Heating coil	670
Pipes	31	Thermostats	113, 166
Tanks	39,156	Differential controller	165

In this section, for the sake of brevity, only a detailed description of the PVT collector, the DAC system, and the thermal comfort and energy models are reported. A detailed description of the other component models used in the simulation is omitted; however, it is available in the TRNSYS's component mathematical reference [22]. The technical data concerning the design and operating parameters of the main types are presented in Table 2.

Table 2. Main design and operation parameters.

Type	Parameter	Symbol	Value	Unit
	Solar Loop			
PVT	Slope	θ_S	35	°
	Azimuth	θ_A	0	°
	PVT fin efficiency factor	f_P	0.96	–
	SCF specific heat	c_f	3.89	kJ/kg K
	Collector plate absorptance	α	0.92	–
	Collector plate emittance	ε_p	0.85	–
	Collector loss coefficient	U	16	kJ/h m^2 K
	Transmission-absorption product	$(\tau\alpha)$	0.85	–
	PV efficiency temperature coefficient	β_{PV}	0.0032	1/°C
	PV efficiency reference temperature	T_{ref}	25	°C
	PVT packing factor	P_f	0.8	–
	PV electrical efficiency at Tref	$\eta_{PV,\,ref}$	0.16	–
Air heater	Heat dissipation capacity	Q_{AH}	20	kW
	Effectiveness	ε_{AH}	0.7	–
	Nominal air flow rate	m_{AH}	1716	kg/h
	Power consumption	P_{AH}	0.12	kWh
Pump 1	Nominal flow rate per PVT area	m_f /A_{PVT}	50	kg/h m^2
	Overall efficiency	$\eta_{p,1}$	0.8	–
	Power consumption	$P_{p,1}$	0.025	kWh

Table 2. *Cont.*

Type	Parameter	Symbol	Value	Unit
	TES loop			
TES	TES volume/PVT area	V_{TES}/A_{PVT}	0.1	m^3/m^2
	Number of nodes	n_{TES}	4	–
	Height	h_{TES}	2	m
	Loss coefficient	H	2.5	kJ/h m^2 K
Pump 2	Nominal flow rate	m_w	236	kg/h
	Overall efficiency	$\eta_{p,2}$	0.8	–
	Power consumption	$P_{p,2}$	0.01	kWh
	HVAC system			
DW	F1 Effectiveness	η_{F1}	0.08	–
	F2 Effectiveness	η_{F2}	0.95	–
HRW	Sensible effectiveness	ε_{HRW}	0.8	–
	Power consumption	P_{HRW}	0.18	kWh
DEC	Saturation efficiency	ε_{DEC}	0.85	–
	Power consumption	P_{DEC}	0.08	kWh
HX	Effectiveness	ε_{HX}	0.85	–
Fan	Air flow rate	m_a	963.6	kg/h
	Motor efficiency	η_a	0.84	–
	Power consumption	P_a	0.12	kWh
	RO module			
RO	Power consumption	P_{RO}	0.11	kWh
	Freshwater production	X_{RO}	0.035	m^3/h
	Tank volume	V_{TK}	1.0	m^3
	Power circuit			
Inverter	Efficiency	η_i	0.9	–

2.2.1. PVT Collector Model

The PVT collectors combine photovoltaic panels, PV, and solar thermal collectors, SC, in a unique sheet-and-tube collector with a PV module over the absorber [34]. It consists of a set of components: a glass cover, a PV film encapsulated in the absorber, flow channels, and thermal insulation [35].

The PVT component has eight operational modes in the TRNSYS library, which vary the calculation method for the thermal loss coefficient and cover transmittance. Type 50, mode 2, simulates a flat-plate photovoltaic thermal solar collector component with a single glazing sheet [22]. The model considers losses as a function of the temperature, wind speed and geometry, and constant cover transmittance. PV cell average temperature, T_{cell}, is calculated through an energy balance according to the modified Hottel–Whillier–Bliss equations [22]. The model calculates PVT electrical efficiency as a linear function of the T_{cell}, as follows in Equation (1):

$$\eta_{PV} = \eta_{PV,ref}\,[1 - \beta_{PV}\cdot(T_{cell} - T_{ref})] \quad (1)$$

$\eta_{PV,ref}$ is the reference efficiency of the PV module, βPV is a temperature coefficient, and T_{ref} is the reference temperature.

The thermal efficiency of the collector is expressed according to Equations (2) and (3):

$$\eta_{th} = FR\cdot(\tau\alpha) - FR\cdot U\cdot\frac{(T_{in} - T_{amb})}{G} \quad (2)$$

$$FR = \frac{m_f\cdot c_f}{U\cdot A_{PVT}}\cdot\left[1 - \exp\left(-\frac{U\cdot A_{PVT}\cdot F'}{m_f\cdot c_f}\right)\right] \quad (3)$$

A_{PVT} is the PVT collector area, T_{amb} is the ambient temperature, T_{in} is the inlet temperature, U is the overall collector heat loss, ($\tau\alpha$) is the transmission-absorption product, and G is the solar radiation. FR is the heat removal efficiency factor given as a function of the average mass flow rate (m_f), the heat capacity of the flowing medium (c_f), and the fin efficiency factor (F′) [36].

Finally, the PVT design parameters chosen for the case study analyzed in this paper are taken from Refs. [37,38] and are listed in Table 2.

2.2.2. Desiccant Air Conditioning Model

DAC is a cooling system that regulates both the temperature and moisture of the air supplied to a building. Thus, it can provide thermal comfort and hygienic conditions [39]. The most common configuration refers to the ventilation mode, enabling 100% indoor air renewal of the building, as seen in Figure 2.

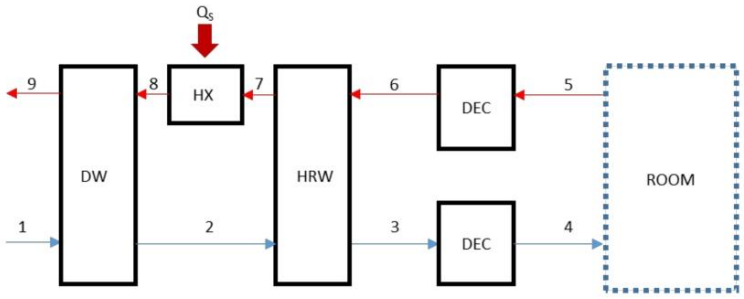

Figure 2. Desiccant air conditioning system (ventilation mode).

A complete desiccant air conditioning system is comprised of a desiccant wheel (DW), two direct evaporative coolers (DEC), and a heat recovery wheel (HRW). The system's operation starts with the DW dehumidifying and heating a supply of ambient air stream (1). At state (2), the process's airflow enters the HRW and is cooled down until state (3). It then passes through a DEC to be cooled down again and humidified, achieving the building's required thermal comfort conditions (4). In the counter flow, the building's exhaust air stream (5), dependent on the internal thermal load, enters the second DEC, where this airflow is first cooled down and then humidified to state (6). Thus, it can absorb sensible heat from the hot and dry process air stream through the HRW (7). At this point, the exhausted airflow needs to reach the regeneration temperature to provide for the DW regeneration. It is achieved by a heat exchanger (HX), releasing a flow at state (8).

Regarding the regeneration heat source, temperatures in the range of 50–80 °C present satisfactory effectiveness. Thus, it allows low-temperature solar thermal energy exploitation, such as with PVT collectors. Finally, the exhaust's air stream passes through the DW. It is cooled, humidified, and released to the environment at state (9) [25].

Another cycle also referred to in the relevant literature is the recirculation mode. According to this configuration (Figure 3), the supply airstream consists of the building's conditioned air.

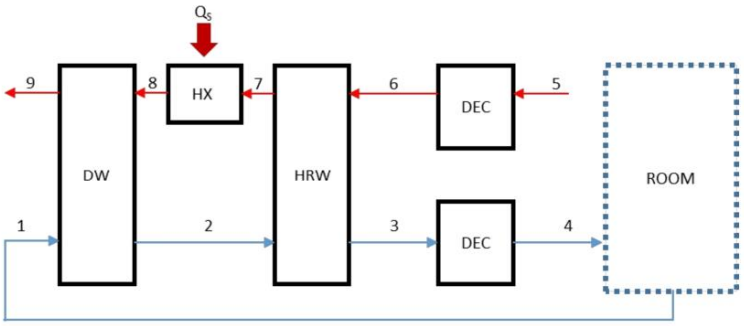

Figure 3. Desiccant air conditioning system (recirculation mode).

The DAC needs five model types for its proper operation in TRNSYS. Types 716 (desiccant wheel), 760 (heat recovery wheel), 506 (direct evaporative cooler), and 670 (heating coil) were used to perform the desiccant cooling system simulation. The DAC design parameters chosen are taken from Panaras et al. [25] and are listed in Table 2.

The main models included in the DAC system are detailed as follows:

Desiccant Wheel

The process's air stream flows through the desiccant material, which retains the moisture of the air. The desiccant capacity of this material can be restored through its regeneration. Type 716 models a rotary desiccant dehumidifier containing nominal silica gel whose performance is based on equations developed by Jurinak [40] for F1 and F2 potentials (ip = 1,2,8):

$$F1_{ip} = \frac{-2865}{(T_{ip} + 273.15)^{1.49}} + 4.344 \times \left(\frac{w_{ip}}{1000}\right)^{0.8624} \quad (4)$$

$$F2_{ip} = \frac{(T_{ip} + 273.15)^{1.49}}{6360} - 1.127 \times \left(\frac{w_{ip}}{1000}\right)^{0.07969} \quad (5)$$

$$\eta F_1 = \frac{F1_2 - F1_2}{F1_8 - F1_1} \quad (6)$$

$$\eta F_2 = \frac{F2_2 - F2_1}{F2_8 - F2_1} \quad (7)$$

It is important to note that the efficiency factor η_{F1} represents the process's approximation to an adiabatic one, whereas the η_{F2} expresses the dehumidification degree.

Heat Recovery Wheel

Type 760 uses the constant effectiveness –minimum capacitance approach (ε_{HRW}) to model this air-to-air heat exchanger. It should be noted that it transfers only sensible energy during its operation [41]:

$$\varepsilon_{HRW} = \frac{T_2 - T_3}{T_2 - T_6} = \frac{T_6 - T_7}{T_6 - T_2} \quad (8)$$

Direct Evaporative Cooler

This model (Type 506) cools an inlet air stream by passing it through a wetted surface, evaporating the water from the surface, and cooling the air stream in the process. The ideal exiting air state for a DEC is if it exits with a dry-bulb temperature equal to its inlet

wet-bulb temperature. It takes the humidity efficiency of the device to calculate the air outlet conditions [22]:

$$\varepsilon_{DEC} = \frac{T_{ip} - T_{ip+1}}{T_{ip} - T_{wb,ip}} \quad (9)$$

ip = 3 for the supply stream humidifier and ip = 5 for the exhaust stream humidifier, and wb is the wet-bulb temperature. Furthermore, Type 506 considers the DEC water consumption as negligible.

Heat Exchanger

Type 670 simulates an air-heating coil (regenerator). The exhausted airflow is heated to provide for the regeneration of the desiccant wheel. It takes the full effectiveness of the device to reach the regeneration temperature. It can be stated that desiccant systems present good thermal effectiveness for a range of regeneration temperatures relevant to the use of simple flat-plate solar collectors [25].

Finally, the coefficient of performance (COP) of the desiccant cooling system is evaluated for the ventilation mode [42]. The purpose of the machine is to cool the building, and to this end, it consumes the regeneration energy:

$$COP = \frac{m_{a,sup} \cdot (h_5 - h_4)}{m_{a,ret} \cdot (h_8 - h_7)} \quad (10)$$

If recirculation mode is considered, the enthalpy of state 5 is replaced by state 1.

2.2.3. Thermal Comfort

TRNSYS includes a built-in subroutine to perform the thermal comfort analysis of building users. This model is developed according to the International Standard Organization's (ISO) 7730 standard [43], described in detail by Fanger [44]. It establishes a statistical correlation between the Predicted Mean Vote (PMV) thermal comfort index and the thermal load acting on the human body:

$$PMV = L\,(0.0303e^{-0.036\,M} + 0.028) \quad (11)$$

The PMV index is calculated according to the energy loss to the environment (L) and the user's metabolic rate (M). It predicts a group of occupants' ambient thermal comfort sensation by the mean value of votes. The index is translated as +3 for a too-hot sensation and −3 for a too-cold feeling. The 0 value represents a neutral comfort condition. To measure the satisfaction level of the occupants in an ambient setting, Fanger developed the Predicted Percentage of Dissatisfied (PPD) index, defined as follows:

$$PPD = 100 - 95e^{-(0.03353\,PMV^4 + 0.2179\,PMV^2)} \quad (12)$$

The TRNBULD comfort subroutine calculates PMV and PPD as a function of the ambient climatic conditions and the person-specific parameters. Regarding the person-specific parameters, metabolism rate, clothing insulation, and air velocity were taken from ASHRAE Standard 55 [45], as shown in Table 3.

Table 3. Thermal comfort parameters.

Parameter	Description	Factor
Clothing factor [clo]	Light outdoor sportswear	0.9
Metabolic rate [met]	Seated, light work	1.2
Air velocity [m/s]	Still air	0.2

2.2.4. Energy Model

The Primary Energy Saving (PES) evaluates the energy performance of the proposed system (PS) through a comparison with a suitable reference system (RS). The PS solely considers the demand unattended to by renewable energy sources. On the other hand, the RS supposes all demands are produced by conventional technologies based on fossil fuels. It is worth noting that electricity demand already aggregates freshwater demand. The reference technologies were an electric vapor compression air conditioning (VC) system with an average coefficient of performance, COP_{VC}, of 2.6, and a natural gas boiler (GB) with average thermal efficiency, η_{th}, of 0.92 [46]. The national grid efficiency was taken from the Spanish resolution published by IDAE [47], η_{el} = 0.42.

The PES and its ratio (PES_R) are calculated as shown in Equations (13) and (14):

$$PES = PE_{RS} - PE_{PS} \quad (13)$$

$$PES_R = \frac{PES}{PE_{RS}} \quad (14)$$

$$PE_{RS} = \left(\frac{P_{Build,\ dem} + P_{Syst,\ dem}}{\eta_{el}} + \frac{Q_{DHW,\ dem} + Q_{Heat,\ dem}}{\eta_{th}} + \frac{Q_{Cool,\ dem}}{COP_{VC} \cdot \eta_{el}} \right)_{RS} \quad (15)$$

$$PE_{PS} = \left(\frac{P_{Grid,aux}}{\eta_{el}} + \frac{Q_{DHW,\ aux} + Q_{Heat,\ aux}}{\eta_{th}} + \frac{Q_{Cool,\ aux}}{COP_{VC} \cdot \eta_{el}} \right)_{PS} \quad (16)$$

$P_{Grid,aux}$ is the electric energy withdrawn from the national grid to meet PS electricity demand, and $Q_{DHW,aux}$, $Q_{Heat,aux}$, and $Q_{Cool,aux}$ are the thermal energy demands required to be supplied by an auxiliary GB for DHW and space heating, and by a VC for space cooling, respectively.

2.2.5. Environmental Model

Similarly, the environmental analysis was evaluated by the saving in CO_2 emissions and its ratio (CO_{2R}) as showed in Equations (17) and (18):

$$CO_2 = CO_{2RS} - CO_{2PS} \quad (17)$$

$$CO2_R = \frac{CO_2}{CO_{2RS}} \quad (18)$$

$$CO_{2RS} = \left[\left(P_{Build,dem} + P_{Syst,dem} \right) \cdot f_{CO_2,EE} + \left(Q_{DHW,dem} + Q_{Heat,dem} \right) \cdot f_{CO_2,NG} + \left(\frac{Q_{Cool,dem}}{COP_{VC}} \right) \cdot f_{CO_2,EE} \right]_{RS} \quad (19)$$

$$CO_{2PS} = \left[\left(P_{Grid,aux} \right) \cdot f_{CO_2,EE} + \left(Q_{DHW,aux} + Q_{Heat,aux} \right) \cdot f_{CO_2,NG} + \left(\frac{Q_{Cool,aux}}{COP_{VC}} \right) \cdot f_{CO_2,EE} \right]_{PS} \quad (20)$$

The CO_2 emission factor of natural gas consumption, $f_{CO_2,NG}$, in Spain is 0.25 $kgCO_2/kWh$ [47]. In the case of the Spanish national grid, $f_{CO_2,EE}$, *REE* [48] provides the emission factor associated with electricity generation, 0.19 $kgCO_2/kWh$.

3. Results

Case study demands are deeply reported by Gesteira et al. [49]. It refers to a single-family townhouse located in the city of Almería, in the Mediterranean European side of Spain. Due to its high summer humidity and, therefore, high cooling latent load, it is suitable for the application of desiccant cooling systems. In these systems, the sensible and latent loads are controlled independently. The latent heat is reduced without cooling the air below its dew point, which is a great advantage [28]. Meteonorm weather data for Almería (36°50′17″ N, 2°27′35″ W) were used for climatic data acquisition.

The dynamic simulation returns temperature, energy, and flowrate profiles, with instantaneous or integrated values. The simulation was performed based on a 1-year time span (from 0 h to 8760 h) with a 5-min time step. This time step allows the controllers to work correctly. First, a design optimization study evaluates the optimal system configuration. For that reason, some design parameters are related to each other. In particular, the PVT field area automatically determines the solar pump flowrate and the TES volume (Table 2). Finally, the dynamic behavior of the optimal system is presented in terms of temperature and energy profiles for representative days of winter and summer. The yearly results show the main performance metrics, and a comparative study with an alternative coastal location is also included to extend the viability of the proposed system.

3.1. Design Optimization

A parametric analysis was developed to provide the optimal system design. In particular, the optimal configuration is obtained when all demands achieve their maximum coverage. The following demand coverages were chosen for the study: electric (C_{El}), heating (C_{Heat}), cooling (C_{Cool}), and DHW (C_{DHW}). The freshwater coverage uses the grid as a backup. Thus, it achieves 100% in all cases. The most critical design parameter of a solar system is the field area, which is related to energy production. For that reason, the sensitivity of the coverages was analyzed as a function of the PVT's size (A_{PVT}). The area varied from 5 m^2 to 30 m^2. Figure 4 shows the parametric study.

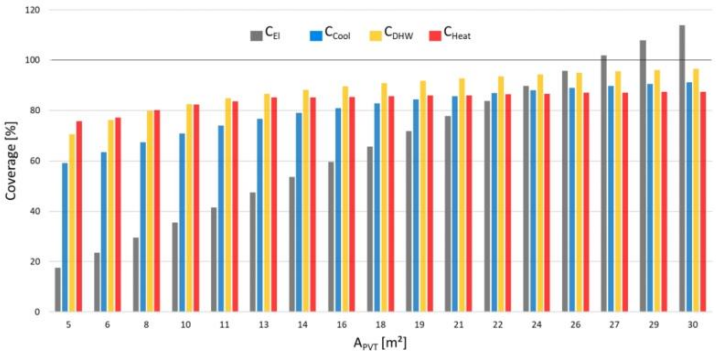

Figure 4. Parametric analysis: performance parameters, PVT collector area.

The increase in the PVT's area directly affects the C_{El}, and realizes 100% at 27.2 m^2 of A_{PVT}. An annual near-zero energy balance for the electricity is desired during the simulation. Consequently, there is no energy convenience in increasing the PVT collectors' area over 27.2 m^2 once 100% electric coverage is already achieved with a slight electricity surplus. It is worth noting that the increase in electric energy produced by the PVT collectors and not utilized by the building determines the non-refundable electricity injected into the grid.

Another relevant parameter for design optimization is the $T_{TES,top}$ setpoint. The AH cools the SCF down whenever the PVT's outlet temperature increases the $T_{TES,top}$ over the setpoint. It controls the SCF temperature and, consequently, the PVT efficiency. Moreover, it determines the available thermal energy for heating, cooling, and DHW. However, the mainly impacted coverage in this study was the cooling coverage. Thus, the parametric study analyzed the cooling coverage versus the PVT efficiency as a function of the $T_{TES,top}$ setpoint. The temperature varied from 50 °C to 80 °C, which is a suitable temperature range for the system's thermal needs. Figure 5 shows the parametric study.

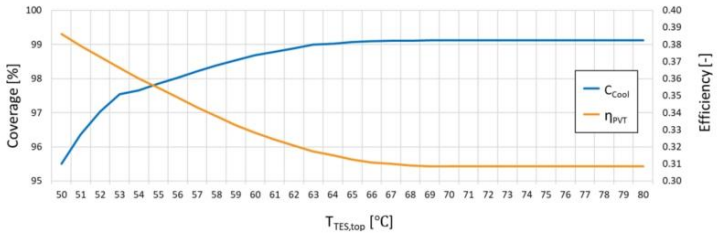

Figure 5. Parametric analysis: cooling coverage versus PVT efficiency, TES top temperature.

The increase in TES's top temperature setpoint directly affects the C_{Cool}, as the greater available thermal energy increases the efficiency of the desiccant wheel. However, it reduces the PVT efficiency due to higher thermal losses (higher mean temperature of the SCF entering the collectors). Thus, the optimal $T_{TES,top}$ setpoint that ensures a sufficient cooling coverage and PVT efficiency is achieved at 55 °C.

Finally, the study compared the ventilation and recirculation modes on the efficiency and coverage metrics (Table 4). The COP_{DAC} showed an enhancement in the ventilation mode, 0.47, against 0.44 for the recirculation case. Thus, the ventilation mode was selected as the optimal DAC configuration.

Table 4. Ventilation vs. recirculation modes.

			Ventilation	Recirculation
Parameter	**Symbol**	**Unit**	**Value**	
PVT total efficiency	η_{PVT}	–	0.35	0.35
DAC thermal COP	COP_{DAC}	–	0.47	0.44
Electricity coverage	C_{El}	%	104.1	101.32
DHW coverage	C_{DHW}	%	96.05	95.48
Heating coverage	C_{Heat}	%	87.01	87.01
Cooling coverage	C_{Cool}	%	97.98	97.85
Freshwater coverage	C_{FW}	%	100	100

3.2. Daily Analysis: A Typical Summer Day

It presents the daily results provided by the simulation for the cooling season. As a representative day, 6 August (from 5208 h to 5232 h) was selected. Figure 6 displays the profile of the main parameters for the representative summer day. The outlet temperature of the PVT collectors ($T_{PVT,out}$) follows the solar thermal gain. $T_{PVT,out}$ starts to increase at 6:30 a.m., reaches its maximum at 2:30 p.m., and then decreases until 8:00 p.m. The TES's top temperature ($T_{TES,top}$) rises from 51 °C to its setpoint (55 °C) during the daylight. Consequently, the air heater signal (y_{AH}) is activated, and heat is dissipated to the environment between 2:30 p.m. and 5:00 p.m. It is worth noting that, during AH activation, the reduction in the SCF's temperature increases the PVT's efficiency; thus, the $T_{PVT,out}$ presents several peaks and valleys.

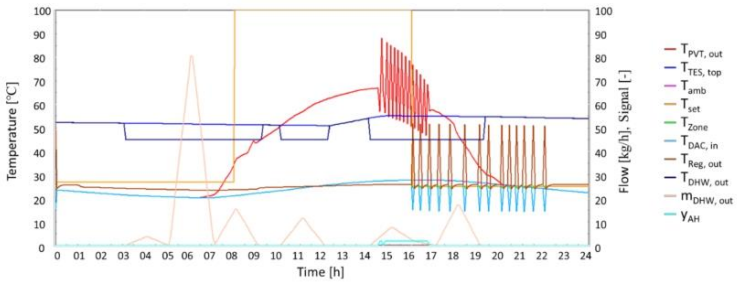

Figure 6. Summer day profile.

The ambient temperature (T_{amb}) varies from 20 °C at 6:00 a.m. to 28 °C at 4:00 p.m. During the morning, due to a mild ambient temperature, the thermostat does not activate cooling. According to the Spanish technical building code (BD-ES) [46], the thermostat setpoint temperature (T_{set}) during the mornings is 27 °C. However, the building's thermal gains increase throughout the day, so cooling is required in the afternoon after 4:00 p.m. This demand also occurs because of the reduction in the T_{set} to 25 °C. The DAC system provides for space cooling, blowing cool air inside the building at 14 °C ($T_{DAC,in}$) and thus reducing the building's zone temperature (T_{Zone}) to 25 °C during the system's operation. T_{Zone} remains around the T_{set} with a dead band of ±1 °C. Moreover, for the desiccant wheel's proper regeneration, the TES thermal energy feeds the regenerator and raises its outlet airflow temperature ($T_{Reg,out}$) up to 51 °C.

Regarding the DHW, the outlet temperature ($T_{DHW,out}$) and the outlet mass flow ($m_{DHW,out}$) are presented. $T_{DHW,out}$ meets the required temperature of 45 °C from 3:00 a.m. to 9:00 a.m., from 10:00 a.m. to 12:30 a.m., and from 2:00 p.m. to 7:30 p.m.

3.3. Daily Analysis: A Typical Winter Day

The selected winter day provided by the simulation in the heating season was 24 January (from 552 h to 576 h). Figure 7 shows the main parameters for the system on the selected day. Here, the solar loop presents a shorter sunlight period. $T_{PVT,out}$ starts to increase at 8:30 a.m., reaches its maximum value at 2:30 p.m. and then decreases until 6:00 p.m., lasting about four hours less than in the summertime. The $T_{TES,top}$ increases from 50 °C to 53 °C during daylight. The AH is not activated during the winter due to lower solar radiation.

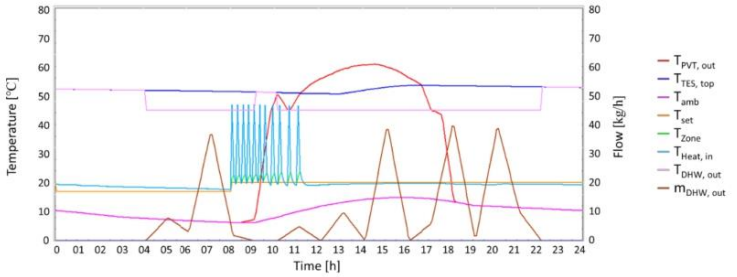

Figure 7. Winter day profile.

T_{amb} achieves its minimum at 9:00 am (6 °C) and maximum at 3:30 pm (15 °C). During the morning, due to a temperature decrease throughout the night and the increase of T_{set} from 17 °C to 20 °C at 8:00 a.m. [46], the thermostat activates heating from 8:00 a.m.

to 11:00 a.m. In the afternoon, the building gains (solar irradiation, occupancy, lighting, and equipment) increase the indoor temperature. Thus, no heating is required. T_{Zone} remains around the T_{set} throughout the day with a dead band of ±1 °C. The heating system provides for space heating, blowing airflow into the building at 47 °C ($T_{Heat,in}$).

Finally, $T_{DHW,out}$ meets the required temperature of 45 °C from 4:00 a.m. to 9:00 a.m. and from 10:00 a.m. to 10:00 p.m., according to the $m_{DHW,out}$ demand.

3.4. Yearly Results

The annual simulation results (from 0 h to 8760 h) are summarized in Table 5. In this table, the integrated amounts of electricity, heat, and water volume are shown for one year. In particular, the building demands were estimated in Ref. [49]. The total electricity demand ($P_{Tot,dem}$) is the sum of the building ($P_{Build,dem}$) and the system's ($P_{Syst,dem}$) electricity demands. The total water demand ($m_{Tot,dem}$) is the sum of the DHW ($m_{DHW,dem}$) and freshwater ($m_{FW,dem}$) demands. The total thermal demand ($Q_{Tot,dem}$) is comprised of the DHW thermal demand ($Q_{DHW,dem}$) and the cooling ($Q_{Cool,dem}$) and heating ($Q_{Heat,dem}$) demands. Note that $Q_{Cool,dem}$ is higher than $Q_{Heat,dem}$ due to local weather conditions.

Table 5. Yearly results.

Parameter	Symbol	Value	Unit
Building electricity demand	$P_{Build,dem}$	3866	kWh/yr [49]
System electricity demand	$P_{Syst,dem}$	1066	kWh/yr
Total electricity demand	$P_{Tot,dem}$	4932	kWh/yr
DHW demand	$m_{DHW,dem}$	41	m^3/yr [49]
Freshwater demand	$m_{FW,dem}$	110	m^3/yr [49]
Total water demand	$m_{Tot,dem}$	151	m^3/yr
DHW thermal demand	$Q_{DHW,dem}$	1260	kWh/yr
Building cooling demand	$Q_{Cool,dem}$	1450	kWh/yr [49]
Building heating demand	$Q_{Heat,dem}$	941	kWh/yr [49]
Total thermal demand	$Q_{Tot,dem}$	3651	kWh/yr
PVT power production	P_{PVT}	5701	kWh/yr
Power losses	P_{Loss}	570	kWh/yr
Total power production	P_{Tot}	5131	kWh/yr
PVT heat production	Q_{PVT}	8990	kWh/yr
Air heater dissipation	Q_{AH}	1857	kWh/yr
Heat losses	Q_{Loss}	1993	kWh/yr
Total useful heat production	Q_{Tot}	5140	kWh/yr
RO freshwater production	m_{RO}	151	m^3/yr

The total power production ($P_{Tot,prod}$) is the PVT power production (P_{PVT}) minus the power loss (P_{Loss}) wasted by the inverter due to its inefficiency during DC to AC conversion (10%). If $P_{Tot,prod}$ is insufficient for attending $P_{Tot,dem}$, electricity can be withdrawn from the national grid. On the other hand, if $P_{Tot,dem}$ exceeds $P_{Tot,prod}$, electricity can be injected into the national grid. An annual near-zero electricity balance is achieved during the simulation.

The total useful heat (Q_{Tot}) is the PVT heat production (Q_{PVT}) minus the heat dissipated by the AH (Q_{AH}) and the heat loss to the environment by the system devices (Q_{Loss}). The energy dissipated by the air heater is around 20.7%, and the thermal losses correspond to 22% of Q_{PVT}. The air heater activates mainly during the autumn and spring due to the lower thermal energy consumption, and during the summer because of the higher solar radiation.

As shown in Table 6, Q_{Tot} is used for attending $Q_{DHW,dem}$, $Q_{Cool,dem}$, and $Q_{Heat,dem}$.

Table 6. Thermal production breakdown.

Parameter	Symbol	Value	Unit
DHW consumption	Q_{DHW}	1210	kWh/yr
Heating coil exchanger	Q_{HX}	798	kWh/yr
DAC regenerator	Q_{Reg}	3000	kWh/yr

Finally, Table 7 presents the energy and environmental results for the proposed polygeneration system.

Table 7. Energy and environmental results.

Parameter	Symbol	Unit	Value
Primary energy saving ratio	PES_R	%	98.62
CO_2 saving ratio	CO_{2R}	%	97.17

3.5. Thermal Comfort

The thermal comfort analysis of the case study is reported in Ref. [49]. It presented two different situations: no indoor temperature control and temperature control as defined by the BD-ES [46]. Here, the thermal comfort of the same case study is provided by the polygeneration system. In particular, Figure 8 shows the thermal comfort analysis described by the PMV and PPD indexes.

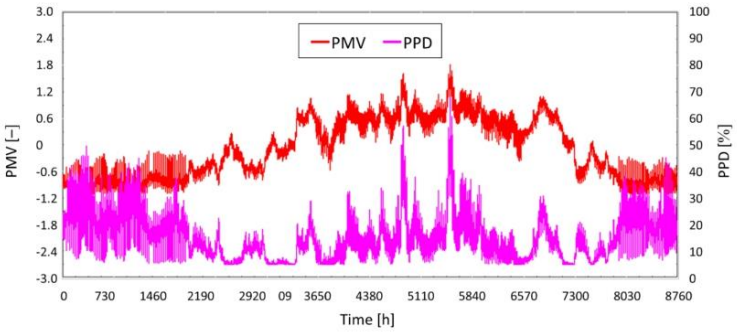

Figure 8. Thermal comfort analysis.

PMV ranges between −1.3 and 1.6 throughout the year, which can be explained as a slightly cool sensation during the winter and a warm feeling during the summer. Consequently, the PPD index presents a maximum occupant dissatisfaction rate of 42% during the winter and 63% in the summer. The thermal comfort analysis showed a remarkable improvement all year long compared to the case study without controls.

3.6. Comparison between Almería and an Alternative Coastal City

The polygeneration system was also applied to an alternative coastal city to evaluate its feasibility. Therefore, Valencia was selected, as it is located along the Spanish Mediterranean coast and presents different climate conditions. Valencia is characterized by lower horizontal global solar radiation per year and over twice the demand for heating (1828 kWh/yr) and slightly more for cooling (1567 kWh/yr) than Almería. By using the previously described methodology, the optimal system configuration was selected for the PVT collectors' area equal to 32 m^2 and a TES top temperature of 57 °C. The comparison between both cities is summarized in Table 8.

Table 8. Almería vs. Valencia efficiency parameters.

			Almería	Valencia
Parameter	**Symbol**	**Unit**	**Value**	
PVT total efficiency	η_{IPVT}	–	0.35	0.35
DAC thermal COP	COP_{DAC}	–	0.47	0.47
Electricity coverage	C_{El}	%	104.1	105.7
DHW coverage	C_{DHW}	%	96.05	90.15
Heating coverage	C_{Heat}	%	87.01	87.31
Cooling coverage	C_{Cool}	%	97.98	97.9
Freshwater coverage	C_{FW}	%	100	100
Primary energy saving ratio	PES_R	%	98.62	97.57
CO_2 saving ratio	CO_{2R}	%	97.17	95.04

Valencia needs a higher PVT collectors' area due to the lower horizontal global solar radiation per year. Furthermore, as it demands more heating and cooling, it thus justifies the increase in the TES's top temperature. The PVT efficiency (η_{PVT}) and the yearly mean COP_{DAC} for both cities are equal, 0.35 and 0.47, respectively. Finally, the polygeneration system applied to Almería presents an advantage in energy and environmental results.

4. Discussion

This work presented a novel simulation of a polygeneration system for residential electricity, heating, cooling, domestic hot water, and freshwater production. The proposed system integrates a solar-assisted desiccant air conditioning system for cooling purposes. The system was applied to a single-family townhouse located on the Mediterranean European side of Spain. The system can be applied to a similar area with moderate relative humidity and ambient temperature, which allows for the operation of desiccant air conditioning. The system's layout was dynamically simulated in the TRNSYS environment by developing comprehensive models suitable for evaluating the transient energy performance (temperatures, heat, power, and efficiency) of all the system's components on an hourly and yearly basis. Design optimization of the system was also performed under different conditions to determine the optimal size for attending to dwelling demands. The main findings of the simulations are summarized in the following:

1. The optimal system configuration for Almería was obtained at a photovoltaic/thermal collector's area of 27.2 m^2 and a top temperature for thermal energy storage of 55 °C;
2. The yearly results showed that the energy dissipated by the air heater is around 20.7% of the produced heat. The device activates mainly during the autumn, spring, and summer due to the lower thermal energy consumption or higher solar radiation;
3. The thermal comfort analysis showed a remarkable improvement compared to the results of the case study performed without temperature controls;
4. Comparing the results for the cities Almería and Valencia, it can be concluded that Valencia presents similar results to Almería. Thus, the proposed polygeneration system works correctly and is reliable.

Finally, the developed polygeneration system showed to be replicable for other cities and introduced solar-assisted desiccant cooling technology for the residential sector. It can be a promising solution for attending to energy demands using renewable energy sources. Further studies will develop an economic analysis and a multiobjective optimization for the proposed system.

Author Contributions: Conceptualization, J.U.; methodology, L.G.G.; formal analysis, L.G.G.; investigation, L.G.G.; resources, J.U.; data curation, L.G.G.; writing—original draft preparation, L.G.G.; writing—review and editing, L.G.G. and J.U.; supervision, J.U. All authors have read and agreed to the published version of the manuscript.

Funding: This research received no external funding.

Institutional Review Board Statement: Not applicable.

Informed Consent Statement: Not applicable.

Data Availability Statement: Not applicable.

Conflicts of Interest: The authors declare no conflict of interest.

References

1. International Energy Agency (IEA), Energy and Climate Change–World Energy Outlook Special Report, Paris. 2015. Available online: https://www.iea.org/reports/energy-and-climate-change (accessed on 9 March 2020).
2. European Commission, Communication from the Commission to the European Parliament, the Council, the European Economic and Social Committee and the Committee of the Regions—An EU Strategy on Heating and Cooling, Brussels. 2016. Available online: https://ec.europa.eu/energy/sites/ener/files/documents/1_EN_ACT_part1_v14.pdf (accessed on 6 April 2020).
3. European Commission. Commission Recommendation (Eu) 2016/1318-on Guidelines for the Promotion of Nearly Zero-Energy Buildings and Best Practices to Ensure that, by 2020, All New Buildings Are Nearly Zero-Energy Buildings. *Off. J. Eur. Union* **2016**, *L 208*, 46–57.
4. Costa, A.; Keane, M.M.; Torrens, J.I.; Corry, E. Building operation and energy performance: Monitoring, analysis and optimization toolkit. *Appl. Energy* **2013**, *101*, 310–316. [CrossRef]
5. European Commission. *SET-Plan ACTION n°5-ISSUES PAPER-Develop New Materials and Technologies for Energy Efficiency Solutions for Buildings*; SET Plan Secretariat: Brussels, Belgium, 2016.
6. Calise, F.; de Notaristefani di Vastogirardi, G.; Dentice d'Accadia, M.; Vicidomini, M. Simulation of polygeneration systems. *Energy* **2018**, *163*, 290–337. [CrossRef]
7. Buonomano, A.; Calise, F.; Palombo, A.; Vicidomini, M. Energy and economic analysis of geothermal-solar trigeneration systems: A case study for a hotel building in Ischia. *Appl. Energy* **2015**, *138*, 224–241. [CrossRef]
8. Calise, F.; d'Accadia, M.D.; Libertini, L.; Quiriti, E.; Vicidomini, M. A novel tool for thermoeconomic analysis and optimization of trigeneration systems: A case study for a hospital building in Italy. *Energy* **2017**, *126*, 64–87. [CrossRef]
9. Calise, F.; d'Accadia, M.D.; Figaj, R.D.; Vanoli, L. A novel solar-assisted heat pump driven by photovoltaic/thermal collectors: Dynamic simulation and thermoeconomic optimization. *Energy* **2016**, *95*, 346–366. [CrossRef]
10. Carotenuto, A.; Figaj, R.D.; Vanoli, L. A novel solar-geothermal district heating, cooling and domestic hot water system: Dynamic simulation and energy-economic analysis. *Energy* **2017**, *141*, 2652–2669. [CrossRef]
11. Angrisani, G.; Entchev, E.; Roselli, C.; Sasso, M.; Tariello, F.; Yaïci, W. Dynamic simulation of a solar heating and cooling system for an office building located in Southern Italy. *Appl. Therm. Eng.* **2016**, *103*, 377–390. [CrossRef]
12. Calise, F. Thermoeconomic analysis and optimization of high efficiency solar heating and cooling systems for different Italian school buildings and climates. *Energy Build.* **2010**, *42*, 992–1003. [CrossRef]
13. Serra, L.M.; Lozano, M.-A.; Ramos, J.; Ensinas, A.V.; Nebra, S.A. Polygeneration and efficient use of natural resources. *Energy* **2009**, *34*, 575–586. [CrossRef]
14. Jana, K.; Ray, A.; Majoumerd, M.M.; Assadi, M.; De, S. Polygeneration as a future sustainable energy solution—A comprehensive review. *Appl. Energy* **2017**, *202*, 88–111. [CrossRef]
15. Acevedo, L.; Uche, J.; del Almo, A.; Círez, F.; Usón, S.; Martínez, A.; Guedea, I. Dynamic Simulation of a Trigeneration Scheme for Domestic Purposes Based on Hybrid Techniques. *Energies* **2016**, *9*, 1013. [CrossRef]
16. Uche, J.; Acevedo, L.; Círez, F.; Usón, S.; Martínez-Gracia, A.; Bayod-Rújula, Á.A. Analysis of a domestic trigeneration scheme with hybrid renewable energy sources and desalting techniques. *J. Clean. Prod.* **2019**, *212*, 1409–1422. [CrossRef]
17. Usón, S.; Uche, J.; Martínez, A.; del Amo, A.; Acevedo, L.; Bayod, Á. Exergy assessment and exergy cost analysis of a renewable-based and hybrid trigeneration scheme for domestic water and energy supply. *Energy* **2019**, *168*, 662–683. [CrossRef]
18. Elmer, T.; Worall, M.; Wu, S.; Riffat, S. An experimental study of a novel integrated desiccant air conditioning system for building applications. *Energy Build.* **2016**, *111*, 434–445. [CrossRef]
19. Angrisani, G.; Minichiello, F.; Roselli, C.; Sasso, M. Desiccant HVAC system driven by a micro-CHP: Experimental analysis. *Energy Build.* **2010**, *42*, 2028–2035. [CrossRef]
20. Jani, D.B.; Mishra, M.; Sahoo, P.K. Performance analysis of a solid desiccant assisted hybrid space cooling system using TRNSYS. *J. Build. Eng.* **2018**, *19*, 26–35. [CrossRef]
21. Elgendy, E.; Mostafa, A.; Fatouh, M. Performance enhancement of a desiccant evaporative cooling system using direct/indirect evaporative cooler. *Int. J. Refrig.* **2015**, *51*, 77–87. [CrossRef]
22. *TRNSYS: A Transient System Simulation Program*; Solar Energy Laboratory, University of Wisconsin: Madison, WI, USA, 2006.
23. Angrisani, G.; Minichiello, F.; Sasso, M. Improvements of an unconventional desiccant air conditioning system based on experimental investigations. *Energy Convers. Manag.* **2016**, *112*, 423–434. [CrossRef]
24. Sopian, K.; Dezfouli, M.M.S.; Mat, S.; Ruslan, M.H. Solar Assisted Desiccant Air Conditioning System for Hot and Humid Areas. *Int. J. Environ. Sustain.* **2014**, *3*, 23–32. [CrossRef]
25. Panaras, G.; Mathioulakis, E.; Belessiotis, V. Solid desiccant air-conditioning systems—Design parameters. *Energy* **2011**, *36*, 2399–2406. [CrossRef]

26. Fabrizio, E.; Seguro, F.; Filippi, M. Integrated HVAC and DHW production systems for Zero Energy Buildings. *Renew. Sustain. Energy Rev.* **2014**, *40*, 515–541. [CrossRef]
27. Farooq, A.S.; Badar, A.W.; Sajid, M.B.; Fatima, M.; Zahra, A.; Siddiqui, M.S. Dynamic simulation and parametric analysis of solar assisted desiccant cooling system with three configuration schemes. *Sol. Energy* **2020**, *197*, 22–37. [CrossRef]
28. Heidari, A.; Roshandel, R.; Vakiloroaya, V. An innovative solar assisted desiccant-based evaporative cooling system for co-production of water and cooling in hot and humid climates. *Energy Convers. Manag.* **2019**, *185*, 396–409. [CrossRef]
29. Villarruel-Jaramillo, A.; Pérez-García, M.; Cardemil, J.M.; Escobar, R.A. Review of Polygeneration Schemes with Solar Cooling Technologies and Potential Industrial Applications. *Energies* **2021**, *14*, 6450. [CrossRef]
30. Pina, E.A.; Lozano, M.A.; Serra, L.M. A multiperiod multiobjective framework for the synthesis of trigeneration systems in tertiary sector buildings. *Int. J. Energy Res.* **2020**, *44*, 1140–1166. [CrossRef]
31. Melgar, S.G.; Cordero, A.S.; Rodríguez, M.V.; Márquez, J.M.A. Matching Energy Consumption and Photovoltaic Production in a Retrofitted Dwelling in Subtropical Climate without a Backup System. *Energies* **2020**, *13*, 6026. [CrossRef]
32. Pinto, E.S.; Serra, L.M.; Lázaro, A. Optimization of the design of polygeneration systems for the residential sector under different self-consumption regulations. *Int. J. Energy Res.* **2020**, *44*, 11248–11273. [CrossRef]
33. Ghalavand, Y.; Hatamipour, M.S.; Rahimi, A. A review on energy consumption of desalination processes. *Desalin. Water Treat.* **2015**, *54*, 1526–1541. [CrossRef]
34. Chow, T.T. A review on photovoltaic/thermal hybrid solar technology. *Appl. Energy* **2010**, *87*, 365–379. [CrossRef]
35. Zondag, H. Flat-plate PV-Thermal collectors and systems: A review. *Renew. Sustain. Energy Rev.* **2008**, *12*, 891–959. [CrossRef]
36. Fudholi, A.; Sopian, K.; Yazdi, M.H.; Ruslan, M.H.; Ibrahim, A.; Kazem, H.A. Performance analysis of photovoltaic thermal (PVT) water collectors. *Energy Convers. Manag.* **2014**, *78*, 641–651. [CrossRef]
37. Calise, F.; Figaj, R.D.; Vanoli, L. A novel polygeneration system integrating photovoltaic/thermal collectors, solar assisted heat pump, adsorption chiller and electrical energy storage: Dynamic and energy-economic analysis. *Energy Convers. Manag.* **2017**, *149*, 798–814. [CrossRef]
38. Zenhäusern, D.; Bamberger, E.; Baggenstos, A.; Häberle, A. PVT Wrap-Up: Energy Systems with Photovoltaic Thermal Solar Collectors. In Proceedings of the IEA SHC International Conference on Solar Heating and Cooling for Buildings and Industry, Abu Dhabi, United Arab Emirates, 29 October–2 November 2017; pp. 1–12. [CrossRef]
39. Rafique, M.M.; Gandhidasan, P.; Rehman, S.; Al-Hadhrami, L.M. A review on desiccant based evaporative cooling systems. *Renew. Sustain. Energy Rev.* **2015**, *45*, 145–159. [CrossRef]
40. Jurinak, J.J. Open Cycle Solid Desiccant Cooling–Component Models and System Simulations. Ph.D. Thesis, University of Wisconsin-Madison, Madison, WI, USA, 1982.
41. Panaras, G.; Mathioulakis, E.; Belessiotis, V.; Kyriakis, N. Theoretical and experimental investigation of the performance of a desiccant air-conditioning system. *Renew. Energy* **2010**, *35*, 1368–1375. [CrossRef]
42. Bourdoukan, P.; Wurtz, E.; Joubert, P. Experimental investigation of a solar desiccant cooling installation. *Sol. Energy* **2009**, *83*, 2059–2073. [CrossRef]
43. International Organization for Standardization (ISO). *ISO 7730:1994, Moderate Thermal Environments—Determination of the PMV and PPD Indices and Specification of the Conditions for Thermal Comfort*; ISO Standard: Geneva, Switzerland, 1994; p. 26.
44. Fanger, P.O. *Thermal Comfort. Analysis and Applications in Environmental Engineering*; Danish Technical Press: Copenhagen, Denmark, 1970.
45. *ANSI/ASHRAE Standard 55*; Thermal Environmental Conditions for Human Occupancy. The Society: New York, NY, USA, 2013.
46. Spanish Ministry of Development. Updating of the Energy Saving Document DB-HE of the Technical Building Code. 2019. Available online: https://www.codigotecnico.org/pdf/Documentos/HE/DBHE.pdf (accessed on 1 October 2021).
47. Instituto para la Diversificación y Ahorro de la Energía (IDAE). CO2 Emission Factors and Primary Energy Coefficients for Different Final Energy Sources Consumed in the Building Sector in Spain. 2014. Available online: https://energia.gob.es/desarrollo/EficienciaEnergetica/RITE/Reconocidos/Reconocidos/Otros%20documentos/Factores_emision_CO2.pdf (accessed on 15 February 2022).
48. Red Eléctrica Española (REE). CO2 Emissions of Electricity Generation in Spain. 2021. Available online: https://api.esios.ree.es/documents/580/download?locale=es (accessed on 15 February 2022).
49. Gesteira, L.G.; Uche, J.; de Oliveira Rodrigues, L.K. Residential Sector Energy Demand Estimation for a Single-Family Dwelling: Dynamic Simulation and Energy Analysis. *J. Sustain. Dev. Energy Water Environ. Syst.* **2021**, *9*, 1–18. [CrossRef]

A.1 Paper IV

sustainability

MDPI

Article

A Polygeneration System Based on Desiccant Air Conditioning Coupled with an Electrical Storage

Luis Gabriel Gesteira [1,2,*], Javier Uche [2,*] and Natalia Dejo-Oricain [3]

[1] Department of Mechanical Technology, Federal Institute of Bahia, Salvador 40301-015, Brazil
[2] CIRCE Research Institute, University of Zaragoza, 50018 Zaragoza, Spain
[3] Department of Management and Business Administration, University of Zaragoza, 50009 Zaragoza, Spain
* Correspondence: 773948@unizar.es (L.G.G.); javiuche@unizar.es (J.U.)

Abstract: This study presents an extension of a previous paper recently published by the authors. In particular, the current paper focuses on adding electrical storage to a polygeneration system developed for residential applications. Different from the previous work, it aims to design an off-grid facility. The polygeneration plant provides electricity, space heating and cooling, domestic hot water, and freshwater for a single-family dwelling in Almería, Spain. The main system technologies are photovoltaic/thermal collectors, reverse osmosis, and desiccant air conditioning. Lead-acid battery storage was added as a backup for the electrical system. The system was performed in the TRNSYS simulation environment for one year with a 5-min time step. A parametric study was carried out to investigate the grid dependence according to the number of batteries installed. Design optimization was also performed to provide the optimal system configuration for the off-grid case. A solar collector efficiency of 0.55 and a desiccant air-conditioning coefficient of performance of 0.42 were obtained. All demands were fully supplied, and the primary energy saving and CO_2 saving achieved 100%. A minimum battery state of charge of 30% was reached for a few hours all year long.

Keywords: polygeneration system; desiccant air conditioning; building; electrical storage; sustainability

Citation: Gesteira, L.G.; Uche, J.; Dejo-Oricain, N. A Polygeneration System Based on Desiccant Air Conditioning Coupled with an Electrical Storage. *Sustainability* **2022**, *14*, 15784. https://doi.org/10.3390/su142315784

Academic Editors: Fontina Petrakopoulou, Maria Vicidomini and Francesco Calise

Received: 10 October 2022
Accepted: 24 November 2022
Published: 27 November 2022

1. Introduction

Buildings are responsible for about 40% of global energy consumption and more than 30% of CO_2 emissions [1]. Consequently, building energy consumption has been calling the attention of the International Energy Agency [2] and the European Union [3]. In 2016, the European Commission introduced the concept of nearly zero-energy buildings (NZEBs) to endorse building energy efficiency [4]. Moreover, the integration of polygeneration systems within buildings is an exciting solution to meet the NZEBs target. Polygeneration plants based on renewable energy sources (RES) can replace the existing conventional technologies and simultaneously produce several energy services. Thus, the primary energy consumption and CO_2 emissions are reduced as the RES are replenished by nature and emit little to no greenhouse gases [5].

It is well known that RES, such as solar and wind technologies, can be highly variable due to climate conditions. This leads to a significant grid dependence as the energy production can be null or insufficient to meet the demand, resulting in a plant's profitability reduction [6]. Therefore, the adoption of electrical storage (ES) to increase the availability of electricity is an attractive option to be investigated [7]. Furthermore, the electricity distribution losses by the grid are dramatically reduced in an off-grid facility [8]. ES refers to converting electricity from a power source into a storage form for conversion back to electricity on demand [9]. They are classified into four main categories: mechanical (e.g., flywheel), electrical (e.g., capacitors), chemical (e.g., electrochemical devices), and fuel cell (e.g., hydrogen storage) [10,11] and can be used as single energy storage or multiple

energy storage to provide better flexibility and lower costs [12]. Among the various storage devices, lead-acid batteries are the most widely used technology [13]. Lead-acid batteries have high efficiency, are low cost, and can supply power on demand without delay [14,15].

RES coupled with batteries has been studied regarding the benefits they can achieve [16–20]. In particular, Goldsworthy [21] carried out a simulation model to analyze the suitability of an off-grid photovoltaic (PV) system with a battery to power a cooling system to provide thermal comfort for a range of buildings of a wide variety of climate zones in Australia. The results showed that a modest-size PV-battery system provided 100% occupant comfort for some buildings and climate combinations. Conversely, Li et al. [22] presented an experimental study to evaluate the operational performance of a PV cooling system applied to the Chinese climate conditions. The system can be installed in offices or residential buildings and can be used in stand-alone or grid-connected modes. In the stand-alone mode, the excess power generated during the daytime was stored in the battery and used on demand.

Some other authors have analyzed hybrid systems coupled with batteries. In this framework, Vick et al. [23] analyzed an off-grid facility based on a wind turbine (WT) and a PV array for water pumping to evaluate the performance of a hybrid system for the Texan climate of Bushland. Results showed 55% as the highest pump efficiency, and the hybrid system pumped 28% more water than the WT and PV systems. Zahnd et al. [24] developed a model of a PV-WT system coupled with lead-acid batteries to supply power to a remote village in Nepal. The results demonstrated that the WT and PV technologies complement each other, and the electricity can be stored in batteries. Nookuea et al. [25] studied the relationship between the life cycle cost and the reliability of some hybrid PV-WT-battery systems for shrimp cultivation in Thailand. The lowest reliability was achieved for WT only due to the low average wind speed of the investigated site. On the other hand, the highest reliability was achieved for PV and battery systems capable of working during the night. Buonomano et al. [26] presented a thermo-economic simulation model of a hybrid renewable power plant based on PV and WT technologies (190 kW and 10 kW, respectively) coupled to an ES system (400 kWh). The system was performed in the TRNSYS environment to boost economic profitability considering the electricity time-dependent tariffs exchanged with the grid and the electrical storage possibility. Results showed a negative system profit index due to the higher capital cost of the ES, although an operating cost contraction was noticed. Rehman and Al-Hadhrami [27] evaluated a PV-diesel hybrid power system with battery backup to decrease diesel demand in a remote area near Rafha, Saudi Arabia. The results presented an optimal system configuration consisting of 2 MW PV panels (21% solar energy), four generators with rated power of 1250, 750, 2250, and 250 kW, and 300 batteries (2280 kWh). Furthermore, the environmental analysis showed a CO_2 emission saving of 3321 tons per year.

Some relevant publications have been found in the literature regarding the integration of ES with buildings. Chabaud et al. [28] investigated an energy management approach in a residential microgrid using energy and economic criteria. In particular, a grid-connected building was modeled and simulated. The authors outlined that combining PV and WT is an interesting option for residential buildings. Moreover, they found that ES affects the system performance and savings, shifting some domestic loads from on-peak to off-peak periods. Koh and Lim [29] studied the feasibility of ES systems in a building. The analysis focused on technical, cost, and environmental aspects. The results outlined a reduction of the system's overall cost by installing an ES system. Stadler et al. [30] evaluated the influence of ES systems on building energy costs and CO_2 emissions by a mixed-integer linear optimization. The case study consisted of 139 different commercial buildings in California, analyzing the economic–environmental benefits. The results showed that the optimization did not affect the battery performance parameters.

Moreover, ES can work in a broad variety of cogeneration systems, improving system stability [13,31]. In particular, Comodi et al. [32] analyzed the operational results of a domestic microgrid system based on a solar PV and thermal energy plant, a geothermal

heat pump, thermal energy storage (TES), and two ES systems. The results showed that the self-consumption of PV energy is increased by the operation of the ES with a decrease in electricity fed back to the grid. Singh et al. [33] developed a PV-WT generation system, including biomass and ES. The system was used to match the electrical load of a small area. The study defined the optimal component sizes through an artificial bee colony and particle swarm algorithms. The results highlighted the system operation in terms of the battery state of charge (*SOC*). The analysis showed a minimum *SOC* of 30% for only a few hours in the whole year. Destro et al. [34] studied the optimal design of a trigeneration system for a small, isolated tourist resort in Northern Italy. It consisted of a PV plant, a diesel engine, a hot and cold TES, lead-acid batteries, and pumped hydro energy storage. The design and operation strategies were optimized through a model based on the particle swarm algorithm to minimize the costs and fulfill the users' demands of electricity, heating, cooling, and potable water. The results showed a PV generation of 35% of the total electricity demand and battery storing of around 88% of all energy stored. Calise et al. [35] developed a thermo–economic analysis of a polygeneration system consisting of photovoltaic/thermal collectors (PVT) coupled with a solar-assisted heat pump, an adsorption chiller, and ES. The plant supplies electricity, space heating and cooling, and domestic hot water. The electricity was self-consumed and/or sent to the grid. The results outlined a share of the ES system on the self-consumed electricity of about 20%. Żołądek et al. [36] presented an energy-economic assessment of an island polygeneration system based on a PV field, small WT, wood chip gasifier, battery, and hydrogen circuit with electrolyzer and fuel cell. The system was designed in TRNSYS to supply electricity for a tourist facility in two European cities. The system was able to meet the user's demand. Cappiello et al. [37] analyzed two technologies for biogas production coupled with PV panels and an ES system. The off-grid arrangement was designed for a sewage sludge treatment plant located in Stuttgart, Germany. The results presented a primary energy saving of around 25–30%. Kim et al. [38] studied a polygeneration system with ES for a hospital. The results showed 30.79% of primary energy saving, 28.35% of CO_2 emission reduction, and 36.86% of operating cost saving compared to the conventional system. Furthermore, the economic feasibility analysis indicated a simple payback period of 6.6 years.

Analyzing the available literature, RES systems coupled with ES are of interest to the research community, especially for buildings. However, the analysis of an off-grid polygeneration plant coupled with battery storage for a residence is scarce. The authors aim to extend the application of the polygeneration system designed by Gesteira et al. [39] for electricity, heating, cooling, domestic hot water (DHW), and freshwater supply for a residential dwelling located in Almeria, Spain. Here, a novel off-grid layout is proposed and modeled with TRNSYS software [40]. To the best of the authors' knowledge, the polygeneration system proposed in this paper was never investigated employing a dynamic simulation of PVT collectors, reverse osmosis (RO), and desiccant air conditioning (DAC) coupled with lead-acid batteries. First, a parametric study analyzed the previous polygeneration system when coupled with batteries. Then, a Hooke–Jeeves optimization was performed to determine the system's off-grid optimal setup regarding the energy and environmental parameters. Finally, the optimal daily and yearly results are presented and analyzed.

2. Materials and Methods

2.1. System Layout

The proposed approach is adapted from the polygeneration system designed by Gesteira et al. [39] (Figure 1). Here, the novelty is the electrical storage replacing the grid to avoid grid dependence and converting it to an off-grid system. Moreover, a new regulator/inverter for monitoring the battery state of charge was added. The solar and TES loops, RO module, and HVAC system are described in more detail in Ref. [39]; therefore, in this work, only the new off-grid power circuit is deeply reported.

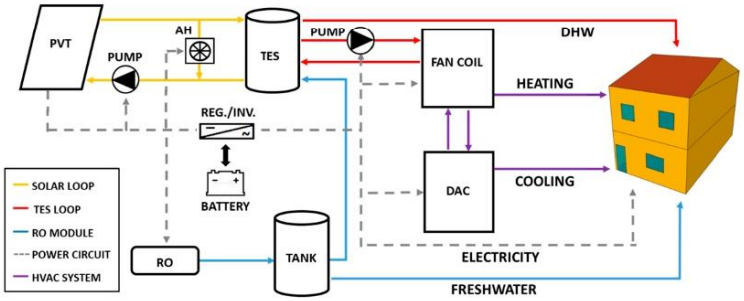

Figure 1. Polygeneration system layout (adapted from Ref. [39]).

The PVT collectors convert solar irradiation into electrical and thermal energy with a fixed slope of 35° (no tracking). The solar collector fluid is a mixture of water/glycol (60/40). The thermal energy storage consists of a fluid-filled sensible vertically stratified (four nodes) energy storage tank with a heat exchanger inside. An air heater (AH) prevents fluid overheating by dissipating heat with a capacity of 20 kW. The TES supplies the HVAC system and the DHW at 45 °C. The RO device consumes 110 W and produces 35 kg/h of freshwater. The freshwater is stored in a tank of 1.0 m^3. In the winter season, heating is provided for the building through a fan coil. During summertime, the thermal energy drives a DAC system and provides cooling.

Regarding the power circuit, the electricity consumption consists of the building's electric demand and the system power load (pumps, fans, etc.). The PVT collector's power is sent to a regulator/inverter with peak-power tracking. Two power-conditioning devices are needed in PV power systems coupled with ES. The first is a regulator, which distributes DC power from the solar array to and from a battery. If the battery is fully charged, excess energy is dumped. The second component is the inverter, which converts the DC power to AC and sends it to the load. Although batteries are expensive and require notable maintenance [41], an economic analysis was not performed. However, they can be economically competitive for isolated dwellings for which the cost of connection to the grid would be high [42].

2.2. System Model

The TRNSYS environment (version 18) [40] was used to model and dynamically simulate the proposed system (PS). The software's built-in library provided all components used to develop the system. Some of them are user-defined, such as calculators, controllers, and data readers set by the authors. Others are required to provide the results, such as integrators and plotters. Here, a detailed description of the regulator/inverter, the battery storage, and the energy and environmental models are reported. The other components' descriptions are available in TRNSYS's component mathematical reference [40]. Table 1 presents the parameters of the novel power circuit of the PS.

Table 1. Main design and operation parameters of the power circuit.

Type	Parameter	Symbol	Value	Unit
Regulator/inverter	Efficiency	η_i	0.96	–
	High limit on fractional state of charge	*HSOC*	1	–
	Low limit on fractional state of charge	*LSOC*	0.3	
	Inverter output power capacity	P_{inv}	4	kW
Battery	Capacity	B_{cap}	2.2	kWh
	Voltage	P_{batt}	12	V

2.2.1. Regulator/Inverter Model

Type 48 models both the regulator and inverter with peak-power tracking. It is a power-conditioning device that distributes DC power from the solar array to and from a battery bank. It converts the input power to an AC output signal waveform [43] and sends it to the load. It also monitors the battery's state of charge (*SOC*). If the *SOC* is between the high limit on the state of charge (*HSOC*) and the low limit on the state of charge (*LSOC*), the battery can discharge (when the power production, P_{prod}, is lower than the power demand, $P_{tot,dem}$) or charge (when P_{prod} is greater than $P_{tot,dem}$). The priority for the power output is to match the electricity demand. It also monitors if the *SOC* is lower than *LSOC* and no further discharging is allowed or if it is higher than *HSOC*, the excess power is dumped. A detailed description of subroutines of such additional controls is reported by Calise et al. [35]. It is important to note that power exchange with the electric grid is not admitted.

2.2.2. Battery Model

A lead-acid storage battery (Type 47) operates with the solar array and the power-conditioning components. It specifies how the battery *SOC* varies over time, given the rate of charge or discharge. This model is based on a simple energy balance of the battery [44]. The battery mathematical model is based on Shepherd equations, which describe the battery charge or discharge [40]. The battery discharge equation ($I < 0$) is given by:

$$V = e_{qd} - g_{dis}H + Ir_{qd}\left(1 + \frac{m_{dis}H}{\frac{Q_{dis}}{Q_m} - H}\right) \quad (1)$$

And the battery charge equation ($I > 0$) is given by:

$$V = e_{qc} - g_{cha}H + Ir_{qc}\left(1 + \frac{m_{cha}H}{\frac{Q_{cha}}{Q_m} - H}\right) \quad (2)$$

The maximum charging and minimum discharging voltages are limited to extend the battery lifetime. The voltage limit on discharge is calculated from the:

$$V_{dis} = e_{dis} - |I|r_{dis} \quad (3)$$

The variation of the battery charge is calculated as follows:

$$\frac{dQ}{dt} = \left\{ \begin{array}{ll} I & if\ I < 0 \\ I.\eta_{cha} & if\ I > 0 \end{array} \right\} \quad (4)$$

2.2.3. Energy and Environmental Models

The energy performance of the PS is evaluated by the primary energy saving (*PES*) index. The PS considers the demands not attended to by the polygeneration system. A reference system (RS) compares all demands provided by traditional energy sources. The RS consists of an electric cooling system (ECS) with a coefficient of performance, COP_{ECS}, of 2.6, and a natural gas boiler (GB) with a thermal efficiency, η_{th}, of 0.92 [45]. The Spanish electric grid efficiency was taken from IDAE [46], η_{el} = 0.42.

The PES and its ratio (PES_R) are calculated as shown in Equations (5) and (6):

$$PES = PE_{RS} - PE_{PS} \quad (5)$$

$$PES_r = \frac{PES}{PE_{RS}} \quad (6)$$

$$PE_{RS} = \left(\frac{P_{build,\,dem} + P_{syst,\,dem}}{\eta_{el}} + \frac{Q_{DHW,\,dem} + Q_{heat,\,dem}}{\eta_{th}} + \frac{Q_{cool,\,dem}}{COP_{ECS} \cdot \eta_{el}}\right)_{RS} \quad (7)$$

$$PE_{PS} = \left(\frac{P_{grid,aux}}{\eta_{el}} + \frac{Q_{DHW,\ aux} + Q_{heat,\ aux}}{\eta_{th}} + \frac{Q_{cool,\ aux}}{COP_{ECS} \cdot \eta_{el}} \right)_{PS} \quad (8)$$

$P_{grid,aux}$ is the electricity withdrawn from the grid, and $Q_{DHW,aux}$, $Q_{heat,aux}$, and $Q_{cool,aux}$ are the thermal demands supplied by a GB and an ECS.

Following the same method, the CO_2 saving was used as the environmental analysis, as shown in Equations (9) and (10):

$$CO_2 \ \ CO_{2RS} - CO_{2PS} \quad (9)$$

$$CO_{2r} \ \ \frac{CO_2}{CO_{2RS}} \quad (10)$$

$$CO_{2RS} \left[\left(P_{build,\ dem} + P_{syst,\ dem} \right) \cdot f_{CO_2,EE} + (Q_{DHW,\ dem} + Q_{heat,\ dem}) \cdot f_{CO_2,NG} + \left(\frac{Q_{cool,\ dem}}{COP_{ECS}} \right) \cdot f_{CO_2,EE} \right]_{RS} \quad (11)$$

$$CO_{2PS} \left[\left(P_{grid,aux} \right) \cdot f_{CO_2,EE} + (Q_{DHW,\ aux} + Q_{heat,\ aux}) \cdot f_{CO_2,NG} + \left(\frac{Q_{cool,\ aux}}{COP_{ECS}} \right) \cdot f_{CO_2,EE} \right]_{PS} \quad (12)$$

The Spanish emission factor for natural gas, $f_{CO_2,NG}$, is 0.25 kg_{CO_2}/kWh [46], and for the grid, $f_{CO_2,EE}$, it is 0.19 kg_{CO_2}/kWh [47].

3. Results and Discussion

The residential building used during the simulation is described in detail by Ref. [48]. Table 2 summarizes all the information regarding the climate zone and the building. In this paper, the authors propose a novel polygeneration system for the same case study. It supplies electricity, heating, cooling, DHW, and freshwater for a residential dwelling located in Almeria, Spain.

Table 2. Main climate and building parameters of the case study.

Climate Zone	
Location	Almeria
Latitude	36°50′ N
Altitude above sea level (m)	0
Annual average outdoor temperature (°C)	18.4
Horizontal global solar radiation (kWh/year)	1829
Average temperature of tap water (°C)	15.7
Building description	
Type	Single-family, semi-detached house
Number of occupants	4
Total conditioned area (m^2)	110
Total area (m^2)	165
No. of floors	2 + attic
Height per floor (m)	3
Total building height (m)	7.5
Total volume (m^3)	371.3
Window-to-wall ratio for north façade (%)	10
Window-to-wall ratio for south façade (%)	15
Building envelope transmittances	
External wall ($W/m^2 \cdot K$)	0.5
External roof ($W/m^2 \cdot K$)	0.47
Floor ($W/m^2 \cdot K$)	0.5
Door ($W/m^2 \cdot K$)	2.2
Window ($W/m^2 \cdot K$)	2.6

Table 2. *Cont.*

Building usage profile			
Setpoint temperature (°C)	Heating season	17 20	00:00–08:00 08:00–24:00
	Cooling season	27 - 25	00:00–08:00 08:00–16:00 16:00–24:00
Occupancy load (W/m^2)	Weekday	3.51 0.88 1.76	00:00–08:00 08:00–16:00 16:00–24:00
	Weekend	3.51	00:00–24:00
Lighting load/equipment load (W/m^2)		1.76 0.44 1.32 2.2 4.4	00:00-01:00 01:00-08:00 08:00-19:00 19:00-20:00 20:00-24:00
Ventilation rate (1/h)	Heating season	0.4	00:00–24:00
	Cooling season	4 0.4	01:00–09:00 09:00–01:00
Infiltration rate (1/h)		0.45	00:00-24:00
Daily DHW demand per person (l/day·person)	28		

The simulation was performed based on one year with a 5-min time step. Firstly, a parametric study was performed to investigate the behavior of the polygeneration system developed in Ref. [39] when coupled with a battery bank. Then, a design optimization was done to determine the system's off-grid optimal setup. For that reason, the number of PVT collectors and batteries was simultaneously optimized. Finally, the optimal system behavior is shown based on typical-day temperature and energy profiles. The yearly results showed the main performance metrics.

3.1. Design of the Storage Capacity

Table 3 comprehends the solar generation parameters of the polygeneration system developed by Ref. [39]. Here, a parametric analysis was conducted to investigate the behavior of this system when coupled with a battery bank. The number of batteries (N_{batt}) varied from 1 to 20. The off-grid configuration is obtained when the PES_r and CO_{2r} achieve their maximum, and the $P_{grid,aux}$ is no longer required by the system. As seen in Figure 2, the addition of batteries to the already developed system solely cannot convert it into an off-grid facility.

Table 3. Solar loop design parameters [39].

Type	Parameter	Symbol	Value	Unit
PVT	Area	A_{PVT}	27.2	m^2
Inverter	Efficiency	η_{inv}	0.9	–
Air heater	Heat dissipation capacity	Q_{AH}	20	kW
Solar pump	Nominal flow rate per PVT area	v_f/A_{PVT}	50	kg/h·m^2
TES	TES volume/PVT area	V_{TES}/A_{PVT}	0.1	m^3/m^2

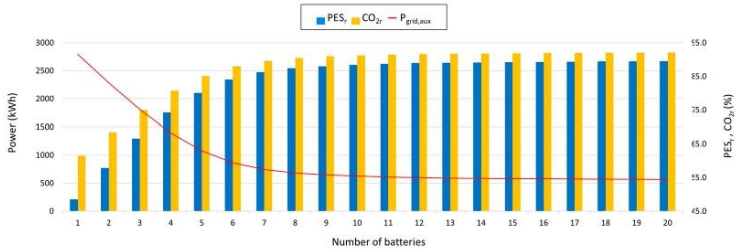

Figure 2. Parametric analysis: performance parameters and grid power, number of batteries.

An annual electricity autonomy is a primary goal. However, $P_{grid,aux}$ was not able to achieve less than 500 kWh per year based only on the batteries addition. It can also be seen by the energy and environmental analysis, which achieved a maximum of 89.4% and 92.0% of PES_r and CO_{2r}, respectively, due to the grid electricity consumption. It is worth noting that selling back electricity to the grid was neglected.

3.2. Design Optimization

To achieve 100% electricity autonomy, an optimization analysis was performed. The TRNOPT plug-in included in the TRNSYS package links the optimization algorithm and the simulation model. This tool uses the algorithms included in the GENOPT package developed by Lawrence Berkeley National Laboratory [49] to perform complex mathematical operations and optimize the system. In particular, the generalized search method was used as this technique avoids the calculation of partial derivatives. The Hooke–Jeeves [50] modified algorithm was selected. The structure of this algorithm avoids the achievement of local minimum points and considers the TRNSYS simulation for approximating the objective function. This optimization method provides the optimum value in a relatively low number of iterations.

The optimization was conducted considering the number of PVT collectors and batteries to achieve an off-grid capable setup. Moreover, the *PES* and CO_2 ratios were selected as optimization objective functions. As they are similar, the results coincided for both parameters. Figure 3 shows the optimized variables as a function of iterations. The optimization process converged in more than 100 simulations. The optimization results are consistent with the ones obtained by the parametric study. The optimum number of PVT collectors was 30 due to roof limitation. Regarding the number of batteries, the optimum value was 22. Moreover, it is worth noting that the optimization algorithm restricted the lower value for both variables to 1, and the maximum number of batteries was not limited.

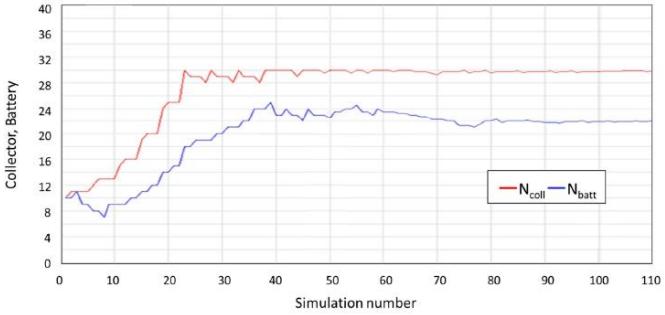

Figure 3. Parametric analysis: performance parameters and grid power, number of batteries.

3.3. Daily Analysis: A Typical Summer Day

A daily result for the summer season is presented next. As a representative day, 6 August was chosen. Figure 4 displays the profile of the main parameters for this typical day. The power produced by the PVT collectors (P_{PVT}) follows the increase in solar radiation. P_{PVT} starts to increase at 6:30, meets its maximum at 12:30 (4197 W), and then decreases until 20:00. The battery power (P_{batt}) meets the electric demand (P_{load}) from 0:00 to 9:00 and from 18:30 to 24:00, which coincides with the overnight period or deficient power production. The excess power produced during the daylight is dumped (P_{dump}) between 13:30 and 19:00 as the battery *SOC* achieves 100%. No electricity is withdrawn from the grid (P_{grid}) during the day. The minimum *SOC* found was around 80%.

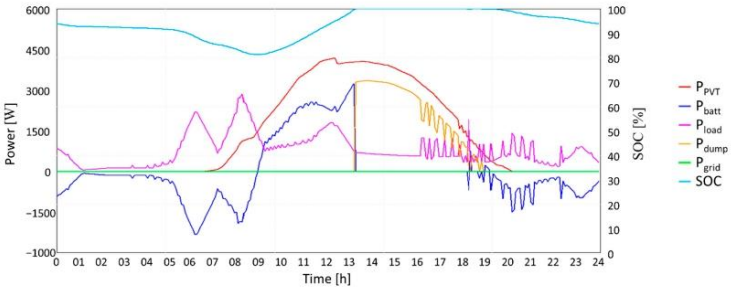

Figure 4. Summer day profile.

3.4. Daily Analysis: A Typical Winter Day

As a winter day, 24 January was selected. Figure 5 shows its main parameters. Here, the sunlight period is shorter. P_{PVT} increases at 8:30, meets its maximum at 13:30 (4292 W), and then decreases until 18:00, four hours less than in the summertime. The battery is fully charged between 9:00 and 12:00. P_{batt} supplies P_{load} from 0:00 to 9:00 and from 18:00 to 24:00, coinciding with the overnight time. P_{dump} occurs between 13:30 and 19:00 as the battery *SOC* achieves 100%. P_{grid} remains null throughout the day. The minimum *SOC* found was greater than the summer case and was around 85%.

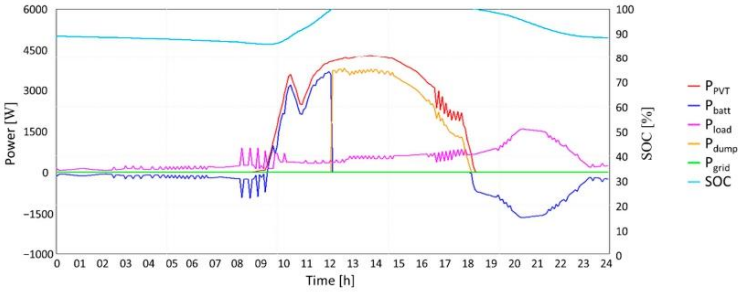

Figure 5. Winter day profile.

3.5. Yearly Results

The state of charge of a lead-acid battery denotes the actual battery capacity as a function of the rated capacity. It can vary between 0% to 100%. In this application, the *SOC* can go down to 30% to minimize the number of batteries during the optimization

process. Therefore, the battery is recharged when the *SOC* reaches 30%. *SOC* over 100% is not permitted. Thus, electricity is dumped whenever 100% *SOC* is achieved.

The annual *SOC* profile found in this study is shown in Figure 6. It is important to note that the *SOC* affects the safe operation, aging, and degradation of the batteries [51]. The minimum *SOC* of 30% was achieved for only a few hours in the year, from 8359 h to 8362 h and from 8408 h to 8409 h.

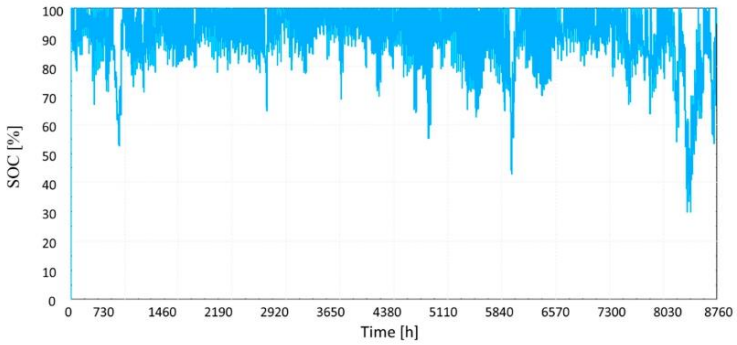

Figure 6. Battery annual SOC profile.

The annual results are summarized in Table 4. Here, P_{prod} is the P_{PVT} minus the regulator/inverter losses due to its inefficiency during the DC to AC conversion (4%). The total useful power production (P_{tot}) is the P_{prod} minus the P_{dump} by the system when the excess power cannot be delivered to the battery because it is fully charged. The off-grid system fully attends to the annual electricity demand during the simulation.

Table 4. Yearly results.

Parameter	Symbol	Value	Unit
Building electricity demand	$P_{build,dem}$	3866	kWh/yr [48]
System electricity demand	$P_{syst,dem}$	2167	kWh/yr
Total electricity demand	$P_{tot,dem}$	6033	kWh/yr
DHW demand	$m_{DHW,dem}$	41	m^3/yr [48]
Freshwater demand	$m_{FW,dem}$	110	m^3/yr [48]
Total water demand	$m_{tot,dem}$	151	m^3/yr
DHW thermal demand	$Q_{DHW,dem}$	1260	kWh/yr
Building cooling demand	$Q_{cool,dem}$	1450	kWh/yr [48]
Building heating demand	$Q_{heat,dem}$	941	kWh/yr [48]
Total thermal demand	$Q_{tot,dem}$	3651	kWh/yr
Power production	P_{prod}	10,018	kWh/yr
Power dumped	P_{dump}	3741	kWh/yr
Total useful power production	P_{tot}	6277	kWh/yr
PVT heat production	Q_{PVT}	39,876	kWh/yr
Air heater dissipation	Q_{AH}	30,599	kWh/yr
Heat losses	Q_{loss}	3234	kWh/yr
Total useful heat production	Q_{tot}	6043	kWh/yr
RO freshwater production	m_{RO}	151	m^3/yr
PVT total efficiency	η_{PVT}	0.55	–
DAC thermal COP	COP_{DAC}	0.42	–
Primary energy saving	*PES*	kWh	12,893
CO_2 saving	CO_2	kg_{CO2}	1380

The total useful heat production (Q_{tot}) is the PVT heat generation (Q_{PVT}) minus the heat released by the AH (Q_{AH}) and the heat dissipated to the environment (Q_{loss}). The energy dissipated by the air heater is around 76.7%, and the thermal losses correspond to 8% of Q_{PVT}. The air heater dissipates much energy as the system prioritizes electricity production. Moreover, Q_{tot} is used for attending $Q_{DHW,dem}$, $Q_{heat,dem}$, and $Q_{cool,dem}$. However, as the DAC thermal *COP* is 0.42, the thermal energy required by the DAC regenerator (3,750 kWh/yr) is much higher than $Q_{cool,dem}$ (1,450 kWh/yr). Nevertheless, the annual thermal demand is also fully supplied by the system.

The previous work [39] simulated a polygeneration system consisting of 17 (27.2 m^2) PVT collectors connected to the national electric grid. An annual near-zero electricity balance was assumed for the electricity withdrawn and sold back to the grid. However, according to the parametric study presented here, this system is not suitable for conversion to an off-grid facility. The addition of lead-acid battery storage on it was not able to provide annual electricity autonomy from the grid.

Consequently, a design optimization was performed to determine a novel polygeneration system setup that is fully independent of the grid. For that case, the number of PVT collectors was increased to 30 (48 m^2), and 22 (48.4 kWh) batteries were established by the optimization algorithm. In particular, the constraints were the roof availability (50 m^2) and the minimum *SOC*, affecting the PVT generation and the storage bank size, respectively.

4. Conclusions

This paper investigated a novel off-grid polygeneration system for residential applications. The proposed system integrates PVT collectors, RO, and DAC coupled with lead-acid batteries. The system was simulated for a single-family townhouse in Spain to meet the demands of electricity, heating, cooling, domestic hot water, and freshwater. The system can be applied to isolated areas with mild relative humidity and temperature, which makes the operation of a DAC possible. The system's layout was dynamically simulated in the TRNSYS environment on an hourly and yearly basis. Design optimization of the system was done under different numbers of PVT collectors and batteries to achieve the optimal off-grid system structure. The main findings are summarized in the following:

1. The introduction of batteries to the already developed on-grid system solely cannot convert it into an off-grid plant. Indeed, the number of PVT collectors and the number of batteries must also be considered.
2. The optimal off-grid system configuration for Almería was obtained for 30 PVT collectors and 22 batteries. This optimization pursued null electricity withdrawn from the grid. For that reason, an energy and environmental approach was used, neglecting the system's economic feasibility.
3. The minimum battery *SOC* was defined as 30%, which may decrease the battery lifespan. However, the yearly results showed that the *SOC* achieved its minimum only for a few hours during the year. Lithium battery would be an interesting choice for avoiding lifespan issues but with higher costs.
4. The energy released by the air heater was around 77% of the generated heat due to an electricity generation priority. The excess heat may be reduced with the addition of PV panels instead of increasing PVT collectors or used in other thermal applications.
5. High *PES* and CO_2 savings were found, and all demands were fully attended.

To sum up, the developed polygeneration system is replicable for other cities, mainly those disconnected from the grid. It can be an interesting option for meeting the energy demands using RES. Future works should investigate the economic feasibility of the capital cost of new and second-life batteries if the grid is not available or determine which system is more attractive if the grid is available, considering the electricity purchase tariff.

Author Contributions: Conceptualization, J.U.; methodology, L.G.G.; formal analysis, L.G.G.; investigation, L.G.G.; resources, J.U.; data curation, L.G.G.; writing—original draft preparation, L.G.G.; writing—review and editing, L.G.G., J.U., and N.D.-O.; supervision, J.U. All authors have read and agreed to the published version of the manuscript.

Funding: This research received no external funding.

Institutional Review Board Statement: Not applicable.

Informed Consent Statement: Not applicable.

Data Availability Statement: Not applicable.

Conflicts of Interest: The authors declare no conflict of interest.

Nomenclature

A	area (m^2)
COP	coefficient of performance
e	open circuit voltages (V)
g	coefficients of H in voltage-current-state of charge formulas (V)
H	complement to 1 of fractional state of charge
$HSOC$	high limit on the fractional state of charge
I	electric current (A)
$LSOC$	low limit on the fractional state of charge
m	cell-type parameter for shapes of the battery I-V-Q characteristics
N	number
P	electric power (kW)
PE	primary energy (kWh/year)
PES	primary energy saving (-)
Q	battery electrical charge or thermal power (Ah or kW)
r	internal resistance (Ω)
SOC	state of charge
t	time (h)
V	volume or voltage (m^3 or V)
v	mass flow rate ($kg\ s^{-1}$)
Greek Symbols	
η	efficiency (-)
Subscripts	
aux	auxiliary
batt	battery
build	referred to the building
cap	capacity
cha	charge
cool	cooling
dem	demand
dis	discharge
dump	electricity dumped
EE	electricity
el	electric
f	collector fluid
grid	referred to the electric grid
heat	heating
inv	inverter
load	referred to the energy load
loss	referred to the energy loss
NG	natural gas
qc	full charge when charging
qd	full charge when discharging
prod	production

R	ratio
syst	referred to the system
th	thermal
tot	total

Abbreviations and acronyms

AC	alternating current
AH	air heater
DAC	desiccant air conditioning
DC	direct current
DHW	domestic hot water
ES	electrical storage
ECS	electric cooling system
FW	freshwater
GB	gas boiler
HVAC	heating, ventilation, and air conditioning
NZEB	nearly zero-energy building
PS	proposed system
PV	photovoltaic panel
PVT	photovoltaic/thermal collector
RO	reverse osmosis
RS	reference system
RES	renewable energy sources
TRNSYS	TRansient SYstem Simulation tool
TES	thermal energy storage
WT	wind turbine

References

1. Costa, A.; Keane, M.M.; Torrens, J.I.; Corry, E. Building Operation and Energy Performance: Monitoring, Analysis and Optimisation Toolkit. *Appl. Energy* **2013**, *101*, 310–316. [CrossRef]
2. International Energy Agency. *Energy and Climate Change: World Energy Outlook Special Report*; IEA: Paris, France, 2015.
3. European Commission. *Communication from the Commission to the European Parliament, the Council, the European Economic and Social Committee and the Committee of the Regions: An EU Strategy on Heating and Cooling*; European Commission: Brussels, Belgium, 2016.
4. European Commission. *Commission Recommendation (EU) 2016/1318: On Guidelines for the Promotion of Nearly Zero-Energy Buildings and Best Practices to Ensure That, by 2020, All New Buildings Are Nearly Zero-Energy Buildings*; Official Journal of the European Union: Brussels, Belgium, 2016; p. 12.
5. Calise, F.; de Notaristefani di Vastogirardi, G.; Dentice d'Accadia, M.; Vicidomini, M. Simulation of Polygeneration Systems. *Energy* **2018**, *163*, 290–337. [CrossRef]
6. Calise, F.; Cappiello, F.L.; Dentice d'Accadia, M.; Vicidomini, M. Thermo-Economic Analysis of Hybrid Solar-Geothermal Polygeneration Plants in Different Configurations. *Energies* **2020**, *13*, 2391. [CrossRef]
7. Olabi, A.G. Renewable Energy and Energy Storage Systems. *Energy* **2017**, *136*, 1–6. [CrossRef]
8. MendezQuezada, V.H.; RivierAbbad, J.; GomezSanRoman, T. Assessment of Energy Distribution Losses for Increasing Penetration of Distributed Generation. *IEEE Trans. Power Syst.* **2006**, *21*, 533–540. [CrossRef]
9. Chen, Y.; Liu, Y.; Wang, Y.; Wang, D.; Dong, Y. The Research on Solar Photovoltaic Direct-Driven Air Conditioning System in Hot-Humid Regions. *Procedia Eng.* **2017**, *205*, 1523–1528. [CrossRef]
10. Yekini Suberu, M.; Wazir Mustafa, M.; Bashir, N. Energy Storage Systems for Renewable Energy Power Sector Integration and Mitigation of Intermittency. *Renew. Sustain. Energy Rev.* **2014**, *35*, 499–514. [CrossRef]
11. Liu, T.; Yang, Z.; Duan, Y.; Hu, S. Techno-Economic Assessment of Hydrogen Integrated into Electrical/Thermal Energy Storage in PV+ Wind System Devoting to High Reliability. *Energy Convers. Manag.* **2022**, *268*, 116067. [CrossRef]
12. Fan, M.; Lu, S. Benefit Analysis and Preliminary Decision-Making of Electrical and Thermal Energy Storage in the Regional Integrated Energy System. *J. Energy Storage* **2022**, *55*, 105816. [CrossRef]
13. Chen, H.; Cong, T.N.; Yang, W.; Tan, C.; Li, Y.; Ding, Y. Progress in Electrical Energy Storage System: A Critical Review. *Prog. Nat. Sci.* **2009**, *19*, 291–312. [CrossRef]
14. Beaudin, M.; Zareipour, H.; Schellenberglabe, A.; Rosehart, W. Energy Storage for Mitigating the Variability of Renewable Electricity Sources: An Updated Review. *Energy Sustain. Dev.* **2010**, *14*, 302–314. [CrossRef]
15. May, G.J.; Davidson, A.; Monahov, B. Lead Batteries for Utility Energy Storage: A Review. *J. Energy Storage* **2018**, *15*, 145–157. [CrossRef]
16. Hazelton, J.; Bruce, A.; MacGill, I. A Review of the Potential Benefits and Risks of Photovoltaic Hybrid Mini-Grid Systems. *Renew. Energy* **2014**, *67*, 222–229. [CrossRef]

17. Wollny, M.; Tapanlis, S. Hybrid Backup Power Solutions for Unstable Grids. In Proceedings of the 4th European Conference on PV-Hybrids and Mini-Grids, Glyfada, Greece, 29–30 May 2008.
18. Dekker, J.; Nthontho, M.; Chowdhury, S. Economic Analysis of PV/ Diesel Hybrid Power Systems in Different Climatic Zones of South Africa. *Int. J. Electr. Power Energy Syst.* **2012**, *40*, 104–112. [CrossRef]
19. Schroeter, A.; Martin, S. Profitable and Affordable Energy Services for Remote Areas in Lao PDR: Private-Public Partnership as Mutual Leverage for Hybrid Village Grids in Areas of the National Grid. In Proceedings of the 4th European Conference on PV-Hybrids and Mini-Grids, Glyfada, Greece, 29–30 May 2008.
20. Wiser, R.; Millstein, D.; Mai, T.; Macknick, J.; Carpenter, A.; Cohen, S.; Cole, W.; Frew, B.; Heath, G. The Environmental and Public Health Benefits of Achieving High Penetrations of Solar Energy in the United States. *Energy* **2016**, *113*, 472–486. [CrossRef]
21. Goldsworthy, M.J. Building Thermal Design for Solar Photovoltaic Air-Conditioning in Australian Climates. *Energy Build.* **2017**, *135*, 176–186. [CrossRef]
22. Li, Y.; Zhang, G.; Lv, G.Z.; Zhang, A.N.; Wang, R.Z. Performance Study of a Solar Photovoltaic Air Conditioner in the Hot Summer and Cold Winter Zone. *Sol. Energy* **2015**, *117*, 167–179. [CrossRef]
23. Vick, B.D.; Neal, B.A. Analysis of Off-Grid Hybrid Wind Turbine/Solar PV Water Pumping Systems. *Sol. Energy* **2012**, *86*, 1197–1207. [CrossRef]
24. Alex, Z.; Clark, A.; Cheung, W.; Zou, L.; Kleissl, J. Minimizing the Lead-Acid Battery Bank Capacity through a Solar PV - Wind Turbine Hybrid System for a High-Altitude Village in the Nepal Himalayas. *Energy Procedia* **2014**, *57*, 1516–1525. [CrossRef]
25. Nookuea, W.; Campana, P.E.; Yan, J. Evaluation of Solar PV and Wind Alternatives for Self Renewable Energy Supply: Case Study of Shrimp Cultivation. *Energy Procedia* **2016**, *88*, 462–469. [CrossRef]
26. Buonomano, A.; Calise, F.; Vicidomini, M.; Dentice d'Accadia. A Hybrid Renewable System Based on Wind and Solar Energy Coupled with an Electrical Storage: Dynamic Simulation and Economic Assessment. *Energy* **2018**, *155*, 174–189. [CrossRef]
27. Rehman, S.; Al-Hadhrami, L.M. Study of a Solar PV–Diesel–Battery Hybrid Power System for a Remotely Located Population near Rafha, Saudi Arabia. *Energy* **2010**, *35*, 4986–4995. [CrossRef]
28. Chabaud, A.; Eynard, J.; Grieu, S. A New Approach to Energy Resources Management in a Grid-Connected Building Equipped with Energy Production and Storage Systems: A Case Study in the South of France. *Energy Build.* **2015**, *99*, 9–31. [CrossRef]
29. Koh, S.L.; Lim, Y.S. Methodology for Assessing Viability of Energy Storage System for Buildings. *Energy* **2016**, *101*, 519–531. [CrossRef]
30. Stadler, M.; Kloess, M.; Groissböck, M.; Cardoso, G.; Sharma, R.; Bozchalui, M.C.; Marnay, C. Electric Storage in California's Commercial Buildings. *Appl. Energy* **2013**, *104*, 711–722. [CrossRef]
31. Zhang, C.; Wei, Y.-L.; Cao, P.-F.; Lin, M.-C. Energy Storage System: Current Studies on Batteries and Power Condition System. *Renew. Sustain. Energy Rev.* **2018**, *82*, 3091–3106. [CrossRef]
32. Comodi, G.; Giantomassi, A.; Severini, M.; Squartini, S.; Ferracuti, F.; Fonti, A.; Nardi Cesarini, D.; Morodo, M.; Polonara, F. Multi-Apartment Residential Microgrid with Electrical and Thermal Storage Devices: Experimental Analysis and Simulation of Energy Management Strategies. *Appl. Energy* **2015**, *137*, 854–866. [CrossRef]
33. Singh, S.; Singh, M.; Kaushik, S.C. Feasibility Study of an Islanded Microgrid in Rural Area Consisting of PV, Wind, Biomass and Battery Energy Storage System. *Energy Convers. Manag.* **2016**, *128*, 178–190. [CrossRef]
34. Destro, N.; Benato, A.; Stoppato, A.; Mirandola, A. Components Design and Daily Operation Optimization of a Hybrid System with Energy Storages. *Energy* **2016**, *117*, 569–577. [CrossRef]
35. Calise, F.; Figaj, R.D.; Vanoli, L. A Novel Polygeneration System Integrating Photovoltaic/Thermal Collectors, Solar Assisted Heat Pump, Adsorption Chiller and Electrical Energy Storage: Dynamic and Energy-Economic Analysis. *Energy Convers. Manag.* **2017**, *149*, 798–814. [CrossRef]
36. Żołądek, M.; Kafetzis, A.; Figaj, R.; Panopoulos, K. Energy-Economic Assessment of Islanded Microgrid with Wind Turbine, Photovoltaic Field, Wood Gasifier, Battery, and Hydrogen Energy Storage. *Sustainability* **2022**, *14*, 12470. [CrossRef]
37. Cappiello, F.L.; Cimmino, L.; Napolitano, M.; Vicidomini, M. Thermoeconomic Analysis of Biomethane Production Plants: A Dynamic Approach. *Sustainability* **2022**, *14*, 5744. [CrossRef]
38. Kim, H.; Jung, Y.; Oh, J.; Cho, H.; Heo, J.; Lee, H. Development and Evaluation of an Integrated Operation Strategy for a Poly-Generation System with Electrical and Thermal Storage Systems. *Energy Convers. Manag.* **2022**, *256*, 115384. [CrossRef]
39. Gesteira, L.G.; Uche, J. A Novel Polygeneration System Based on a Solar-Assisted Desiccant Cooling System for Residential Buildings: An Energy and Environmental Analysis. *Sustainability* **2022**, *14*, 3449. [CrossRef]
40. *TRNSYS: A Transient System Simulation Program*; Solar Energy Laboratory, University of Wisconsin: Madison, WI, USA, 2006.
41. Gómez Melgar, S.; Sánchez Cordero, A.; Videras Rodríguez, M.; Andújar Márquez, J.M. Matching Energy Consumption and Photovoltaic Production in a Retrofitted Dwelling in Subtropical Climate without a Backup System. *Energies* **2020**, *13*, 6026. [CrossRef]
42. Lubello, P.; Pasqui, M.; Mati, A.; Carcasci, C. Assessment of Hydrogen-Based Long Term Electrical Energy Storage in Residential Energy Systems. *Smart Energy* **2022**, *8*, 100088. [CrossRef]
43. Havrlík, M.; Libra, M.; Poulek, V.; Kouřím, P. Analysis of Output Signal Distortion of Galvanic Isolation Circuits for Monitoring the Mains Voltage Waveform. *Sensors* **2022**, *22*, 7769. [CrossRef]
44. Souza, R.P.S. Dynamic Simulation and Optimization of an Off-Grid Solar Photovoltaic Driven Drinking Fountain with Battery Storage. *Int. J. Smart Grid Sustain. Energy Technol.* **2021**, *4*, 13. [CrossRef]

45. Spanish Ministry of Development. Updating of the Energy Saving Document DB-HE of the Technical Building Code. 2019. Available online: https://www.codigotecnico.org/pdf/Documentos/HE/DBHE.pdf (accessed on 1 October 2022).
46. Instituto para la Diversificación y Ahorro de la Energia (IDAE). *CO2 Emission Factors and Primary Energy Coefficients for Different Final Energy Sources Consumed in the Building Sector in Spain*; IDAE: Madrid, Spain, 2014.
47. Red Eléctrica Española (REE). *CO2 Emissions of Electricity Generation in Spain*; REE: Madrid, Spain, 2021.
48. Gesteira, L.G.; Uche, J.; de Oliveira Rodrigues, L.K. Residential Sector Energy Demand Estimation for a Single-Family Dwelling: Dynamic Simulation and Energy Analysis. *J. Sustain. Dev. Energy Water Environ. Syst.* **2021**, *9*, 1080358. [CrossRef]
49. Wetter, J.F. A generic optimization program. In Proceedings of the 7th IBPSA Conference, Rio de Janeiro, Brazil, 13–15 August 2001.
50. Hooke, R.; Jeeves, T.A. "Direct search" solution of numerical and statistical problems. *J. Assoc. Comput. Mach.* **1961**, *8*, 17. [CrossRef]
51. Vetter, J.; Novák, P.; Wagner, M.R.; Veit, C.; Möller, K.-C.; Besenhard, J.O.; Winter, M.; Wohlfahrt-Mehrens, M.; Vogler, C.; Hammouche, A. Ageing Mechanisms in Lithium-Ion Batteries. *J. Power Sources* **2005**, *147*, 269–281. [CrossRef]

A.1 Paper V

sustainability

MDPI

Article

Thermoeconomic Optimization of a Polygeneration System Based on a Solar-Assisted Desiccant Cooling

Luis Gabriel Gesteira [1,2,*], Javier Uche [2], Francesco Liberato Cappiello [3] and Luca Cimmino [3]

[1] Department of Mechanical Technology, Federal Institute of Bahia, Salvador 40301-015, Brazil
[2] CIRCE Research Institute, University of Zaragoza, 50018 Zaragoza, Spain
[3] Department of Industrial Engineering, University of Naples Federico II, P.le Tecchio 80, 80138 Naples, Italy
* Correspondence: 773948@unizar.es

Abstract: This paper presents a thermoeconomic analysis of a polygeneration system based on solar-assisted desiccant cooling. The overall plant layout supplies electricity, space heating and cooling, domestic hot water, and freshwater for a residential building. The system combines photovoltaic/thermal collectors, photovoltaic panels, and a biomass boiler coupled with reverse osmosis and desiccant air conditioning. The plant was modeled in TRNSYS and simulated for 1 year. A parametric study defined the system's setup. A thermoeconomic optimization determined the set of parameters that minimize the simple payback period. The optimal structure showed a total energy efficiency of 0.49 for the solar collectors and 0.16 for the solar panels. The coefficient of performance of the desiccant air conditioning was 0.37. Finally, a sensitivity analysis analyzed the influence of purchase electricity and natural gas costs and the electricity sell-back price on the system. The optimum simple payback was 20.68 years; however, the increase in the energy cost can reduce it by up to 85%.

Keywords: renewable energy; building; polygeneration system; desiccant air conditioning; optimization

Citation: Gesteira, L.G.; Uche, J.; Cappiello, F.L.; Cimmino, L. Thermoeconomic Optimization of a Polygeneration System Based on a Solar-Assisted Desiccant Cooling. *Sustainability* **2023**, *15*, 1516. https://doi.org/10.3390/su15021516

Academic Editor: Alberto-Jesus Perea-Moreno

Received: 6 December 2022
Revised: 4 January 2023
Accepted: 9 January 2023
Published: 12 January 2023

1. Introduction

In the last 20 years, climate change has become a relevant issue in the global scenario [1]. As a matter of fact, the global average temperature is constantly increasing, and the effects of greenhouse gas (GHG) emissions in the atmosphere are dramatic [2]. EU countries have established several strategies to face the climate change issue by increasing the usage of renewables in their systems [3]. The ever-increasing primary energy consumption in all the energy sectors has led to the necessity of exploiting alternative renewable sources [4]. Polygeneration systems based on renewable energy sources (RESs) can replace traditional machinery and supply several energy demands, consequently reducing CO_2 emissions and increasing primary energy saving, as renewables are renewed by the environment and release little or even no carbon dioxide [5]. The concept of the polygeneration system is to exploit one or more renewable sources to simultaneously provide electricity, heating, cooling, and fuels [6]. In the case of residential applications, instead of producing fuels, these systems are used to produce freshwater [7]. The adoption of innovative renewable-based systems for residential applications is becoming increasingly proposed in the scientific literature [8]. Moreover, the study of innovative control strategies to optimize building heating and cooling systems performances is increasingly developing [9].

Several technologies may be adopted for polygeneration systems, based on the different energy source that is supposed to be exploited [10]. The most commonly adopted source in the case of residential applications is the solar one. In recent work, Alqaed et al. [11] proposed a comparative analysis of three polygeneration systems combining in different configurations a desiccant cooling system, an organic Rankine cycle, and a humidification–dehumidification desalination device. N-octane was used as an organic fluid for the ORC

cycle. Results for the optimal configuration showed a production of 102 kW for electricity (all systems), 214.7 kg/h of freshwater (System 2), 29.94 kW of heating (System 2), 225.6 kW of cooling (System 1), and an overall energy efficiency of 0.6303 (System 1). In a more recent study [12], the n-octane solution was compared with other organic fluids such as R245fa, R113, isopentane, and toluene. R113 showed the best result in terms of the energy efficiency of the system.

The polygeneration structure can vary widely to be suitable for different types of buildings and be assessed based on three main indicators, i.e., technical, economic, and environmental [13]. In particular, Chabaud et al. [14] evaluated a novel energy resource management approach in a residential microgrid, using energy and economic criteria. A grid-connected building equipped with energy production and storage systems was modeled and simulated. The authors outlined that the combination of photovoltaic (PV) and wind turbine (WT) systems is an interesting energy mix option for residential buildings. Figaj et al. [15] investigated the energy performance and economic feasibility of polygeneration systems based on biomass, wind turbine, and solar energy for small isolated districts. The polygeneration system also includes thermal and electrical energy storage, an adsorption chiller, and a reverse-osmosis water desalination unit. The proposed system is modeled and simulated through TRNSYS software to dynamically analyze space heating and cooling, electrical energy, and fresh and domestic hot water demands of 10 households located on Pantelleria Island, Italy. Economic results showed that without considering any incentive fee, the simple payback (SPB) of the system proposed ranges between 7 and 12 years. Ceglia et al. [16] recently presented an environmental, energy, and economic analysis of a polygeneration plant based on a geothermal source for district heating and cooling. The residential district is located in Naples, Italy, and the dynamic energy demand is simulated in TRNSYS. Parametric analyses were performed by ranging the depth of the geothermal well and the usage time of the district. The SPB and the net present value are 7 years and EUR 6.11 M, respectively. From the energy point of view, the yearly saved primary energy is 27.2 GWh, with 5490 tons of carbon dioxide emissions avoided.

Buonomano et al. [17] showed a thermoeconomic analysis of a polygeneration system consisting of PV and WT (190 kW and 10 kW, respectively), connected to an energy storage system (ESS) (400 kWh). The plant was modeled in TRNSYS to maximize economic benefits. It was considered time-dependent tariffs applied to the electricity exchanged with the grid and the possibility to store electricity. Results presented a remarkable reduction in operating costs. Calise et al. [18] investigated a thermoeconomic simulation of a polygeneration plant consisting of a solar-assisted heat pump, photovoltaic/thermal collectors (PVT), an adsorption chiller, and an ESS. The system provides domestic hot water (DHW), space cooling and heating, and electricity. Comodi et al. [19] presented the operational results of a residential microgrid system, consisting of a photovoltaic and solar thermal energy plant, a geothermal heat pump, a tank, and an ESS. The results showed that the self-consumption of photovoltaic energy is maximized by the operation of the ESS, with a reduction of electricity fed back to the grid.

Many of the works presented have been proposed for residential applications in warm countries where the large availability of solar energy allows one to make the polygeneration system more profitable. Many interesting works have been proposed in Spain for polygeneration applied to residential buildings analyzing energy and exergy performances [20]. Sigarchian et al. [21] proposed instead a comparative analysis of polygeneration systems in several weather conditions in Iran to analyze the optimal configuration for each case. The analysis shows that in the case of the coldest climate the CO_2 emissions avoided are by 27%, whereas in the warmest case, this value rises to 41%. Unfortunately, the economic feasibility is still far since incentives are needed from the Government to make the systems proposed profitable.

Solar-based systems, namely PV and PVT, are thus widely exploited as renewable energy technologies for the refurbishment of the residential sector. Because of their relevance in this framework, many experimental studies were recently developed to improve their

performance. Praveenkumar et al. [22] recently proposed an experimental study on the optimization of a PV module employing thermos-electric cooling. According to their study, a reduction of roughly 12 °C of the PV module temperature, from about 45 °C to 33 °C, lead to an increase in the cell efficiency of 5%. The drawback of the system is the higher capital cost of the technology than the conventional one. Conversely, the levelized cost of electricity (LCE) is almost the same, around 0.41 USD/kWh, for 8760 hours/year of functioning. The reason is the high power generated thanks to the increase in performance. Ultimately, the same author proposed a 5E analysis of a PV module cooled using a fanless central processing unit (CPU) heat pipe [23]. In this case, the module temperature reduction is 6.7 °C, with a consequent increase in the average power of 1.66 W. The increase in the electric efficiency is 2.98% for the cooled panel, and the embodied energy recorded is 438.52 kWh. The main findings of the LCE analysis show that in the case of a cooled panel, the cost may range from 0.277 to 0.964 USD/kWh, depending on the hours of functioning. Results for the uncooled panel are close, with an LCE from 0.205 to 0.698 USD/kWh, confirming the relevance of the results obtained.

Furthermore, optimization techniques can be used in polygeneration systems to find their best configuration or to improve performance parameters. Stadler et al. [24] examined 139 different commercial buildings in California, performing an analysis of the economic and environmental benefits. A mixed-integer linear algorithm was developed to evaluate the building energy costs and CO_2 emissions. Singh et al. [25] built up a PV–wind system, including biomass and electrical storage. The system matched the electrical load demand of a small-scale zone. In the work, the ideal sizing of components was defined through an artificial bee colony and particle swarm algorithms. The results highlighted the robustness of the algorithm in terms of good-quality results. Destro et al. [26] investigated the ideal design and management strategy of a trigeneration plant for an isolated hotel in the North of Italy consisting of a PV field, a thermal energy storage (TES), a diesel combined heat and power (CHP) engine, and two ESSs, namely, a pumped hydro and a lead–acid battery. The configuration and operation strategies were defined by applying a particle swarm optimization algorithm to reduce costs and meet the hotel's consumption of electricity, heating, cooling, and freshwater.

A large number of papers present polygeneration schemes for cooling, heating, electricity, DHW, and desalinated water production. However, to the best of the authors' knowledge, none of the papers already published include a detailed dynamic thermoeconomic optimization of a polygeneration system based on a solar-assisted desiccant air conditioning (DAC) to supply five demands for the residential sector. To cover such a lack of literature, the present study aims to perform a Hooke–Jeeves optimization to minimize the SPB of a polygeneration system. Furthermore, a sensitivity analysis was performed to investigate the system's behavior according to the electricity and natural gas prices.

2. Materials and Methods

2.1. System Layout

The system's layout is presented in Figure 1. The plant attends to a domestic dwelling. It consists of PVT collectors, PV panels, and a biomass boiler (BB) for electricity and heating production, as well as reverse osmosis (RO) for potable water and DHW demands and a DAC for cooling. Extra devices were used, and all parameters were accurately selected to allow the system proper operation.

The proposed system (PS) is an improvement of the polygeneration plant reported by Gesteira et al. [27]. Here, PV panels, a BB, and a second TES were added to increase the system's robustness. Solar energy is converted into electricity and heat through PV panels and PVT collectors. The best irradiation yield was found for a slope of 35° for the city. The demand of electricity includes all power loads and the building's consumption. The PV panels and PVT collectors are connected to an inverter with peak-power tracking. It allows electricity purchase and sale back to the utility. The grid behaves as a backup as

the solar energy is intermittent, and there is a non-simultaneity between generation and demand [28].

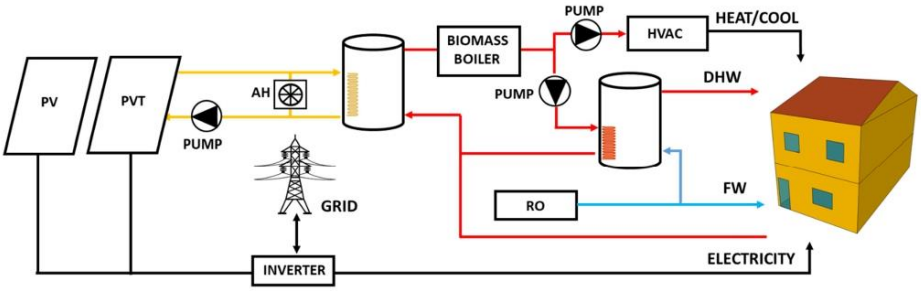

Figure 1. Polygeneration system layout.

A primary TES is used to mitigate the intermittence of solar radiation and a secondary TES supplies DHW for the residence on demand. Moreover, an air heater (AH) dissipates heat whenever the PVT's outlet temperature increases over 100 °C. The primary TES works as a preheater for the boiler, which feeds the heating, ventilation, and air conditioning (HVAC) system, and the secondary TES. The HVAC system supplies heating in the winter season and cooling in the summer. In the winter period, the thermal energy is directly exploited for building space heating. On the other hand, during summer, a DAC system consumes thermal energy to supply building space cooling. Moreover, a tempering valve merges the water heated in the secondary TES with the freshwater and supplies DHW at 45 °C.

2.2. System Model

The PS was modeled in the TRNSYS simulation studio (version 18) [29]. Most of the components come from the software's built-in library. However, some of them are user-defined. A detailed description of the component models used in the simulation is available in TRNSYS's component mathematical reference. In this section, a detailed description of the PV panels and the inverter models are reported. The user-defined and manufacturer's technical data of the PV panels are presented in Table 1.

Table 1. Main parameters of the PV panels.

Component	Parameter	Symbol	Value	Unit
PV	Slope	θ_S	35	°
	Azimuth	θ_A	0	°
	Module area	A_{PV}	1.93	m^2
	Short-circuit current at reference conditions	$I_{sc,ref}$	9.38	A
	Open-circuit voltage at reference conditions	$V_{oc,ref}$	46.2	V
	Reference cell temperature	$T_{c,ref}$	25	°C
	Reference insolation	$G_{T,ref}$	1	kW/m^2
	Voltage at max power point and reference conditions	$V_{mp,ref}$	37.5	V
	Current at max power point and reference conditions	$I_{mp,ref}$	8.81	A
	Temperature coefficient of Isc at reference condition	μ_{Isc}	0.0032	1/°C
	Temperature coefficient of Voc at reference condition	μ_{voc}	25	°C
	Module temperature at NOCT	$T_{c,NOCT}$	45	°C

2.2.1. PV Panel Model

The PV model (Type 103) is a polycrystalline photovoltaic panel. The array works through a maximum power point tracker. The model is based on the "four parameters"

model based on the manufacturers' data for generating an IV curve at each time step [30,31]. The first parameter is the $I_{L,ref}$, which is the photocurrent at reference condition; the second one is the $I_{0,ref}$, which is the diode reverse saturation current at reference condition; γ is the third parameter and means the empirical PV curve-fitting and finally the R_s, which is the module series resistance [32]. The IV curve slope at the short-circuit condition is null. The current-voltage equation of the circuit is shown in Equation (1):

$$I = I_{L,ref}\frac{G_T}{G_{T,ref}} - I_{o,ref}\left(\frac{T_c}{T_{c,ref}}\right)^3\left[\exp\left(\frac{q}{\gamma k T_c}(V + IR_s)\right) - 1\right] \quad (1)$$

The current (I_{mp}) and the voltage (V_{mp}) at the maximum power point are analyzed using an iterative process. Algorithms are used to solve the four equivalent circuit characteristics. Firstly, the voltage and current are replaced in Equation (1) at the short-circuit, open-circuit, and maximum power conditions. Then by considering a rearrangement the following Equations (2)–(4) are obtained depending on $I_{L,ref}$, γ, and $I_{0,ref}$:

$$I_{L,ref} \approx I_{sc,ref} \quad (2)$$

$$\gamma = \frac{q\left(V_{mp,ref} - V_{oc,ref} + I_{mp,ref}R_s\right)}{kT_{c,ref}\ln\left(1 - \frac{I_{mp,ref}}{I_{sc,ref}}\right)} \quad (3)$$

$$I_{o,ref} = I_{sc,ref}\exp^{-\left(\frac{qV_{oc,ref}}{\gamma kT_{c,ref}}\right)} \quad (4)$$

The last unknown parameter needs another equation to be determined, i.e., the analytical derivative of voltage:

$$\frac{\partial V_{oc}}{\partial T_c} = \mu_{voc} = \frac{\gamma k}{q}\left[\ln\left(\frac{I_{sc,ref}}{I_{o,ref}}\right) + \frac{T_c\mu_{isc}}{I_{sc,ref}} - \left(3 + q\varepsilon\left(\frac{\gamma}{N_s}kT_{c,ref}\right)^{-1}\right)\right] \quad (5)$$

N_s is the number of cells in the module, q is the constant of the electron charge, k is the Boltzmann constant, and ε is the bandgap of the semiconductor.

2.2.2. Inverter Model

The inverter (Type 48) is a peak-power tracking device, with no battery as backup. The inverter converts the DC power to AC and sends it to the load and/or to the utility. It allows the power purchase or sale back with the grid. When the production is higher than the consumption, the excess is sent to the utility. When the production is not sufficient to meet the consumption, the power is taken from the utility.

2.2.3. Energy Model

Primary energy saving (PES) analyzes the energy performance of the PS. A reference system (RS) supposes all demands produced by conventional technologies. The assumptions considered were a national grid efficiency (η_{el}) of 0.42 [33] and a natural gas boiler efficiency (η_{th}) of 0.92 [34]. A cooling coefficient of performance based on an electric chiller (COP_{ECH}) of 2.6 [34]. Freshwater is fully provided by the RO unit powered by the national grid, as it is considered a coastal area with water scarcity. Thus, electricity consumption aggregates freshwater demand.

The PES and its ratio (PES_R) are calculated as shown in Equations (6) and (7):

$$PES = PE_{RS} - PE_{PS} \quad (6)$$

$$PES_R = \frac{PES}{PE_{RS}} \quad (7)$$

$$PE_{RS} = \left(\frac{P_{el,dem}}{\eta_{el}} + \frac{Q_{DHW,dem} + Q_{heat,dem}}{\eta_{th}} + \frac{Q_{cool,dem}}{COP_{ECH} \cdot \eta_{el}} \right)_{RS} \quad (8)$$

$$PE_{PS} = \left(\frac{P_{grid,aux}}{\eta_{el}} + \frac{Q_{DHW,aux} + Q_{heat,aux}}{\eta_{th}} + \frac{Q_{cool,aux}}{COP_{ECH} \cdot \eta_{el}} \right)_{PS} \quad (9)$$

$P_{grid,aux}$ is the electricity taken from the utility to match PS consumption, and $Q_{DHW,aux}$, $Q_{heat,aux}$, and $Q_{cool,aux}$ are the thermal need to be provided by a gas boiler (GB) for DHW and space heating, and by an electric chiller (ECH) for space cooling, respectively.

2.2.4. Environmental Model

Following the same approach, the environmental analysis is presented by the CO_2 saving as displayed in Equations (10) and (11):

$$CO_2 = CO_{2RS} - CO_{2PS} \quad (10)$$

$$CO_{2R} = \frac{CO_2}{CO_{2RS}} \quad (11)$$

$$CO_{2RS} = \left(P_{el,dem} + \frac{Q_{cool,dem}}{COP_{ECH}} \right) \cdot f_{CO_2,EE} + \frac{Q_{DHW,dem} + Q_{heat,dem}}{\eta_{th}} \cdot f_{CO_2,NG} \quad (12)$$

$$CO_{2PS} = \left(P_{grid,aux} + \frac{Q_{cool,aux}}{COP_{ECH}} \right) \cdot f_{CO_2,EE} + \frac{Q_{DHW,aux} + Q_{heat,aux}}{\eta_{th}} \cdot f_{CO_2,NG} \quad (13)$$

The CO_2 emission factor of natural gas usage $f_{CO_2,NG}$ in Spain is 0.204 $kgCO_2/kWh$ [35]. The emission factor associated with the Spanish national grid $f_{CO_2,EE}$ is 0.19 $kgCO_2/kWh$ [36].

2.2.5. Economic Model

In this section, a detailed economic analysis is presented to assess the economic feasibility of the polygeneration plant. The operating cost of all components was estimated. Cost functions were introduced to calculate the capital costs of the PS. In particular, the PVT capital cost, Equation (14), is computed as a function of the solar field area A_{PVT} [37]:

$$C_{PVT} = 200 \cdot A_{PVT} \quad (14)$$

The PV unit capital cost per kW, Equation (15), is defined as [38]:

$$CPV = 1000 \text{ EUR/kW} \quad (15)$$

The thermal storage cost, Equation (16), is obtained as a function of its volume, V_{TK} [39]:

$$C_{TK} = 494.9 + 808.0 \cdot V_{TK} \quad (16)$$

The capital cost of the inverter C_{inv} is calculated as a function of the nominal power of the PVT collectors and PV panels (P_{PVT}, P_{PV}) assuming a specific cost equal to 180 EUR/kW_{el} [17]:

$$C_{inv} = 180 \cdot (P_{PVT} + P_{PV}) \quad (17)$$

The biomass boiler capital cost, C_{boiler}, is estimated by IDAE [40] as:

$$C_{boiler} = 282 \text{ EUR/kW} \quad (18)$$

RO device cost C_{RO} was taken from the TRHIBERDE project reported by Acevedo et al. [41]:

$$C_{RO} = \text{EUR } 4650 \quad (19)$$

Regarding the DAC cost, it is a heat-driven component and an effective air conditioner for residential buildings in regions where the use of thermal energy is more economical than electrical power, or when thermal energy is available, i.e., coming from solar collectors. The cost of a desiccant-based air handling unit was presented by Angrisani et al. [42]. Its

specific investment cost C_{DAC} related to the nominal cooling capacity of the system was also reported by the same author [43]:

$$C_{DAC} = 1090\ EUR/kW_{th} \quad (20)$$

Finally, the cost of the pumps was reported by Buonomano et al. [44]:

$$C_{pump} = 1.08 \cdot \left(-0.00000002 \cdot Q_{pump}^2 + 0.0285 \cdot Q_{pump} + 388.14\right) \quad (21)$$

For the cost of all other components required in the system (pipes, valves, controllers, etc.), 20% of the capital cost was assumed. Thus, the total capital cost of the PS was estimated as:

$$C_{PS,tot} = 1.2 \cdot \left(C_{PVT} + C_{PV} + C_{TK} + C_I + C_{boiler} + C_{DAC} + C_{RO} + C_{pump}\right) \quad (22)$$

In addition, the PVT maintenance yearly cost is estimated equal to 2% of the capital cost of the PVT field [37]:

$$M_{PVT} = 2\% \cdot C_{PVT} \quad (23)$$

A PV maintenance annual cost is equal to [38]:

$$M_{PV} = 1\% \cdot C_{PV} \quad (24)$$

A RO unit maintenance cost is estimated as 1.5% of its capital cost [45]:

$$M_{RO} = 1.5\% \cdot C_{RO} \quad (25)$$

Regarding the operating cost of the biomass boiler, a maintenance cost is estimated as 1% of the boiler investment cost [46]:

$$M_{boiler} = 1\% \cdot C_{Boiler} \quad (26)$$

DAC systems are very reliable, so their maintenance cost was neglected.

The economic yearly saving of the PS considers the economic profits with respect to the RS. In the RS, the national utility provides electricity. Conversely, in the PS, the PV panels, the PVT collectors, and the grid match the electric user load. Moreover, the PS is allowed to sell back electricity to the utility at 80% of the purchase price. Considering time-dependent tariffs, the electricity is withdrawn from the national grid with a cost, c_{el}, composed of a fixed, $c_{el,fix}$, and a variable, $c_{el,var}$, parts. $c_{el,fix}$ is proportional to the contracted power, and it is considered in both RS and PS systems; thus, it can be negligible. Conversely, the $c_{el,var}$ is calculated based on the electricity consumption. Values of purchased electricity in EUR/kWh depend on time-of-use tariff are shown in Table 2 [35].

Table 2. Electricity tariffs in Spain.

Period	Hours	$c_{el,fix}$ (EUR/kWy)	$c_{el,var}$ (EUR/kWh)
P1	14–23	47.816	0.173941
P2	1, 8–13, 24		0.099554
P3	2–7		0.076838

In the case of natural gas costs, c_{ng}, the contract depends on the annual gas consumption, which is related to a fixed cost, $c_{ng,fix}$. The variable cost of natural gas, $c_{ng,var}$, is proportional to its usage (Table 3) [35].

Table 3. Natural gas tariff in Spain.

$c_{ng,fix}$ (EUR/y)	$c_{ng,var}$ (EUR/kWh)
61.8	0.063125

Regarding the tap water cost, c_w, in Mediterranean cities, a unit cost of 2 EUR/Sm^3 was considered [47]. Furthermore, for the biomass boiler operation, a biomass (wood-chip) cost, c_b, was reported by IDEA [40] as 0.193 EUR/kg with a Lower Heating Value (LHV) set to 5.2 kWh/kg and a combustion efficiency of 0.85 [46].

So, the annual savings of the PS concerning the RS were calculated as:

$$J_{tot} = C_{op,RS} - C_{op,PS} \quad (27)$$

$$C_{op,RS} = \left(P_{el,dem} + \frac{Q_{cool,dem}}{COP_{ECH}}\right) \cdot c_{el,var} + \frac{Q_{DHW,dem} + Q_{heat,dem}}{\eta_{th}} \cdot c_{ng,var} + c_{ng,fix} + FW_{dem} \cdot c_w \quad (28)$$

$$C_{op,PS} = \left(P_{el,purc} - P_{el,sold}\right) \cdot c_{el,var} + \frac{Q_{boiler}}{\eta_{th} \cdot LHV_b} \cdot c_b + M_{PVT} + M_{PV} + M_{RO} + M_{boiler} \quad (29)$$

Finally, the economic performance of the PS was evaluated by the SPB, Equation (22), calculated as the ratio of the total capital cost and the savings obtained by PS. A lifetime of 20 years for the entire system was assumed, except for the inverter and the RO unit, for which 10 years was considered [18,45].

$$SPB = \frac{J_{tot}}{Cop, RS - Cop, PS} \quad (30)$$

In this study, the annual savings are assumed to be constant over the 20 years life span. In other words, it is assumed that electricity costs remain unchanged and that PV and PVT degradation are neglected. Similarly, it is also assumed that the solar radiation profile is the same for all periods. Therefore, in this work, the cash flow is developed considering an annual cost-saving constant over the system's lifetime.

3. Results

The case study is reported by Gesteira et al. [48]. It consists of a single family dwelling based in Almería, Spain. Meteonorm weather data for Almería (36°50′17″ N, 2°27′35″ W) were used during the simulation. It is worth noting that polygeneration systems applied to European Mediterranean countries can reach up to 80% of energy savings with a suitable level of energy mixture [49]. Figure 2 displays the building's 3D view and its floor plan.

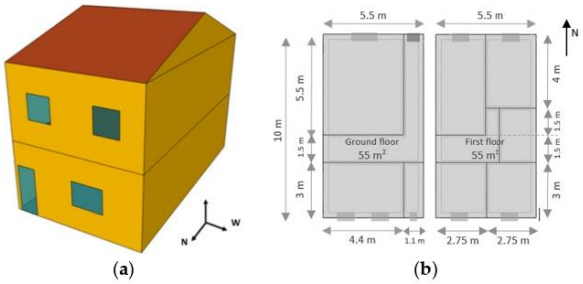

Figure 2. Building geometrical (**a**) and architectural models (**b**).

The simulation was performed from 0 h to 8760 h (1 year) with a 5 min time step. Firstly, to investigate the system's best configuration, a parametric study was carried out. Then, a thermoeconomic optimization was used to determine the set of parameters that minimize the simple payback period. For that reason, the number of PV panels, PVT collectors, and primary and secondary TES volumes was optimized. The yearly results of the optimal structure are presented for the main parameters. Finally, a sensitivity analysis was performed to investigate the system's behavior according to the electricity and natural gas prices.

3.1. Parametric Study

A parametric study was carried out to investigate the most significant design variables when all other parameters remain fixed. The top temperature of the secondary TES ($T_{TES2,top}$) and the boiler outlet temperature ($T_{boiler,out}$) were analyzed as they affect the thermal demand coverages. Furthermore, the study was also performed to define the minimum boiler power capacity (P_{boiler}). $T_{TES2,top}$ and $T_{boiler,out}$ were both varied from 45 °C to 55 °C, while P_{boiler} ranged from 8 to 20 kW.

3.1.1. Parametric Study: Secondary TES Top Temperature

Increasing the $T_{TES2,top}$ leads to an increase in the DHW coverage, as this temperature ensures the achievement of the hot water setpoint defined for the house. As seen in Figure 3, the coverage is almost constant for $T_{TES2,top}$ higher than 49 °C. Thus, it is not convenient to increase $T_{TES2,top}$ over 49 °C, as the maximum DHW coverage is already achieved.

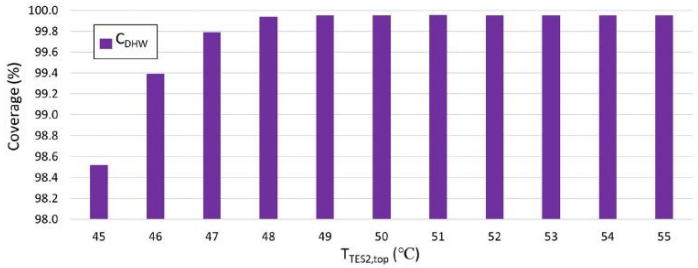

Figure 3. Domestic hot water coverage, the top temperature of the secondary TES.

3.1.2. Parametric Study: Boiler Outlet Temperature

The boiler outlet temperature affects all thermal demands. The minimum $T_{boiler,out}$ is equal to $T_{TES2,top}$, which was already defined in the previous analysis. $T_{TES2,top}$ of 49 °C ensures the maximum DHW coverage. However, the maximum HVAC coverage was not achieved yet. The increase in the $T_{boiler,out}$ provides a higher temperature for the heating fan coil and the DAC regenerator. Figure 4 shows that the coverages are directly proportional to the boiler outlet temperature. The heating and cooling coverages increased from 96% to 102% and from 97% to 104%, respectively. Therefore, there is no energy convenience to increase $T_{boiler,out}$ to values higher than 51 °C. This temperature was selected as a setpoint for the boiler as it provided the maximum coverage for both cooling and heating demands.

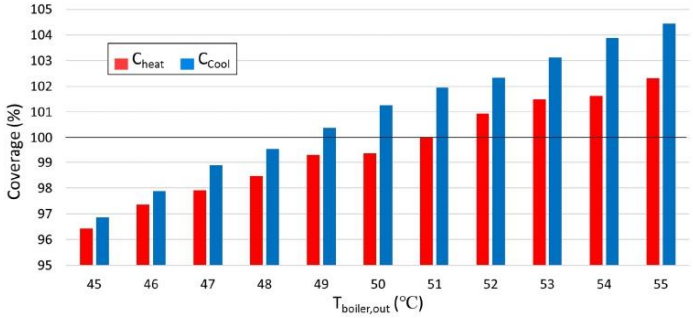

Figure 4. Cooling and heating coverages, boiler outlet temperature.

3.1.3. Parametric Study: Boiler Power Capacity

The BB adds heat to the flow stream at its power capacity (P_{boiler}) whenever the boiler outlet temperature ($T_{boiler,out}$) is less than a setpoint. It performs like an auxiliary heater with an internal control to maintain $T_{boiler,out}$ fixed. The boiler power is related to the capacity of providing an outlet temperature whenever it is required during the simulation. The minimum power capacity commercially available was considered 8 kW. Figure 5 shows the correlation between the P_{boiler} and the thermal coverages. The DHW coverage can be satisfied for all capacities due to its lower temperature requirement. Lower power capacities affect cooling, which achieves 100% at 9 kW. Heating shows the same trend as the others' demands; however, it only meets full coverage at 12 kW. Thus, the power capacity of 12 kW was selected for the boiler as it provided 100% coverage for all house thermal demands.

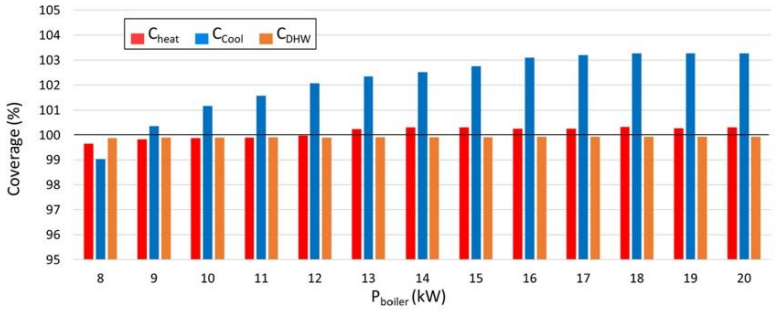

Figure 5. Heating, cooling, and DHW coverages, boiler power capacity.

3.2. Thermoeconomic Optimization

A thermoeconomic optimization was implemented using the TRNOPT tool included in the TRNSYS simulation studio. TRNOPT is designed to link the optimization algorithm and the dynamic simulation. A complex mathematical algorithm is performed by the GENOPT package developed by Lawrence Berkeley National Laboratory [50]. In particular, the Generalized Search Method was used in the optimization by the Hooke–Jeeves [51] modified algorithm. The optimization was performed considering the main design variables, namely: the number of PVT collectors (N_{coll}), number of PV panels (N_{pan}), primary TES volume (V_{TES1}), and secondary TES volume (V_{TES2}). Moreover, the SPB was selected as the optimization objective function. Table 4 shows the details of the main variables. The optimization range is defined by its minimum and maximum values. The first attempt starts with the initial value and proceeds with the iterations according to the step size.

Table 4. Optimization variables breakdown.

Variables	Ncoll	Npan	V_{TES1}	V_{TES2}
Initial Value	15	15	2.5	0.15
Minimum Value	1	1	0.3	0.05
Maximum Value	30	25	5	0.3
Step Size	1	1	0.1	0.05

Figure 6 shows the SPB and the design variables as a function of the optimization iteration. The optimization process converged in a bit over 150 iterations. The optimal configuration is obtained when the SPB achieves its minimum value. The optimum SPB value of 20.68 years was obtained for 9 PVT collectors, 25 PV panels, and a primary and secondary TES volume of 1.35 m^3 and 0.25 m^3, respectively. Moreover, it is worth noting

that the number of collectors and panels was limited to 50 m^2 due to the available roof area at the house.

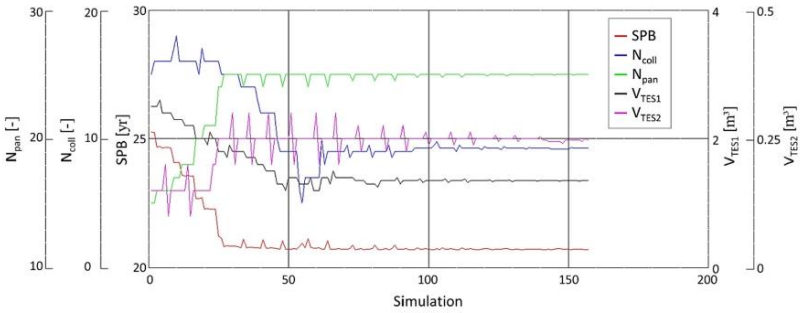

Figure 6. SPB and the design variables, optimization iteration.

3.3. Yearly Results

The annual results for the optimal solution are summarized in Table 5. The table presents the yearly integrated number of electricity, heat, and water volume. Moreover, the performance parameters are also presented. The building demands were taken from Ref. [48].

Table 5. Yearly results.

Parameter	Symbol	Value	Unit
Freshwater demand	$m_{FW,dem}$	151	m^3/yr
Electricity demand	$P_{el,dem}$	5.11	MWh/yr
DHW demand	$Q_{DHW,dem}$	1.26	MWh/yr
Cooling demand	$Q_{cool,dem}$	1.45	MWh/yr
Heating demand	$Q_{heat,dem}$	0.94	MWh/yr
RO freshwater production	m_{RO}	151	m^3/yr
PV power production	P_{PV}	16.81	MWh/yr
PVT power production	P_{PVT}	2.91	MWh/yr
Power loss	P_{loss}	1.97	MWh/yr
Total power production	$P_{tot,prod}$	17.75	MWh/yr
PVT heat production	Q_{PVT}	9.53	MWh/yr
Biomass boiler production	Q_{boiler}	1.54	MWh/yr
Air heater dissipation	Q_{AH}	1.18	MWh/yr
Heat loss	Q_{loss}	3.13	MWh/yr
Total useful heat production	$Q_{tot,prod}$	6.75	MWh/yr
PV efficiency	η_{PV}	0.16	–
PVT efficiency	η_{PVT}	0.49	–
DAC thermal COP	COP_{DAC}	0.37	–
Primary energy saving	PES	12.9	MWh
CO_2 saving	CO_2	1.29	$tonCO_2$
Simple payback	SPB	20.69	yr

The power generation ($P_{tot,prod}$) is the PV (P_{PV}) and PVT (P_{PVT}) generation minus the losses (P_{loss}) due to the inverter's inefficiency (10%). The excess power is injected into the grid (12.64 MWh/yr).

The total useful heat production ($Q_{tot,prod}$) is the PVT heat generation (Q_{PVT}) and the BB production (Q_{boiler}) subtracted by the energy released by the AH (Q_{AH}) and the total energy dissipated to the surroundings (Q_{loss}). The heat released by the AH is about

12% of Q_{PVT}. Moreover, $Q_{tot,prod}$ is used for attending $Q_{DHW,dem}$, $Q_{heat,dem}$, and $Q_{cool,dem}$; however, as the DAC thermal COP is equal to 0.37, the heat requested by the regenerator was 4.43 MWh/yr.

3.4. Sensitivity Analysis

A sensitivity analysis investigated how electricity purchase, electricity sell-back, and natural gas prices affect the economic performance of the PS. Thus, the purchasing costs were progressively increased, and the sell-back price was reduced (Table 6). Each parameter was evaluated for each case, and the optimization results were collected.

Table 6. Sensitivity analysis variables.

Parameter	Case 1	Case 2	Case 3	Case 4	Case 5
Electricity purchase cost	+50%	+100%	+150%	+200%	+250%
Natural gas purchase cost	+50%	+100%	+150%	+200%	+250%
Electricity sell-back cost	−10%	−20%	−30%	−40%	−50%

3.4.1. Sensitivity Analysis: Purchase Cost of Electricity

Considering that the RS is based on the consumption of electricity, the increase in the energy price worsens economic performance. Conversely, in the PS, electricity may be sold back to the grid. Thus, higher energy cost enhances its economic performance because the sell-back cost of electricity is a ratio of the electricity purchase cost. The increase in the electricity cost leads to an increase in the operational cost of the RS and improves the economic savings of the PS. Figure 7 displays the sensitivity analysis of the electricity purchase cost.

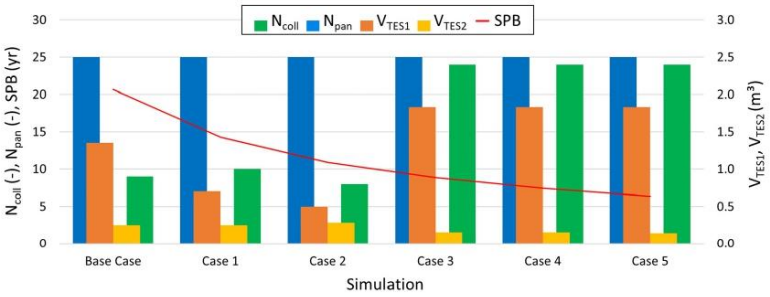

Figure 7. SPB and the design variables, optimization case (purchase cost of electricity).

The number of PV panels remains constant at 25 for all cases simulated. The number of PVT collectors increases from 9 to 24 between the second and third cases. At the same point, the volume of the primary TES increases, following the higher thermal energy availability, and the secondary TES volume decreases. It demonstrates that as of Case 3, the energy cost becomes very expensive; thus, the electricity sold back to the grid is more attractive, as it is proportional to the purchase cost. Therefore, electricity production increased to its maximum. The SPB decreases to 6.38 years when the purchase cost of electricity increases up to 250%.

3.4.2. Sensitivity Analysis: Purchase Cost of Natural Gas

The RS is also dependent on natural gas consumption; thus, the increase in the energy price worsens the economic performance. On the other hand, the PS is not affected by the natural gas cost. The increase in the natural gas cost leads solely to an increase in the

operational cost of the RS. Therefore, the SPB decrease is slighter compared to the previous case. Figure 8 displays the sensitivity analysis of the natural gas purchase cost.

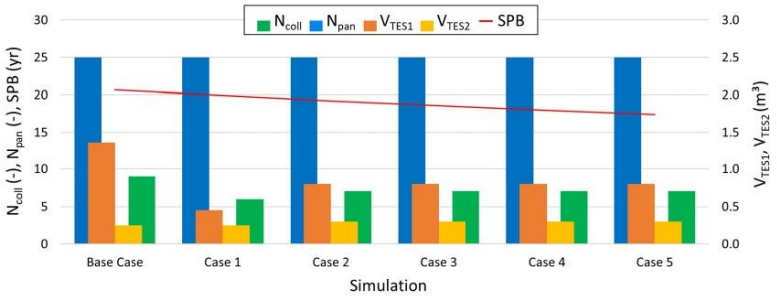

Figure 8. SPB and the design variables, optimization case (purchase cost of natural gas).

The number of PV panels remains constant at 25 for all cases simulated. The number of PVT collectors and the primary and secondary TES volumes present a minor variation around 7, 0.8 m^3, and 0.3 m^3, respectively. The SPB decreases 15.81% from the base case to the last case, while the purchase cost of natural gas increases up to 250%.

3.4.3. Sensitivity Analysis: Sell-Back Cost of Electricity

In the PS, electricity may be sold back to the grid with a price defined as a ratio of the electricity purchase cost. Thus, a lower sell-back cost worsens its economic performance. The decrease in this ratio leads to an increase in the operational cost of the PS. Figure 9 displays the sensitivity analysis of the sell-back cost of electricity.

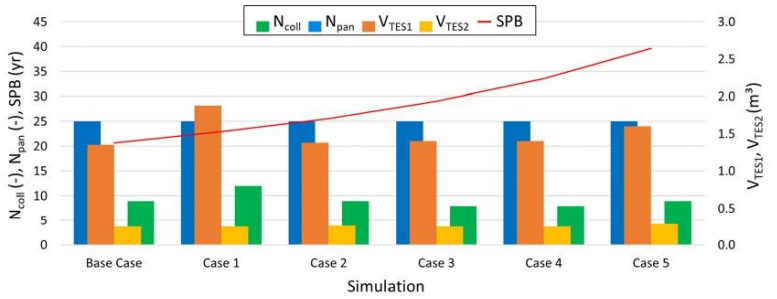

Figure 9. SPB and the design variables, optimization case (sell-back cost of electricity).

Again, the number of PV panels remains constant at 25 for all cases simulated. The number of PVT collectors and primary and secondary TES varies between 8 to 12, 1.35 to 1.88 m^3, and 0.25 to 0.28 m^3, respectively. It indicates that the system design is relatively constant along the iterations. However, the SPB increases to 39.61 years when the sell-back cost of electricity decreases to 30% of the purchase cost.

4. Conclusions

This study performed a thermoeconomic analysis of a solar-assisted desiccant cooling polygeneration plant. The facility provides electricity, space heating and cooling, DHW, and potable water for a residential building. The system combines photovoltaic/thermal collectors, photovoltaic panels, and a biomass boiler coupled with reverse osmosis and

desiccant air conditioning. The plant was applied to a dwelling for a Spanish single family. The system's model was performed in the TRNSYS simulation studio. A parametric study, a thermoeconomic optimization, and a sensitivity analysis of the system were performed. The main findings are summarized below:

1. The top temperature of the secondary TES and the boiler outlet temperature and power capacity were defined as 49 °C, 51 °C, and 12 kW, respectively.
2. The optimum SPB value of 20.68 years was obtained for 9 PVT collectors, 25 PV panels, and a primary and secondary TES volume of 1.35 m^3 and 0.25 m^3, respectively.
3. The optimal structure showed a total energy efficiency of 0.49 for the solar collectors, 0.16 for the solar panels, and a desiccant air conditioning coefficient of performance of 0.37
4. The yearly results showed that 12.64 MWh/yr of electricity was injected into the grid.
5. The increase in the electricity purchase cost makes the proposed polygeneration system economically profitable. On the other hand, the decrease in the electricity sell-back cost reduces its feasibility. The increase in the natural gas cost is not very relevant to the system's profitability decision making.
6. The highest prices of electricity and natural gas (+250%) and the sell-back cost of electricity (base case) can reduce the SPB by up to 85%.

Regarding the system, variations in solar energy can be found over the 20-year life span. Moreover, the time-dependent tariff may vary year by year due to inflation or energy scarcity periods. However, it is impossible to predict the behavior of climate conditions and the future time-dependent prices of electricity over such a long period. Furthermore, PV and PVT degradation may be neglected (around 1% per year). Finally, the system may be a good solution for matching the energy consumption using renewables mostly if a capital investment subsidy is considered.

Author Contributions: Conceptualization, J.U.; methodology, F.L.C., L.C. and L.G.G.; formal analysis, L.G.G.; investigation, L.C. and L.G.G.; resources, J.U.; data curation, F.L.C. and L.G.G.; writing—original draft preparation, L.C. and L.G.G.; writing—review and editing, F.L.C. and J.U.; supervision, J.U. All authors have read and agreed to the published version of the manuscript.

Funding: The author J.U. has been funded by European Regional Development Funds (FEDER, UE)/Spanish Ministry of Science, Innovation, and Universities (MCIU)–Spanish State Research Agency (AEI), grant number RTI2018-09886-A-100.

Institutional Review Board Statement: Not applicable.

Informed Consent Statement: Not applicable.

Data Availability Statement: Not applicable.

Conflicts of Interest: The authors declare no conflict of interest.

References

1. Perkins-Kirkpatrick, S.; Green, D. Chapter 2—Extreme Heat and Climate Change. In *Heat Exposure and Human Health in the Context of Climate Change*; Elsevier: Amsterdam, The Netherlands, 2023; pp. 5–36. ISBN 978-0-12-819080-7.
2. Borie, M.; Mahony, M.; Obermeister, N.; Hulme, M. Knowing like a Global Expert Organization: Comparative Insights from the IPCC and IPBES. *Glob. Environ. Chang.* **2021**, *68*, 102261. [CrossRef]
3. Köhl, M.; Linser, S.; Prins, K.; Talarczyk, A. The EU Climate Package "Fit for 55"—A Double-Edged Sword for Europeans and Their Forests and Timber Industry. *For. Policy Econ.* **2021**, *132*, 102596. [CrossRef]
4. Saint Akadiri, S.; Alola, A.A.; Akadiri, A.C.; Alola, U.V. Renewable Energy Consumption in EU-28 Countries: Policy toward Pollution Mitigation and Economic Sustainability. *Energy Policy* **2019**, *132*, 803–810. [CrossRef]
5. Calise, F.; de Notaristefani di Vastogirardi, G.; Dentice d'Accadia, M.; Vicidomini, M. Simulation of Polygeneration Systems. *Energy* **2018**, *163*, 290–337. [CrossRef]
6. Gimelli, A.; Muccillo, M. Development of a 1 KW Micro-Polygeneration System Fueled by Natural Gas for Single-Family Users. *Energies* **2021**, *14*, 8372. [CrossRef]

7. Khoshgoftar Manesh, M.H.; Mousavi Rabeti, S.A.; Nourpour, M.; Said, Z. Energy, Exergy, Exergoeconomic, and Exergoenvironmental Analysis of an Innovative Solar-Geothermal-Gas Driven Polygeneration System for Combined Power, Hydrogen, Hot Water, and Freshwater Production. *Sustain. Energy Technol. Assess.* **2022**, *51*, 101861. [CrossRef]
8. Calise, F.; Cappiello, F.L.; Cimmino, L.; Dentice d'Accadia, M.; Vicidomini, M. Dynamic Simulation and Thermoeconomic Analysis of a Hybrid Renewable System Based on PV and Fuel Cell Coupled with Hydrogen Storage. *Energies* **2021**, *14*, 7657. [CrossRef]
9. Sawant, P.; Villegas Mier, O.; Schmidt, M.; Pfafferott, J. Demonstration of Optimal Scheduling for a Building Heat Pump System Using Economic-MPC. *Energies* **2021**, *14*, 7953. [CrossRef]
10. Calise, F.; Dentice D'Accadia, M. Simulation of Polygeneration Systems. *Energies* **2016**, *9*, 925. [CrossRef]
11. Alqaed, S.; Fouda, A.; Elattar, H.F.; Mustafa, J.; Almehmadi, F.A.; Refaey, H.A.; Alharthi, M.A. Performance Evaluation of a Solar Heat-Driven Poly-Generation System for Residential Buildings Using Various Arrangements of Heat Recovery Units. *Energies* **2022**, *15*, 8750. [CrossRef]
12. Almehmadi, F.A.; Elattar, H.F.; Fouda, A.; Alqaed, S.; Mustafa, J.; Alharthi, M.A.; Refaey, H.A. Energy Performance Assessment of a Novel Solar Poly-Generation System Using Various ORC Working Fluids in Residential Buildings. *Energies* **2022**, *15*, 8286. [CrossRef]
13. Jana, K.; Ray, A.; Majoumerd, M.M.; Assadi, M.; De, S. Polygeneration as a Future Sustainable Energy Solution—A Comprehensive Review. *Appl. Energy* **2017**, *202*, 88–111. [CrossRef]
14. Chabaud, A.; Eynard, J.; Grieu, S. A New Approach to Energy Resources Management in a Grid-Connected Building Equipped with Energy Production and Storage Systems: A Case Study in the South of France. *Energy Build.* **2015**, *99*, 9–31. [CrossRef]
15. Figaj, R.; Żołądek, M.; Homa, M.; Pałac, A. A Novel Hybrid Polygeneration System Based on Biomass, Wind and Solar Energy for Micro-Scale Isolated Communities. *Energies* **2022**, *15*, 6331. [CrossRef]
16. Ceglia, F.; Macaluso, A.; Marrasso, E.; Roselli, C.; Vanoli, L. Energy, Environmental, and Economic Analyses of Geothermal Polygeneration System Using Dynamic Simulations. *Energies* **2020**, *13*, 4603. [CrossRef]
17. Buonomano, A.; Calise, F.; d'Accadia, M.D.; Vicidomini, M. A Hybrid Renewable System Based on Wind and Solar Energy Coupled with an Electrical Storage: Dynamic Simulation and Economic Assessment. *Energy* **2018**, *155*, 174–189. [CrossRef]
18. Calise, F.; Figaj, R.D.; Vanoli, L. A Novel Polygeneration System Integrating Photovoltaic/Thermal Collectors, Solar Assisted Heat Pump, Adsorption Chiller and Electrical Energy Storage: Dynamic and Energy-Economic Analysis. *Energy Convers. Manag.* **2017**, *149*, 798–814. [CrossRef]
19. Comodi, G.; Giantomassi, A.; Severini, M.; Squartini, S.; Ferracuti, F.; Fonti, A.; Nardi Cesarini, D.; Morodo, M.; Polonara, F. Multi-Apartment Residential Microgrid with Electrical and Thermal Storage Devices: Experimental Analysis and Simulation of Energy Management Strategies. *Appl. Energy* **2015**, *137*, 854–866. [CrossRef]
20. Picallo-Perez, A.; Sala-Lizarraga, J.M. Design and Operation of a Polygeneration System in Spanish Climate Buildings under an Exergetic Perspective. *Energies* **2021**, *14*, 7636. [CrossRef]
21. Ghaem Sigarchian, S.; Malmquist, A.; Martin, V. Design Optimization of a Small-Scale Polygeneration Energy System in Different Climate Zones in Iran. *Energies* **2018**, *11*, 1115. [CrossRef]
22. Experimental Assessment of Thermoelectric Cooling on the Efficiency of PV Module. *Int. J. Renew. Energy Res.* **2022**. [CrossRef]
23. Praveenkumar, S.; Gulakhmadov, A.; Agyekum, E.B.; Alwan, N.T.; Velkin, V.I.; Sharipov, P.; Safaraliev, M.; Chen, X. Experimental Study on Performance Enhancement of a Photovoltaic Module Incorporated with CPU Heat Pipe—A 5E Analysis. *Sensors* **2022**, *22*, 6367. [CrossRef] [PubMed]
24. Stadler, M.; Kloess, M.; Groissböck, M.; Cardoso, G.; Sharma, R.; Bozchalui, M.C.; Marnay, C. Electric Storage in California's Commercial Buildings. *Appl. Energy* **2013**, *104*, 711–722. [CrossRef]
25. Singh, S.; Singh, M.; Kaushik, S.C. Feasibility Study of an Islanded Microgrid in Rural Area Consisting of PV, Wind, Biomass and Battery Energy Storage System. *Energy Convers. Manag.* **2016**, *128*, 178–190. [CrossRef]
26. Destro, N.; Benato, A.; Stoppato, A.; Mirandola, A. Components Design and Daily Operation Optimization of a Hybrid System with Energy Storages. *Energy* **2016**, *117*, 569–577. [CrossRef]
27. Gesteira, L.G.; Uche, J. A Novel Polygeneration System Based on a Solar-Assisted Desiccant Cooling System for Residential Buildings: An Energy and Environmental Analysis. *Sustainability* **2022**, *14*, 3449. [CrossRef]
28. Pina, E.A.; Lozano, M.A.; Serra, L.M. A Multiperiod Multiobjective Framework for the Synthesis of Trigeneration Systems in Tertiary Sector Buildings. *Int. J. Energy Res.* **2019**, *44*, 1140–1166. [CrossRef]
29. *TRNSYS: A Transient System Simulation Program*; Solar Energy Laboratory, University of Wisconsin: Madison, WI, USA, 2006.
30. Duffie, J.A.; Beckman, W.A. *Solar Engineering of Thermal Processes*; John Wiley & Sons: New York, NY, USA, 1991.
31. Eckstein, J.H. Detailed Modeling of Photovoltaic Components. Master's Thesis, University of Wisconsin, Solar Energy Laboratory, Madison, WI, USA, 1990.
32. Buonomano, A.; Calise, F.; Vicidomini, M. Design, Simulation and Experimental Investigation of a Solar System Based on PV Panels and PVT Collectors. *Energies* **2016**, *9*, 497. [CrossRef]
33. Instituto para la Diversificación y Ahorro de la Energia (IDAE). *CO_2 Emission Factors and Primary Energy Coefficients for Different Final Energy Sources Consumed in the Building Sector in Spain*; IDAE: Madrid, Spain, 2014.
34. Spanish Ministry of Development. Updating of the Energy Saving Document DB-HE of the Technical Building Code. 2019. Available online: https://www.codigotecnico.org/pdf/Documentos/HE/DBHE.pdf (accessed on 1 October 2021).

35. Pinto, E.S.; Serra, L.M.; Lázaro, A. Optimization of the Design of Polygeneration Systems for the Residential Sector under Different Self-consumption Regulations. *Int. J. Energy Res.* **2020**, *44*, 11248–11273. [CrossRef]
36. Red Eléctrica Española (REE). *CO_2 Emissions of Electricity Generation in Spain*; REE: Madrid, Spain, 2021.
37. Calise, F.; Cappiello, F.L.; Dentice d'Accadia, M.; Vicidomini, M. Dynamic Simulation, Energy and Economic Comparison between BIPV and BIPVT Collectors Coupled with Micro-Wind Turbines. *Energy* **2020**, *191*, 116439. [CrossRef]
38. Calise, F.; Cappiello, F.L.; Dentice d'Accadia, M.; Petrakopoulou, F.; Vicidomini, M. A Solar-Driven 5th Generation District Heating and Cooling Network with Ground-Source Heat Pumps: A Thermo-Economic Analysis. *Sustain. Cities Soc.* **2022**, *76*, 103438. [CrossRef]
39. Calise, F.; Dentice d'Accadia, M.; Figaj, R.D.; Vanoli, L. A Novel Solar-Assisted Heat Pump Driven by Photovoltaic/Thermal Collectors: Dynamic Simulation and Thermoeconomic Optimization. *Energy* **2016**, *95*, 346–366. [CrossRef]
40. Instituto para la Diversificación y Ahorro de la Energía (IDAE). *Biomass Price Report for Thermal Uses*; IDEA: Madrid, Spain, 2020.
41. Acevedo, L.; Uche, J.; Del Almo, A.; Círez, F.; Usón, S.; Martínez, A.; Guedea, I. Dynamic Simulation of a Trigeneration Scheme for Domestic Purposes Based on Hybrid Techniques. *Energies* **2016**, *9*, 1013. [CrossRef]
42. Angrisani, G.; Roselli, C.; Sasso, M.; Tariello, F. Dynamic Performance Assessment of a Micro-Trigeneration System with a Desiccant-Based Air Handling Unit in Southern Italy Climatic Conditions. *Energy Convers. Manag.* **2014**, *80*, 188–201. [CrossRef]
43. Angrisani, G.; Roselli, C.; Sasso, M. Experimental Assessment of the Energy Performance of a Hybrid Desiccant Cooling System and Comparison with Other Air-Conditioning Technologies. *Appl. Energy* **2015**, *138*, 533–545. [CrossRef]
44. Buonomano, A.; Calise, F.; Ferruzzi, G.; Vanoli, L. A Novel Renewable Polygeneration System for Hospital Buildings: Design, Simulation and Thermo-Economic Optimization. *Appl. Therm. Eng.* **2014**, *67*, 43–60. [CrossRef]
45. Calise, F.; Cappiello, F.L.; Vanoli, R.; Vicidomini, M. Economic Assessment of Renewable Energy Systems Integrating Photovoltaic Panels, Seawater Desalination and Water Storage. *Appl. Energy* **2019**, *253*, 113575. [CrossRef]
46. Mouaky, A.; Rachek, A. Thermodynamic and Thermo-Economic Assessment of a Hybrid Solar/Biomass Polygeneration System under the Semi-Arid Climate Conditions. *Renew. Energy* **2020**, *156*, 14–30. [CrossRef]
47. Uche, J.; Acevedo, L.; Círez, F.; Usón, S.; Martínez-Gracia, A.; Bayod-Rújula, Á.A. Analysis of a Domestic Trigeneration Scheme with Hybrid Renewable Energy Sources and Desalting Techniques. *J. Clean. Prod.* **2019**, *212*, 1409–1422. [CrossRef]
48. Gesteira, L.G.; Uche, J.; de Oliveira Rodrigues, L.K. Residential Sector Energy Demand Estimation for a Single-Family Dwelling: Dynamic Simulation and Energy Analysis. *J. Sustain. Dev. Energy Water Environ. Syst.* **2021**, *9*, 1–18. [CrossRef]
49. Serra, L.M.; Lozano, M.-A.; Ramos, J.; Ensinas, A.V.; Nebra, S.A. Polygeneration and Efficient Use of Natural Resources. *Energy* **2009**, *34*, 575–586. [CrossRef]
50. Wetter, M. GenOpt—A Generic Optimization Program. In Proceedings of the Seventh International IBPSA Conference, Rio de Janeiro, Brazil, 13–15 August 2001; pp. 601–608.
51. Hooke, R.; Jeeves, T.A. "Direct Search" Solution of Numerical and Statistical Problems. *J. ACM* **1961**, *8*, 212–229. [CrossRef]

A.1 Paper VI

applied sciences

MDPI

Article

A Sustainable Polygeneration System for a Residential Building

Javier Uche *, Ignacio Zabalza, Luis G. Gesteira, Amaya Martínez-Gracia and Sergio Usón

CIRCE Research Institute, University of Zaragoza, 50018 Zaragoza, Spain
* Correspondence: javiuche@unizar.es

Abstract: In line with the decarbonization of the domestic sector to meet the 2050 climate neutrality targets, this paper describes the energy, economic, and environmental analysis of a set of different novel configurations of polygeneration installations to provide electricity, air conditioning, domestic hot water, and desalinated water for a building of 80 dwellings. All arrangements were designed to cover 100% of the five demands required in the building with renewable energy only, from photovoltaic (PV) and photovoltaic-thermal (PVT) panels and biomass backup boilers (BB). Electricity can be sold to or purchased from the grid without electrical storage with batteries. Additional electricity generation with thermoelectric generators (TEG) coupled to the PVTs, and the BB was explicitly analyzed. The choice of electrically or thermally activated technologies (heat pump, HP/single-effect absorption chiller, SEAC for cooling and multi-effect distillation, MED/reverse osmosis, RO for desalination) created four configurations from the basic structure based on solar and biomass sources. Thus, the paper has studied four designs in detail and applied them to three case studies corresponding to different locations in Spain. They were modeled with TRNSYS and included specific models for desalination technologies. Both structures provide important energy and CO_2 savings concerning the conventional supply of the building demands. The novel life-cycle analysis approach further increases the lifetime CO_2 savings for all configurations as well. The electric option (the combination of HP and RO for cooling and desalting) was, by far, the most attractive solution in terms of liability and lower investment required in the three case studies.

Keywords: polygeneration; desalination; buildings; renewable sources self-consumption

Citation: Uche, J.; Zabalza, I.; Gesteira, L.G.; Martínez-Gracia, A.; Usón, S. A Sustainable Polygeneration System for a Residential Building. *Appl. Sci.* **2022**, *12*, 12992. https://doi.org/10.3390/app122412992

Academic Editor: Angelo Algieri

Received: 23 November 2022
Accepted: 15 December 2022
Published: 18 December 2022

1. Introduction

In Europe, buildings are responsible for 40% of energy consumption and 36% of CO_2 emissions, and similar figures are reported in the United States [1]. The decarbonization of the building sector by 2050 is an ambitious objective requiring the implementation of energy transition strategies. To do so, the actions needed to perform that plan must be helped by regulatory changes and the support for investments in energy efficiency, especially for existing buildings, in which improvements are easier to reach since present references are relatively high in terms of energy consumption.

Since 2002, three progressive Directives on Energy Performance of Buildings have been approved (Directive 2002/91/CE [2], Directive 2010/31/EU [3], and Directive (EU) 2018/844 [4]). This has led to a gradual improvement in enclosures to reduce losses, which has been transposed into national regulations. Consequently, from 2020, all new residential, office, and service buildings are expected to be nearly zero-energy buildings. In the next few years, new rules will try to account for many new and existing decarbonized buildings by the year 2050. A new directive is currently being drafted, which would limit the use of fossil fuels for community heating and promote high-efficiency heat pumps. A new energy rating for buildings is to be upgraded in quality in each country depending on the age of the building.

To reduce final energy consumption, it is evident that improving the thermal envelope could lead to significant cuts in demand. It could also lead to better thermal comfort [5].

Note that around 50% of the primary energy demands in buildings are linked to heating, ventilation, and air conditioning. Building energy codes (BECs) have been one of the keys in reducing buildings' energy consumption. Unfortunately, their effectiveness is based on their mandatory and enforced nature [6]. This can be shown in comparative studies of BECs in neighboring countries with similar climate conditions [7,8].

On the other hand, energy demands have to be served more sustainably. A sustainable and safe solution for a building is a polygeneration scheme that simultaneously produces electricity, heating, cooling, and freshwater (partly converted into domestic hot water) from a single or several primary resources. Polygeneration schemes have been used in industry, in many cases with products other than those described above, and not always using only renewable energy sources [9,10]. Several studies on providing electricity, freshwater, and heating and cooling for diverse uses have recently presented sustainable solutions in isolated and/or rural areas [11–18], coming from solar and biomass resources. In the case of these four basic demands for a building, the number of scientific references is already somewhat smaller according to our state-of-the-art review [19–24]. In all cases, simulations are carried out, including the optimization of their design, their energy, environmental, and economic analysis, and their sensitivity to the externalities of the proposed plant. Still, there are no experimental studies analyzing the feasibility of this integrated approach, given its complexity and the significant investment required.

A polygeneration scheme mainly based on RES heat-producing technologies, such as PVTs and biomass boilers, is a natural solution since these are the only available renewable sources in a water-scarce area near the coast. Anyway, at the tail of the scheme, different options to produce cooling and desalinated water should be checked to find the best integration. In other words, consuming heat or electricity will lead to different designs for the same purpose. In most of the previously analyzed papers, only a configuration has been performed for a case study. Therefore, the main novelty of this paper is the analysis of different structures of a polygeneration scheme based on renewable energies, essentially thermal, to cover the five typical demands of a building of 80 dwellings. The building already has a good energy standard in its envelope, so the integrated production scheme generates the minimum energy demand for its occupants. The additional electricity contribution of the TEGs to the system has also been analyzed as a novelty in the proposed schemes.

Three case studies in Spain have been conducted to compare four configurations for the same building type. Every combination will differ, using HP or SEAC for cooling and RO or MED for desalination. In all, 100% coverage of electricity (in annual net balance), heating, cooling, cold, cold water, and domestic hot water are pursued. Energy analysis is based on primary energy saving (PESR). Environmental benefits were estimated by comparing the CO_2 emitted by the integrated scheme proposed along its life cycle following an LCA approach, that is, also including the impact on the materials, transport, and end-life of the analyzed installation, apart from the operational phase. This approach also constitutes a novelty since, to our knowledge, it is the first time that it has been applied to a polygeneration scheme. Economic analysis uses the simple payback period (SPB), net present value (NPV), and internal rate of return (IRR) of the investment required, as well as the levelised costs of any of the five covered demands (LCO_x).

2. Materials and Methods

This research combines different software to carry out the study. Design Builder was used to estimate the building demands. EES was taken to model some devices that were not available in TRNSYS. The former was the core for simulations of the proposed four polygeneration arrangements. Excel has been used to analyze the performance of each design based on the monthly results obtained from TRNSYS. Finally, SimaPro was required to perform the environmental assessment of the four schemes along their life cycle. A sequential process has been followed to find the results; thus, any modification must be carefully attended.

2.1. Building Demands

The building type was located in Spain, a country characterized by its mild climate and water scarcity. The choice of the typical residential building in Spain has been based on data collected from the Population and Housing Census [25]. It corresponds to the average surface of new real estate developments in the expansion areas of medium and large cities. Their main geometric characteristics are detailed in Table 1.

Table 1. Geometric characteristics of the building type considered.

Parameter	Value
Building type	Medium/large block of flats
No. of homes	80
Total number of people	240
Useful surface per dwelling (m^2)	70
Total conditioned area (m^2)	5600
Total area (m^2)	7190
Height per plant (m)	3
Total volume (m^3)	21,568.8
No. of floors above ground	11 (10 + ground floor)
No. of floors below ground	0
Total building height (m)	33
No. of bedrooms per home	2
Orientation	North-South

The following figures include a 3D view (Figure 1) and floor plans (Figure 2) of the building type considered. The floor plan of the building corresponds to a simple layout with landings every two floors and carpentry oriented to the north and south for all the dwellings.

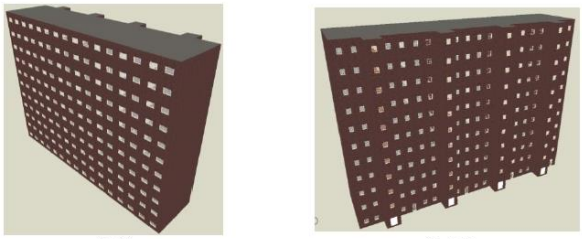

(**left**) (**right**)

Figure 1. 3D view of the building type's south façade (**left**) and north façade (**right**).

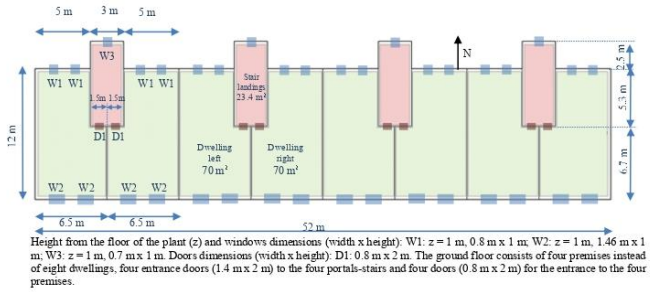

Figure 2. Typical floor plan of the building type. Source: [26].

As this article focuses on an integrated energy and water supply solution for the demands, it is assumed that the building meets the best energy efficiency standards. The amendments introduced with Directive 2010/31/EU [3] led to an update of the Basic Document HE on Energy Saving of the Technical Building Code in 2013 [27], which has to be applied to the buildings in the period 2014–2019. Finally, this document was updated again in 2019 [28] to include the new requirements of Directive (EU) 2018/844 [4].

The Spanish regulation included in the Basic Document HE on Energy Saving of the Technical Building Code [27] establishes 15 climate zones classified according to their winter (5, from A to E) and summer (4, from 1 to 4) climate severities. They are ranked from each zone's degree days and solar radiation. Three cities were selected for the analysis. Two correspond to a specific location in the Mediterranean area, with different heating and cooling demands and water scarcity. The third one is an inland location with a higher climate severity but not a freshwater shortage, despite being an arid area. They were then coded as A4 (Almeria), B3 (Valencia), and D3 (Zaragoza). Table 2 shows a description of the leading climate conditions of these localities.

Table 2. Description of the main climate conditions of the selected cities. Source: [28–30].

Zone	1	2	3
Location	Almería	Valencia	Zaragoza
Climate zone	A4	B3	D3
Latitude	36°50′ N	39°28′ N	41°39′ N
Altitude above sea level (m)	0	8	207
Annual average outdoor temperature (°C)	18.4	17.6	15.2
Horizontal global solar radiation (kWh/y)	1829	1615	1656
Average annual wind speed (m/s)	4.1	3.1	4.5
Average annual temperature of tap water (°C)	15.7	14.6	13.3

Detailed calculations on the building demands are shown in Appendix A. Table 3 presents the annual demands based on the hourly estimates following the methodology presented in Annex A. Unitary consumptions per dwelling and year are also included in the table.

Table 3. Annual energy and water consumption for the same building in the three selected cities.

Location	Almería	Valencia	Zaragoza
Heating demand (HD, kWh/y)	21,449.7	59,572.9	101,297.2
per dwelling (kWh/y·dwelling)	268.1	744.7	1265.0
Cooling demand (CD, kWh/y)	75,691.8	46,907.0	48,271.0
per dwelling (kWh/dwelling)	946.1	587.3	603.4
Electricity demand (ED, kWh/y)	151,905.3	151,905.3	236,655.1
per dwelling (kWh/dwelling)	1888.7	1888.7	2958.2
Freshwater demand (FWD, m^3/y)	8555.1	8555.1	8555.1
per dwelling (m^3/y·dwelling)	106.95	106.95	106.95
Domestic hot water demand (DHWD, kWh/y)	93,887.0	93,887.0	150,101.0
per dwelling (kWh/y·dwelling)	1173.6	1173.6	1876.26

2.2. System Layouts

The main integrated scheme starts with a solar loop consisting of PVTs, a storage tank (ST), and a heat sink to avoid overheating (AE). Additional electricity generation to cover the demands of the building is provided by a PV field and supported by the installation of TEGs on 50% of the solar aperture of the resulting PVT field. The facility will have the corresponding inverter according to the absolute power, buying and selling energy to the grid depending on the demand (ED) and instantaneous production.

The DHW demand is covered by a mixture of the secondary tank (HWDT) and cold freshwater to serve the required flow rate at 45 °C. The heating demand (HD) is covered in

the same way as DHW, but in this case, it is done at 35 °C and returned at 25 °C, considering there is underfloor heating in the building.

The fundamental difference between the configurations analyzed for the three sites with the same base building is the production of cooling and desalinated water. They may require either heat, which will come from the secondary tank, or electricity. For cooling (CD), a single-effect lithium bromide absorption cycle (SEAC) or a high-efficiency heat pump (HP) connected to an aquifer with a stable temperature (15 °C) can be chosen. A membrane technique (RO) or distillation (MED) is proposed for seawater desalination. The biomass boiler (BB) allows the secondary tank to maintain a setpoint temperature according to the cooling and desalinated water demands since they operate at the highest temperatures. TEGs were also incorporated at its top to produce more electricity for the system.

Finally, a 50 m^3 tank (FWT) has been foreseen to regulate desalinated water production concerning consumption (FWD). The selected cooling technology has a third storage tank to avoid system start-ups and shutdowns while meeting demand.

Thus, the four combinations analyzed for the polygeneration system differ in selecting technology for cooling and desalination (whose flows are marked as dashed lines in Figure 3 depending on the chosen technology), as shown in the attached Table 4. In any case, the final design of each option will be different in terms of the number of PV/PVTs, biomass boiler power, HP/SEAC capacity, and size of the hot and cold water storage tanks. Moreover, the setpoints of the boiler and start-up of the thermally activated technologies (MED, SEAC) may differ slightly depending on the overall integration scheme.

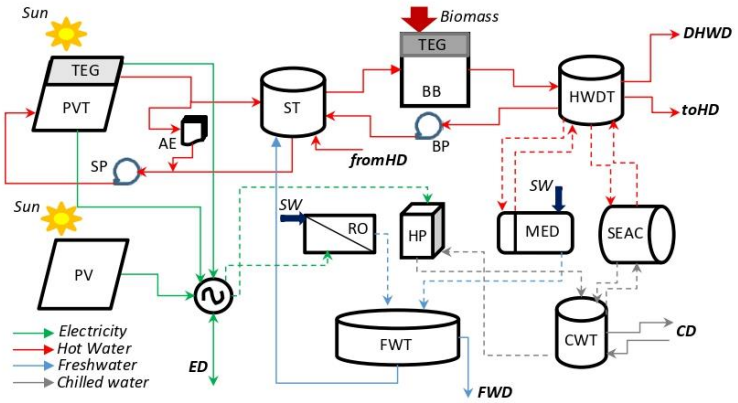

Figure 3. The general layout of the polygeneration schemes to serve the building demands.

Table 4. Configurations analyzed in the polygeneration scheme.

Service	A	B	C	D
Electricity	PV + PVT + TEG			
Heating and DHW	PVT + (AE) + SP + ST + BB + BP + HWDT			
Cooling (CWT+)	HP	HP	SEAC	SEAC
Freshwater (FWT+)	MED	RO	RO	MED

2.3. System Model

The configurations have been modeled in TRNSYSv18, using its types whenever possible. There are two unusual situations in this regard: The first is that the regression models available for the HP and SEAC types have been used to adapt the capacities required in the installation with variable load performances. The second is that there is

no specific type for this technology in the case of desalination. Consequently, complex models were first developed in the EES software for RO and MED. However, given the slowness of calculation observed when integrating both software, a simplified version of each technology has been incorporated into the TRNSYS scheme through a new DHW demand and its return or additional electricity consumption but with fixed performance parameters (see the next table). In the case of TEGs, a simple EES model was carried out and then immersed in the PVTs and the BB types as other equations to estimate the power generation.

The following Table 5 summarizes the essential information of the components included in the analyzed configurations. If no parameter number is given, it will depend on the end design of each composition (Var.). Auxiliary types for integrating variables and graphical representation have not been included for simplicity.

Table 5. Summary of main components of the TRNSYS installation.

Component	Type	Parameter	Value	Unit
Weather	15–6	Slope surface	37	°
Tap water	14-a	Temperature	Var.	°C
PV	103-b	Module area I_{sc} at RC V_{oc} at RC	1.93 9.38 46.2	m^2 A V
PVT	50-a	Module area Cell efficiency Collector absorptance Cover transmittance	1.63 16 92 89	m^2 % % %
Aerotherm (AE)	5-g	Cooling airflow	285,600	kg/h
TEG	–	ZT	0.72	
Inverter	48-a	Efficiency	95	%
Solar loop pipes	31	Overall loss coefficient	0.3	$W/m^2 \cdot K$
Solar controller	113	Cooling setpoint	90	°C
Solar pump (SP)	3b	Power Flowrate	Var. Var.	W L/h
Solar tank (ST)	156	Capacity Number of nodes Overall loss coefficient	Var. 10 0.35	m^3 - $W/m^2 \cdot K$
Demands (5.txt files)	9-c	Periodicity	Var.	h
Hot water demands tank (HWDT)	534	Capacity Number of ports Overall loss coefficient	Var. Var. 0.35	m^3 - $W/m^2 \cdot K$
Biomass boiler (BB)	122	Output power Efficiency Minimum load	Var. 80 5	kW_{th} % %
Boiler pump (BP)	3b	Power Flowrate	Var. $50 \cdot A_{PVT}(m^2)$	W L/h

Table 5. *Cont.*

Component	Type	Parameter	Value	Unit
Demand controller	106	Heating setpoint	Var.	°C
Heat Pump (HP)	927	Cooling capacity Inlet source temperature Return temperature Load flowrate Source flowrate	Var. 15 12 Var. Var.	kW_{cl} °C °C kg/h kg/h
Single-effect LiBr absorption chiller (SEAC)	107	Cooling capacity Return temperature Load flowrate Cooling flowrate Hot Water flowrate Cooling temperature Hot Water temperature Operating range	Var. 12 Var. Var. Var. 20 Var. 70–85	kW_{cl} °C kg/h kg/h kg/h °C °C °C
Cooling water tank (CWT)	156	Capacity Number of nodes Overall loss coefficient	Var. 10 0.35	m^3 - $W/m^2 \cdot K$
Multi-effect distillation unit (MED)	–	Desalting capacity Recovery factor Source flowrate Source temperature Operating range	1309 20.65 Var. Var. 60–82	L/h % L/h °C °C
Reverse osmosis unit (RO)	–	Desalting capacity Recovery factor Reject factor	3216 45 99.31	L/h % %
Freshwater tank (FWT)	39	Capacity Minimum volume Level (off-desalting)	50 5 35	m^3 m^3 m^3

The simulation was performed for the entire annual period in the four configurations and three locations, with a time step of 5 min. Several key performance indicators (KPI) have been used from the annual results with TRNSYS to evaluate the best alternative comprehensively. They will be presented next.

2.4. Energy Analysis

The energy KPI selected is the primary energy saving ratio (PESR). It compares the energy performance of the proposed system (PS) through a comparison with a suitable reference system (RS). The PS solely considers the demand unattended by electricity from the grid, because, in all cases, the demand for air conditioning and water is served at 100%. The RS supposes all demands are produced by conventional technologies based on fossil fuels and appropriate conversion efficiencies (see Table 6 for details). The PES and its ratio (PESR) are calculated as shown in Equations (1) and (2):

$$PES = PE_{RS} - PE_{PS} \tag{1}$$

$$PESR = \frac{PES}{PE_{RS}} \tag{2}$$

$$PE_{RS} = \frac{E_D}{\eta_E} + \frac{Q_{SH}}{\eta_Q} + \frac{Q_{DHW}}{\eta_Q} + \frac{Q_{CL}}{COP_R \cdot \eta_E} + \frac{W_D}{SEC_R \cdot \eta_E} \tag{3}$$

$$PE_{PS} = \frac{E_{FG}}{\eta_E} \quad (4)$$

where PES is the primary energy saving, and PE_{RS} and PE_{PS} are, respectively, the energy consumption in the reference and proposed system. E_D is the electricity demand of the building, Q_{SH}, Q_{DHW}, and Q_{CL} are the building's space heating, domestic hot water, and cooling demands, and W_D is its freshwater demand. Regarding the technical parameters, η_E is the electric efficiency of the Spanish grid system, and η_Q is the thermal efficiency of the auxiliary boiler. For the reference system, COP_R is the coefficient of performance of the cooling system, and SEC_R is the specific energy consumption of the desalting system. E_{FG} is the electricity demand of the building taken from the grid.

Table 6. Main economic and environmental parameters of the study.

Item	Parameter	Value	Unit(s)	Reference
PV	Inv. & OM cost	1000, 1	€/kW_P, %/y	[31]
PVT	Inv. & OM cost	200, 2	€/m^2, %/y	[32]
Water tanks	Investment cost	495 + 808·V(m^3)	€	[33]
Inverter	Investment cost	180	€/kW	[34]
Pumps	Inv. & OM cost	419 + 0.03 ·Q-2.16·10^{-8}·Q^2, 0.5	€, %/y	[35]
BB	Inv. & OM cost	282, 1	€/kW_{th}, %/y	[24,36]
Heat pump	Inv. & OM cost	350, 0.5	€/kW_{cl}, %/y	[31,37]
SEAC	Inv. & OM cost	600, 0.2	€/kW_{cl}, %/y	[32,37]
MED	Inv. & OM cost	1500, 0.5	€/(m^3/d), %/y	[38]
RO	Inv. & OM cost	800, 1.5	€/(m^3/d), %/y	[39]
$p_{E,p}$	Price	0.2	€/kWh	
$p_{E,s}$	Price	0.08	€/kWh	
p_{NG}	Price	0.07	€/kWh	
$p_{E,b}$	Price	0.052	€/kWh	
p_W	Price	2.0	€/m^3	[40]
$f_{CO_2,E}$	Emission factor	0.19	kgCO_2/kWh	[41]
$f_{CO_2,NG}$	Emission factor	0.204	kgCO_2/kWh	[42]
r	Interest rate	2	%	
COP_R	Efficiency	2.6	–	[43]
η_E	Efficiency	0.42	–	[44]
η_Q	Efficiency	0.92	–	[43]
SEC_R	Specific cons.	4	kWh/m^3	[40]

2.5. Economic Analysis

The simple payback (SPB) has been selected first in this section. It is calculated as the ratio of the total capital cost and the savings achieved by PS concerning RS. In particular, 25 years of a lifetime is considered.

$$SPB = \frac{TI_{PS}}{AS_{PS}} \quad (5)$$

$$AS_{PS} = OC_{RS} - OC_{PS} \quad (6)$$

In Equations (5) and (6), SPB is the simple payback of the investment, TI_{PS} is the total investment in the proposed system, AS_{PS} is the annual saving in the proposed system, and OC_{RS} and OC_{PS} are the operating cost in the reference system and proposed system, respectively.

The yearly economic saving of the proposed system takes into account the economic gains concerning the reference system. In RS, electricity is provided only by the national grid. On the other hand, in PS, the electric user load is matched by the PV, PVT, and TEG in an overall yearly balance, but sometimes the electricity is supplied by the grid. Moreover, different prices are found when electricity is purchased or sold to the grid. A fee for natural

gas, biomass pellets (assuming a fixed low heating value, LHV), and water from the grid is also necessary to establish the annual cost of the reference facility to compare with the proposal (see Table 6). The yearly operating costs (OC) also include a percentage of the investment required for each central technology as a maintenance cost. These investment and installation costs for each technology have been taken from the bibliography of similar studies and are also compiled in Table 6.

$$TI_{PS} = C_{PV} + C_{PVT} + C_{INV} + C_{ST,DHT,CWT} + C_{SP,BP} + C_{BB} + C_{HP/SEAC} + C_{RO/MED} \quad (7)$$

$$OC_{RS} = E_D \cdot p_{E,p} + \left(\frac{Q_{SH}}{\eta_Q} + \frac{Q_{DHW}}{\eta_Q} \right) \cdot p_{NG} + \frac{Q_{CL}}{COP_R \cdot \eta_E} \cdot p_{E,p} + W_D \cdot p_W \quad (8)$$

$$OC_{PS} = E_{FG} \cdot p_{E,p} - E_{TG} \cdot p_{E,s} + E_B \cdot p_{E,b} + OM_{PV,PVT,BB,HP/SEAC,RO/MED} \quad (9)$$

The right side of Equation (7) includes the investment costs of all the devices composing the system: PV field, PVT field, inverters, solar, demand hot water and cooling water tanks, solar and boiler pumps, biomass boiler, selected cooling technology (HP or SEAC), and chosen desalination technology (RO or MED). To focus on the comparative analysis of alternative production systems, the cost of the distribution system to the dwellings is not included, nor is the assembly of the central drive system itself. In Equations (8) and (9), to provide the operating costs of the compared alternatives, the terms $p_{E,P}$, $p_{NG,}$ and p_W are the purchase cost of electricity, natural gas, and water from their respective grids. On the other hand, $p_{E,s}$ is the electricity price of surplus electricity, E_B is the energy supplied by the biomass boiler, $p_{E,b}$ is the purchase energy cost of biomass pellets, and OM_x are the operating and maintenance costs of the x technology.

As an additional economic indicator, the levelized costs of each demand (LCO_x) have also been estimated. Taking into account that some driving technologies provide energy for several demands, heat (and even electricity) and distribution factors ($f_{E,x}$ and $f_{Q,x}$) based on the electrical or thermal energy required for each need concerning the total produced by the system must first be estimated. As an example, the estimation of the LCO_W is shown. Note that it is one of the most complex demands to assess at the tail end of the integrated system. The total cost, O&M, and energy required for the desalination plant also consider the upstream equipment's fractional costs, with the distribution factors described above.

$$LCO_W = \frac{\left[C_w + \sum_{n=1}^{25} OM_w \cdot (1+r)^{-n} \right]}{\sum_{n=1}^{25} E_w \cdot (1+r)^{-n}} \quad (10)$$

In Equation (10), C_W is the total investment cost associated with water, OM_W is the total cost for O&M associated with water, r is the rate of return, and E_W is the total energy required for water, depending on the seawater desalting facility adopted.

Finally, the internal rate of return (IRR) and the net present value (NPV) of the investment have also been estimated as fundamental economic indicators.

2.6. Environmental Analysis during the Operational Phase

Similarly, the environmental analysis was first checked by using a KPI based on the calculation of the saving in CO_2 emissions (ΔCO_2) and its ratio (CO_{2R}) as shown in Equation (11) to (12):

$$\Delta CO_2 = CO_{2,RS} - CO_{2,PS} \quad (11)$$

$$CO_{2R} = \frac{\Delta CO_2}{CO_{2,RS}} \quad (12)$$

$$CO_{2,RS} = E_D \cdot f_{CO_2,E} + (Q_{SH} + Q_{DHW}) \cdot f_{CO_2,NG} + \frac{Q_{CL}}{COP_R \cdot \eta_E} \cdot f_{CO_2,E} + W_D \cdot SEC_R \cdot f_{CO_2,E} \quad (13)$$

$$CO_{2,PS} = E_G \cdot f_{CO_2,E} \quad (14)$$

In these equations, the values of the CO_2 produced in the reference and proposed systems ($CO_{2,RS}$ and $CO_{2,PS}$) used the CO_2 emission factor for electricity generation in Spain ($f_{CO_2,E}$), and the CO_2 emission factor for heat provided by natural gas combustion (reference, $f_{CO_2,NG}$). These factors are also presented in Table 6.

2.7. Lifecycle Environmental Performance

The environmental KPI mentioned above does not consider the CO_2 emissions along the life cycle of the installations proposed. Furthermore, their values are similar to those found with the PES, especially when CO_2 factors for electricity and natural gas combustion are similar (that is the Spanish case).

Therefore, the life cycle assessment (LCA) of the proposed installations and the alternative reference to cover the building demands have been analyzed in detail. In this manner, the environmental impacts of the proposed solution are compared by considering the whole life cycle of the alternatives. That is, they included the impact associated with the construction and transport of the materials used in each technology as the end phase after the installation dismantle. Those impacts are added to the impact generated during its operation, which is usually the easiest to estimate (see the previous section), in order to give a more comprehensive vision of the environmental burdens. Despite its complexity, this method is being progressively introduced in the thorough analysis of experimental solutions based on RES for this purpose [45–47], but never for a polygeneration scheme providing five services.

The LCA requires the selection of a life cycle impact assessment method (LCIA) that evaluates, through diverse impact categories (in the mid- or end-point vision), which are grouped into three damage categories (human health, ecosystems, and resources depletion), the environmental impact of the resources supplied or consumed in the life cycle of the product analyzed. Thus, several steps are compulsory to carry out to perform this LCA. First, a functional unit must be defined, and the system limits must be clearly marked. Second, a complete inventory with the list of the materials used and resources consumed in the life-cycle time of the system has to be completed. Third, an LCIA method is usually selected from existing software. Finally, a critical analysis of the results found and further recommendations from the environmental penalties of the study are desirable, this being a non-mandatory phase after the previous ones.

The functional unit here is a rather complex issue. Considering that five demands are produced (heating, cooling, domestic hot water, electricity, and water), the functional unit is the installation itself, which makes 100% of the five demands throughout the year. In any case, it is possible, through the consideration of the equipment involved in the production, to assign an impact for each demand (in % of the total) and per unit of demand (kWh, or m^3).

Regarding the life cycle inventory (LCI) of this study, since each option A, B, C, or D incorporates a different number of units of PV, PVT, etc., the inventory of materials and transportation, as well as their final destination, has been carried out for each of these units. In this way, it is easier to build the total inventory for the four alternatives in the LCA software SimaPro v9.0. As a general rule, the Ecoinvent database (EIDB [48]) has been used to compute the emissions generated by the various materials and other databases using European standards (ELCD [49]). The transport required for the equipment depends on the distance to the supplier. This value may vary if there is another data source for similar equipment in terms of performance. Concerning the end-of-life phase, the most conservative option of landfilling the entire facility has been chosen in line with other studies [45]. The following table shows the global inventory of the four alternatives, grouped by the different equipment involved in each configuration. It includes the data source to perform such a list for the various equipment. For each technology, the inventory of similar equipment from published studies or selected from internal databases has been taken as a basis and then extrapolated to its final capacity in each configuration (see Table 7). In the conventional case, only one natural gas boiler is included, and the impacts

of electricity (low voltage, LV) and water will be taken from 1 kWh and 1 m^3 obtained from the aforementioned databases.

Table 7. Reference items to perform the LCI of the four options and the conventional supply.

Item	Reference	Capacity	Unit	km Truck	km Ship
PV	[45]	320	W_p	300	16,500
PVT	[45]	320	W_p	20	–
Aerotherm	[50]	24	kW_{th}	150	–
Inverter	[45]	2.5	kW_e	1892	–
Water tanks	[50]	2000	L	100	–
Water pumps	[48]	40	W	20	–
Heat Pump	[48]	10	kW_{cl}	1500	–
SEAC	[50]	19	kW_{cl}	2500	200
MED	[51]	2.8	m^3/d	50	–
RO	[40]	35	L/h	500	1000
Piping	[45]	5	kW_p	300	–
Wiring	[50]	3	kW_p	1500	–
Expansion vessel	[48]	80	L	150	–
Foundations (solar field)	[48]	260	W_p	80	–
Biomass boiler	[48]	50	kW_{th}	50	–
Natural gas boiler	[47]	300	kW_{th}	900	–
LV Electricity, Spanish grid	[48]	1	kWh_e	–	–
Heat demand (to a DH)	[47]	1	MJ	–	–
De-ionized water by RO	[48]	1	L	–	–

When choosing an environmental impact assessment method and considering the previous KPI analysis with the CO_2 savings in operation, we have opted for a simple but well-recognized LCIA method in the more generalist field, such as the IPCC 100-year GWP method that computes in kg of CO_2 equivalent. It is a single-indicator method. In any case, the analysis of the installation has been considered for 25 years, after which all its components should be replaced.

3. Results

3.1. End Design for Each Option

Given the complexity of supplying five demands at 100%, the optimal configuration for each site (1–3) and technology selection (A–D) imply a different final design. Most of them correspond to the *Var.* values included in Table 5, which also contains the technical data of each technology. The following table summarizes the final design required for each case, the objective being to cover all demands at around 100%. However, in the case of electricity, this is done through an approximated annual net balance with the grid. For cooling, the buffer tank also prevents covering precisely 100% of the demand (see Table 8).

Table 8. The final design for each proposed configuration (A-D) and site (1–3).

Item	Location	A	B	C	D
Number of PV panels	1	210	320	270	210
	2	210	320	270	210
	3	300	430	370	325
Number of PVT panels	1	180	60	140	160
	2	190	70	140	160
	3	300	90	200	200
TEG capacity (kW_p)	1	1,20	0.40	1.06	1.13
	2	1.23	0.44	1.07	1.13
	3	2.00	0.92	1.67	1.67

Table 8. *Cont.*

Item	Location	A	B	C	D
BB nominal capacity (kW_{th})	1	300	100	300	300
	2	300	100	300	300
	3	500	300	500	500
BB setpoint temperature (°C)	1	75	55	80	82
	2	75	55	80	82
	3	75	55	78	82
Solar tank capacity (m^3)	1	10	7	10	12
	2	10	7	10	12
	3	15	10	15	18
Hot water demand capacity (m^3)	1	10	5	10	12
	2	10	5	10	12
	3	12	8	15	18
HP/SEAC capacity (kW_{CL})	1	120	100	150	170
	2	80	70	105	140
	3	80	70	100	140
Coldwater tank capacity (m^3)	1	5	7	7	10
	2	5	7	7	10
	3	5	5	7	10
Electricity annual demand coverage (%)	1	99.7	102.3	102.2	101.5
	2	100.3	102.1	101.5	101.1
	3	100.7	100.2	100.5	101.1
Cooling annual demand coverage (%)	1	101.9	99.7	98.9	99.5
	2	103.1	99.9	100.7	102.0
	3	101.7	101.2	99.8	101.9

The comparative analysis by configuration and location of the results presented in the table above is summarised below.

- The solar field required for Zaragoza (3) is higher than Almería and Valencia (see annex A for details) to cover its higher electricity and DHW demand. Moreover, its heating demand is also higher due to its continental climate.
- A much larger solar field with PVT, a boiler, and hot water tanks is necessary when the desalination technology is the MED, and to a lesser extent, when the cold production comes through the SEAC. That is, options D and A require a higher dimension of the thermal supply side than the others.
- In that case, the share of PV and PVT is reduced for the first technology to complete the electricity demand.
- The PVT required in configuration A (HP and MED) is higher than the theoretical maximum one (configuration D) for each location. This is mainly due to the lower setpoint temperature of the BB, which was adjusted only to activate the MED.
- Rapidly following thermal demand sometimes forces a biomass boiler to upsize. However, the BB is a modulable device, and the equivalent number of operating hours may differ significantly for the same capacity. Especially in the spring and autumn periods where cooling is unnecessary, it is really underutilised.
- The heat demand required by the SEAC matches better with the solar resource in summer. Thus, its choice does not provoke a substantial increase in the final configuration (number of PVT panels) needed to cover the cooling demand.
- Heat-activated technologies provide better control to avoid overheating and, therefore, the use of the dissipative device (AE). When the option only requires low temperatures (case B) to cover the heating and DHW demands, the highest portion of exhausted heat was found when setting up 55 °C in the boiler.

- According to its technical characteristics, the response to cold demand is slower for the SEAC than for the HP. This means that higher capacities and associated CWT are required for the same purpose. Almeria (1) had the highest cooling capacity for both options due to its most demanding summer weather.

Regarding the impact of the electricity supplied by the TEGs, we must say that is almost irrelevant. First, it should be clarified that the capacity finally installed in each configuration (see the third block of Table 8) depends on the size of the PVT field and the boiler. In addition, the production in the boiler also depends on its operation. Experimental tests carried out by the authors [52] measured the low ΔT available in the PVTs, which is not enough to work with appreciable conversion efficiencies in this device. This means that TEG in PVTs is less than 0.5% of the total electricity generated by PV and PVT fields, respectively. In the case of BB, tests integrating TEGs [53] indicate that the hot temperature is maintained at 300 °C in its operation, and the cold side depends on the service temperature. Therefore, it is possible to obtain more electrical generation with better efficiencies (up to the 1% of the total demand, see the fourth block in Table 9). In any case, it is much less than the specific one of photovoltaic technologies. The following table shows the electrical generation fractions of each technology analyzed.

Table 9. Gross electricity fraction obtained by each power technology.

Electricity Generator	Location	A	B	C	D
PV	1	73.82	96.82	85.04	76.32
	2	72.66	95.34	85.38	77.00
	3	72.41	95.95	85.36	82.00
PVT	1	31.22	8.56	20.27	28.82
	2	32.38	10.04	19.94	28.15
	3	32.73	9.46	19.97	23.23
TEG in PVT	1	0.51	0.17	0.25	0.42
	2	0.5	0.17	0.23	0.40
	3	0.40	0.14	0.22	0.32
TEG in BB	1	0.85	0.11	0.24	0.98
	2	0.88	0.13	0.23	0.98
	3	0.57	0.16	0.22	0.72

3.2. Performance Analysis

Once the designs for each site and configuration have been presented, the results from the KPIs and the LCO_x of each demand establish the best arrangement, with slight variations in the results according to the three sites analyzed. These results can be seen in the following Table 10.

Table 10. Performance analysis of the proposed configurations for each site.

KPI Parameter	Location	A	B	C	D
Primary energy saving ratio (PESR)	1	0.640	0.646	0.651	0.645
	2	0.648	0.654	0.658	0.652
	3	0.683	0.683	0.685	0.682
CO_2 emissions saving ratio ($CO_{2,R}$)	1	0.720	0.726	0.733	0.728
	2	0.746	0.750	0.755	0.751
	3	0.778	0.778	0.781	0.779
Total investment (TI_{PS}, €)	1	348,256	293,445	421,824	408,448
	2	338,021	286,710	394,825	390,299
	3	477,903	398,157	519,016	517,594

Table 10. *Cont.*

KPI Parameter	Location	A	B	C	D
Annual saving (AS_{PS}, €/y)	1	21,679.5	48,177.6	39,278.6	9415.0
	2	8484.1	46,729.8	40,209.3	10,391.4
	3	34,821.7	62,266.6	55,296.9	24,635.5
Simple payback (SPB, years)	1	16.06	6.09	10.74	43.38
	2	39.84	6.14	9.82	37.56
	3	13.72	6.39	9.39	21.01
Levelised cost of electricity (LCO_E, €/kWh_E)	1	0.035	0.033	0.038	0.041
	2	0.037	0.036	0.038	0.042
	3	0.037	0.035	0.038	0.039
Levelised cost of heating (LCO_{SH}, €/kWh_H)	1	0.013	0.029	0.035	0.011
	2	0.012	0.023	0.036	0.011
	3	0.017	0.030	0.040	0.014
Levelised cost of DHW (LCO_{DHW}, €/kWh_H)	1	0.013	0.029	0.035	0.011
	2	0.012	0.023	0.036	0.011
	3	0.017	0.030	0.040	0.014
Levelised cost of cooling (LCO_{CL}, €/kWh_c)	1	0.041	0.039	0.126	0.095
	2	0.048	0.045	0.137	0.120
	3	0.045	0.041	0.139	0.123
Levelised cost of water (LCO_W, €/m^3)	1	1.237	0.593	0.597	1.079
	2	1.204	0.598	0.598	1.083
	3	1.558	0.587	0.589	1.363

The analysis of the above table is detailed below, row by row.

- From the point of view of the PESR, all configurations yield similar data (0.64–0.68), and the remaining is due to the net electricity balance in periods of higher demand than production. Zaragoza has the best PESR due to its higher demands, followed by Valencia and, finally, Almería, with the lowest overall needs (see Table 3).
- A similar pattern was found with CO_2 savings. All configurations and alternatives also show similar relative values to PESR. A higher value is found (0.72–0.78) since natural gas emission factors exceed the Spanish grid's electricity factor (see Table 6).

In the economic analysis, the major findings are:

- The highest investment is found in option C, due to the largest solar field required and the SEAC cost. Option B requires the minimum investment. MED technology is, in general, expensive but used throughout the year.
- However, electrically activated technologies (HP and RO) have better energy performances. The use of thermal energy displacing PV to PVTs is penalized electrically. In addition, a high number of operating hours of the boiler are needed to maintain the required temperature for MED (throughout the year) and SEAC (in summer). This makes the cost of pellet supply the most significant component of expenditure in the polygeneration installation, thereby reducing the annual savings significantly.
- Thus, the highest annual savings was found with the B option (HP + RO), then option C is the second in this term (SEAC + RO), followed by A (HP + MED), and finally, D (SEAC + MED).
- Therefore, by combining investment and annual savings, the order found according to the feasibility of configurations (measured in terms of the SPB) is relatively straightforward: option B is the best option (HP + RO), followed by option C (SEAC + RO), option A (HP + MED), and finally, option D (SEAC + MED).

The analysis of internalized costs requires a particular study:

- Similar and attractive costs were found for electricity production in both configurations (less than 0.04 €/kWh), coming from the PV + PVT field.

- As heating and DHW demands take the heat from the same tank (DHWT), equal costs are found.
- Lower costs for heat are estimated if thermally activated technologies take part in the configuration. This is because heat infrastructure is divided into additional demands (MED and SEAC).
- Cooling provided by HP is cheaper (about one-third) than using the SEAC for the same purpose. This is explained by its respective COPs, despite the higher cost of electricity versus heat.
- The same was found for freshwater provided by RO against MED, taking into account the SEC values of both alternatives.

Anyway, the lower costs found in HD and DHW do not compensate for the remaining services, and B is globally the more profitable solution for the three buildings.

3.3. Sensitivity to Externalities

The above results for the base scenario take economic data on the prices of the demands served and the performance and costs of the equipment set by the (Spanish) regulations or taken from the scientific literature. But as expected, the effect of externalities on the polygeneration plant liability is significant, such as the purchase and sale prices of electricity, natural gas, and biomass. However, the interest rate was not found as a crucial parameter for the SPB. The following Figure 4 shows a sensitivity analysis of two selected parameters, which demonstrates the above. In any case, it must be remembered that in the annual savings section, the possible avoidance of CO_2 has not been considered as income; therefore, in the current context of decarbonization, some details not considered in the study (O&M of some equipment piping, etc.) can be compensated in the applied economic balance.

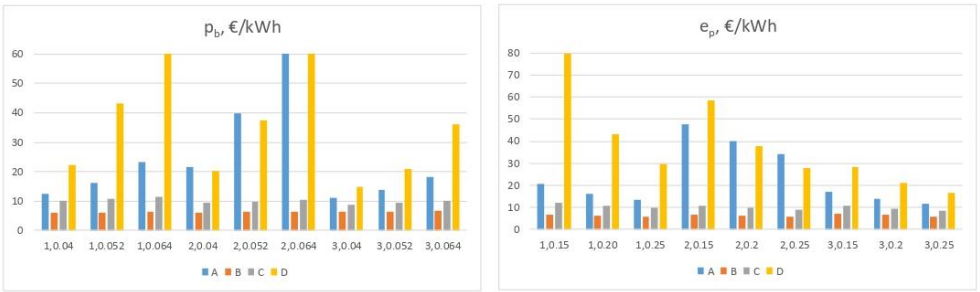

Figure 4. Sensitivity analysis of the proposed configurations for each site: SPB (years) as a function of the biomass p_b (0.04, 0.052, 0.064) and electricity purchase e_p prices (0.15, 0.20, 0.25) in €/kWh for the three locations (1–3) and four configurations (A–D).

3.4. Environmental Life-Cycle Analysis

The life-cycle analysis of the polygeneration facility has only been carried out due to the extensive complexity and as a comparative example to the results previously obtained in Table 10 with the main energy, economic, and environmental KPIs on site 2 (Valencia). Table 11 shows the more interesting results from the applied LCA, especially the associated emissions in the life cycle of the installation for each one of the five demands covered in the study.

Table 11. Total emissions (in $kgCO_{2eq}$) of the polygeneration scheme.

Items	Conventional	A	B	C	D
PVs	–	45,738.7	69,697.0	58,806.8	45,738.7
PVTs	–	51,342.6	18,915.7	37,831.4	43,235.9
Aerotherms (AE)	–	23,081.3	8503.6	17,007.3	19,436.9
Inverters	–	6822.4	10,396.1	8771.7	6822.4
Water tanks	–	2425.0	18,430.0	26,190.0	32,980.0
Water pumps	–	653.3	284.8	904.5	938.0
Heat pump	–	14,480.0	12,670.0	–	–
SEAC	–	–	–	6742.1	8989.5
MED	–	57,571.4	–	–	57,571.4
RO	–	–	33,828.6	33,828.6	–
Piping	–	1493.7	550.3	1100.6	1257.8
Wiring	–	3328.6	5072.1	4279.6	3328.6
Expansion vessels	–	627.6	231.2	462.5	528.5
Foundations (solar field)	–	23,650.2	22,439.7	23,947.3	21,791.8
Biomass boiler	–	40,380.0	13,460.0	40,380.0	40,380.0
Total polygeneration	–	293,419.8	214,479.1	260,252.3	282,999.5
% materials		94.55	93.44	92.87	93.35
% transport		0.98	1.75	1.69	1.39
% end life		4.47	4.81	5.44	5.26
Electricity (from the grid)	–	162,000	159,000	152,000	155,000
Natural gas boiler	67,455	–	–	–	–
LV Electricity, Spanish grid	723,650	–	–	–	–
Heat, from DH network	942,510	–	–	–	–
De-ionized water by RO	1,803,830	–	–	–	–
$kgCO_{2,eq}/m^3$	1.670	0.701	0.322	0.326	0.666
$kgCO_{2eq}/m^3_{DHW}$	6.314	0.219	0.488	0.667	0.201
$kgCO_{2eq}/kWh_H$	0.188	0.006	0.013	0.018	0.005
$kgCO_{2eq}/kWh_C$	0.537	0.026	0.023	0.036	0.017
$kgCO_{2eq}/kWh_E$	0.477	0.067	0.060	0.061	0.068

The results are overwhelming in terms of the minimal impact (1 to 10 approximately) of the four polygeneration schemes using renewable energies, even though by using a net electricity balance, it is necessary to take a significant amount of electricity from the grid, which computes the environmental impact in the same way as the conventional solution that uses the external supply of the demands. It is also worth noting the low contribution of the transport of the equipment and its dismantling after 25 years of operation.

With respect to the unit emissions obtained for each demand, it can be observed that it presents similar patterns to those obtained for the LCO_x, in the sense that the MED technology has a more significant environmental impact within the integration, and the use of SEAC for the production of cold also concerning the use of HP. It is important to note that for the four schemes, the unit impact of kWh electricity is very similar and that producing heat has a lower impact than the rest of the demands, as it is the first source of secondary energy produced from the sun. In any case, the unit values are generally an order of magnitude lower than the emissions of the conventional alternative.

4. Discussion

The first consequence of this configurational analysis is the appropriate selection of the number of PVs or PVTs in the solar field to meet downstream demands. Although PVT technology has a higher overall performance than PV since it also produces heat simultaneously, it could not be the best solution. Suppose such heat serves a demand that can be generated with an electrical technology of lower equivalent consumption and lower investment cost. In that case, it does not justify the purely thermal integration for a polygeneration scheme, including desalinated water. This case is clearly shown in our comparative analysis A-D, when HP and RO are used to produce cooling and water with

an electrical rather than thermal technology. This is especially the case when using MED to cover water demand, as it overstretches the required solar field too much compared with having RO as an alternative. The subject of SEAC is more compatible with the higher solar input in summer, and its effect concerning an HP is lower than in the case of desalination.

In any case, it is important to note that this four-option analysis arises from the selection of desalination and cooling technologies. Therefore, this optional analysis is meaningless outside the scope of an area with water scarcity and similar building cooling and heating demands.

At this point, it is worth remembering that this analysis focused on polygeneration with equipment that produces thermal energy, particularly those equipped with the possibility of integrating TEG devices within them to provide free electricity generation. Finally, it should be remarked that the TEG devices integrated with the PVTs and the BB do not represent a substantial additional advantage in electricity generation. They only contribute a mere 1.5% to the generation obtained with the PVs and PVTs, and they are a dispensable option in any proposed configuration.

This analysis covers three locations within Spain, which essentially influence the required air conditioning demands and the appropriate building standards to meet a similar energy efficiency (see annex). In any case, the values obtained for the KPIs are pretty similar for all three, with the choice of cooling and water technologies leaving the best integrations in terms of liability. The 100% RES solution (that is, not using an energy balance with the grid and using (or not using) energy storage systems, ESS) has not been included here for economic reasons. Still, the authors have also studied it for an isolated domestic dwelling [54,55]. In these analyses, the polygeneration configuration only includes PVT panels, the RO being the desalination technique but including the desiccant wheel (SDW) as the cooling system. In addition, the economy of scale criterion is met; the required configuration and its feasibility were worse than those obtained here, giving a more extensive installation and worse SPB.

The economic analysis started from an energy price scenario (the end of 2021 in Spain) that has changed significantly from then. With the current trend in the energy sector, it is true that it predicts an increase in biomass costs, which reduces the viability of this basic configuration (see Section 3.2). However, the rest of the parameters favor the schemes' viability with respect to the values initially estimated in Table 6. These include the price of natural gas, the price of buying and selling electricity, as well as the unit investment costs of solar panels and biomass boilers. Suppose we also include as income the CO_2 avoided (with data from the CO_2 emissions trading market) with their alternative operation with respect to the supply from conventional grids. In that case, the results obtained can be considered clearly conservative. Therefore, this trend dramatically encourages the liability of those integrated schemes based on RES and efficient energy management. In short, the promising environmental and energy KPIs found in this preliminary assessment will undoubtedly be improved with the corresponding economic ones in the following years.

As for the reliability of the results, unfortunately, it is impossible for the authors to make any reasonable comparison with other references, given that the configurations analyzed do not coincide with the rest of the proposals. Moreover, as previously mentioned, the external input parameters significantly affect these values. Even in defining some parameters, the criteria applied are not precisely the same. Despite this limitation, we consider that given the complexity of the simulations performed, their reduced time step, and the verification of the internal temperature profiles of the scheme allow us to ensure that the results obtained have very reasonable reliability.

Finally, it is worth highlighting the contribution made by the novel life-cycle analysis applied to these polygeneration facilities, in the sense that its results further improve those obtained with the study of the operation in terms of CO_2 avoided. It, therefore, reinforces the idea that distributed generation of services close to consumers is a more sustainable solution in the long term.

5. Conclusions

A 3E (energy, environmental, and economic) analysis was performed for a set of novel polygeneration configurations based on thermal technology (PVT, TEG, and biomass boiler, BB). Each arrangement could produce cold and desalinated water from heat or electricity, thus having four different polygeneration schemes based on solar and biomass energy. This analysis was tested for two similar sites on the Mediterranean coast in Spain and the same building site in a more continental climate. An LCA approach was also added to include the environmental penalties associated with the installation's construction and end phase, apart from the CO_2 saved in the operation phase with respect to a conventional supply based on external grids. The results found from the three analyzed case studies are presented next:

- The four schemes present good values for PESR and CO_{2R} (around 0.65 and 0.75, respectively). These values are penalized by the constraint imposed here, which balances the generation and demand of electricity throughout the year, according to a better installation liability.
- The "electric" alternative (B) was the more economical option, i.e., the combination of PV + PVT + TEG + BB with HP and RO as the best integration. In this case, SPB of about six years was found to be much worse in the rest of the configurations.
- The levelised costs of the five demands provided by the polygeneration schemes are lower than the regular supply of commodities. The financial results are strongly dependent on the current prices of electricity and fuels; future trends will surely improve the economic KPIs of these schemes.
- The LCA approach gives even better results if the scheme is compared with the infrastructure required for the conventional supply based on external grids.

Further research centered on including new technologies or the benefits supplied by a well-designed ESS in these polygeneration RES-based schemes are pending issues that could contribute to the sustainable management of the urban sector.

Author Contributions: Conceptualization, methodology, J.U.; software, J.U., I.Z. and L.G.G.; validation, J.U., L.G.G. and A.M.-G.; formal analysis and data curation, I.Z. and A.M.-G.; writing—original draft preparation, J.U.; writing—review and editing, L.G.G.; visualization, S.U.; supervision, S.U.; project administration, S.U. and A.M.-G. All authors have read and agreed to the published version of the manuscript.

Funding: This research was funded by European Regional Development Funds (FEDER, UE) / Spanish Ministry of Science, Innovation and Universities (MCIU)–Spanish State Research Agency (AEI), grant number RTI2018-09886-A-100.

Institutional Review Board Statement: Not applicable.

Informed Consent Statement: Not applicable.

Data Availability Statement: Not applicable.

Conflicts of Interest: The authors declare no conflict of interest.

Appendix A

Table A1 shows the different U-values for the elements of the thermal envelope based on the standard and three chosen climate zones.

More information regarding infiltration, thermal bridges, and ventilation can be supplied to the readers upon request as supplementary information. The heating and cooling demands were estimated using a user profile. Here it follows the Spanish regulation [23] and consists of the following aspects:

Design Builder was used as the energy simulation tool, considering the abovementioned characteristics and typical internal loads. Regarding the climate data, the SWEC (Spanish Weather for Energy Calculations) was considered according to the reference

adopted in the technical code. This software also estimates electricity demand following recommendations [28] in the case of Valencia and Almería:

In the case of Zaragoza, an alternative pattern based on existing Spanish regulation [56] for on-grid PV domestic installations was used to estimate the hourly electricity demand for every day of the year, also accounting for statistical data of the sector in Spain [57].

Freshwater and DHW hourly demands were calculated using a statistical study with measurements on domestic consumption carried out by the public water management company in Madrid [58]. Additionally, the average monthly temperature of tap water has been compiled from the Spanish regulation [28] to estimate the DHW demand.

Table A1. Characteristic U-values (W/m^2K) of the thermal envelope of buildings in each climate zone and the selected building standard. Source: own elaboration based on [27].

Element	U-Value
External wall	1:0.50 2:0.38 3:0.27
Roof	1:0.47 2:0.33 3:0.22
Party walls and horizontal/vertical internal partitions between zones with different uses	1:1.25 2:1.10 3:0.85
Horizontal internal partitions between zones with the same use	1:1.80 2:1.55 3:1.20
Vertical internal partitions between zones with the same use	1:1.40 2:1.20 3:1.20
Ground floor	1:0.50 2:0.38 3:0.27
South-facing windows without obstacles (high solar gain) considering the window-to-wall ratio of 15%	1:2.60 2:2.10 3:1.80
North-facing windows without obstacles (low solar gain) considering the window-to-wall ratio of 10%	1:2.60 2:2.00 3:1.40

Table A2. Air-conditioning timetables and set points.

	Period	Setpoint	Time
Heating service	October to May	20 °C 17 °C	8:00–23:59 0:00–7:59
Cooling service	June to September	25 °C 27 °C None	16:00–23:59 0:00–7:59 8:00–15:59

Table A3. Internal loads to estimate the building demands.

Internal Load	Characteristics	Occupancy Rate (%)	Time
Metabolic rate	117.21 W/person 0.03 people/m^2 3.51 W/m^2 61% sensitive, 39% latent	100 25 50 100	0:00–7:59 8:00–15:59 16:00–23:59 Weekend and holidays
Equipment and lighting	Both 4.40 W/m^2 90% sensitive*, 10% latent** *70% by convection, 30% by radiation **50% by convection, 30% Long-Wave Radiation (thermal), 20% Short-Wave Radiation (visible)	10 30 50 100	1:00–7:59 8:00–18:59 19:00–19:59 20:00–23.59

References

1. United Nations Environment Programme. *2020 Global Status Report for Buildings and Construction: Towards a Zero-Emission, Efficient and Resilient Buildings and Construction Sector*; Report; United Nations Environment Programme: Nairobi, Kenya, 2020.
2. European Union. Directive 2002/91/EC of the European Parliament and of the Council of 16 December 2002 on the Energy Performance of Buildings. Available online: https://eur-lex.europa.eu/ (accessed on 22 March 2022).
3. European Union. Directive 2010/31/EU of the European Parliament and of the Council of 19 May 2010 on the Energy Performance of Buildings. Available online: https://eur-lex.europa.eu/ (accessed on 22 March 2022).
4. European Union. Directive (EU) 2018/844 of the European Parliament and of the Council of 30 May 2018 amending Directive 2010/31/EU on the Energy Performance of Buildings and Directive 2012/27/EU on Energy Efficiency. Available online: https://eur-lex.europa.eu/legal-content/ (accessed on 22 March 2022).
5. Reis, I.F.G.; Figueiredo, A.; Samagaio, A. Modelling the evolution of construction solutions in residential buildings' thermal comfort. *Appl. Sci.* **2021**, *11*, 2427. [CrossRef]
6. Nejat, P.; Jomehzadeh, F.; Taheri, M.M.; Gohari, M.; Majid, M.Z. A global review of energy consumption, CO_2 emissions and policy in the residential sector (with an overview of the top ten CO_2 emitting countries). *Renew. Sustain. Energy Rev.* **2015**, *43*, 843–862. [CrossRef]
7. Allard, I.; Nair, G.; Olofsson, T. Energy performance criteria for residential buildings: A comparison of Finnish, Norwegian, Swedish, and Russian building codes. *Energy Build.* **2021**, *250*, 111276. [CrossRef]
8. Bienvenido-Huertas, D.; Oliveira, M.; Rubio-Bellido, C.; Marín, D. A comparative analysis of the international regulation of thermal properties in building envelope. *Sustainability* **2019**, *11*, 5574. [CrossRef]
9. Jana, K.; Ray, A.; Majoumerd, M.M.; Assadi, M.; De, S. Polygeneration as a future sustainable energy solution—A comprehensive review. *Appl. Energy* **2017**, *202*, 88–111. [CrossRef]
10. Calise, F.; Notaristefani di Vastogirardi, G.; Dentice d'Accadia, M.; Vicidomini, M. Simulation of polygeneration systems. *Energy* **2018**, *163*, 290–337. [CrossRef]
11. Luqman, M.; Al-Ansari, T. Thermodynamic analysis of an Energy-Water-Food (Ewf) nexus driven polygeneration system applied to coastal communities. *Energy Convers. Manag.* **2020**, *205*, 112432. [CrossRef]
12. Kumar, P.; Rajagopal, S.; Coronas, A. Integrated polygeneration system for coastal áreas. *Therm. Sci. Eng. Prog.* **2020**, *20*, 100739.
13. Ahmadi, P.; Dincer, I.; Rosen, M.A. Thermoeconomic multi-objective optimization of a novel biomass-based integrated energy system. *Energy* **2014**, *68*, 958–970. [CrossRef]
14. Hogerwaard, J.; Dincer, I.; Naterer, G.F. Solar energy based integrated system for power generation, refrigeration and desalination. *Appl. Therm. Eng.* **2017**, *121*, 1059–1069. [CrossRef]
15. Xi, Z.; Eshaghi, S.; Sardari, F. Energy, exergy, and exergoeconomic analysis of a polygeneration system driven by solar energy with a thermal energy storage tank for power, heating, and freshwater production. *J. Energy Storage* **2021**, *36*, 102429. [CrossRef]
16. Jana, K.; De, S. Polygeneration for power, utility heat, desalination and refrigeration: Comparative performance evaluation for different biomass inputs. *Mater. Today Proc.* **2018**, *5*, 22908–22915. [CrossRef]
17. Thomas, S.; Sahoo, S.S.; Ajithkumar, G.; Thomas, S.; Rout, A.; Mahapatra, S.K. Socio-economic and environmental analysis on solar thermal energy-based polygeneration system for rural livelihoods applications on an Island through interventions in the energy-water-food nexus. *Energy Convers. Manag.* **2022**, *270*, 116235. [CrossRef]
18. Kumar, G.P.; Ayou, D.S.; Narendran, C.; Saravanan, R.; Maiya, M.P.; Coronas, A. Renewable heat powered polygeneration system based on an advanced absorption cycle for rural communities. *Energy* **2023**, *262*, 125300. [CrossRef]
19. Rong, A.; Su, Y. Polygeneration systems in buildings: A survey on optimization approaches. *Energy Build.* **2017**, *151*, 439–454. [CrossRef]

20. Calise, F.; Cipollina, A.; Dentice d'Accadia, M.; Piacentino, A. A novel renewable polygeneration system for a small Mediterranean volcanic island for the combined production of energy and water: Dynamic simulation and economic assessment. *Appl. Energy* **2014**, *135*, 675–693. [CrossRef]
21. Calise, F.; Dentice d'Accadia, M.; Piacentino, A. Exergetic and exergoeconomic analysis of a renewable polygeneration system and viability study for small isolated communities. *Energy* **2015**, *92*, 290–307. [CrossRef]
22. Calise, F.; Macaluso, A.; Piacentino, A.; Vanoli, L. A novel hybrid polygeneration system supplying energy and desalinated water by renewable sources in Pantelleria Island. *Energy* **2017**, *137*, 1086–1106. [CrossRef]
23. Calise, F.; Cappiello, F.L.; Vicidomini, M.; Petrakopoulou-Robinson, F. Water-energy nexus: A thermoeconomic analysis of polygeneration systems for small Mediterranean islands. *Energy Convers. Manag.* **2020**, *220*, 113043. [CrossRef]
24. Mouaky, A.; Rachek, A. Thermodynamic and thermo-economic assessment of a hybrid solar/biomass polygeneration system under the semi-arid climate conditions. *Renew. Energy* **2020**, *156*, 14–30. [CrossRef]
25. Spanish National Institute of Statistics. Population and Housing Census. Available online: www.ine.es/censos2011_datos/cen11_datos_inicio.htm (accessed on 11 November 2021).
26. Zabalza, I.; Gesteira, L.G.; Uche, J. The impact of building energy codes evolution on the residential thermal demand. *J. Braz. Soc. Mech. Sci. Eng.* **2022**, *44*, 588. [CrossRef]
27. Spanish Ministry of Development. Order FOM/1635/2013, of September 10th, Which Updates the Basic Document DB-HE of Energy Saving of the Technical Building Code, Approved by Royal Decree 314/2006, of March 17th. BOE no. 219, 12/09/2013. Available online: https://www.boe.es/eli/es/ (accessed on 22 March 2022).
28. Spanish Ministry of Development. Royal Decree 732/2019, of December 20th, Which Modifies the Technical Building Code, Approved by Royal Decree 314/2006, of March 17th. BOE no. 311, 27/12/2019. Available online: https://www.boe.es/diario_boe/ (accessed on 15 May 2022).
29. State Meteorological Agency of Spain. Municipal Climate Data. Available online: http://www.aemet.es (accessed on 11 November 2021).
30. Meteotest AG. Meteonorm 8. Handbook Part I: Software. Available online: https://meteonorm.com/assets/downloads/mn81_software.pdf (accessed on 11 November 2021).
31. Calise, F.; Cappiello, F.L.; Dentice d'Accadia, M.; Petrakopoulou, F.; Vicidomini, M. A solar-driven 5^{th} generation district heating and cooling network with ground-source heat pumps: A thermo-economic analysis. *Sustain. Cities Soc.* **2022**, *76*, 103438. [CrossRef]
32. Calise, F.; Cappiello, F.L.; Dentice d'Accadia, M.; Vicidomini, M. Dynamic simulation, energy and economic comparison between BIPV and BIPVT collectors coupled with micro-wind turbines. *Energy* **2020**, *191*, 116439. [CrossRef]
33. Calise, F.; d'Accadia, M.D.; Figaj, R.D.; Vanoli, L. A novel solar-assisted heat pump driven by photovoltaic/thermal collectors: Dynamic simulation and thermoeconomic optimization. *Energy* **2016**, *95*, 346–366. [CrossRef]
34. Buonomano, A.; Calise, F.; d'Accadia, M.D.; Vicidomini, M. A hybrid renewable system based on wind and solar energy coupled with an electrical storage: Dynamic simulation and economic assessment. *Energy* **2018**, *155*, 174–189. [CrossRef]
35. Buonomano, A.; Calise, F.; Ferruzzi, G.; Vanoli, L. A novel renewable polygeneration system for hospital buildings: Design, simulation and thermo-economic optimization. *Appl. Therm. Eng.* **2014**, *67*, 43–60. [CrossRef]
36. Instituto para la Diversificación y Ahorro de la Energía (IDAE). Renewable Energy Plan in Spain 2005–2010 (2005). Available online: https://www.idae.es (accessed on 31 March 2022).
37. Pina, E.A.; Lozano, M.A.; Serra, L.M. Allocation of economic costs in trigeneration systems at variable load conditions including renewable energy sources and thermal energy storage. *Energy* **2018**, *151*, 633–646. [CrossRef]
38. Mata-Torres, C.; Escobar, R.A.; Cardemil, J.M.; Simsek, Y.; Matute, J.A. Solar polygeneration for electricity production and desalination: Case studies in Venezuela and northern Chile. *Renew. Energy* **2017**, *101*, 387–398. [CrossRef]
39. Esrafilian, M.; Ahmadi, R. Energy, environmental and economic assessment of a polygeneration system of local desalination and CCHP. *Desalination* **2019**, *454*, 20–37. [CrossRef]
40. Uche, J.; Acevedo, L.; Círez, F.; Usón, S.; Martínez-Gracia, A.; Bayod-Rújula, Á.A. Analysis of a domestic trigeneration scheme with hybrid renewable energy sources and desalting techniques. *J. Clean. Prod.* **2019**, *212*, 1409–1422. [CrossRef]
41. Red Eléctrica Española (REE). CO_2 Emissions of Electricity Generation in Spain. 2021. Available online: https://api.esios.ree.es/documents/580/download?locale=es (accessed on 15 February 2022).
42. Pinto, E.S.; Serra, L.M.; Lázaro, A. Optimization of the design of polygeneration systems for the residential sector under different self-consumption regulations. *Int. J. Energy Res.* **2020**, *44*, 11248–11273. [CrossRef]
43. Spanish Ministry of Development. Updating of the Energy Saving Document DB-HE of the Technical Building Code. 2019. Available online: https://www.codigotecnico.org/pdf/Documentos/HE/DBHE.pdf (accessed on 1 October 2021).
44. Instituto para la Diversificación y Ahorro de la Energía (IDAE). CO_2 Emission Factors and Primary Energy Coefficients for Different Final Energy Sources Consumed in the Building Sector in Spain. 2014. Available online: https://energia.gob.es/desarrollo/EficienciaEnergetica/RITE/Reconocidos/Reconocidos/Otros%20documentos/Factores_emision_CO2.pdf (accessed on 15 February 2022).
45. Herrando, M.; Elduque, D.; Javierre, C.; Fueyo, N. Life cycle assessment of solar energy systems for the provision of heating, cooling and electricity in buildings: A comparative analysis. *Energy Convers. Manag.* **2022**, *257*, 115402. [CrossRef]

46. Solano-Olivares, K.; Romero, R.J.; Santoyo, E.; Herrera, L.; Galindo-Luna, Y.R.; Rodríguez-Martínez, A.; Santoyo-Castelazo, E.; Cerezo, J. Life cycle assessment of solar absorption air-conditioning system. *J. Clean. Prod.* **2019**, *240*, 118206. [CrossRef]
47. Lozano, J.A.; López, R.; Palomar, J.M.; Rey, F.J. Comparative study of heat pump system of biomass boiler system to a tertiary building using the Life Cycle Assessment (LCA). *Renew. Energy* **2020**, *152*, 1439–1450. [CrossRef]
48. *Ecoinvent Data Base*, Version 3.4.; Swiss Centre for Life Cycle Inventories: Dübendorf, Switzerland, 2018.
49. *ELCD Data Base, Database of LCI Data Sets with European Market or Production Scope*, Version 3.2; The European Platform on LCA: Bruxelles, Belgium, 2013.
50. Beccali, M.; Cellura, M.; Longo, S. *IEA Solar Heating and Cooling Program (Task 48). Final Deliverable*; Report on Life Cycle Analysis; IEA: Paris, France, 2014.
51. Raluy, G.; Serra, L.; Uche, J. Life cycle assessment of MSF, MED and RO desalination technologies. *Energy* **2006**, *31*, 2361–2372. [CrossRef]
52. Pintanel, M.T.; Martínez-Gracia, A.; Galindo, M.P.; Bayod-Rújula, A.A.; Uche, J.; Tejero, J.A.; Del Amo, A. Analysis of the Experimental Integration of Thermoelectric Generators in Photovoltaic–Thermal Hybrid Panels. *Appl. Sci.* **2021**, *11*, 2915. [CrossRef]
53. Usón, S.; Royo, J.; Canalís, P. Experimental tests of the integration of thermoelectric generators in a biomass boiler. In Proceedings of the 7th International Conference on Contemporary Problems of Thermal Engineering (CPOTE22), Warsaw, Poland, 20–23 October 2022.
54. Gesteira, L.G.; Uche, J. A Novel Polygeneration System Based on Solar-Assisted Desiccant Cooling System for Residential Buildings: An Energy and Environmental Analysis. *Sustainability* **2022**, *14*, 3449. [CrossRef]
55. Gesteira, L.G.; Uche, J.; Dejo, N. A Polygeneration System Based on Desiccant Air Conditioning Coupled with an Electrical Storage. *Sustainability* **2022**, *14*, 15784. [CrossRef]
56. Boletín Oficial del Estado (BOE-A-2020-17282). Resolution of 18 December 2020, of the Directorate General for Energy Policy and Mines, which approves the consumption profile and the calculation method for the purposes of energy settlement, applicable to type 4 and type 5 consumers who do not have an hourly consumption register, in accordance with Royal Decree 1110/2007, of 24 August, which approves the Unified Regulation of Measuring Points of the Electricity System, for the year 2021. Available online: https://www.boe.es/eli/es/ (accessed on 15 May 2022). (In Spanish).
57. Instituto de Diversificación y Ahorro de Enegía (IDAE). Informe Anual de Indicadores Energéticos. Sector Doméstico. 2018. Available online: https://www.idae.es (accessed on 18 October 2020).
58. Canal de Isabel II. Cuadernos de I+D+i. No. 28. Las Claves del Consumo Doméstico en la Comunidad de Madrid. 2018. Available online: https://www.canaldeisabelsegunda.es/documents/ (accessed on 18 June 2022). (In Spanish).